A Study On The Roles And Effects Of Syndecans On Endothelial Cell Biology During Angiogenesis

De Rossi, Giulia

Alla mia splendida famiglia,

A Study On The Roles And Effects Of Syndecans On Endothelial Cell Biology During Angiogenesis

A thesis submitted in partial fulfilment of the requirements of the Degree of Doctor of Philosophy

By

Giulia De Rossi

Centre for Microvascular Research

William Harvey Research Institute

Barts & The London School of Medicine and Dentistry

Queen Mary University of London

Charterhouse Square

London EC1M 6BQ

United Kingdom

List of contents

Acknowledgments

It’s been amazing.

I’d like to express my gratitude to my first supervisor, James Whiteford. Although rumour has it James only picked me because the other candidate showed up at the interview with a love bite on his neck, I’m sure he doesn’t regret his choice. Over the past 4 years I’ve grown so much professionally and this is largely due to his supervision. James is probably the best scientist I’ve encountered in my career so far, his passion for science is inspirational and his friendly personality makes him the best lab mate you could have. I couldn’t have hoped for a better supervisor, not one single idea I had during the course of my PhD hasn’t been acknowledged and encouraged by him. We made a formidable team. We only had 2 limits for what we could achieve: time and money. Apart from that, nothing has proven impossible.

A big thank you goes to the head of the centre for microvascular research and my second supervisor, Sussan Nourshargh. First of all for welcoming me in her lab but mostly for supporting me throughout the whole journey. I’ve always felt encouraged by her to reach for the stars. She taught me that nothing comes easy in this job and that if something is worth a shot then you should give it your best one. Know your goals and stay focused. Learn from failures and always stay positive and endure because hard work pays off eventually.

So many people made this journey memorable and pleasant: Michi and Krishma, my first desk buddies, my first friends, who made me feel at home in such a new environment. Suborno, Chris, Thomas, Kate and Fu for the #bants, of course. To all the past and present members of the lab and the institute, too many to name, none of this would’ve been possible without the lovely environment you created in the lab every day.

To my friends in Rome, Chiara C., Chiara D.V., Maria, Mario, Silvia, Valeria, because I’m pretty sure they still don’t have a clue about what the heck it is that I study but they always show me their support and love regardless.

To Snoops, for believing in me more than I do.

E per finire, alla mia famiglia. Che mi tiene per mano, sempre.

Giulia

Statement of originality

I, Giulia De Rossi, confirm that the research included within this thesis is my own work or that where it has been carried out in collaboration with, or supported by others, that this is duly acknowledged below and my contribution indicated. Previously published material is also acknowledged below.

I attest that I have exercised reasonable care to ensure that the work is original, and does not to the best of my knowledge break any UK law, infringe any third party's copyright or other Intellectual Property Right, or contain any confidential material.

I accept that the College has the right to use plagiarism detection software to check the electronic version of the thesis.

I confirm that this thesis has not been previously submitted for the award of a degree by this or any other university.

Signature: 

Date: 07.12.2015

List of presentations and prizes awarded at scientific meetings

Oral presentations

- Angiogenesis and Vascular remodelling meeting, **Chester**, July 2014
- 5th International meeting on Angiogenesis VU university medical center, **Amsterdam**, March 2014
- WHRI New year celebration, **London**, January 2014
- London Matrix group half-day Symposium, **London**, October 2013
- Wellcome Trust Symposium Get Connected 3: Immuno Matrix, **Manchester**, September 2013
- WHRI annual research review, **London**, July 2013

Posters

- William Harvey Day, **London**, October 2015
- 9th International Conference On Proteoglycans And 10th Pan-Pacific Connective Tissue Societies Symposium, **Seoul**, August 2015
- Angiogenesis and Vascular Remodelling meeting, **Chester**, July 2014
- 5th International meeting on Angiogenesis VU university medical center, **Amsterdam**, March 2014
- Wellcome Trust Symposium Get Connected 3: Immuno Matrix, **Manchester**, September 2013
- WHRI annual research review, **London**, July 2012
- UK Adhesion Meeting, **Sheffield**, April 2012
- BSMB Spring meeting, **Oxford**, April 2012

Prizes

- **Outstanding Young Investigator Award** at the WHRI annual review, London, January 2014
- **Best Talk** at the Wellcome Trust Symposium Get Connected 3: Immuno Matrix, Manchester, September 2013
- **Best Poster** at the Wellcome Trust Symposium Get Connected 3: Immuno Matrix, Manchester, September 2013

List of publications arising from this work

- **De Rossi G**, Whiteford JR. (2013) - *Novel insight into the biological functions of syndecan ectodomain core proteins.* Biofactors 39(4):374-82

- **De Rossi G**, Scotland RS, Whiteford JR. (2013) - *Critical factors in measuring angiogenesis using the aortic ring model.* J Genet Syndr Gene Ther 4(5)

- **De Rossi G**, Whiteford JR. (2013) - *A novel role for syndecan-3 in angiogenesis.* F1000Research 2:270

- **De Rossi G**, Evans A, Kay E, Woodfin A, McKay T, Nourshargh S, Whiteford J. (2014) - *Shed syndecan-2 inhibits Angiogenesis.* J Cell Sci, 127, 4788-4799

- **De Rossi G**, Whiteford JR. (2014) - S*yndecans in angiogenesis and EC biology.* Biochem Soc Trans, 42(6):1643-6

- **De Rossi G**, Cristante E, Kojima T, Bainbridge J, Greenwood, J, Whiteford JR - S*yndecan-4 is required for VEGF-induced angiogenesis*, in preparation.

Abstract

Angiogenesis, the formation of new blood vessels from pre-existing ones, is a key process during development, wound healing and the female reproductive cycle. However, it is also a pathological feature of many diseases such as cancer, age-related macular degeneration and chronic inflammatory pathologies. Given the complexity underlying the fine regulation of this process, despite the great number of studies, our understanding of it is not yet exhaustive.

Syndecans are heparan sulphate proteoglycans with roles in cell adhesion, migration and growth factor interactions. The aim of this body of work was to investigate the role of these molecules in the regulation of angiogenesis. For this purpose, in the first part of my project, I investigated the effects of the extracellular core proteins of all four syndecans on endothelial cell functions. These studies identified that all four proteins are able to inhibit angiogenesis and strongly suppress endothelial cell migration, invasion and tube formation. On the basis of these discoveries, I focused on the syndecan-2 extracellular core protein and showed that it is shed during inflammation and can interact with the endothelial cell surface tyrosine phosphatase receptor CD148. Upon binding to CD148, the syndecan-2 extracellular core protein reduces the expression of active β1 integrins on endothelial cell surface and inhibits endothelial cell migration. This provides a mechanism through which shed syndecan-2 can regulate angiogenesis. Critically, this is an entirely novel pathway for the reduction of angiogenesis which is independent to the main angiogenic factor VEGF. Lastly, since previous works suggested that the syndecan-4-null mouse may exhibit angiogenic defects, I set out to determine the role of syndecan-4 in angiogenesis. Here, I observed an up-regulation of syndecan-4 on endothelial cells in angiogenic settings both *in vitro* and *in vivo*. Furthermore, through analysis of *in vivo* models of pathological angiogenesis, I observed that syndecan-4 is critical for VEGF-A-mediated angiogenesis. This effect was partially explained by impaired activation of VEGFR2 in syndecan-4-null endothelial cells. This data suggests that syndecan-4 is the main heparan sulphate proteoglycan to act as VEGFR2 co-receptor during pathological angiogenesis.

Collectively, the findings of this research have identified previously unknown roles for syndecans in the regulation of angiogenesis.

Table of contents

List of Figures

List of tables

List of appendices

Appendix 1

- **De Rossi G**, Whiteford JR. (2013) - *Novel insight into the biological functions of syndecan ectodomain core proteins.* Biofactors 39(4):374-82

Appendix 2

- **De Rossi G**, Scotland RS, Whiteford JR. (2013) - *Critical factors in measuring angiogenesis using the aortic ring model.* J Genet Syndr Gene Ther 4(5)

Appendix 3

- **De Rossi G**, Whiteford JR. (2013) - *A novel role for syndecan-3 in angiogenesis.* F1000Research 2:270

Appendix 4

- **De Rossi G**, Evans A, Kay E, Woodfin A, McKay T, Nourshargh S, Whiteford J. (2014) - *Shed syndecan-2 inhibits Angiogenesis.* J Cell Sci, 127, 4788-4799

Appendix 5

- **De Rossi G**, Whiteford JR. (2014) - S*yndecans in angiogenesis and EC biology.* Biochem Soc Trans, 42(6):1643-6

List of Acronyms and abbreviations

Ab	Antibody
ADAM	A Disintegrin And Metalloproteinase
AIDS	Acquired Immune Deficiency Syndrome
ANG	Angiopoietin
ARD	Adhesion-Regulatory Domain
ASMC	Artherial Smooth Muscle Cell
BALB/c	Bagg Albino Inbred Research Mouse Strain
BM	Basement Membrane
BMDC	Bone-Marrow Derived Cell
BSA	Bovine Serum Albumin
CASK	Calcium/Calmodulin-Dependent Serine Protein Kinase
CBD	Cell-Binding Domain
CCL	CC Chemokine Ligand
CCR	CC Chemokine Receptor
CD	Cluster Of Differentiation
cDNA	Complementary DNA
CS	Chondroitin Sulphate
CTF	C-Terminal Cleavage Fragment
CXCL	CXC Chemokine Ligand
DAPI	4',6-Diamidino-2-Phenylindole
DC	Dendritic Cell
DLL4	Delta-Like 4
DMEM	Dulbecco's Modified Eagle's Medium
DS	Dermatan Sulphate
EC	Endothelial Cell
ECM	Extracellular Matrix

EC-SOD	EC-Superoxide Dismutase
EDTA	Ethylenediaminetetraacetic Acid
EGF	Epidermal Growth Factor
ELISA	Enzyme-Linked Immunosorbent Assay
ERK	Extracellular-Signal-Regulated Kinases
ERM	Ezrin–Radixin–Moesin
EtOH	Ethanol
EV	Empty Vector
EXT1	Exostosin Glycosyltransferase 1
FA	Focal Adhesion
FACS	Fluorescence Associated Cell Sorting
FBS	Foetal Bovine Serum
FGF	Fibroblast Growth Factor
FGFR	Fibroblast Growth Factor Receptor
FN	Fibronectin
GAG	Glycosaminoglycan
GST	Glutathione S-Transferase
HBD	Heparin-Binding Domain
HB-EGF	Heparin-Binding Egf-Like Growth Factor
HEK293T	Human Embryonic Kidney 293 Cells
HG	Haemoglobin
HGF	Hepatocyte Growth Factor
HIF	Hypoxia-Inducible Factors
HIV	Human Immunodeficiency Virus
HMEC	Human Microvascular EC
HRE	Hypoxia-Responsive Element
HRP	Horseradish Peroxidase
HS	Heparan Sulphate
HSPG	Heparan Sulphate Proteoglycan

HUVEC	Human Umbilical Vein ECs
IGF	Insulin-Like Growth Factor
IL-8	Interleukin-8
IPF	Idiopathic Pulmonary Fibrosis
KC	Keratinocyte Chemoattractant
MAP	Mitogen-Activated Protein
MIP-2	Macrophage Inflammatory Protein 2
MLEC	Mouse Lung EC
MMP	Matrix Metalloproteinase
MT-MMP	Membrane-Type MMP
MvEC	Mouse Vascular EC
NDST	N-Deacetylase–N-Sulphotransferase
NO	Nitric Oxide
NRP	Neuropilin
ON	Over-Night
OST	O-Sulphotransferase
P/S	Penicillin/Streptomycin
PAGE	Polyacrylamide Gel Electrophoresis
PAI	Plasminogen Activator Inhibitor
PBS	Phosphate-Buffered Saline
PDGF	Platelet-Derived Growth Factor
PDH	Pyruvate Dehydrogenase
PECAM	Platelet EC Adhesion Molecule
PGE	Prostaglandin
PI3K	Phosphoinositide 3-Kinase
PKC	Protein Kinase C
PLA	Proximity-Ligation Assay
PlGF	Placental Growth Factor
PMA	Phorbol 12-Myristate 13-Acetate

PTK	Protein Tyrosine Kinase
RANTES	Regulated On Activation, Normal T Expressed And Secreted
REF	Rat Embryo Fibroblasts
RGD	Tripeptide Arg-Gly-Asp
RNA	Ribonucleic Acid
RPE	Retinal Pigmented Epithelium
RPF	Renal Periphery Fibroblast
RT	Room Temperature
RT-PCR	Reverse Transcription Polymerase Chain Reaction
S1ED	Syndecan-1 ectodomain
S4	Syndecan-4
SCID	Severe Combined Immunodeficiency
SDC	Syndecan
SDF	Stromal Cell Derived Factor
SDS	Sodium Dodecyl Sulfate
SSTN	Synstatin
syndecan-4 KO	Syndecan-4 Knock-Out
TBST	Tris-Buffered Saline And Tween 20
TGF	Transforming Growth Factor
TNF	Tumor Necrosis Factor
TRAP	Thrombin Receptor-Activating Peptide
TSP	Thrombospondin
uPA	Urokinase-Type Plasminogen Activator
UT	Untreated
VCAM	Vascular Cell Adhesion Molecule
VE-Cadherin	Vascular Endothelial Cadherin
VEGF	Vascular Endothelial Growth Factor
VN	Vitronectin
VPF	Vascular Permeability Factor

WT	Wild-Type
ZO	Zona Occludens Protein

1. Introduction

Heparan sulphate proteoglycans (HSPGs) are a class of glycoproteins composed of a core protein to which long linear heparan sulphate (HS) chains are attached. HSPGs can be found on the cell surface, anchored to the plasma membrane via a transmembrane domain as is the case for syndecans or via a glycosylphosphatidylinositol molecule as is the case for glypicans, or they can be directly released in the extracellular space like in the case of agrin, collagen XVIII and perlecan (Gallagher et al., 1986).

HSPGs are absent in protista, plantae and fungi, and they only appear in the animal kingdom with the advent of eumetazoa, animals that display true tissues, where they are found to be ubiquitously expressed in all tissues and species analysed (Dietrich et al., 1983). HSPGs have therefore a long evolutionary history, which is usually indicative of fundamental roles. HSPGs, in fact, participate in many different activities in cells and tissues: ligand-receptor clustering and signalling, endocytosis and trafficking of cytoplasmic vesicles, cytoskeletal dynamics, cell adhesion and motility, basement membrane organisation, chemotactic gradient formation and cell-cell cross talk (Bishop et al., 2007; Sarrazin et al., 2011).

Perhaps unsurprisingly, given their key roles in cell and tissue biology, HSPGs have often been associated with the pathogenesis of many diseases including cancer (Soares et al., 2015), arthritis (De Ceuninck et al., 2003), vascular diseases (David et al., 1995), dysregulated inflammation (Gordts and Esko, 2015) and Alzheimer's disease (van Horssen et al., 2003). However, despite the large amount of studies aimed at understanding the roles of HSPGs in health and disease, our understanding of these structures is still elusive.

This thesis aimed at examine the role of the syndecan family of HSPGs with a specific focus on how they impact on angiogenesis, the process of new blood vessel formation from pre-existing ones.

1.1. The syndecan family

Syndecans were discovered in 1989 while studying cell surface proteins substituted by HS and chondroitin-sulphate chains and were initially called Syndenins ("to link" in Greek, as it was thought to link the cytoskeleton to the interstitial matrix) (Saunders et al., 1989). Syndecans are HSPGs expressed at up to 1 million copies per cell in nearly every cell of the body as transmembrane proteins. Vertebrates possess 4 different syndecan genes each encoding one type of syndecan i.e. syndecan-1 (syndecan, CD138), syndecan-2 (fibroglycan, CD362), syndecan-3 (N-syndecan) and syndecan-4 (ryudocan, amphiglycan) (Fig. 1.1).

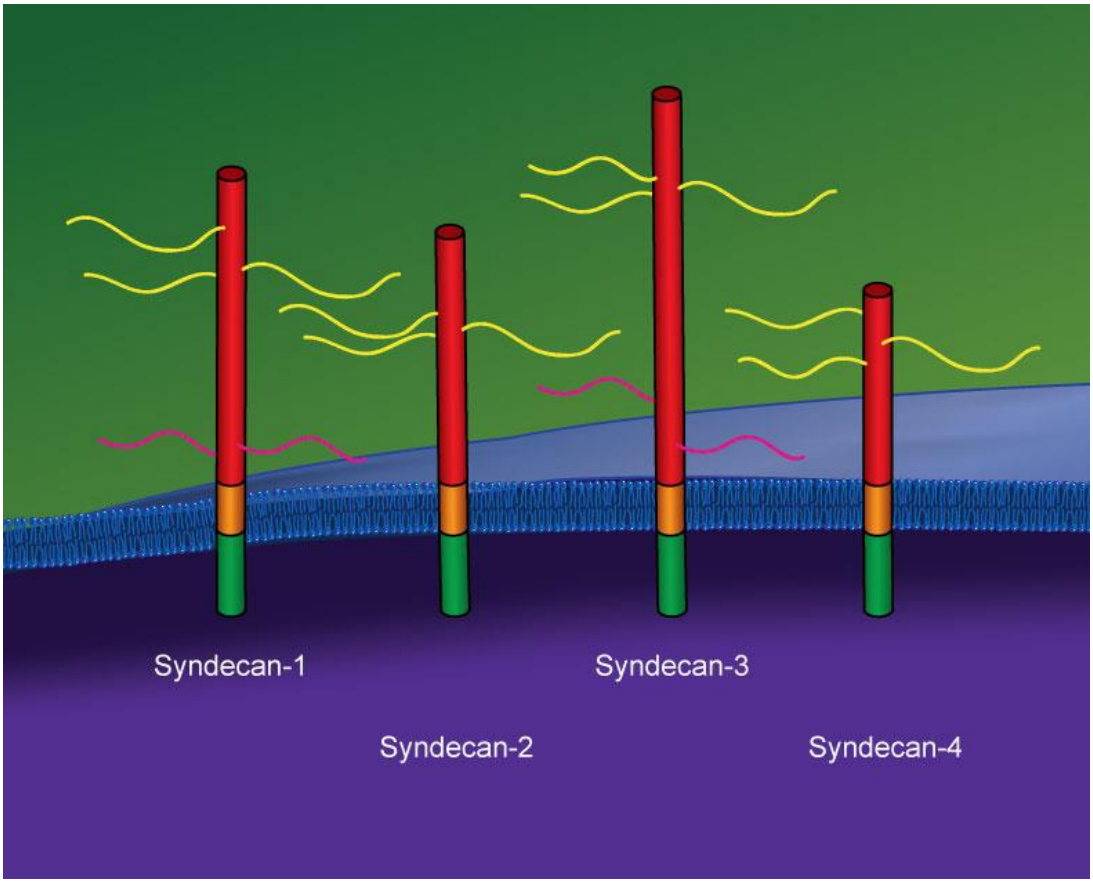

Fig. 1.1 **The mammalian syndecan family.** The diagram shows the 4 members of the mammalian syndecan family. Based on sequence homology, the 4 syndecans are additionally grouped into 2 sub-families, one composed of syndecan-1 and -3 and one composed of syndecan-2 and -4. The syndecan numbers reflect the order in which the cDNAs for each family member were cloned. In red is shown the extracellular domain, in orange the transmembrane domain and in green the cytoplasmic domain. (Figure modified from De Rossi et al. 2013).

Each family member has a distinctive spatial and temporal expression pattern. Syndecan-1 is primarily expressed on epithelial and plasma cells, syndecan-2 on fibroblasts, endothelial cells (ECs), neurons and smooth-muscle cells, syndecan-3 is mainly expressed in the nervous system and on chondrocytes, while syndecan-4 is ubiquitous. However, new patterns of expression for each of the four vertebrate syndecan are continuously revealed, meaning that our current understanding of syndecan distribution is yet far from comprehensive. Syndecan functions have been difficult to discern, and the situation is compounded by the finding that syndecan-1 and -4 knock-out mice develop normally (Ishiguro et al., 2000b) (Stepp et al., 2002). They both, however showed impairment in tissue repair, skin and cornea in the case of syndecan-1 (Pal-Ghosh et al., 2008) and skin in the syndecan-4 null mice (Echtermeyer et al., 2001a). Long-term potentiation defects were noted in the syndecan-3 null mouse, the major syndecan of the neural tissue (Hienola et al., 2006). Interestingly, in the invertebrate *Caenorhabditis elegans*, the only syndecan present is also widely enriched in the developing and adult nervous system, suggesting that syndecan-3 is most closely related to the invertebrate member.

1.1.1. Structure

The 4 members that comprise the syndecan family in vertebrates originated after 2 gene duplication events of the invertebrate syndecan. The first duplication event produced what will later become 2 sub-families, syndecan-2 and -4 and syndecan-1 and -3 which in pairs share a high degree of homology (Chakravarti and Adams, 2006). All 4 members have a common linear structure and lack a tertiary structure with their conformation determined by interacting molecules (Leonova and Galzitskaya, 2013). Syndecan-2 and -4 have a shorter polypeptide chain compared to syndecan-1 and -3 and are substituted only by HS chains, while syndecan-1 and -3 may also possess chondroitin-sulphate chains. The polypeptide chain of the core protein is synthesized on membrane-bound ribosomes and then transferred to the lumen of the endoplasmic reticulum. Attachment of the sugar chains proceeds in the Golgi apparatus. The sugar chains are attached covalently to the syndecan extracellular core protein's serine residues, provided that those are followed by a glycine in the sequence. The HS chains are composed of repetitions of the disaccharides N-acetylglucosamine plus glucoronic acid and N-acetylglucosamine plus iduronic acid, while chondroitin-sulphate consists of N-acetylgalactosamine and glucuronic acid. The glycosaminoglycan (GAG) chains may contain 50 to 200 repetitions of the afore mentioned disaccharides. Importantly, these GAG chains are substituted with sulphate groups conferring them a highly negative charge which is key to both

syndecan functions and structure. First, GAG chains repulse each other by which mean they can extend in space increasing their area of action; second, they can interact and sequester a large repertoire of positively charged molecules. Not much is known about the different sulphation patterns of syndecan GAG chains, but it is clear that there is an alternation of sites with low and high degrees of sulphation (Manon-Jensen et al., 2010) (Gallagher et al., 1992).

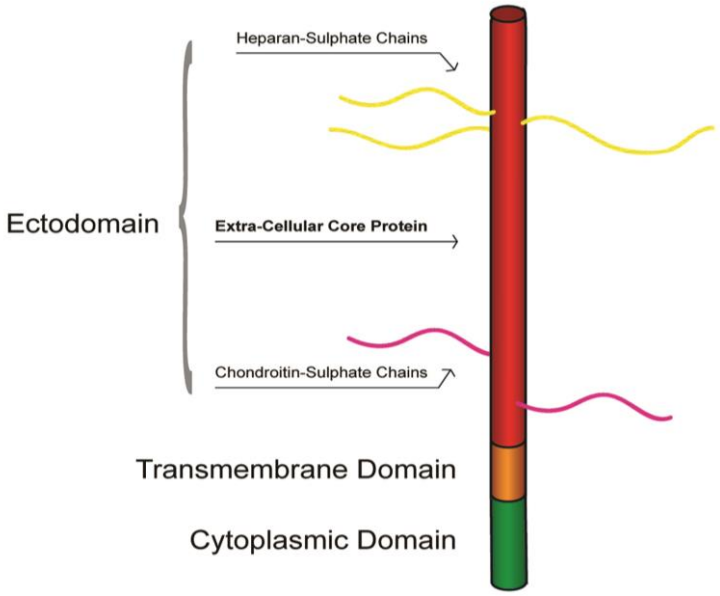

Fig. 1.2 **Syndecan ectodomain structure.** Shown in red is syndecan ectodomain which projects outside the cellular space and is composed of a linear proteic backbone substituted by 3 HS chains only, in the case of syndecan-2 and -4, or with the addition of 2 chondroitin-sulphate chains in the case of syndecan-1 and -3. (Figure modified from De Rossi et al. 2013).

The transmembrane domain of all syndecans contains a conserved motif GXXXG which is necessary for syndecan dimerization at the cell surface and for retaining cholesterol into lipid rafts (Barrett et al., 2012). Syndecan cytoplasmic domains are quite short (~33 aa) and do not possess any intrinsic enzymatic activity. They are divided into 3 regions, C1 and C2, which are very conserved amongst all 4 members, flanking a more variable region (V). At the C-terminus of syndecan cytoplasmic domains, on the C2 region, are the 4 amino acids EFYA which represent a binding site for PDZ-containing proteins, such as synbindin (Ethell et al., 2000), synectin (also known as GIPC1) (Gao et al., 2000) and syntenin (Grootjans et al., 1997). The C1 region also interacts with proteins, especially actin-binding ones (e.g. ezrin, moesin, etc.) (Beauvais and Rapraeger, 2004). The V region, as stated above, is quite divergent amongst vertebrate syndecans. Unfortunately, not much is known about its function/interactions. There are some indications suggesting that the syndecan-4 V region

interacts with phosphatidyl inositol 4,5 bisphosphate (PIP2) and protein kinase Cα (PKCα) (Horowitz et al., 1999; Keum et al., 2004; Lim et al., 2003). Interestingly, a single serine phosphorylation at the C1-V junction is able to promote a substantial shape change in the syndecan-4 cytoplasmic tail which seems to decrease the interaction with PIP2 and PKCα. On the other hand the afore mentioned phosphorylation appears to increase the affinity of the V region to another cytoskeleton protein, α actinin (Chaudhuri et al., 2005) (Choi et al., 2008) (Greene et al., 2003) (Okina et al., 2012), suggesting the presence of alternative binding partners depending on the phosphorylation status of syndecan-4 cytoplasmic domain. Syndecan ectodomains will be covered extensively in 1.1.7.

1.1.2. Glycosaminoglycan chain biosynthesis

The molecular interactions mediated by syndecan GAG chains (HS or/and chondroitin-sulphate) are key to syndecan functions chains (Deepa et al. 2004).

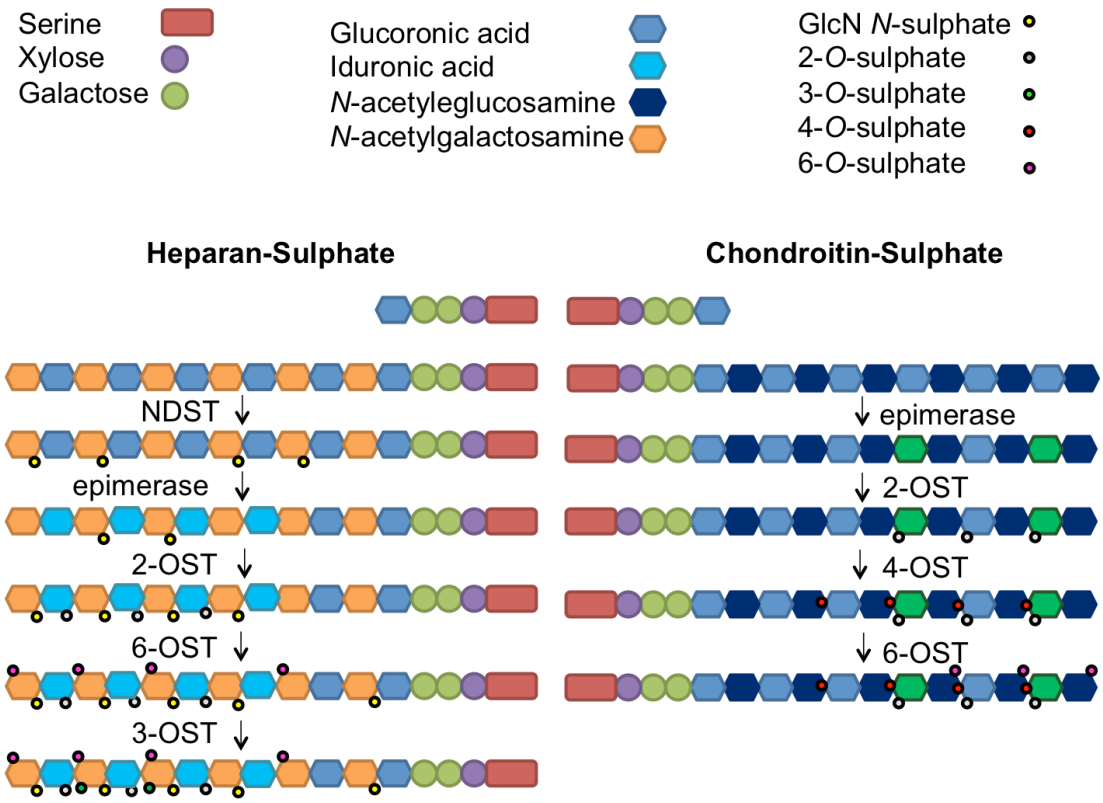

Fig. 1.3 **GAG chains structure and assembly.** GAGs are attached to a serine residue in the core protein by a tetrasaccharide linker (xylose–galactose–galactose–uronic-acid) on which the sugar chain is assembled. Synthesis of N-acetylgalactosamine (GalNAc)- and glucuronic acid (GlcA)-containing disaccharide units generates chondroitin sulphate (CS) or dermatan sulphate (DS); synthesis of N-acetylglucosamine (GlcNAc)- and GlcA-containing disaccharide units generates HS. Successive modification by epimerization of GlcA to iduronic acid, 2-O-sulphation, 4-O-sulphation and 6-O-sulfation in the case of CS or DS, and N-deacetylation–N-sulphation, epimerization, 2-O-sulphation, 6-O-sulphation and 3-O-sulphation in the case of HS, results in mature GAG chains. Note that not all biosynthesis or modification steps occur in a linear sequence. Some modification steps depend on previous steps to occur first, whereas others are independent. The nature of the modification reactions leads to the generation of an almost infinite diversity of polysaccharide chains. NDST, N-deacetylase–N-sulphotransferase; OST, O-sulphotransferase.

The complex biosynthetic pathway that leads to the formation of HS chains of up to 100 kDa in weight begins with a linker tetrasaccharide composed of xylose, two galactoses and glucoronic acid residues. This is then elongated by the action of a heterodimeric complex of

EXT1 and EXT2 enzymes within the Golgi which will add an alternation of N-acetylglucosamine (GlcNAc) and glucoronic acid (GlcA). During the elongation process, some of the GlcNAc is N-deacetylated and N-sulphated by the action of N-deacetylase/N-sulphotransferas (NDST). Subsequently, some GlcA residues can undergo epimerization to Iduronic acid (IdoA), which can then be sulphated by 2-O sulphotransferases. Adjacent exosamine can then be further sulphated on 6-O and less frequently on 3-O (Murphy et al., 2004) (Skidmore et al., 2008). Interestingly, these modifications lead to considerable heterogeneity in syndecan GAG chains which can potentially, and most likely, be regulating their affinity for ligands. Many genetic experiments in invertebrates and the mouse showed that HS is required in development. For example, the Ext1 and 2 proteins, which are the most piviotal enzymes involved in heparan synthesis, were shown to be essential in development (Lin et al., 2000) (Stickens et al., 2005). Deletion of the 2-O-sulphotransferase leads to renal agenesis in the mouse, a condition in which the pup is missing one or both kidneys at birth (Bullock et al., 1998).

1.1.3. Syndecan signalling

Syndecans possess a short (less than 40 amino acids) cytoplasmic domain with no intrinsic enzymatic activity. This domain can be divided into 3 regions: a variable region V flanked by two conserved region C1 and C2 (Fig. 1.4). The C1 region is proximal to the membrane, it is highly conserved across all syndecans and participates in linkage to the cytoskeleton. The C1 region interacts with ezrin–radixin–moesin (ERM) proteins, tubulin, cortactin and Src (Kinnunen et al., 1998). In addition, the MKKK sequence of syndecan-1 seems to be alone required for clustering and endocytosis (Chen and Williams, 2013). The phosphorylation of tyr180 at the end of the C1 region of syndecan-4 has been shown to be a key control point for cell migration in fibroblasts. c-Src seems to be the kinase responsible for syndecan-4 phosphorylation and its activity is probably initiated by ECM-interactions and/or growth factor receptors, although further studies are needed to elucidate this point. Nevertheless, c-Src-mediated phosphorylation of syndecan-4 leads to suppression of the small G protein Arf6 activity and promotes the movement of αVβ3 from the recycling endosomes to the plasma membrane while promoting the opposite route for α5β1. The resultant elevation in αVβ3 engagement promotes stabilization of focal adhesions. On the other hand, when syndecan-4 is not phosphorylated the surface expression of α5β1 destabilizes adhesion complexes and disrupts cell migration (Morgan et al., 2013). The second conserved region C2 is located at the C-terminus of syndecan-4 and comprises a hydrophobic motif (FYA) that interacts with

PDZ-domain-containing proteins. Examples include syntenin, synectin and Ca2+/calmodulin-associated serine/threonine kinase (CASK) (Multhaupt et al., 2009).

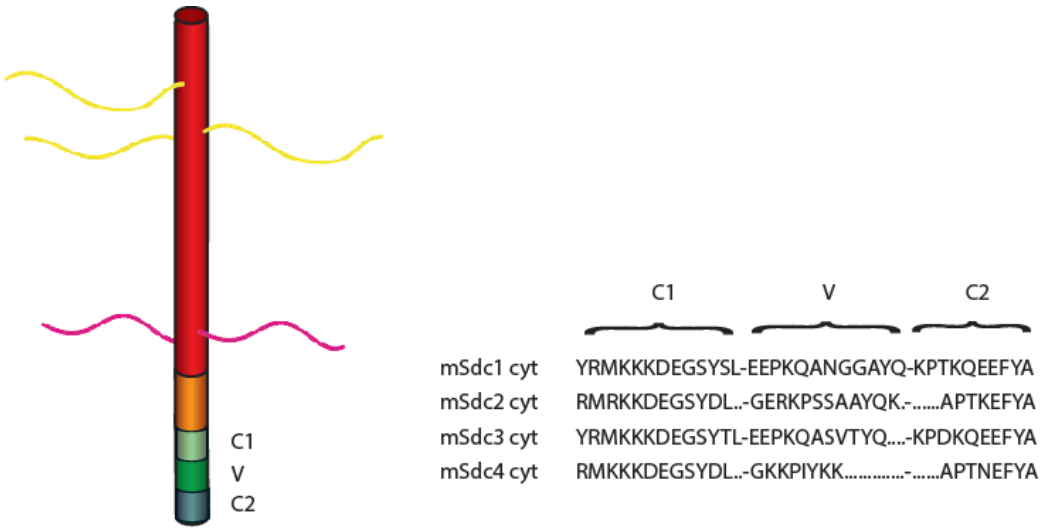

Fig. 1.4 **Syndecan cytoplasmic domain sequence and conservation.** In the highly conserved cytoplasmic domains, a juxtamembrane C1 region is exactly conserved among the syndecan across all species and has been implicated in binding protein ezrin, radixin and moesin (ERM) domains. A C-terminal C2 region consisting of the amino acid sequence is present in all syndecans and binds to post-synaptic density 95, PSD-95; discs large, Dlg; zonula occludens-1, ZO-1 (PDZ) domains in several proteins including calcium/calmodulin-dependent serine protein kinase (CASK), syntenin, synbindin and synectin. The variable (V) region is distinct for each of the four family members, but its syndecan-specific identity is conserved across species. The function of this domain is largely unknown except in the case of syndecan-4.

The interaction of syndecans with syntenin seems to be important for syndecan trafficking and recycling (Zimmermann et al., 2005). Moreover, it has been recently described how a complex composed of syndecan, syntenin and ALIX regulates exosome formation (Baietti et al., 2012). Exosomes are considered signalling particles important in cellular communication and are recently attracting a lot of attention, particularly in the field of tumor–host crosstalk. Interestingly, exosome formation by tumor cells has been shown to be enhanced by heparanase, an enzyme which cleaves HS chains (Ramani et al., 2013; Thompson et al., 2013). Lately, it has also been shown that the Arf6 and its target phospholipase D are implicated in syntenin-based exosome biogenesis (Ghossoub et al., 2014).

Synectin is another binding partner for syndecan-4 PDZ-binding domain. The formation of the synectin-syndecan-4 complex allows the binding of the inhibitor RhoGDI-α (Elfenbein et al., 2009) which sequesters and suppresses the activity of the GTPases RhoG, Rac1 and RhoA

(Burridge and Wennerberg, 2004) leading to low rate of cell motility. However, upon ligand binding, such as fibronectin or growth factors, syndecan-4 oligomerizes promoting the activation of the kinase PKCα through a mechanism which will be described later. PKCα will in turn phosphorylate serine 96 on RhoGI-α which allows the release of RhoG and Rac1, leading to increased cell migration (Elfenbein et al., 2009).

Between the two conserved regions C1 and C2, there is a variable region (V) which is specific to each syndecan but is conserved across species, for example zebrafish, avian and mammalian syndecan-4 V regions are highly homologous (Whiteford et al., 2008). Because these regions are divergent amongst syndecan family members, they probably assert different functions. V region functions, however, have so far only been elucidated for syndecan-4. The syndecan-4 V region can bind and activate PKCα, and this interaction is dependent on phosphatidylinositol 4, 5 bisphosphate (PIP2) (Oh et al., 1997a) (Oh et al., 1997b) (Oh et al., 1998). The conserved serine residue at position 183 (in human syndecan-4) is potentially phosphorylated by PKCδ (Murakami et al., 2002a). When serine 179 (in mouse syndecan-4) is phosphorylated, syndecan-4 cannot oligomerize, does not associate with PIP2 (Koo et al., 2006), cannot bind PDZ protein and in turn PKCα does not get activated (Horowitz and Simons, 1998). PKCα activation seems to be key for syndecan-4's role in cell adhesion and several substrates for PKCα have been proposed, including p190RhoGAP and RhoGDI (Bass et al., 2008) (Dovas and Couchman, 2005). Phosphorylation of G proteins and their regulators, known to be essential in focal adhesion and microfilament bundle assembly (Dovas and Couchman, 2005), would explain the prominent role of syndecan-4 in the formation of these structures (Couchman, 2010). Interestingly, during wound healing, syndecan-4 seems to be responsible for increased fibroblast motility and therefore tissue repair. In fact, syndecan-4 interactions with the extracellular matrix (ECM) molecule fibronectin (abundant during tissue remodelling) induces association with PKCα and RhoG activation which in turn results in caveolin- and dynamin-mediated endocytosis of integrin α5β1 (Bass et al., 2011). The V region of syndecan-4 has also been shown to interact with a protein called syndesmos (Denhez et al., 2002), unfortunately little is known about this protein apart from it interacts with the focal adhesion protein paxillin. α-actinin also binds directly to syndecan-4 V region, and fibroblasts in which syndecan-4 has been knocked out show disordered α-actinin patterns, loss of microfilament bundles and fewer focal adhesions (Okina et al., 2012). It appears that the phosphorylation of a serine residue at position 183 favours interactions with α-actinin instead of that with PKCα (Chaudhuri et al., 2005). However, other studies didn't support this hypothesis (Okina et al., 2012).

1.1.4. Syndecan shedding

Shedding is an important regulatory mechanism of syndecan function, common to many cell surface molecules, that allows the generation of soluble ectodomains (Fig. 1.5). These can have autocrine or paracrine effects and/or compete with their membrane-anchored counterpart for ligand-binding. Not long after their discovery, syndecans were shown to undergo low-rate constitutive shedding in cultured cells (Jalkanen et al., 1987; Saunders et al., 1989) and since then a huge number of studies have emerged describing regulated syndecan shedding *in vitro* and *in vivo* highlighting its biological significance.

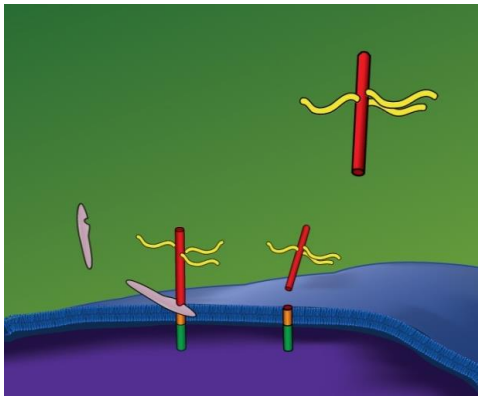

Fig. 1.5 **Syndecan shedding.** Diagram depicting syndecan ectodomain being shed from the cell surface by the action of protease.

1.1.4.1. Syndecan shedding during tissue injury

Little was known concerning regulated shedding of syndecans during biological processes until Subramanian et al. tested agents active during wound healing for their ability to stimulate accelerated shedding of syndecan-1 and -4 from the cell surface of ECs (SVEC4-10). They could demonstrate that both HSPGs are shed upon the addition of Phorbol 12-Myristate 13-Acetate (PMA), Epidermal growth factor (EGF), Heparing-binding EGF-like growth factor (HB-EGF), thrombin and plasmin but not upon addition of Vascular endothelial growth factor (VEGF), Fibroblast growth factor-2 (FGF-2) or Urokinase-type Plasminogen activator (uPA). Since thrombin, besides binding to its cell surface receptor, also has intrinsic proteolytic activity, it was unclear whether shedding occurred from direct cleavage or signalling. Given that the addition of TRAP, a peptide that activates thrombin R but has no proteolytic activity, increased syndecan shedding, it was suggested that both mechanisms were present. Moreover, shed syndecan-1 and -4 were found in the fluids that surround injured tissue. This was the first time a regulated shedding mechanism for syndecans in a biological process was described (Subramanian et al., 1997).

The first indications of possible cleavage sites on the syndecan ectodomains was derived from cell-free system studies. In these settings, plasmin and thrombin cleave syndecan-4 in two sites, Lys114-ARg115 and Lys129-Val130. Surprisingly, no syndecan-1 is shed in these

conditions. This result, in apparent contrast with the data from Subramanian et al. showing that thrombin mediates syndecan-1 shedding from ECs, would suggest that thrombin-triggered shedding requires the thrombin receptor (Schmidt et al., 2005).

An interesting aspect of syndecan shedding is that once syndecans are shed they can be further enzymatically modified: extracellular endosulfatases, for instance, can remove 6-O sulfate groups influencing shed syndecans binding properties (Ai et al., 2003) and heparanases can cleave heparan sulfate chains, releasing biologically active fragments (Ilan et al., 2006). The latter modification has great impact on the regulation of the syndecan-1 and FGF-2 interaction. Soluble S1ED is an inhibitor of FGF activation because of its poorly sulphated HS domains, however, during wound healing heparanase is released in the microenvironment where it cleaves the HS chains from the peptide backbone producing highly mitogenic heparin-like oligosaccharide fragments (Kato et al., 1998).

In idiopathic pulmonary fibrosis (IPF), a disease characterized by progressive fibrosis of the lungs due to an uncontrolled healing response in the lungs, syndecan-1 may represent an important target for the development of a therapy. It was shown that extracellular superoxide dismutase (EC-SOD) binds syndecan-1 and this protects it from oxidative stress-induced cleavage. When EC-SOD expression is altered, like during IPF, syndecan-1 is cleaved and this induces neutrophil chemotaxis, impaired epithelial wound healing and fibrogenesis (Kliment et al., 2009; Kliment and Oury, 2011). In severely injured patients undergoing haemorrhagic shock, syndecan-1 is shed from the endothelial glycocalyx and this causes an increase in vascular permeability and disruption of ECs integrity (Haywood-Watson et al., 2011). These studies indicate that syndecan shedding is a feature of inflammation and that shed syndecan moieties are present in the inflamed tissue.

1.1.4.2. Syndecan shedding during inflammation

The first syndecan-1 sheddase identified was matrylisin (MMP-7). In 2002, a study on acute lung injury gave important insight into the role of shed syndecans in inflammation: they proposed a model in which, in response to lung injury, the chemokine KC gets anchored to syndecan-1 on epithelial cells and, at the same time, matrilysin, released from the wound-edge epithelia, cleaves syndecan-1; the complex composed of S1ED (syndecan-1 ectodomain) and KC is then transported to the apical surface to create a chemotactic gradient to direct inflammatory neutrophils to the site of injury (Li et al., 2002). Another study on syndecans in inflammation showed that IL-8, which is bound to ECs to form a gradient and direct neutrophil

trans-endothelial migration, is constitutively shed from ECs in culture as a complex with HS and syndecan-1. This study showed that the plasminogen activator system is involved in regulating the shedding of the cell-bound tri-molecular complex, thus influencing the formation of the chemoattractant form of IL-8 at the cell surface and therefore neutrophil recruitment (Marshall et al., 2003). Syndecan-1 and -4 shedding from lung epithelial cells is mediated by ADAM17. This enzyme was shown to mediate both constitutive shedding and that triggered by inflammatory stimuli such as PMA, thrombin or IFNγ/TNFα. Interestingly, shedding stimulated by IFNγ/TNFα requires longer treatment times than that by PMA, increased shedding is not mediated by an up-regulation of ADAM17 expression but rather changes in its activity. Moreover, syndecans undergo a sequential cleavage, ADAM17 releases the ectodomain, leaving a CTF (C-terminal cleavage fragment) which is then degraded by γ-secretase (Pruessmeyer et al., 2010). In mice, shed syndecan-1 is often released in body fluids upon inflammatory stimulation. Syndecan-1 null mice show an exaggerated inflammatory response following allergen-exposure suggesting that syndecan-1 shedding is involved in the resolution phase of inflammation (Xu et al., 2005). Syndecan-1 seems to also have a protective role in LPS-induced multi-organ injury and mortality. In particular, syndecan-1 appears to be responsible for the clearance of KC and MIP-2 which regulates neutrophil infiltration. Interestingly, this function is only HS-dependent (Hayashida et al., 2009). Airway smooth muscle cells (ASMCs) augmented production of the chemokine CXCL10 has a key role in asthma pathogenesis. Interestingly, syndecan-4 on ASMC binds to CXCL10 and it is shed in response to inflammatory conditions, suggesting that syndecan-4 shedding could regulate CXCL10 availability during the development of the disease (Brightling et al., 2005; Tan et al., 2012). In a recent study on mouse, shed syndecan-4 was found in the ECM of the heart after LPS injection. The authors could show that shed syndecan-4 plays part in the response to LPS in the heart via promoting immune cell recruitment (cytotoxic T-cells, in particular) and stimulating the synthesis of collagen by cardiac fibroblasts, affecting ECM remodelling (Strand et al., 2015).

1.1.4.3. Syndecan shedding in cancer

Syndecan shedding has been often associated with disease onset and progression. In pancreatic cancer MMP-7 mediates FGF-2-induced syndecan-1 shedding and then complexes with it. This phenomenon could have at least three implications: first, MMP-7 complexed with S1ED could be protected from the action of TIMPs; second, HS chains could enhance MMP-7 proteolytic activity; third, in a manner similar to that of KC in epithelial cells (Li et al., 2002),

S1ED could help MMP-7 transportation to sites far from the tumor into the stroma (Ding et al., 2005). Notably, up-regulation of heparanase and soluble syndecan-1 was detected in tumors with poor prognosis (Yang et al., 2007). In aggressive myeloma, heparanase has been shown to induce syndecan-1 shedding via stimulation of ERK phosphorylation resulting in an up-regulation of MMP-9, which then acts as a syndecan-1 sheddase (Purushothaman et al., 2008). Shed syndecan-1 then binds to VEGF when released by the tumor and navigate into the tumor microenvironment where it promotes EC invasion and angiogenesis. Syndecan-1 can mediate this effect by presenting VEGF to ECs and also interacting with integrins on the cell surface (Purushothaman et al., 2010). Another study using the fibrosarcoma cell line (HT1080) revealed that MT1-MMP shedding of syndecan-1increases cell migration and that the cleavage site resides between Gly245-Leu246 (Endo et al., 2003). Syndecan-3 is shed from rat Schwann cells by the action of an MMP. This occurs also *in vivo* in rat peripheral nerves in an age dependent way (shedding is lower in P10 nerves compared to P4 ones) and the inhibition of MMP activity not only decreases cell surface syndecan-3 but also the soluble form, suggesting that MMPs are also involved in the degradation of syndecan-3 once released in the ECM. Studies with chimeric syndecans also showed that the ectodomains contain the information necessary for their shedding (Asundi et al., 2003). Interestingly, carcinoma cells stimulate the expression of syndecan-1 on fibroblasts, syndecan-1 is then shed and diffuses to cancer cells, here S1ED stimulate cancer cell proliferation probably by forming a complex on the cell surface with FGF2 and FGFR1 (Su et al., 2007). The first study specifically aimed at understanding the intracellular signalling involved in syndecan shedding showed that the syndecan-1 cytoplasmic domain associates with Rab5, preferentially to the inactive GDP-bound form. Interestingly, shedding stimuli such as PMA, induce the switch from GDP-Rab5 to GTP-Rab5 which then dissociates from syndecan-1. Since Rab5 is involved in intracellular trafficking, it was speculated that Rab5 activation could induce the internalization of a cell surface receptor associated with syndecan-1 on the cell surface, if this receptor was protecting a cleavage site on the syndecan-1 ectodomain from the action of sheddases then it may explain why upon Rab5 activation syndecan-1 is shed (Hayashida et al., 2008). MCF-7 Cells (breast carcinoma cell line) engineered to over-express a soluble form of syndecan-1 are less proliferative but more invasive when compared to cells over-expressing an uncleavable mutant form of syndecan-1 (Nikolova et al., 2009). Syndecan-2 has been shown to activate MMP-7 in colon cancer cells (Park et al., 2002), and in a negative feedback MMP-7 cleaves syndecan-2 N-terminally at Leu149 in the extracellular domain (Choi et al., 2012).

Syndecan	Cell type/tissue	Stimuli	Proteases	Ref.
Syn-1, -4	ECs	PMA, EGF, HB-EGF, Thrombin, Plasmin	?	(Subramanian et al., 1997)
Syn-1, -4	ECs	Cellular stress (hyperosmolarity and ceramide)	TIMP-3-sensitive MP	(Fitzgerald et al., 2000)
Syn-1, -4	Lung epithelial cells	PMA, Thrombin, IFNγ/TNFα	ADAM17	(Pruessmeyer et al., 2010)
Syn-1	Myeloma cells	PMA	Non-matrix MP	(Holen et al., 2001)
Syn-1	Epithelial cells	Acute lung injury	MMP-7	(Li et al., 2002)
Syn-1	Pancreatic tumor cells	FGF-2	MMP-7	(Ding et al., 2005)
Syn-1	Myeloma cells	Heparanase	MMP-9	(Purushothaman et al., 2008)
Syn-1	Fibrosarcoma		MT1-MMP	(Endo et al., 2003)
Syn-1	Lungs	Oxidative-stress	?	(Kliment et al., 2009; Kliment and Oury, 2011)
Syn-2	Colon cancer cells		MMP-7	(Choi et al., 2012)
Syn-3	Schwann cells		Matrix MP	(Asundi et al., 2003)
Syn-4	Airway smooth muscle cells	IL-1β, TNFβ	?	(Tan et al., 2012)

Table 1 S**yndecan shedding and associated sheddases.**

1.1.5. Syndecans as extracellular matrix receptors

Syndecans can interact with a large repertoire of ECM components; in most cases the HS chains are required (Fig. 1.6) but in some instances these interactions are mediated by syndecan ectodomains (reviewed in 1.1.7). The ECM is an intricate network for macromolecules (mostly proteins and polysaccharides) which is produced and secreted by cells and serve not only as a scaffold but has also an active role in regulating the behaviour of the cells that contact it. Each tissue contains specific amounts of different types of matrix macromolecules and the way in which they are organized is well-designed to the requirements of that particular tissue. Fibronectin for example is found abundantly in the serum and it is, together with fibrin, the main constituent of the matrix which forms during clotting. It has been shown that fibroblasts are able to attach and spread on fibronectin fragments containing the RGD domain, a binding site for integrin α5β1, but only the addition of the fragment containing the heparin-binding site allows the proper formation of focal adhesion via an integrative signal of syndecan-4 (Bass et al., 2008; Gopal et al., 2010; Okina et al., 2009; Xian et al., 2010). Similarly, co-operation between integrin α5β1 and HS chains, possibly from syndecan 4, is necessary for fibroblast focal adhesion formation (Bax et al., 2007). This synergistic co-operation of syndecans and integrins in mediating cell adhesion is a recurrent mechanism which takes place on various ECM substrates. In the basement membrane, for example, syndecan-1 works closely with integrin α3β1 to promote keratinocyte adhesion on the precursor of Laminin-322. This co-operation allows the formation of fascin-containing protrusions, which is dependent on the GTPases Rac and Cdc42 (Bachy et al., 2008). Finally, collagens, the most abundant ECM proteins with 29 different types in several different classes, can interact with syndecans. Many collagen types, in fact, possess a heparin- and HS-binding domain. Interestingly, it has been shown that co-binding of syndecan-1 and integrin α2β1 to collagen promotes the transcription of the matrix-metalloproteinase-1 with implications for tissue remodelling (Vuoriluoto et al., 2008).

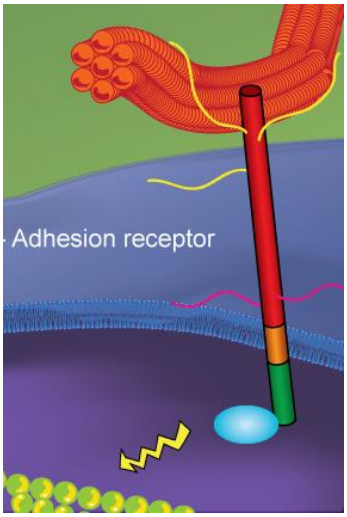

Fig. 1.6 **Syndecans as adhesion receptors.** Syndecan can function as adhesion receptor by linking the ECM to the cell cytoskeleton. (Figure modified from De Rossi et al. 2013).

1.1.6. Syndecans as co-receptors

In addition to ECM molecules, syndecans can also interact with a large repertoire of pericellular molecules such as growth factors, cytokines, chemokines and pathogens (Fig. 1.7).

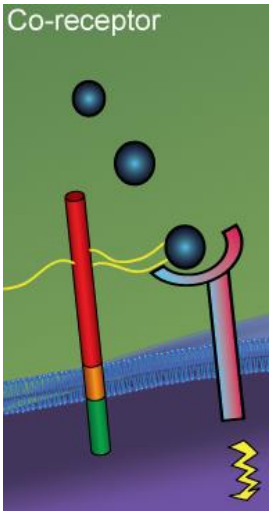

Fig. 1.7 **Syndecans as co-receptors.** Syndecan can act as co-receptor by presenting ligands to their receptors. (Figure modified from De Rossi et al. 2013).

Many growth factors possess a heparin-binding domain that can interact with syndecan HS chains. FGF2 has been thoroughly investigated in this context as its binding to FGF receptor 1 is facilitated by syndecan-1, -2 and -4 and the receptor activation increased. The binding of FGF2 to syndecan results in high concentration of FGF2 on the cell surface of mouse mammary epithelial cells (NMumG), which in turns facilitates the activation of FGFR (Reiland and Rapraeger, 1993) (Steinfeld et al., 1996). A similar function has been suggested for syndecan-2 in the context of VEGF-A-mediated signalling in zebrafish. Here, syndecan-2 is key for sprouting angiogenesis during development and the authors of the study provide good indication that syndecan-2 binds to VEGF-A165 (the isoform of VEGF-A containing the heparin-binding domain) and presents it to its receptor VEGFR2 (Chen et al., 2004b) (Kaji et al., 2006). Syndecan-1, instead, has been reported to mediate HGF- and EGF-mediated signals in multiple myeloma, and members of the hepatocyte growth factor HGF and epidermal growth factor EGF family have been shown to associate with syndecan-1 for induction of cell survival and proliferation. The association of syndecan-1 with HGF or EGF has been shown to promote clustering and activation of their respective receptors (Mahtouk et al., 2006) (Andersen et al., 2005) (Mahtouk et al., 2004) (Derksen et al., 2002) (Seidel et al., 2000a). Results from a recent study also suggest that syndecan-2 and -4 can bind HGF and FGF2, in this case mediating Sema3A expression in early-differentiated myoblasts (Do et al., 2015).

Syndecan-1, -2, -3 interact with Interleukin-8 (IL-8) on the surface of ECs and the implication for the immune response is remarkable, as this interaction not only creates a gradient of IL-8 that promotes neutrophil accumulation to the site of inflammation, but also protects the cytokine from proteolytic degradation (Halden et al., 2004; Marshall et al., 2003) (Goger et al., 2002; Patterson et al., 2005). Syndecan-2 has also been shown to facilitate the interaction of granulocyte-macrophage colony-stimulating factor (GM-CSF) with its receptor on the surface of osteoblasts (Modrowski et al., 2000).

Syndecan-1 interacts via its HS chains with the chemokines CCL7, CCL11 and CCL17 and this results in an inhibition of chemokine-mediated T cell migration and suppression of allergen-induced accumulation of Th2 cells in the lung (Xu et al., 2005). Moreover, disturbing syndecan-4 signalling (using blocking antibody or syndecan-4 knock-out mice) resulted in a diminished CCR7 expression on dendritic cells and in a reduced directional DC migration to the draining lymph nodes, leading to a reduced asthma phenotype (Polte et al., 2015). Syndecan-1, together with syndecan-4, has also been shown to associate with RANTES on macrophages, facilitating its interaction with CCR5 (Slimani et al., 2003a, b). Syndecan-4 is also able to interact with stromal-cell derived factor 1 (SDF-1) and the receptor CXCR4 on the cell surface of the hepatocarcinoma cells Huh7, leading to a mitogenic effect (Sutton et al., 2007).

Interestingly, syndecans can also interact with pathogens. All 4 syndecans, for example, have been shown to been able to capture HIV-1 via their HS chains (Bobardt et al., 2003). In addition, syndecan-2 also binds HIV-2 and simian immunodeficiency virus. Many other viruses exploit syndecans as attachment sites to facilitate their entry in the host cell, the list includes: herpes simplex virus, papilloma virus, dengue virus, human T-cell leukemia virus and hepatitis C virus (Bernfield et al., 1999a) (Hilgard and Stockert, 2000) (Pinon et al., 2003) (Shafti-Keramat et al., 2003). Syndecans can also bind and therefore participate in and influence the pathogenesis of several bacteria including *Chlamidia trachomatis*, *Staphylococcus aureus*, *Pseudomonas aeruginosa*, *Neisseria gonorrhoeae* and *Neisseria meningitides* (Freissler et al., 2000) (Chen et al., 2008).

1.1.7. Syndecan ectodomains

As discussed above, the two main functions of syndecans described to date are as adhesion receptors and co-receptors. Both of these roles are dependent on the ability of syndecans to interact with a large repertoire of molecules present in the extracellular space. These interactions are mainly mediated by the glycosaminoglycan chains of syndecans; however, the studies summarized in the following paragraphs will prove that the proteic component of syndecan ectodomain also possesses biological properties. These studies cover a variety of biological processes including cell adhesion, migration and morphology in many different cell types.

1.1.7.1. Syndecan-1

Syndecan-1 was the first member of the syndecan family to be described in 1989. Early studies revealed a strong correlation between syndecan-1 and tumor cell proliferative, adhesive and invasive properties (Inki et al., 1994a; Inki et al., 1994b; Inki et al., 1994c). Syndecan-1 presence on a mouse mammary tumor (S115), for example, inhibits its proliferative potential, a function for which the syndecan-1 ectodomain (S1ED) is required (Mali et al., 1994). Moreover, when ARH-77, a B-lymphoid cell line that expresses low amounts of HS, is transfected with syndecan-1 cell migration through the collagen layer is repressed.

S1ED is sufficient to inhibit invasion and this effect is not solely due to the ability of syndecan-1 to promote adhesion by engaging the substratum (Liu et al., 1998). Further studies characterized an "invasion regulatory domain" mapped to an AVAAV sequence (aa 222-226) on syndecan-1 extracellular core protein (Langford et al., 2005).

Interestingly, transfection of syndecan-1 in Raji cells, a human lymphoblastoid cell line that does not express syndecan-1 and grows in suspension, is sufficient to stimulate attachment and spreading on both thrombospondin and fibronectin. More interestingly, attachment and spreading on Abs against S1ED occurs after heparinase addition (Lebakken and Rapraeger, 1996).

In MDA-MB-231 (human mammary carcinoma cells) syndecan-1 is required for cell spreading on Vitronectin (VN) via activation of αVß3. Moreover, since the addition of soluble S1ED or transfection with a mutant form of syndecan-1 lacking a portion of the ectodomain (mS1Δ88-252) inhibits cell spreading on VN, this implies S1ED interacts with a partner on the cell surface to activate αVß3 integrin (Beauvais et al., 2004). Further studies revealed that the minimal sequence able to block cell spreading on VN corresponds to aa 82 to 130 of the syndecan-1 extra-cellular core protein; this peptide is called Synstatin or SSTN, and it is able to inhibit co-precipitation of αVß3 with syndecan-1. More interestingly, it can also inhibit adhesion and spreading of B82L fibroblasts on VN, which is mediated only by αVß5. SSTN inhibits association of syndecan-1 with both integrins and it is also able to inhibit their activation in ECs, impeding their attachment and spreading. It is therefore unsurprising that SSTN is able to inhibit angiogenesis *in vivo* in the aortic ring outgrowth assay, in the corneal angiogenesis model and, also, in an *in vivo* orthotopic tumor model (MDA-MB-231 injected subcutaneously into a BALB/c nude mouse). Interestingly, syndecan-1 Knock Out mice are viable with no angiogenic defect, meaning that they have compensated for the loss of syndecan-1 by developing an alternative pathway for integrin activation (Beauvais et al., 2009). Integrin is activated when a conformational change increases the affinity of its extra-

cellular head for its ligand; this is usually triggered by an energy-dependent inside-out signal (O'Toole et al., 1994). Treatment of MDA-MB-231 with metabolic inhibitors showed that syndecan-1-mediated integrin activation is energy-dependent and, by the use of different kinase inhibitors, it became clear that there is an involvement of insulin-like growth factor-1 receptor (IGF1R) in this process. In the model proposed by Beauvais and Rapraeger, syndecan-1, once clustered by engaging VN, interacts with αVß3 and ß5 integrin through its ectodomain, this complex is then able to engage with IGF1R. The formation of the syndecan-1/integrin/IGF1R is an indispensable step for later events, in fact, it is essential for IGF1R auto-phosphorylation on Y1131, subsequent activation of Talin (cytoskeletal protein key for inside-out integrin activation) which then binds integrin ß subunit, triggers a conformational shift and activates it (Beauvais and Rapraeger, 2010).

The correlation between syndecan-1 loss and poor prognosis in many human cancers could be well explained by the ability of this HSPG to promote adhesion and inhibit invasion as described above (Beauvais and Rapraeger, 2004; Sanderson, 2001). Nonetheless, in some tumors with poor prognosis the expression of syndecan-1 is up-regulated (Barbareschi et al., 2003; Beauvais and Rapraeger, 2004; Burbach et al., 2003; Matsuda et al., 2001). Burbach et al, transfected syndecan-1 in three different human breast carcinoma cell lines to mimic syndecan-1 over expression, a characteristic often found in breast carcinomas *in vivo*. Upon transfection, cells which usually grow as adherent cohesive epithelial islands (T47D), spread poorly and assumed a rounded morphology in 2D and were more invasive in 3D culture. Interestingly, this effect was maintained regardless of the absence of GAG chains or transmembrane and cytoplasmic domains, and abolished when syndecan-1 was expressed as a mutant lacking aa 88-252 from the ectodomain. Moreover, since syndecan-1-dependent morphology change could be blocked by Genistatin (a protein tyrosin kinase inhibitor), this suggests the involvement of a signal transduction. They could show that carcinoma cells didn't spread on integrin ligand and attachment was also blocked by Abs against the ß1 subunit, suggesting that syndecan-1 disrupts ß1-mediated signalling or attachment. Syndecan-1 expression level alters adhesion signalling in epithelial cells (Burbach et al., 2004).

Syndecan-1's role in cell adhesion and migration is not limited to tumor cells, in fibroblasts (B82L), for example, spreading on a native matrix ligand is dependent on αVß5 integrin complexing with S1ED. This mechanism is similar to that proposed for the regulation of αVß3 in epithelial tumor cells (Beauvais et al., 2004) although they differ in some features: in B82L syndecan-1 is probably constitutively associated with ß5 integrin through its extra-cellular core protein and only if the integrin is in a complex with S1ED then it can signal upon binding to VN or FN; in epithelial cells, instead, the engagement of syndecan-1 with a substratum

(through its HS chains) is necessary to bring S1ED and αVß3 together in a complex and signal and in this case αVß3, unlike αVß5 in fibroblasts, does not need a ligand (McQuade et al., 2006).

One of the most recent works on syndecan-1 added further evidence to support the presence of a close interaction between syndecan-1 extra-cellular core protein and integrins, in particular, they showed, in a human bronchial epithelial cell line (B2b), that S1ED promotes cell adhesion by activating the ß1 subunit and therefore regulating the affinity of α2ß1 integrin (Altemeier et al., 2012).

1.1.7.2. Syndecan-2

While in normal epithelium syndecan-2 is usually expressed at low levels, during epithelial cancer progression its expression increases; in colon carcinoma, for instance, syndecan-2 is highly expressed on cancer cells (both highly and weakly metastatic) when compared to normal colon cell lines. S2ED has specific roles in adhesion and tumorigenicity of these epithelial cancer cells. Not only can recombinant S2ED (HS chains free) inhibit tumor cell attachment to the ECM, but it can also promote cell cycle arrest through an up-regulation of p53, p21 and p27 and down-regulation of cyclin E and D2. Moreover, the addition of S2ED in the medium of colon cancer cells inhibits the EGF-mediated mitogen-activated protein kinase activation which is critical for the growth of many tumors (Park et al., 2002).

Syndecan-2 also has key roles in the development of fibrosis. TGF-ß is a growth factor with multiple roles, among which is the ability to promote fibrosis by up-regulating matrix proteins and down-regulating metalloproteinases. TGF-ß RIII binds TGF-ß and transfers it to TGF-ß RII. Intriguingly, TGF-ß RII is a cell surface proteoglycan with very similar characteristics to syndecan-2. Since syndecan-2 controls left-right axis asymmetry in *X. laevis* through TGF-ß, a role for syndecan-2 in TGF-ß-induced fibrosis was suggested. Syndecan-2 was indeed shown to regulate TGF-ß mediated matrix deposition via its cytoplasmic domain which is fundamental for its interaction with TGF-ß R III. More interestingly, syndecan-2 in RPFs (renal periphery fibroblasts) was shown to interact with TGF-ß via its ectodomain (and partially through its HS chains) independently of the presence of the cytoplasmic domain (Chen et al., 2004c). In brain microvascular ECs, S2ED is also able to induce an increase in cell migration and tube formation on both fibronectin and growth factor-reduced Matrigel (Fears et al., 2006).

A broad-spectrum adhesion study revealed a tendency for mesenchymal cells to attach to GST-mS2ED, while the epithelial ones fail to do so. When compared to those seeded on FN, REF (rat embryo fibroblasts) seeded on GST-mS2ED spread more slowly, formed less focal adhesions (FA) (and those formed were more peripheral) and showed reduced phosophorylation of FA components such as FAK and paxilin. Interestingly, REF attached to FN spread but didn't form FA when treated with heparinase, whereas the same treatment on cells attached to S2ED has no effect, indicating that HS chains are important when cells are on native matrix ligands. Attachment could be avoided by the addition of ß1 blocking antibody (Ab), but since ß1 is expressed also by cells that didn't adhere, this suggested the presence of one or more intermediate cell surface molecules able to interact with S2ED and communicate the adhesion signal to ß1 integrin (Whiteford et al., 2007). A parallel study on S4ED revealed that the phosphatase cell surface receptor CD148 is key to ß1-mediated adhesion to S4ED; a study with siRNA confirmed that this is also true for S2ED. Indeed, the addition of the soluble extracellular domain of CD148 (comprising the 8 N-terminal type III FN repeats) blocks cell attachment on S2ED but not on FN and a solid-phase binding assay could show that the extracellular part of CD148 interacts with the C-terminal 18 aa of S2ED. The same study showed that the adhesion regulatory domain comprises the last 18 aa at the C-terminal of S2ED (P124 -> F141), of particular importance seems to be the sequence DNLF. Solid-phase binding assays, however, demonstrated no direct interaction between ß1 integrin and CD148 and, moreover, cells weren't able to adhere to CD148 extracellular domain when provided as a substrate, suggesting an involvement of an intra-cellular signalling pathway that functionally connects CD148 to ß1 integrin. Analysis of the possible intracellular substrates for CD148 revealed that ß1-mediated adhesion requires activated Src and PI3k-C2ß and there is evidence for the involvement of a de-phosphorylation step of p85 (subunit of PI3K) (Whiteford et al., 2011).

1.1.7.3. Syndecan-3

Whether the syndecan-3 ectodomain has biological properties remains unclear. Adhesion assays with human dermal fibroblasts, Swiss 3T3 and NIH 3T3 on immobilized GST fused to the syndecan-3 ectodomain suggested that this protein could not support the cell attachment and spreading responses seen with the syndecan-1, -2, and -4 ectodomains (McFall and Rapraeger, 1998). However, the syndecan-3 ectodomain is unique as it possesses a mucin rich domain which may be extensively substituted with O-linked sugars and confer novel functionality (Carey, 1996). Experiments to date have utilized fusion proteins expressed in

bacteria which would not be post-translationally modified in the same way as if they were expressed in eukaryotic cells.

1.1.7.4. Syndecan-4

RGD-dependent integrins (e.g. α5ß1) interact with the RGD sequence within the cell-binding domain (CBD) of fibronectin, promoting cell attachment and spreading (Burridge et al., 1992). Although the CBD fragment alone triggers fibroblast attachment, it is not sufficient, unlike intact fibronectin, to induce the formation of focal adhesions (FAs) (Woods et al., 1986). In both fibronectin (Woods et al., 1986) and laminin (Couchman et al., 1983) induction of FA formation requires the heparin binding domain (HBD) present in both molecules. This made syndecans plausible candidates for providing the second signal to generate FAs. Later it was found that Syndecan-4 is the only syndecan co-localizing with FAs (Baciu and Goetinck, 1995; Woods and Couchman, 1994). In 1999, an elegant work demonstrated that it is indeed syndecan-4 which provides the second signal for FA assembly in fibroblasts on fibronectin. Using $FN^{-/-}$ fibroblasts, the studies showed that, once fibroblasts are spread on the CBD, they can subsequently form FAs either when the HBD is provided (as expected) but also when a bivalent anti-body against S4ED is added to the medium (Saoncella et al., 1999). Syndecan-4 is able to oligomerize on the cell surface and the clustering of S4 V region is necessary for its interaction with PKC-α (Oh et al., 1997a), therefore when HS chains are present, they can interact with HBDs, control S4 clustering on the cell surface allowing oligomerization of the V region and activation of PKC and finally promotion FA formation. Surprisingly, however, unglycanated syndecan-4 over-expression leads to the same effect (Echtermeyer et al., 1999), probably because once clustering reaches a critical level, oligomerization might be spontaneous and independent of ligand binding (Couchman and Woods, 1999) (Fig. 1.8).

Interestingly, as evidences were accumulating delineating a role for the HS chains and the cytoplasmic domain of syndecan-4 in adhesion, McFall and Rapraeger were testing the ectodomain of syndecan-4 in a series of adhesion assays. Between 1997 and 1998, using a bacterially-derived (GAG-free) mS4ED, they were able to show that, in the presence of divalent cations, the ectodomain is able to bind a cell surface receptor through a domain mapped to aa 56-109, which is specific to S4 and the effect was conserved amongst species (mouse and chicken) and retained when syndecan-4 is physiologically shed. For the first time, it was speculated that S4ED could act *in trans*, as a matrix-embedded or soluble adhesive ligand for cells (McFall and Rapraeger, 1997, 1998).

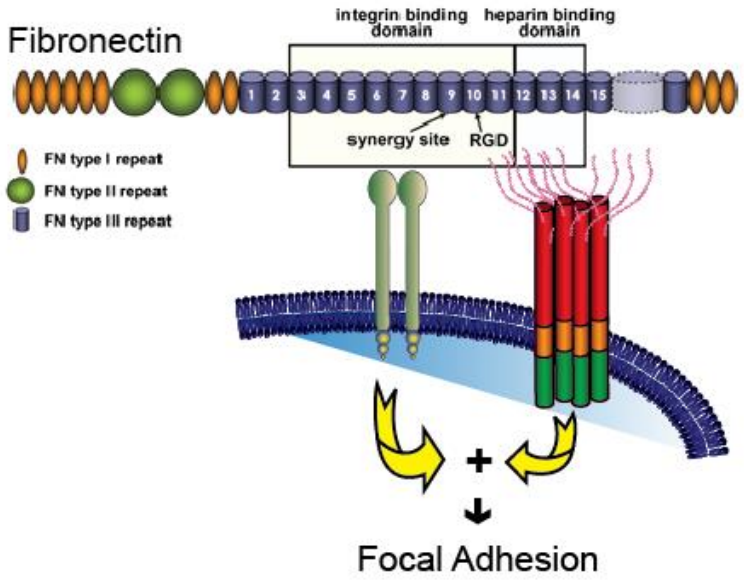

Fig. 1.8 **Syndecan-4 is required for the formation of focal adhesions in fibroblasts on fibronectin.** Fibronectin contains domains that can specifically engage α5β1 integrin and heparin. Focal adhesion formation in fibroblasts requires both α5β1 integrin to engage the integrin binding domain and syndecan-4 HS chains to engage the heparin binding domain.

A decade later, Whiteford et al., further characterized S4ED adhesive properties and found that an NXIP motif, contained within the previously described cell-binding domain, is fundamental for attachment. Testing of different cell lines showed that only mesenchymal, Jurkat T-lymphocytes and ECs were able to attach to mS4ED, and not epithelial or other lymphoblastic lines. Interestingly, Jurkat cells were able to bind only after PMA treatment (PMA is necessary for Jurkat integrin activation, (Faull et al., 1994)) and addition of EDTA stopped adhesion of all cell lines suggesting a role for integrins which was later confirmed by showing that the use of Abs against ß1 integrin stopped mS4ED-dependent cell attachment (Whiteford and Couchman, 2006). Additional studies showed that adhesion of rat embryo fibroblasts (REF) to GST-mS4ED induced a polygonal morphology, slow forming peripheral focal adhesions and overall a slower spreading process. Also, FAs induced by S4ED contain ß1 integrin subunits both in REFs and Jurkat cells. In the case of Jurkat cells, adhesion is mediated by α4ß1; interestingly, REF, which lacks the α4 subunit, still attach to GST-mS4ED revealing that the α subunit which mediates S4ED adhesive properties might be cell-specific (Whiteford et al., 2007).

1.2. Angiogenesis

Angiogenesis is the process that allows the formation of new blood vessels from pre-existing vasculature. This occurs throughout life in both health and disease. A well-organized and functional vascular system allows the diffusion of nutrients, metabolites and oxygen to metabolically active cells, which is why every cell in our body is no more than a few hundred micrometres away from a blood capillary. Angiogenesis is a dynamic process that allows growth and regression of capillaries in healthy tissues according to functional demands. Physical exercise, for example, stimulates angiogenesis in skeletal muscle and heart and an increase in the adipose tissue during weight gain demands an increase in capillarity too. The correlation between metabolic demand and angiogenesis was already hypothesized in the late 18th century when the Scottish surgeon John Hunter wrote: *"In short, whenever Nature has considerable operations going on, and those are rapid, then we find the vascular system in a proportionable degree enlarged."* The study of angiogenesis, however, emerged as a new attractive field only 200 years later when Judah Folkman published in 1971 his results showing that tumor growth is angiogenesis-dependent (Folkman, 1971).

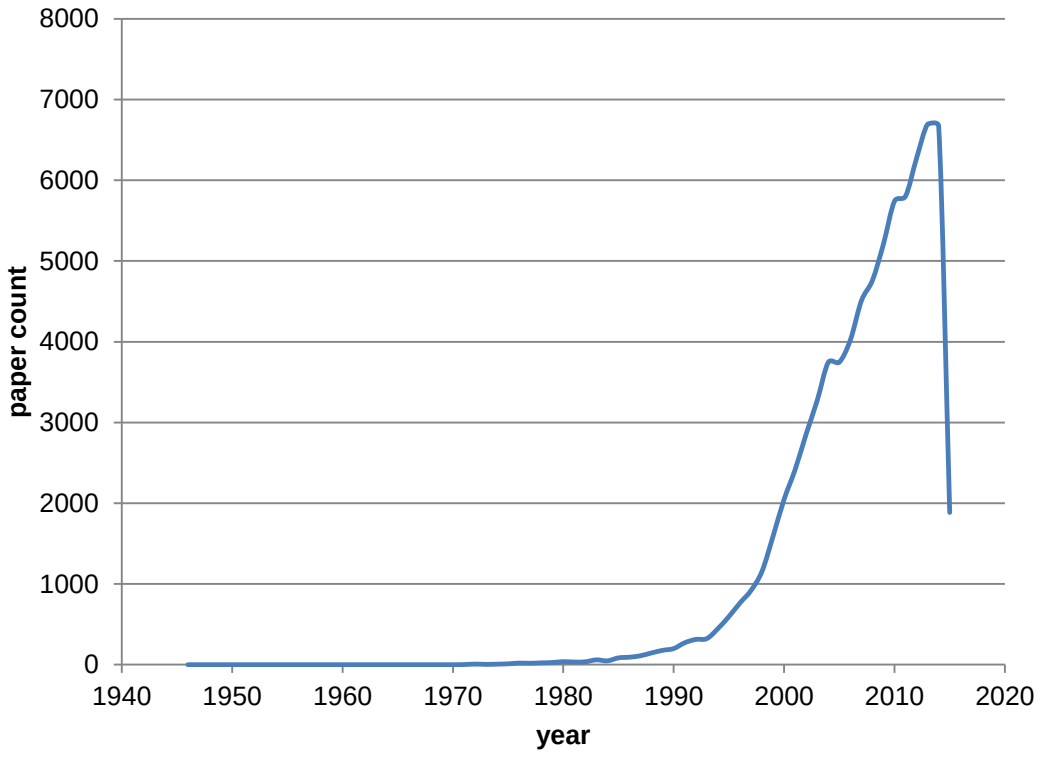

Fig. 1.9 **Papers on angiogenesis published over the years.** Data analysis was performed on PubMed http://www.ncbi.nlm.nih.gov/pubmed/.

1.2.1. The angiogenic process

1.2.1.1. Origin of blood vessels

Angiogenesis is the process of formation and remodelling of new blood vessels from pre-existing ones. The primary vascular network which develops at embryonic stage is in fact the result of a different process called Vasculogenesis. Vasculogenesis gives rise to the heart and the first primitive vascular plexus inside the embryo and in its surrounding membranes, as the yolk sac circulation (Risau, 1997).

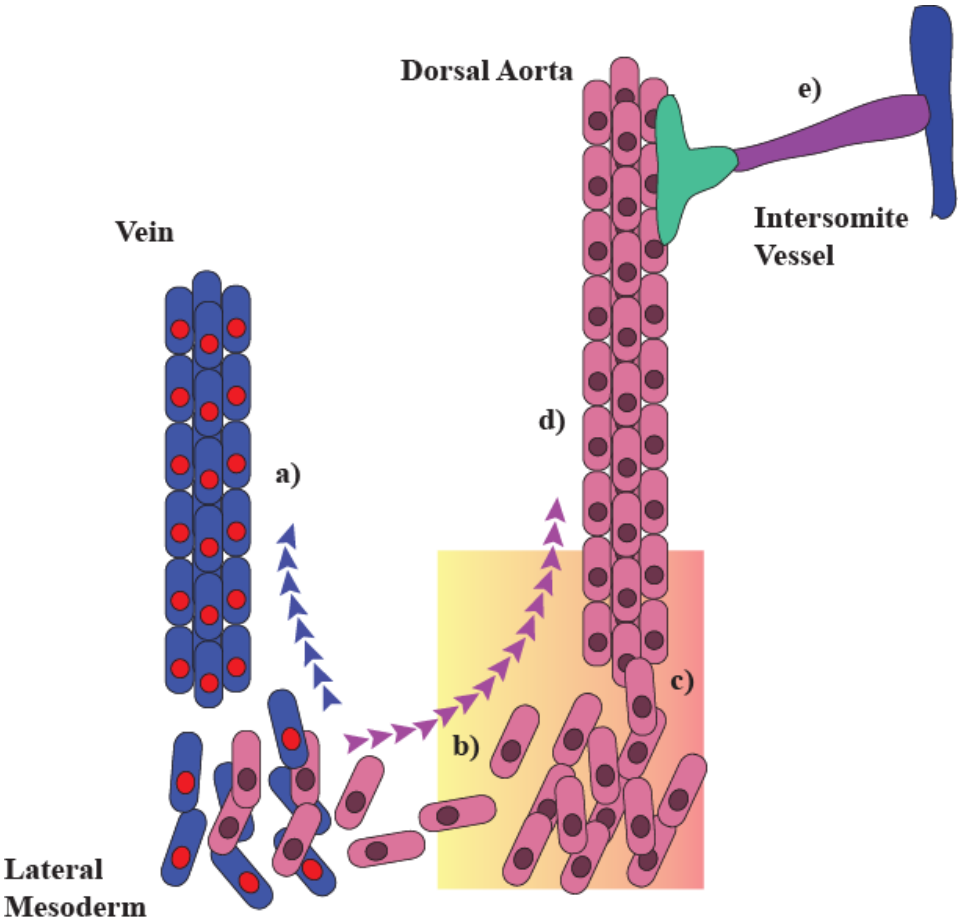

Fig. 1.10 **Vasculogenesis.** The cardinal veins assemble from precursor cells (blue) that remain in a lateral position (a). Artery precursor cells (pink) migrate toward a vascular endothelial growth factor A (VEGF-A) gradient secreted from cells in the midline (b). The migrating arterial angioblasts align into cords forming a plexus (c). Arterial angioblasts merge forming the dorsal aorta (d). Intersomite vessels are assembled from three types of ECs with different morphologies indicated as green, purple, and blue.

During vasculogenesis mesodermal derived hemangioblasts differentiate into hematopoietic stem cells and angioblasts; the latter will eventually differentiate into ECs but do not yet express EC markers at this stage. Angioblasts which are derived from the lateral mesoderm are committed to become arteries or veins. The cardinal veins assemble from precursor cells that endure in a lateral position. Artery precursor cells migrate following a VEGF gradient which is created by cells in the midline. The migrating arterial angioblasts align into cords forming a plexus. Arterial angioblasts merge forming the dorsal aorta. Intersomite vessels are made up of three types of ECs with different morphologies indicated as blue, purple, and green. (Hogan and Kolodziej, 2002). Angiogenesis is responsible for the remodelling and expansion of this network.

1.2.1.2. Types of angiogenesis

There are two types of angiogenesis which happen both in utero and in adults and are thought to occur in virtually all tissues and organs; these are called sprouting and intussusceptive angiogenesis. Sprouting angiogenesis is certainly better understood having been discovered around 200 years ago, while intussusceptive angiogenesis has only been recently described (Caduff et al., 1986) and therefore is less well characterized. The common feature is that both processes lead to formation of new blood vessels. However, while sprouting angiogenesis forms entirely new vessels, intussusceptive angiogenesis increases capillarity by splitting vessels which already exist.

Intussusceptive angiogenesis is also called splitting angiogenesis because the vessel wall extends into the lumen causing a single vessel to split in two. Amongst the two, intussusceptive angiogenesis is generally considered the fast form of angiogenesis as it only requires reorganization of existing ECs rather than their proliferation and migration. It is therefore unsurprising that it plays a prominent role in embryonic development where growth is fast and resources are restricted (Kurz et al., 2003) (Djonov et al., 2003) (Djonov et al., 2002). Evidence for the occurrence of intussusceptive angiogenesis is based upon the presence of trans-capillary tissue pillars.

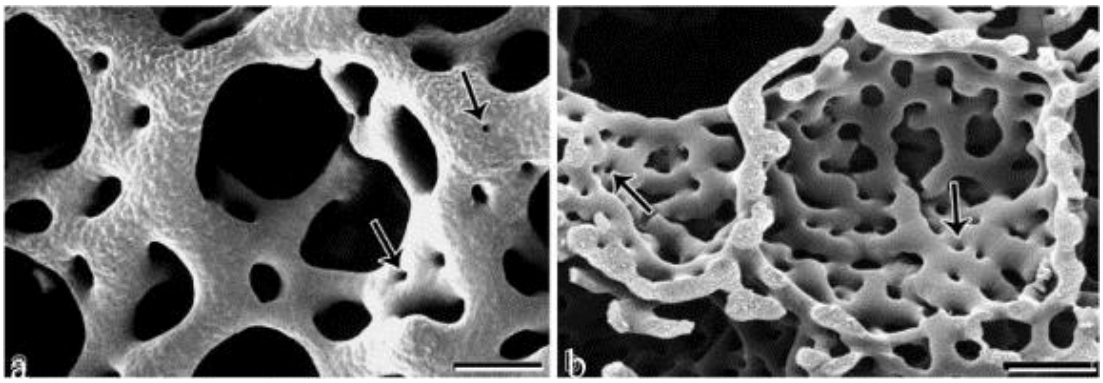

Fig. 1.11 **Trans-capillary tissue pillars in Mercox casts.** (a) Fetal chicken lung microvasculature. (b) Rat lung microvasculature at postnatal day 44. The small holes indicated by arrows have diameters of about 2 µM. The holes correspond to tissue pillars that extend across the capillary lumina. Scale bars: (a) 12 and (b) 20 µM. From (Djonov et al., 2002).

The regulation of intussusceptive angiogenesis is poorly understood compared with sprouting angiogenesis. This is partly due to its recent discovery (Caduff et al., 1986) but also to the fact that proving its presence involves determining the frequency of tissue pillars from scanning electron micrographs of vascular casts, which is challenging. However, since its discovery in postnatal lungs of rats and humans (Burri and Tarek, 1990; Caduff et al., 1986), intussusceptive angiogenesis has been revealed in other tissues, especially in capillary networks that are adjacent to an epithelial surface, e.g., choroid of the eye, vascular baskets around glands, intestinal mucosa, kidney, ovary, and uterus (Burri et al., 2004) (Patan et al., 1992). In addition to forming new capillary structures, intussusceptive growth plays a major role in the formation of artery and vein bifurcations as well as pruning of larger microvessels. Interestingly, mechanical stresses related to increases in blood flow can initiate intussusceptive growth in some high flow regions of the circulation (Kurz et al., 2003) (Djonov et al., 2002).

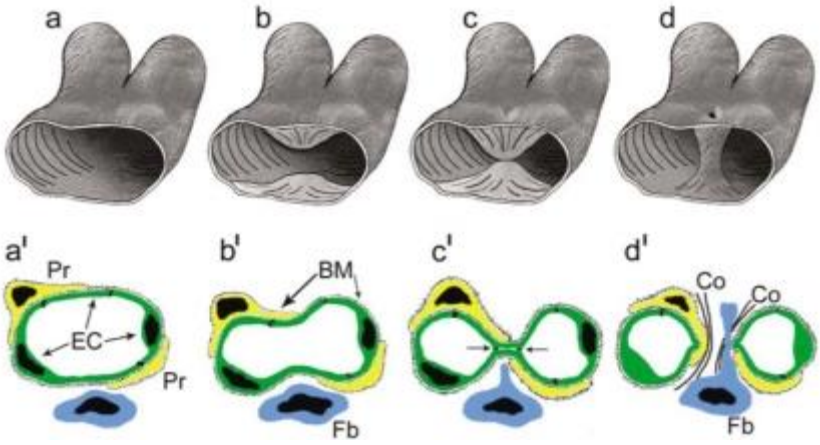

Fig. 1.12 **Intussusceptive angiogenesis in three dimensions (a–d) and two dimensions (a'–d')**. (a,b,a',b') The process begins with protrusion of opposing ECs into the capillary lumen. (c,c') An interendothelial contact is established and endothelial junctions are reorganized. (d,d') The endothelial (EC) bilayer and basement membranes (BM) are perforated centrally allowing growth factors to enter. Fibroblasts (Fb) and pericytes (Pr) migrate into the site of perforation where they produce collagen fibrils (Co) and other components of ECM forming a tissue pillar. From (Djonov et al., 2002).

Angiogenesis may also take place in another way. Sprouting angiogenesis is commenced in poorly perfused tissues when oxygen sensing mechanisms perceive a level of hypoxia that demands the formation of new blood vessels to satisfy the metabolic requirements of parenchymal cells. The basic steps of sprouting angiogenesis include: tip cell selection, tip cell navigation, stalk elongation, tip cell fusion and pericyte stabilization.

1.2.1.3. Tip cell selection

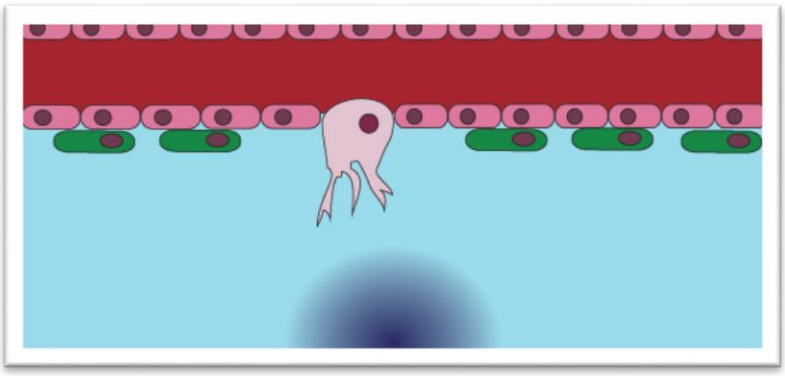

Fig. 1.13 **Sprouting angiogenesis: Tip cell selection.** ECs exposed to the highest VEGF-A concentration (blue gradient) become tip cells (central, light pink cell).

In conditions of decreased oxygen tension, the cytoplasmic enzyme prolyl hydroxylase (PDH) becomes unable to hydroxylate Hypoxia Inducible Factor 1α (HiF1α), which is then not degraded and instead accumulates in the cell, forming heterodimers with HIF1β. HIFα and β are basic Helix-Loop-Helix (bHLH) transcription factors and HIFα/β heterodimers initiate the transcription of genes with a Hypoxia Responsive Element (HRE) in their promoter. Hypoxia responsive genes change the cellular behaviour leading to altered metabolism, erythropoiesis and, importantly, the induction of angiogenesis. One such gene is VEGF-A. When VEGF-A is released in the microenvironment some ECs within the vessel wall will sense high VEGF-A concentration and will be selected for sprouting. These cells are called tip cells, they possess a migratory phenotype and they will guide the growth of the new vessel. Flanking the tip cell are the stalk cells whose phenotype favours proliferation and they will support sprout elongation. The specification of this two different types of ECs is regulated by the Notch pathway (Eilken and Adams, 2010; Phng and Gerhardt, 2009), in particular low Notch signalling activity is present on tip cells while it is upregulated on stalk cells, conversely tip cells express high level of the Notch ligand DDL4. The mechanism by which Notch-DLL4 directs EC behaviour seems to be linked to VEGF-A signalling. DLL4 expression by tip cells is in fact induced by their sensing of high concentrations of VEGF-A, while the activation of stalk cell-Notch by tip cell-DLL4 suppress the expression of VEGF-A receptor, VEGFR2, in the stalk cells (Sainson and Harris, 2008; Suchting et al., 2007). It is therefore lateral inhibition that select tip and stalk cells. Although there are several Notch receptors expressed on ECs, Notch1 is the main factor responsible for inhibiting tip cell behaviour in stalk cells (Moya et al., 2012). JAGGED1, another Notch ligand, is primarily expressed by stalk cells and,

interestingly, it is a poor activator of the receptor hence it is thought to help maintain low Notch activation on tip cells by competing with DLL4 (Eilken and Adams, 2010). Tip cells, which express high levels of VEGFR2, will guide the new blood vessel formation by sensing a concentration gradient of VEGF-A anchored to the surrounding ECM. VEGF-A exists in different isoforms (which will be reviewed in 1.2.2.1.2), VEGF-A 165 in human (VEGF-A 164 in mouse) possess a heparin-binding domain which allows it to interact with the ECM and provide directional guidance to the tip cell. On the other hand, VEGF-A 121 lacks this property but has been shown to be able to promote EC proliferation as opposed to tip cell guidance (Gerhardt et al., 2003; Ruhrberg et al., 2002).

1.2.1.4. Tip cell navigation

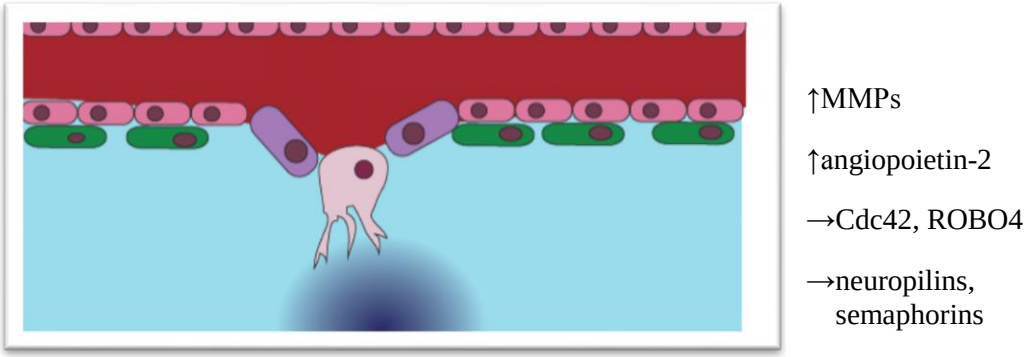

Fig. 1.14 **Sprouting angiogenesis: Tip cell navigation.** The tip cell (light pink) leads the developing sprout by extending numerous filopodia through the ECM (light blue) towards the VEGF gradient (blue).

Endothelial and mural cells share a basement membrane comprised of ECM proteins that form an envelope around the vessels (Eble and Niland, 2009). This retains ECs in their positions. Once the tip cell has been selected, for angiogenesis to occur, ECs must therefore be liberated, a process requiring proteolytic breakdown of the basement membrane and detachment of mural cells. Basement membrane degradation is mediated by matrix metalloproteases (MMPs) such as MT-MMP1, enriched in tip cells. Proteolysis is finely regulated, too little and the ECs will not migrate, whereas excessive degradation of the ECM, as occurs in plasminogen activator inhibitor 1 (PAI1) deficiency, leaves too little matrix support for the branch to sprout (Blasi and Carmeliet, 2002). MMPs have another key function which is to release pro-angiogenic growth factors that are sequestered in the matrix (Arroyo and Iruela-Arispe, 2010). They also generate anti-angiogenic molecules by cleaving plasma proteins, matrix molecules,

or proteases themselves to prevent inappropriate sprouting and coordinate branching (Nyberg et al., 2005). Detachment of mural cells, such as pericytes, is stimulated by Angiopoietin-2 (ANG2), a proangiogenic growth factor stored by ECs for rapid release (Augustin et al., 2009) (Huang et al., 2010). These steps are necessary for tip and stalk cells to liberate from the old vessels and migrate to the site where new blood vessels are needed.

Tip cell migration is guided by filopodia, thin protrusions with a core of parallel bundles of actin filaments that extend from the plasma membrane. Little is known regarding the molecular mechanisms regulating tip cell filopodia, apart from that activation of Cdc42 by VEGF triggers their formation (De Smet et al., 2009). ECs express guidance receptors including ROBO4, UNC5B, PLEXIN-D1, NRPs, and EPH family members, which they use to probe the environment. ROBO4 is expressed in ECs and maintains vessel integrity, and ROBO4 deficiency induces leakiness and hyper vascularisation (London et al., 2009). At the molecular level, ROBO4 inhibits the VEGFR2-mediated activation of Src kinase and therefore src-mediated permeability. The ROBO4 ligand is unknown however, ROBO4 binds to UNC5B, another guidance receptor, and it is thought that ROBO4/ UNC5B maintains vessel integrity via UNC5B activation (Koch et al., 2011). UNC5B is a receptor for Netrins whose expression is enriched in tip cells. Netrin1 prompts filopodia retraction on ECs, consistent with a suppressive function of netrins and UNC5B on sprouting (Adams and Eichmann, 2010). Interestingly, when UNC5B is not engaged with a ligand, it induces EC apoptosis (Castets and Mehlen, 2010). Semaphorins are secreted or membrane-bound guidance cues that interact with receptor complexes, formed by Neuropilins (NRPs) alone or NRP/plexin family proteins (Carmeliet and Tessier-Lavigne, 2005). SEMA3E induces vessel repulsion through interaction with PLEXIN-D1. As ECs express PLEXIN-D1, its loss causes aberrant sprouting into SEMA3E-expressing tissues in zebrafish embryos (Adams and Eichmann, 2010). In the mouse retina, SEMA3E activates PLEXIN-D1 on tip cells to fine-tune the balance of tip and stalk cells necessary for even-growing vascular fronts by coordinating VEGF's activity in a negative feedback (Kim et al., 2011). NRPs have several ligands in addition to semaphorins, including VEGF. The vessel abnormalities of NRP1-deficient embryos are in fact related to defective VEGF/NRP1 signalling (Fantin et al., 2009) as most semaphorins are suppressors of angiogenesis (Serini et al., 2009). EPH receptors and their ephrin ligands are regulators of cell contact-dependent signalling (Pitulescu and Adams, 2010). Eph-ephrin binding leads to bidirectional signalling in cells expressing the receptor (forward signalling) or ligand (reverse signalling). Eph-ephrins generate mostly repulsive signals. Ephrin-B2 is expressed in arterial ECs, whereas EphB4 is present on venous ECs. Both of them regulate vessel morphogenesis, and loss of ephrin-B2 or EphB4 leads to vascular remodelling defects (Pitulescu and Adams,

2010). Ephrin-B2-mediated reverse signalling has also been shown to regulate VEGFR internalization and tip cell behaviour. When eprhin-B2 is not knocked-out in ECs, they become unable to internalize VEGFR2 and VEGFR3 and cannot transmit VEGF signals properly, resulting in impaired sprouting (Sawamiphak et al., 2010) (Wang et al., 2010).

1.2.1.5. Stalk elongation / lumen formation

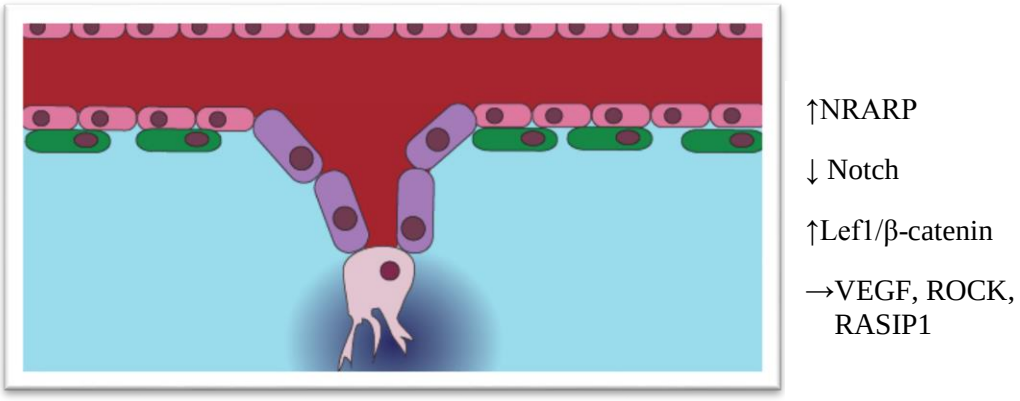

Fig. 1.15 **Sprouting angiogenesis: Stalk elongation / lumen formation.** The developing spout elongates by proliferation of endothelial stalk cells (purple) that trail behind the tip cell.

Compared to tip cells, stalk cells produce fewer filopodia and are more proliferative. Importantly, they also form junctions with neighbouring cells and produce basement membrane components to ensure the integrity of the new vessel (Phng and Gerhardt, 2009). As stated before, stalk cell specification is regulated by Notch signalling (Jakobsson et al., 2010). Upon activation, Notch receptor is cleaved leading to the release of the intracellular domain (NICD), forming a complex with the transcription factor RBPj/CBF1 and Mastermind-like proteins to initiate the transcription of target genes. This mechanism not only drives targeted gene expression but also prevents continuous Notch activation on the cell surface. The Notch-regulated ankyrin repeat protein (NRARP) disassembles Notch complex and induce NICD degradation to counterbalance Notch activation. This balance in Notch activation is fundamental to stalk cell proliferation. NRARP also promotes Lef1/β-catenin pathway to preserve stability of nascent vessel (Phng et al., 2009). Reversible acetylation of NICD represents another level of Notch regulation (Guarani et al., 2011). Acetylation enhances Notch responses by interfering with NICD1 turnover, whereas deacetylation by SIRT1 opposes NICD1 stabilization, thereby limiting Notch activity.

A functional vessel possesses a luminal space which will allow the circulation of blood throughout the vascular network. Lumen formation can occur via different mechanisms (Iruela-Arispe and Davis, 2009; Zeeb et al., 2010). During development, for instance, ECs in intersomitic vessels form a lumen by coalescence of intracellular (pinocytic) vacuoles, which interconnect with vacuoles from neighboring ECs (cell hollowing). Recently, it has been observed that, in large axial vessels, ECs adjust their shape and reorganize their junctions to open up a lumen (cord hollowing). During this process, ECs first define apical-basal polarity, then the apical (lumenal) membrane starts expressing negatively charged glycoproteins that confer a repulsive signal, opening up the lumen. Subsequently, changes in EC morphology, driven by VEGF and Rho-associated protein kinase (ROCK), enlarge the lumen (Strilic et al., 2009) (Zeeb et al., 2010). Ras-interacting protein 1 (RASIP1), a regulator of GTPase signalling controlling cytoskeletal rearrangements, adhesion, and EC polarity, seems also required for tube genesis (Xu et al., 2011).

1.2.1.6. Tip cell fusion

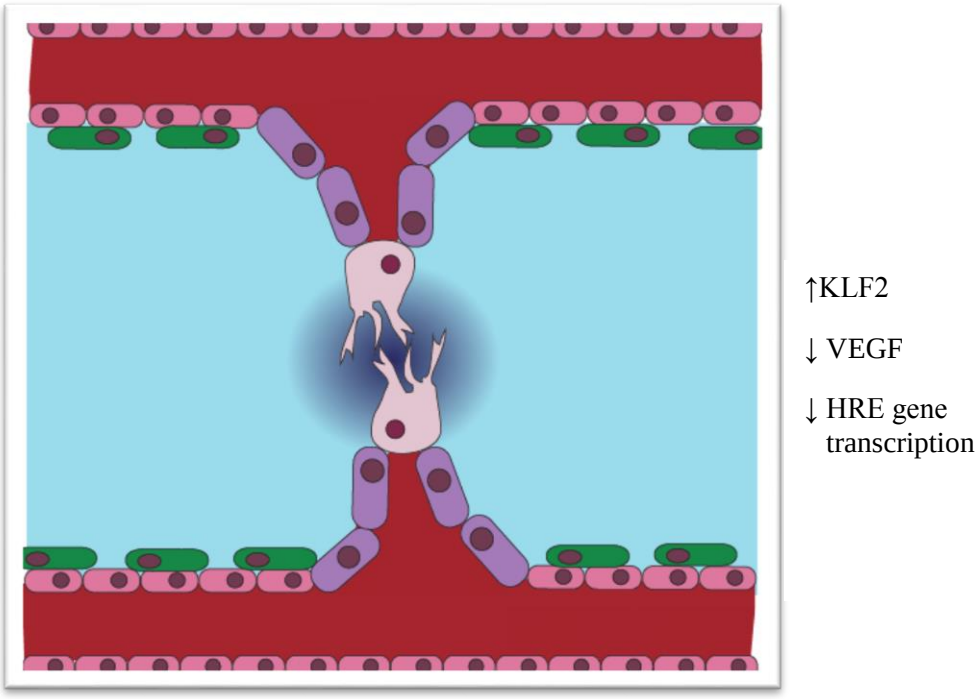

Fig. 1.16 **Sprouting angiogenesis: Tip cell fusion.** The tip cells from two developing sprouts fuse and create a lumen. Blood flowing through the new capillary oxygenates the tissues, thus reducing the secretion of VEGF-A.

Multiple newly formed vessels, guided by tip cells, will eventually converge to the site of the tissue with the highest concentration of angiogenic factors. At this point, a key step is represented by the interactions between the tip cells. Interestingly, macrophages have been shown to facilitate these interactions but are not strictly required (Fantin et al., 2010). Following the establishment of the first cell-cell contacts, new EC junctions are created. Subsequently, ECM is deposited into the basement membrane, supporting pericytes are recruited, EC proliferation decreases to basal level, and more cell junctions are formed. Blood will now start to flow in the new lumen and this is key to the shaping and remodeling of the vessel connections. Blood flow will also activate the shear stress-responsive transcription factor Krüppel-like factor 2 (KLF2). In zebrafish, KLF2 has been shown to upregulate the EC-specific miR-126 that modulates PI3K and MAPK signalling which then promotes vessel remodelling (Nicoli et al., 2010). Following perfusion, oxygen and nutrient delivery reduces VEGF production and inactivates endothelial oxygen sensors (Hypoxia-inducible factors), together re-directing ECs toward a quiescent phenotype.

1.2.1.7. Pericyte stabilization

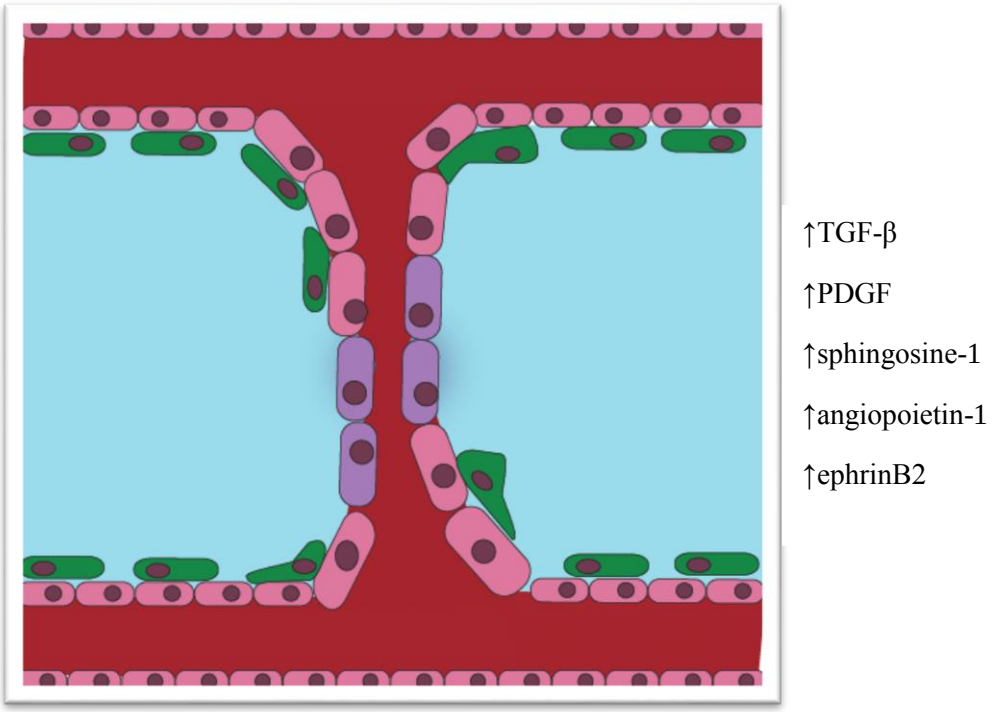

Fig. 1.17 **Sprouting angiogenesis: Stalk elongation / lumen formation.** The newly developed capillary is stabilized by pericyte recruitment (green), deposition of ECM, shear stress and other mechanical forces associated with blood flow and blood pressure.

Functional vessels are the result of a maturation process which involves the formation of a vessel wall. This implicates recruitment of mural cells and deposition of ECM (Jain, 2003). ECs also acquire tissue-specific differentiation adapted to meet local homeostatic demands and thus differ in phenotype (Dyer and Patterson, 2010). Pericytes are in direct contact with ECs in capillaries and immature vessels, whereas vascular smooth muscle cells cover arteries and veins and are separated from ECs by a matrix (Gaengel et al., 2009). Transforming growth factor β (TGF-β) signalling plays a major role during vessel maturation. TGF-β stimulates mural cell induction, differentiation, proliferation, and migration and promotes production of ECM (Pardali et al., 2010). Unsurprisingly, loss of function of TGF-β receptor 2 (TGFBR2) in mice causes vessel fragility in part due to impaired mural cell development (Pardali et al., 2010).

Platelet-derived growth factor (PDGF) receptor-β (PDGFR-β) is instead key to recruitment of mural cells (Gaengel et al., 2009). Endothelial PDGFB signals to PDGFR-β expressed by mural cells, stimulating their migration and proliferation. In fact, inactivation of either Pdgfb

or Pdgfrb genes induces pericyte deficiency, vascular dysfunction, micro-aneurysm formation, and bleeding (Gaengel et al., 2009). Sphingosine-1-phosphate receptor (S1PR) signalling also controls EC/mural cell interactions. Endothelial-derived S1P binds to G protein-coupled S1PRs (S1PR1–5) (Lucke and Levkau, 2010) and promotes cytoskeletal and junctional changes affecting cell migration, proliferation, and survival. Disruption of S1PR1 or loss of both S1PR2 and S1PR3 in mice causes defective coverage of vascular smooth muscle cells and pericytes, a phenotype reminiscent of Pdgfb and Pdgfrb mutant mice. However, the main defect is related to ECs, where S1P1 controls trafficking of N-cadherin to the ablumenal side of ECs in order to reinforce EC-pericyte contacts.

Angiopoietin-1 (ANG1), produced by mural cells, activates its endothelial receptor TIE2 (Augustin et al., 2009) (Huang et al., 2009) and stabilizes vessels by promoting pericyte adhesion and tightening EC junctions. Mural cells also require ephrinB2 for association around ECs, as mural cell-specific ephrinB2 deficiency causes mural cell migration and vascular defects (Pitulescu and Adams, 2010). Notch signalling also controls maturation and arterial differentiation of vascular smooth muscle cells (Gridley, 2010).

Recently, notch signalling (notch 1 and 3) has been shown to be required for proper pericyte coverage, interaction with the endothelium and vascular basement membrane formation in the mouse retina (Kofler et al., 2015).

1.2.2. Angiogenic factors

1.2.2.1. Vascular Endothelial Growth Factors

The identification of what is considered the strongest pro-angiogenic factor, VEGF or Vascular endothelial growth factor dates to 1983 when Senger et al. described for the first time a novel protein, partially purified from conditioned medium of a tumor cell line, which possessed the ability to induce vascular leakage in guinea pig skin and named it VPF or vascular permeability factor (Senger et al., 1983). Later that decade, Ferrara and Henzel (Ferrara and Henzel, 1989) discovered that pituitary follicular cells secrete a novel heparin-binding growth factor specific for vascular ECs and named it VEGF or vascular endothelial growth factor. Soon after, cDNA cloning of VPF (Leung et al., 1989) and VEGF (Keck et al., 1989) demonstrated that they were the same molecule.

VEGF family	
Type	***Function***

VEGF-A	• Angiogenesis
	  • ↑ Migration of ECs
	  • ↑ Mitosis of ECs
	  • ↑ Matrix metalloproteinase activity
	  • ↑ αvβ3 activity
	  • Blood vessel lumen formation
	  • Fenestrations
	• Chemotactic for macrophages and granulocytes
	• Vasodilation (indirectly by NO release)

VEGF-B	Embryonic angiogenesis in the myocardium
VEGF-C	Lymphangiogenesis
VEGF-D	Needed for the development of lymphatic vasculature surrounding lung bronchioles
PlGF	Important for Vasculogenesis, also needed for angiogenesis during ischemia, inflammation, wound healing, and cancer

Table 2 **Vascular endothelial growth factor family member functions.**

The VEGF family comprises in mammals five members: VEGF-A, VEGF-B, VEGF-C, VEGF-D and placenta growth factor (PlGF). A number of VEGF-related proteins encoded by viruses (VEGF-E) (Ogawa et al., 1998) and in the venom of some snakes (VEGF-F) (Tokunaga et al., 2005) have also been discovered.

1.2.2.1.1. VEGF-A activities

VEGF-A is a potent mitogen for micro- and macro-vascular ECs from arteries, veins and lymphatics with a ED_{50} of 2-10 picomolar (Ferrara and Henzel, 1989). Although initially this effect seemed limited and very specific to ECs, hence the name vascular endothelial growth factor, further studies have demonstrated that other cell types are susceptible to VEGF-A mitogenicity, such as retinal pigment cells (Guerrin et al., 1995), pancreatic duct cells (Oberg-Welsh et al., 1997) and Schwann cells (Sondell et al., 1999).

Beside promoting growth of ECs, VEGF-A is also a survival factor. *In vitro* studies showed that VEGF-A is able to protect ECs from serum starvation-induced apoptosis via the activation of the PI3 kinase / Akt pathway (Gerber et al., 1998b); in addition, VEGF-A can induce the expression of the anti-apoptotic proteins Bcl-2, A1 (Gerber et al., 1998a), XIAP (Tran et al., 1999) and Survivin (Tran et al., 2002) in ECs. Interestingly, *in vivo* the anti-apoptotic effect of VEGF-A seems to be limited to newly formed vessels, as such is important in neonatal vasculature in mice, but not in adult (Gerber et al., 1999), and in newly formed vessels within the tumors but not in fully established ones (Yuan et al., 1996). Since pericyte coverage marks the stabilization of newly formed blood vessels, this has been proposed to be the event that determines loss of VEGF-A dependency in ECs (Benjamin et al., 1999).

VEGF-A has been shown on several occasions to be able to promote angiogenesis both *in vivo* and *in vitro*. EC tube formation, for instance, an *in vitro* assay that recapitulates key events during angiogenesis, is promoted by VEGF-A (Pepper et al., 1992) and so is the *ex vivo* sprouting of rat aortic ring (Nicosia et al., 1994) and chorioallantoic membrane (Leung et al., 1989; Plouet et al., 1989). VEGF-A can also promote angiogenesis *in vivo* as shown in the rabbit cornea (Phillips et al., 1994), primate iris (Tolentino et al., 1996) and matrigel plug in mice (Mesri et al., 1995).

As mentioned before, VEGF-A was originally described as a protein capable of inducing vascular leakage in the skin (Senger et al., 1983). The link between vascular permeability and angiogenesis is still a grey area, some believe that an increase in permeability is a step necessary for angiogenesis to occur as it allows the extravasation of fibrin which will serve as

a scaffold for EC proliferation and migration (Dvorak et al., 1987), however, some others could argue that factors such as bFGF can induce angiogenesis without having an effect on vascular permeability (Cao et al., 2004). Another confusing aspect of the matter is the reported dependency of VEGF-A-induced permeability on Src and Yes and yet mice lacking these two kinases display a normal angiogenic response to VEGF-A (Eliceiri et al., 1999).

1.2.2.1.2. VEGF-A isoforms

The VEGF-A gene is localized in humans on chromosome 6p21.3, it is composed of 8 exons which by undergoing alternative splicing result in the generation of 4 different isoforms: VEGF-A121, VEGF-A165, VEGF-A189, VEGF-A206 (where the numbers are indicative of the amount of amino acids they retain after signal peptide cleavage) (Houck et al., 1991) (Fig. 1.18).

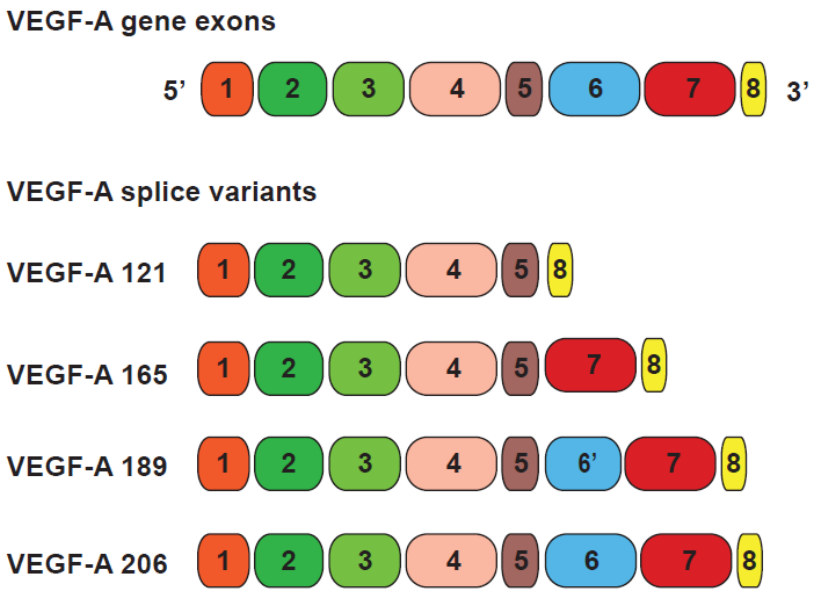

Fig. 1.18 **VEGF-A isoform exon composition.** Signal sequence (1), N-terminus (2), VEGF-R1 binding site, dimerization domain (3), VEGF-R2 binding site (4), Plasmin cleavage site (5), Heparin-binding site (6, 6', 7), C-terminus (8).

The 165 isoform is the predominant one, lacks the residues encoded by exon 6, and is a heparin-binding homodimeric glycoprotein of 45 kDa (Houck et al., 1992). Crystallography resolved VEGF homodimer structure showing their anti-parallel engagement by 2 disulphide bridges between cys-51 and cys-60 (Muller et al., 1997). An important difference between 165 and 121 is the absence of the heparin-binding domain in the latter. This is due to lack of the

exon 7 in the VEGF-A121 transcript. The 121 isoform is acidic and freely diffusible, while isoforms 189 and 206 which are highly basic and bind to heparin with high affinity (Houck et al., 1992) are almost completely sequestered in the ECM. VEGF-A165 has intermediate properties as it is secreted but can diffuse or stay anchored to the cell surface or the ECM (Park et al., 1993). However, even the ECM-bound isoforms can become freely diffusible when cleaved by specific proteases such as plasmin or sugar-degrading enzymes like heparinase. Interestingly, when VEGF-A loses its heparin-binding properties this reflects in loss of its mitogenic activity (Keyt et al., 1996). The importance of the predominant form of VEGF-A (165) became clear when it was shown to be the only isoform able to rescue a tumorigenic phenotype in mice lacking the VEGF gene (Grunstein et al., 2000), moreover, mice expressing only VEGF-A120 die shortly after delivery, emphasizing the importance of the heparin-binding domain for VEGF properties.

1.2.2.1.3. VEGF Receptors

VEGF family members bind to their cognate receptor tyrosine kinases Vascular Endothelial Growth Factor Receptors (VEGFR) 1, 2 and 3, respectively encoded by the genes flt1, flk1and flt4 (Fig. 1.19).

VEGFRs belong to the type III receptor tyrosine kinase family, single-pass transmembrane proteins containing seven extracellular immunoglobulin domains and a split intracellular tyrosine kinase domain. VEGF ligands have different affinities for the 3 receptors, with VEGFR1 binding VEGF-A, B and PLGF, VEGFR2 binding VEGF-A, C, E and D (following processing) and VEGFR3 with VEGFC and D (Olsson et al., 2006) (Fig. 1.19). These receptors are mainly expressed on ECs but VEGFR2 also plays a role in neuronal maturation (Khaibullina et al., 2004) and VEGFR1 is involved in macrophage migration (Sawano et al., 2001). VEGFR3 drives lymphatic development but also has a role in developmental angiogenesis (Tammela et al., 2008).

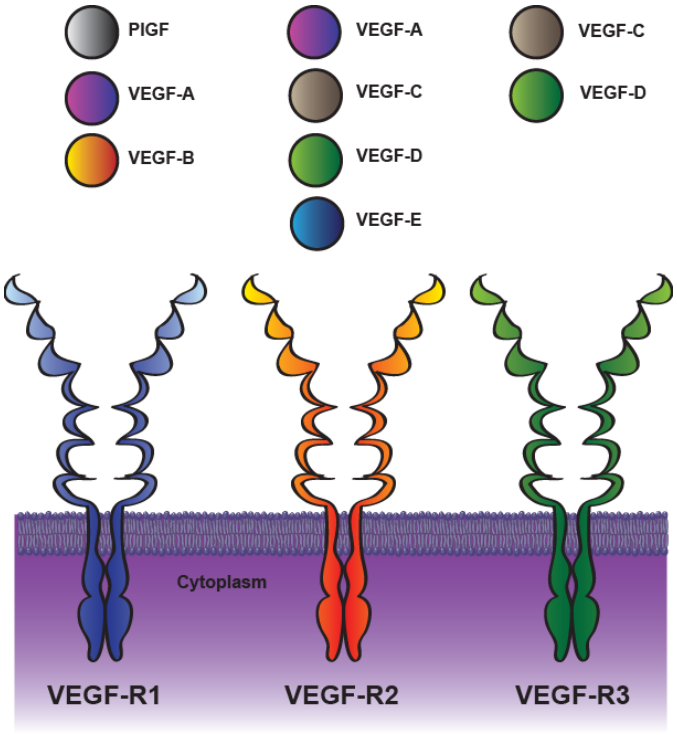

Fig. 1.19 **Vascular endothelial growth factor receptors and their ligands.**

Upon binding of VEGF dimers to VEGFR, the receptor itself dimerises and this is followed by trans-autophosphorylation on specific cytoplasmic tyrosine residues. Activation of VEGFR1 raises the levels of urokinase plasminogen activator (uPA) and plasminogen activator inhibitor-1 (PAI-1), which in turn regulate ECM degradation and cell migration. Both uPA and PAI-1 modulate the actin cytoskeleton dynamics via p38 MAPK, thus impacting EC migration (Robinson and Stringer, 2001) (Kanno et al., 2000) (Landgren et al., 1998b) (Olofsson et al., 1998). When VEGFR1is phosphorylated at residue Y1169, it can also recruit phospholipase Cγ1 (PLCγ1), generating a binding site for the Src homology (SH2) domains in PLCγ (Roskoski, 2007). However, ligand-activated VEGFR1 does not seem to directly affect cellular behaviour such as cell proliferation.

6–7 tyrosine residues in the cytoplasmic tail of VEGFR2 can be phosphorylated, particularly residues Y1175, Y951 and Y1214 (Fig. 1.20). Phosphotyrosines will then function as binding sites for SH2 domain-containing proteins or phosphotyrosine binding domains. PLCγ1 binds to the pY1175 site and this promotes phosphatidylinositol-4,5-bisphosphate hydrolysis to diacylglycerol (DAG) and inositol 1,4,5-triphosphate (IP3). IP3, in turn, activates the IP3 receptor. IP3 acts as a calcium channel on the ER, by mediating IP3-activated translocation of calcium ions from the ER to the cytosol. In the meantime, DAG activates the protein kinase C

(PKC) enzyme, which activates the MAPK pathway and signalling. Moreover, VEGFR2 phosphorylation promotes the activation of the phosphatidylinositol 3-kinase (PI3K) pathway, which leads to increased c-Akt (protein kinase B) activity, followed by endothelial nitric oxide synthase (eNOS) phosphorylation resulting in the production of nitric oxide (NO) (Olsson et al., 2006; Roskoski, 2007). NO then induces the expression of the hypoxia inducible factor complex which stimulates the transcription of VEGF-A (Karar and Maity, 2011). Once PKC enzymes are activated they phosphorylate and activate MEK (MAPK and ERK kinases), which in turn phosphorylates and activates p42/44 MAPK, leading to changes in gene transcription culminating in cell proliferation. Interestingly, it has been shown that PKCe isoform is implicated in VEGF-A–induced phosphorylation and activation of c-Akt and eNOS (Rask-Madsen and King, 2008). Shb (SH2 domain-containing adaptor protein b) similarly binds to the VEGFR2-pY1175 and activates PI3K, which in turn activates c-Akt and eNOS, promoting cell survival and NO production, respectively. Binding of a T-cell–specific adaptor protein (TSAd) to VEGFR2-pY1175 is also implicated in c-Src–regulated EC migration and vascular permeability. The VEGFR2-pY1214 is linked to actin remodelling and cell migration through a pathway involving CDC42, p38 MAPK and heat shock protein 27 kDa. The phosphorylation of Y1214 site is also linked to focal adhesion dynamics and cell motility.

VEGFRs can heterodimerise in a context and cell-specific manner, such as VEGFR2/3 complexes (Tammela et al., 2008) (Nilsson et al., 2010) but the signalling events downstream of such heterodimers are yet to be elucidated. VEGFR2 and VEGFR3 effectively induce receptor phosphorylation and downstream signalling whereas VEGFR1 has weak signalling activity in ECs. VEGFR1 has a much higher binding affinity for VEGF-A, with Kd of 2-10pM whereas the affinity of VEGFR2 is at least one order of magnitude lower (Shibuya, 2006). This has led to the hypothesis that flt1 acts as a VEGF-A sink and sequesters it, thus preventing binding to VEGFR2 and activation of downstream signalling. VEGFR1 negatively regulates tip cell formation by antagonizing the effects on VEGF-A in zebrafish (Krueger et al., 2011). Expression of a soluble isoform of VEGFR1 results in decreased angiogenesis (Zygmunt et al., 2011), which is necessary to keep certain clear tissues avascular i.e. the cornea (Ambati et al., 2006).

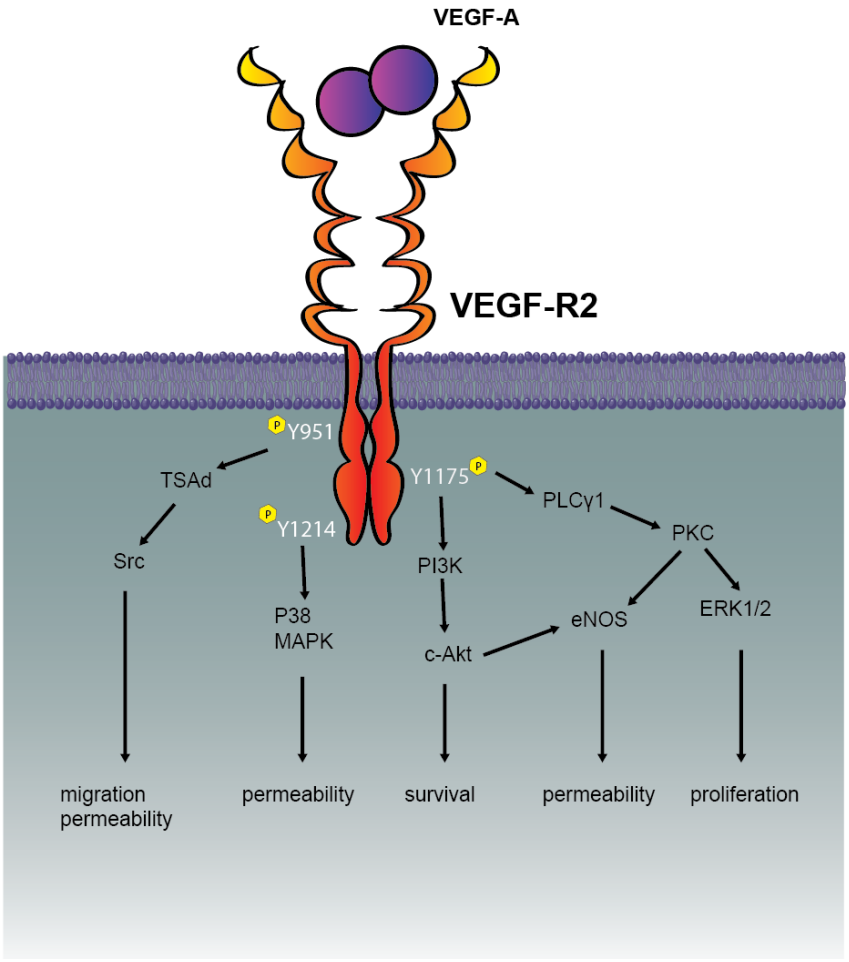

Fig. 1.20 **VEGFR2 signalling.**

Loss of VEGFR1 increases EC proliferation and network formation resulting in embryonic lethality by E9 (Fong et al., 1995), suggesting this may be due to increased VEGFR2-driven signalling. Loss of both VEGFR2 alleles induces embryonic lethality at E8.5, with defects in vascular network formation as in VEGF knockouts, but also defects in EC specification and early migration (Shalaby et al., 1995). Recently, a soluble isoform of VEGFR2 has been described and is important for modulation of lymphangiogenesis by blocking VEGF-C function (Albuquerque et al., 2009). Apart from its role in lymphangiogenesis VEGFR3 is involved in vasculogenesis, with associated embryonic lethality at E9.5 in knockout mice (Dumont et al., 1998), as well positively influencing angiogenic post-natal sprouting (Tammela et al., 2008), findings that have been observed in zebrafish (Ober et al., 2004). The longer isoforms of VEGF-A can bind neuropilins, single pass transmembrane receptors best known for their expression in the nervous system and ability to bind semaphorins (Larrivee et

al., 2009). Nrp1 and 2 are expressed during early vascular development with nrp2 becoming restricted to the lymphatic endothelium. Nrp1 co-immunoprecipitates with VEGFR2 whilst nrp2 associates with VEGFR2 and 3. Nrp1 deficiency leads to embryonic lethality caused by early heart and vascular defects, along with neuronal guidance defects (Kawasaki et al., 1999). These defects are dependent on aberrant sprouting and arterial differentiation but not EC proliferation. Accordingly, nrp1 becomes preferentially expressed in arterial ECs later in development (Stalmans et al., 2002). Similarly, in zebrafish loss of nrp1 expression abrogates VEGF-dependent ISA sprouting (Lee et al., 2002). Nrp2 loss affects the lymphatic vasculature but not the blood vasculature (Yuan et al., 2002). Overexpression of nrp1 induces ectopic vascular sprouting that ultimately leads to embryonic lethality, similar to loss of VEGFR1. The co-binding of Nrp1 to VEGF is not important in the activation of VEGFR2 and its phosphorylation (Larrivee et al., 2009), but recent work suggests a role in the sorting of the endocytosed receptors to different endosomal compartments in a synectin-dependent mechanism, leading to altered downstream signalling (Ballmer-Hofer et al., 2011). The guidance of EC tip cell migration is dependent on the presence of functional Nrp1 (Gerhardt et al., 2004). Evidence also points to the requirement of Nrp1 for p38MAPK phosphorylation downstream of VEGFR2, important for EC sprouting, branching and interaction with pericytes (Kawamura et al., 2008). A recent hypothesis on the VEGF-A specificity of Nrp1 hint that Nrp1 binds both VEGF-A164 and VEGF120, but the latter cannot induce Nrp1-VEGFR2 complex formation and thus fails to activate downstream signalling (Pan et al., 2007). Overall the above data suggest nrp1 is an important player in sprouting angiogenesis through its interaction and effect on VEGFR2 downstream signalling. Blood flow can also influence VEGFR2 signalling through interactions with VE-cadherin and PECAM-1 (Tzima et al., 2005) and this mechanosensory complex can activate integrin-mediated shear stress responses.

1.2.2.2. Fibroblast Growth Factors

The Fibroblast growth factors (FGFs) are pleiotropic factors acting on different cell types, including ECs. They exert their biological activities by binding to high affinity tyrosine kinase receptors FGFRs on the surface of target cells. ECs from different vascular beds express FGFR1, *in vitro* at least, and in some cases FGFR2 while FGFR3 and FGFR4 expression has never been reported on ECs (Bastaki et al., 1997; Dell'Era et al., 2003; Javerzat et al., 2002). A lot of evidence suggests that members of the FGF family, in particular FGF1 and FGF2, can promote a pro-angiogenic switch in ECs *in vitro*. They can, for instance, promote EC proliferation. This involves the autophosphorylation of FGFR followed by the recruitment of

adaptor molecules such as Shc, FRS2 and Crk (Cross and Claesson-Welsh, 2001). In addition, activation of PKC is also required for FGF2 to exert a full mitogenic response in ECs (Presta et al., 1991). Interestingly, FGF1, FGF2 and FGF4 upregulate urokinase-type plasminogen activator (uPA) which is important for the matrix degradation phase at the initial stage of angiogenesis. Additionally, they modulate the expression of uPA receptor on the EC surface, allowing the localization of the proteolytic activity to the leading edge of the migratory EC (Mignatti et al., 1989). Moreover, FGF2 promotes the shedding of cell surface membrane vesicles containing MMP-2, MMP-9 and MMP-14, which, together with the uPA system, contribute to remodelling the ECM during angiogenesis (Taraboletti et al., 2002). FGF2 has also been shown to promote cell migration in ECs. This effect, similarly to that on EC proliferation, requires the activation of the MAPK signalling pathway and is abolished by downregulation of PKC (Daviet et al., 1990; Shono et al., 2001). Interestingly, the capacity of FGFR1 to mediate FGF2 chemotactic effect is independent of its auto-phosphorylation and requires the activation of a Wortmannin-sensitive pathway (Landgren et al., 1998a). FGF2 also regulates the expression of different integrins such as αVβ3 and cadherins. This happens in a very finely tuned manner, as a brief exposure of FGF2 disrupts EC junctions while a prolonged exposure promotes a slow redistribution of junctional adhesion molecules such as PECAM-1, VE-Cadherin and Plakoglobulin (Underwood et al., 2002). In contrast with the potent angiogenic response elicited by exogenous FGF2 *in vitro*, the role of endogenous FGF2 remains uncertain. For one, fgf2 Knock-out mice are morphologically normal (Zhou et al., 1998) and do not even show impairment in neovascularization after injury (Tobe et al., 1998) or hypoxia (Ozaki et al., 1998). The same is true for the double knock out fgf2/fgf1 (Miller et al., 2000). This may reflect compensatory effects amongst members of the FGF family or/and the contribution to angiogenesis of several other growth factors including VEGF. In this regard, an intimate cross-talk exists among FGF2 and different members of the VEGF family during angiogenesis. Several lines of evidence suggest that FGF2 induces new blood vessel formation indirectly by activation of the VEGF/VEGFR system. For instance, expression of a dominant negative FGFR1 or FGFR2 in glioma cells leads to decreased tumor angiogenesis and down-regulation of VEGF (Auguste et al., 2001). Moreover, VEGFR-2 antagonists not only inhibit VEGF but also FGF-mediated angiogenesis both *in vitro* and *in vivo* (Tille et al., 2001), and FGF2 upregulates the expression of both VEGF (Seghezzi et al., 1998) and VEGFR2 (Gabler et al., 2004) in ECs.

1.2.2.3. Angiopoietins

Angiopoietin-1 (Ang1) was first discovered in 1996 as the ligand of the previously orphan receptor TIE-2 (tyrosine kinase with immunoglobulin-like loop and EGF homology domains) expressed exclusively on ECs (Davis et al., 1996) and on leukocytes at early stage of development. Angiopoietin-2 (Ang2) was later discovered as a natural antagonist of Ang1 with similar binding affinity to TIE2 but diminished capacity to activate the receptor (Maisonpierre et al., 1997). Angiopoietins contain a C-terminal fibrinogen-like domain, bearing six cysteine residues, which is the site of interaction with TIE2. It has been shown the Ang1 and Ang2 differ in the ability to activate TIE2 reside in this C-terminal domain. Ang1 is constitutively and widely expressed in adult highly vascularised tissues (Thurston et al., 2000), while Ang2 is only expressed in the ovary, placenta and uterus, organs in which physiological angiogenesis happens (Maisonpierre et al., 1997), and in pathological conditions characterised by new blood vessel formation such as rheumatoid arthritis (Scott et al., 2002). Angiogenic factors such as VEGF, FGF2 and hypoxia up-regulate Ang2, while Ang1, TGFβ and Ang2 (in an autocrine fashion) promote its down-regulation (Mandriota and Pepper, 1998).

Binding of angiopoietin clusters Tie2 molecules, a minimum of four monomers assembling in a tetrameric conformation is required to stimulate the tyrosine kinase domains (Kim et al., 2005). Tie2 is ubiquitous in the vascular endothelium. Tie2 appears to be constitutively phosphorylated in quiescent vasculature (Wong et al., 1997), indicating an active role in vascular maintenance. Tie2 is also expressed to a variable extent on non-ECs, such as monocytes, synovial membrane cells, cancer cells and neurons (Brkovic et al., 2007) (Kosacka et al., 2005) (Nakayama et al., 2005) (Voskas et al., 2005) (Uchida et al., 2000). The cellular effects of ang1 are generally protective. The ligand inhibits endothelial apoptosis in response to a serum-deprivation and TNF-a (Kwak et al., 2000). Ang1 promotes migration of endothelial and some non-ECs such as smooth muscle cells (Iurlaro et al., 2003) (Jones et al., 2003). Ang1 also induces sprouting and reorganisation of ECs into tubules (Kim et al., 2000a) (Koblizek et al., 1998). Ang1 exerts potent anti-inflammatory effects on ECs, suppressing VEGF-induced upregulation of E-selectin, ICAM- 1 and VCAM-1, and inhibiting leucocyte adhesion and transmigration in response to VEGF and TNF-a (Kim et al., 2001) (Gamble et al., 2000). Ang1 also reduces endothelial permeability in response to VEGF and thrombin in HUVECs (Gamble et al., 2000). Ang1 stimulates the localisation to cellular junctions of proteins involved in promoting junctional integrity, such as PECAM-1 (Gamble et al., 2000), occludin (Hori et al., 2004) and ZO-2 (Lee et al., 2009). Whilst ang1 is an agonist to Tie2, ang2 is a partial agonist, with high concentrations of ang2 leading to competitive inhibition of ang1 signalling through Tie2 (Yuan et al., 1999). As ang1 and ang2 form similar structural

complexes with Tie2 (Barton et al., 2006), the mechanisms for this have been suggested to be related to a greater ability of ang1 to dissociate the inhibitory co-receptor Tie1 (Seegar et al., 2010) (Hansen et al., 2010), or possibly to the different oligomerisation patterns of ang1 and 2 allowing differential receptor activation (Kim et al., 2005) (Kim et al., 2009). Ang2 is best currently regarded as an inducible inhibitor of endothelial quiescence, inhibiting the tonic vascular maintenance activities of ang1 at times where endothelial remodelling is required, for example during inflammation or angiogenesis.

1.2.3. Angiogenesis in diseases

A well-organized and functional vascular system allows the diffusion of nutrients, metabolites and oxygen to metabolically active cells. Malignant tumors, for instance, are composed of fast-growing highly-metabolic cells and without a good blood supply to bring nutrients and oxygen and remove waste products they wouldn't grow larger than 1 to 2 mm across. For this reason, tumor cells produce and release pro-angiogenic factors which stimulate neighbouring blood vessels to grow new capillaries within the tumor mass. Tumor angiogenesis not only allows tumor growth but also represents a mechanism of tumor evasion and metastasis to distant organs (Weis and Cheresh, 2011). Angiogenesis is also characteristic of chronic inflammatory conditions such as Rheumatoid Arthritis. During Rheumatoid Arthritis, the highly proliferative synovial cells cause a growing metabolic demand for oxygen and nutrients. In addition, the accumulation of synovial fluid exacerbates hypoxia in an already ischemic environment. Such a combination of increased metabolic demand and hypoxia is a potent signal for angiogenesis. On the other hand during Rheumatoid Arthritis, angiogenesis in itself sustains the inflammatory response. New blood vessels allow more inflammatory cells to migrate from the circulation into the already inflamed synovium (Konisti et al., 2012). Age-related macular degeneration (AMD) is a progressive retinal disease associated with multiple environmental and genetic factors and the leading cause of central vision loss in developed countries, affecting 1 in 10 people older than 50 years. The late or more severe disease progression is often referred to as "wet" AMD. Wet AMD is caused by the growth of abnormal blood vessels, or choroidal neovascularisation (CNV), under the macula. These abnormal vessels leak fluid and blood into the tissue at the back of the eye, causing a blister to form in the retina. The resulting scar tissue leads first to distortion and eventually to retinal detachment and loss of central vision (van Lookeren Campagne et al., 2014). Also cardiovascular diseases, blindness, complications of AIDS, diabetes, Alzheimer's disease and more than 70 other major health conditions affecting children and adults worldwide are characterized by angiogenesis.

1.2.4. Anti-angiogenic therapies

1.2.4.1. Targeting VEGF/VEGFR

VEGF has become the prime antiangiogenic drug target with approval by the US Food and Drug Administration of several VEGF- and VEGF receptor-based inhibitors for clinical use (Crawford and Ferrara, 2009). The anti-VEGF Ab Bevacizumab (Avastin) is approved in combination with chemotherapy or cytokine therapy for several advanced metastatic cancers, including non-squamous non-small cell lung cancer, colorectal cancer, renal cell cancer, and metastatic breast cancer. Based on a randomized phase II trial, bevacizumab monotherapy has been approved for recurrent glioblastoma. Additionally, four multi-targeted pan-VEGF receptor tyrosine kinase inhibitors (RTKIs) have been approved: Sunitinib (Sutent) and Pazopanib (Votrient) for metastatic renal cell carcinoma (RCC), Sorafenib (Nexavar) for metastatic RCC and unresectable hepatocellular carcinoma, and Vandetanib (Zactima) for medullary thyroid cancer. Sunitinib has also been recommended for treatment of advanced pancreatic neuroendocrine tumors. Beside several types of cancer, VEGF has been found overexpressed also in patients with wet AMD, and anti-VEGF Ab therapy is the current standard treatment (Group et al., 2011). Clinical agents for wet age-related macular degeneration, characterized by neovascularization of leaky vessels, include an anti-VEGF Fab Ranibizumab (Lucentis) and a VEGF aptamer Pegaptanib (Macugen), with Avastin being used off-label. Since 2013, Aflibercept (Eylea) has become the drug of choice for the treatment of Wet AMD. Aflibercept is a fully human fusion protein of VEGFR1 and VEGFR2. It uniquely blocks all forms of VEGF-A, as well as PlGF, each arm binding to each pole of an active growth factor dimer. This forms a stable and inert 1:1 complex. Its high affinity allows it to bind growth factors more tightly than naturally occurring VEGF receptors or antibodies, perhaps leading to more complete blockade of VEGF signaling and potentially an increased duration of efficacy. Aflibercept has demonstrated encouraging efficacy and safety in phase 1 and 2 clinical trials in the treatment of wet AMD and in a phase 1 study for diabetic macular edema. Phase 3 studies for the treatment of exudative AMD (VIEW1 and VIEW2) have shown comparable efficacy of Aflibercept when injected every 2 months compared to Ranibizumab injected every month (Heier et al., 2012).

VEGF blockade prolongs progression-free survival or overall survival of cancer patients in the range of weeks to months and improves visual acuity in patients with age-related macular degeneration. The clinical benefit of treatment with VEGF (receptor) inhibitors is attributable to several mechanisms. First, these blockers inhibit tumor vessel expansion by blocking vascular branching or inhibiting homing of BMDCs. Additionally, these drugs induce regression of pre-existing tumor vessels and sensitize ECs to effects of chemotherapy and

irradiation by depriving them of VEGF's survival activity. Normalization of abnormal tumor vessels by pruning immature pericyte-devoid vessels and by promoting maturation into more functional vessels is another mechanism (Goel et al., 2011). The resulting sensitization to cytotoxic or radiation therapies relying on conversion of oxygen to radicals in combination with improved chemotherapeutic delivery may explain partly why combination delivery of bevacizumab/cytotoxic agents is often superior (Jain, 2005). However, the importance of vessel normalization versus pruning for the overall anticancer effect of VEGF (receptor) inhibitor treatment requires future study. Furthermore, vessel normalization observed with treatment is transient, as these drugs induce excessive vessel regression, or tumor vascularization escapes VEGF blockade. In conditions where vascular leakage causes life-threatening intracranial edema (e.g., in glioblastoma) or blindness (e.g., in wet age-related macular degeneration), restoration of normal barrier properties by VEGF (receptor) blockade may be a relevant mechanism (Goel et al., 2011). Besides targeting tumor vessels, these inhibitors also target tumor cells expressing VEGF (receptor), whose growth is stimulated by VEGF.

Although anti-VEGF (receptor) therapies are the current standard in the clinic to treat both tumor angiogenesis and choroidal neovascularization in wet-AMD, therapies that target VEGF directly are raising several concerns. One of which is that VEGF not only drives new vessel growth but it also has an important role for trophic maintenance of the healthy vasculature. Prolonged anti-VEGF therapy for cancer treatment, for example, is associated with a number of severe adverse effects associated with endothelial dysfunction including: hypertension, microangiopathy, proteinuria in the kidney; cardiac ischemia/infarct, thromboembolic events in the heart, and bleeding in the gastrointestinal system (Meadows and Hurwitz, 2012). Moreover, Kurihara et al. have recently described a dramatic and rapid loss of ECs of the choriocapillaries and severe vision loss in mice following genetic deletion of the VEGF gene from the retinal pigment epithelial cells. These data suggesting that an indiscriminate suppression of VEGF signalling, an effect similar to that reached by the anti-VEGF therapies currently in use, might carry with it very dramatic side effects for the patients in the long run (Kurihara et al., 2012). This has highlighted the need to identify novel therapeutic targets to develop better therapies.

1.2.4.2. Targeting Integrins

Integrins have been shown to play key roles in tumor angiogenesis (Foubert and Varner, 2012), and antagonists of several integrins have shown promising results in pre-clinical studies on

several types of cancer. An attractive aspect of targeting integrins is that there are specific family members which are only expressed or activated in remodelling tissues such as tumors; targeting those has therefore the potential to spare toxic effect on the remaining healthy tissues. Anti-integrin blocking monoclonal Abs usually have high affinity and specificity and have been well-characterized over the years; these were, unsurprisingly, the first anti-integrin compounds to reach the clinic. Abegrin (MEDI-522), a humanised version of the anti-integrin αvβ3 monoclonal Ab LM609 (block angiogenesis by inducing apoptosis of tumor-associated ECs), was the first anti-integrin therapy to be tested in cancer clinical studies. The early version of MEDI-522, Vitaxin, was well-tolerated in phase I studies (Gutheil et al., 2000) (McNeel et al., 2005). Vitaxin led to disease stabilization in relapsed/refractory patients with metastatic cancer. However, in a second clinical study, Vitaxin did not show any anti-tumor activity in leiomyosarcoma patients. In 2001, MedImmune started clinical studies using Vitaxin (renamed MEDI-522 and Abegrin) and in 2003 initiated phase II trials in advanced metastatic melanoma and prostate cancer patients (Hersey et al., 2010). In one melanoma trial, 112 patients with late stage melanoma received MEDI-522 weekly, a sub-group also received standard chemotherapy Dacarbizin. Both MEDI-522 treatment groups showed prolonged survival compared with historical clinical trial results (Hersey et al., 2010). Correlative science studies showed that MEDI-522 had functional efficacy by reducing FAK activity in blood vessels (Zhang et al., 2007). Based on these encouraging results, phase III cancer clinical trials are planned.

Integrins αvβ3 and αvβ5 regulate angiogenesis and promote tumor cell invasion in pre-clinical studies (Brooks et al., 1997). The pharmaceutical company Centocor has developed CNTO 95, a human monoclonal Ab directed against both αvβ3 and αvβ5 integrins. CNTO 95 reduced angiogenesis and tumor growth in human melanoma xenografts (mice) (Trikha et al., 2004) and showed little toxicity in preclinical safety studies (Macaca fascicularis) (Martin et al., 2005). This Ab has completed phase I safety trials (Mullamitha et al., 2007) and is now under evaluation in phase II clinical trials for melanoma and prostate cancer. In addition, a cyclic RGD-peptide antagonist of αvβ3 and αvβ5, cilengitide (EMD 121974), has been developed as a potential tumor therapeutic. Phase I clinical trials showed a favourable safety profile (Nabors et al., 2007) and may work well in combination with radiotherapy in cancer patients (Albert et al., 2006). This drug was evaluated in phase I/II clinical trials for glioblastoma and significantly increased progression-free survival (Nabors et al., 2007). Cilengitide has gone to phase II trials for glioblastoma, non-small cell lung cancer, melanoma and pancreatic cancer and in phase I for different types of B cell malignancies (Beekman et al., 2006; Bradley et al., 2011; Friess et al., 2006). Cilengitide has however failed clinical trial phase III in the treatment

of newly diagnosed glioblastoma. Therefore, two distinct αv integrin-targeting drugs offer promise as cancer therapeutics and the results of clinical trials are eagerly anticipated.

As β1 integrins also have important roles in regulating angiogenesis, targeting these integrins in addition to αv integrins could be a beneficial therapeutic strategy to block tumor angiogenesis and progression. Antagonists of one β1 integrin, α5β1, have undergone clinical testing. A chimeric mouse–human anti-α5β1 Ab, M200 (volociximab) has shown low toxicity in phase I studies. M200 was evaluated in phase II trials for metastatic melanoma, renal cell carcinoma and non-small cell lung cancer (Kuwada, 2007). In renal cell carcinoma studies, M200 was well-tolerated and stable disease was noted in 87% of patients. In a melanoma trial, combining M200 with dacarbazine was well-tolerated and anti-cancer activity was noted in 62% of patients. Another drug in clinical trials, ATN-161, is a peptide inhibitor of integrin α5β1. In animal models of colon cancer, ATN-161 reduced metastases and improved survival when combined with chemotherapy (Stoeltzing et al., 2003). In phase I safety trials, ATN161 was well-tolerated and several patients exhibited stable disease. ATN-161 has currently completed phase II clinical trials for multiple myeloma and other tumors (Cianfrocca et al., 2006). Thus, these two integrin α5β1-inhibiting drugs might offer future benefit to cancer patients.

Despite some promising results in phase I and II clinical trials, clear evidence that integrin inhibitors are efficient in inhibiting tumor angiogenesis in cancer patients has yet to be obtained. In this regard, it is fundamental to bear in mind that integrins are widely expressed by cells within the tumor microenvironment and the effect seen in clinical trials are likely to be derived by the combinatorial effect of blocking both EC and tumor cell integrins. Moreover, studies have revealed that nanomolar concentrations of RGD-mimetic inhibitor cilengitide can actually enhance the growth of tumors *in vivo* by promoting VEGF-mediated angiogenesis (Reynolds et al., 2009). These results raise concerns about the use of these agents as anticancer drugs. In conclusion, although phase I and II clinical trials appear promising, further pre-clinical studies are needed to elucidate the mechanism of action of anti-integrin drugs in regard to their target (tumor cells, tumor microenvironment, or both) and their optimal dosing.

1.3. Syndecans in angiogenesis

1.3.1. Syndecan-1

Syndecan-1 is probably the best characterized of the syndecans, it appears to be implicated in a variety of physiological processes associated with the endothelium both during development and adulthood. This is unsurprising since syndecan-1 is a major constituent of the endothelial glycocalyx (Zeng et al., 2014). In an interesting study, increased new blood vessel formation in syndecan-1 deficient mice was observed where corneal neo-vascularization was induced by inflammation rather than pro-angiogenic growth factors. However, a direct correlation between increased EC-leukocyte interactions in these animals and increased angiogenesis was observed which suggested that the increase in the latter is due to an increased local accumulation of leukocytes (Gotte et al., 2002). Other studies have shown that syndecan-1 can associate directly via its extracellular domain with the αVβ3 and αVβ5 integrins leading to their activation and this is true for a variety of cell types (Beauvais et al., 2004; Beauvais and Rapraeger, 2003; McQuade et al., 2006) including ECs from both mice and humans. In fact, immuno-precipitation experiments with HMEC (human microvascular ECs) revealed it was possible to co-precipitate β3 and β5 integrins in complex with syndecan-1 and that by silencing syndecan-1 expression HMEC-1 were not able to spread on the αVβ3 ligand Vitronectin (VN) (Beauvais et al., 2009). The same group previously showed that fibroblasts seeded on syndecan-1 Ab would spread and activate αVβ3 and αVβ5 even in the absence of integrin ligands (McQuade et al., 2006). They could replicate this result with ECs and show that integrin activation could be prevented by adding Synstatin ($SSTN_{82-130}$ a peptide corresponding to aa 82-130 of the syndecan-1 extracellular core protein). Interestingly, the SSTN peptide showed promising results in being able to inhibit tumor angiogenesis in a mouse model of mammary carcinoma (Beauvais et al., 2009).

Later, the same group discovered the mechanism through which syndecan-1 is able to activate αVβ3 and α5β3 integrins. They were able to co-precipitate syndecan-1 with αVβ3 and IGF1R (insulin like growth factor receptor 1) from ECs in a way which suggested integrin and syndecan-1 were acting as a docking site for IGFR1. Also, they showed the presence of this ternary complex on focal contacts when cells were plated on VN (Beauvais and Rapraeger, 2010). In further investigations they found that SSTN, the peptide able to disrupt syndecan-1-αVβ3 interaction, can block VEGF-induced angiogenesis but only in the early phase (in the aortic ring assay) when EC dissemination is preceded by breakdown of adherens junctions. VEGF-stimulated migration of ECs depends on αVβ3 and can be blocked by SSTN, suggesting that syndecan-1 has a role VEGF-dependent migration in ECs. Indeed, stimulation

of cells with VEGF not only activates VEGFR2 but also IGFR1 and αVβ3, activation of the latter can be abolished by adding SSTN. They propose a model whereby during the early phase of angiogenesis, syndecan-1, in its ternary complex with αVβ3 and IGFR1, is necessary for VEGF-induced integrin activation. This is key to EC dissemination and can be prevented by SSTN but also by disruption of the VE-Cadherin homophilic interaction thus supporting the finding that SSTN is not able to stop angiogenesis in its late phase when adherens junctions are already disrupted (Rapraeger et al., 2013). A recent study has also revealed that melanoma cells which are able to perform vascular mimicry (in which cells of a highly aggressive malignant tumor can form vascular-like channels without the need for endothelial cells) are VEGFR2, CD144 and Syndecan-1 positive. Critically, the use of a syndecan-1 blocking Ab abolishes the vascular mimicry ability of melanoma cells (Orecchia et al., 2015).

1.3.2. Syndecan-2

The most important study linking syndecan-2 to angiogenesis dates back to 10 years ago when Chen et al. showed that lack of syndecan-2 in zebrafish (achieved by morpholino gene-targeting approach) dramatically impairs developmental angiogenesis. In the least severe case, corresponding to a less efficient syndecan-2 knock-down, intersegmental vessels either sprouted abnormally or failed to form and the vascular plexus of the tail region was less complex compared with that of wild-type embryos. Primary formation of the axial vessels was normal. However while axial expression of fli-1, flk-1 and tie-1 was retained in the trunk, this was lost in the intersegmental vessels. In an elegant twist to the work, they not only showed that the phenotype could be reverted by injection of exogenous zebrafish syndecan-2 cDNA but that a similar effect could be obtained by injecting human syndecan-2 cDNA, giving clear clues of an important functional conservation amongst species. The exact mechanism through which syndecan-2 asserts its pro-angiogenic function remains unclear. However, they showed that injection of a cytoplasmically-truncated form of syndecan-2 phenocopied the lack of its full-length form, suggesting the importance of its cytoplasmic domain in syndecan-2 vascular function (Chen et al., 2004b).

Syndecan-2 may also play a role in pathological angiogenesis. It was found up-regulated both on vessels in gliomas and from normal brain while not present in the surrounding parenchyma (Fears et al., 2006). The same study showed that knock-down of syndecan-2 in Murine vein ECs (MvEC) resulted in decreased migration on fibronectin and tube formation on matrigel. However, those same pro-angiogenic factors such as EGF, bFGF and VEGF, known to be up-regulated in gliomas, showed an ability to promote syndecan-2 shedding from MvECs. Further

studies showed that the shed molecule can have pro-angiogenic effect on MvECs, suggesting that the vascular function of syndecan-2 might result from a quite complicated balance of its functions on the cell surface, the regulation of its shedding and a possible autocrine or paracrine role as a shed effector (Fears et al., 2006).

Furthermore, Human microvascular ECs (HMEC-1) predominantly express syndecan-2 (around 80% of all HSPG on the cell surface) and its expression is increased in response to angiogenic stimuli (especially FGF) and is dependent on the type of matrix cells are seeded on. Interestingly, down-regulation of syndecan-2 resulted in decreased cell attachment and spreading and accelerated cell migration but also impaired HMEC-1 cells' ability to form capillary-like structures on Matrigel (Noguer et al., 2009).

In light of these few but important studies, it appears that syndecan-2 plays a pivotal role in angiogenesis. Unfortunately, unlike the other three members of the syndecan family, a knock-out mouse model for syndecan-2 has not yet been developed, therefore the question as to whether a syndecan-2 knock-out mouse would develop normally or die prematurely due to angiogenic defects is still left unanswered.

1.3.3. Syndecan-3

Syndecan-3 knock-out mice are viable and develop normally. Syndecan-3 is considered the main syndecan of the nervous system and as such it's been mainly investigated in behavioural studies.

However, a recent work highlighting a role for syndecan-3 in the inflammatory response of different tissues also served to demonstrate that its expression is not limited to the nervous system but it can also be found on the endothelium of different vascular beds (joints, dermis and cremaster muscle) (Kehoe et al., 2014).

We recently showed a potential therapeutic effect of the syndecan-3 extracellular core protein in pathologies where angiogenesis is increased. Recombinant bacterially-derived (hence lacking the glycosaminoglycan chains) syndecan-3 extra-cellular domain was shown to being able to significantly inhibit angiogenesis in the *ex vivo* model of the aortic ring assay and also inhibit skin and brain EC tube formation and cell migration through collagen in 2D and 3D (De Rossi and Whiteford, 2013). These data support the idea that syndecan core proteins when released from the cell surface can act as important effectors of cell behaviour.

1.3.4. Syndecan-4

Although syndecan-4 was found up-regulated throughout the granulation tissue during skin injury on ECs (Gallo et al., 1996b), the first clear evidence of a functional role in angiogenesis came from the work of Echtermeyer et al. in 2001. Here they generated a syndecan-4 knock-out mouse which showed significantly delayed wound healing in a model of skin injury. Although the number of newly generated vessels populating the healing tissue was not affected by the lack of syndecan-4, the vessels were smaller compared to the wild-type littermates (Echtermeyer et al., 2001a).

Syndecan-4 has later been found to be essential in mediating the pro-angiogenic effects of Thrombospondin-1 (TSP-1). The study proposed a model whereby two heparin-binding sequences contained within TSP-1 are able to compete with fibronectin for the interaction with syndecan-4, thus interfering with syndecan-4-mediated EC adhesion (Nunes et al., 2008).

In vitro experiments on ECs have shown that syndecan-4 is also key player in FGF signalling (Murakami et al., 2002b; Volk et al., 1999). Interestingly, it is not just by facilitating the interaction between FGF2 and its receptor FGFR1, but syndecan-4 cytoplasmic domain seems to have a key role as chimeras and deletion mutants of this portion lacking the V or the C2 regions fail to promote an effective intracellular response to FGF2. In particular, lack of the C2 region (which contains the PDZ binding domain) prevents the binding of GIPC/Synectin which results in a failure to activate Rac1 and thus inhibits EC migration (Tkachenko et al., 2006; Tkachenko et al., 2004).

Quite recently syndecan-4 has been shown to participate in the signalling initiated by another pro-angiogenic molecule, Prostaglandin E_2 (PGE_2). The study revealed that in murine ECs lacking syndecan-4 PGE_2-mediated pro-angiogenic effects (i.e. EC migration and tube formation) were decreased. They also show that syndecan-4 activation of PKCα is necessary for the phosphorylation of ERK following PGE_2 stimulation. This molecular mechanism was confirmed *in vivo* by showing a diminished angiogenic response to PGE_2 both in the syndecan-4 and in the PKCα knock-out mice compared to the wild type (Corti et al., 2013).

2. General aims of the work

Angiogenesis, the formation of new blood vessels from pre-existing ones, is both a physiological process and a key pathological feature of many diseases such as cancer, chronic inflammatory conditions and diseases of the eye. As a consequence, numerous anti-angiogenic therapies have been developed over the past few years and are currently used in the clinic or are in the clinical trial phase. The principal targets of these therapies are the VEGF/VEGFR2 pathway and the integrin family of adhesion receptors, as these molecules have pivotal roles in the process of new blood vessel formation. Unfortunately, anti-angiogenic therapies have not quite met with the expectations: their efficiency is very heterogeneous, with a large number of patient non-responders, and often produce toxic side effects due to unspecificity. Nonetheless, the huge potential of blocking new blood vessel formation to stop angiogenesis-dependent disease progression or even revert it is undeniable. There is therefore a critical need to better understand the process of angiogenesis and endothelial cell biology to improve the current anti-angiogenic therapies or develop new therapeutic strategies.

Why study the roles and effects of syndecans on endothelial cell biology during the process of angiogenesis?

The studies reviewed in section 1.3 indicate important roles of the syndecan family of HSPGs in EC biology. The original work presented in this thesis aimed to build on these works by focussing on the role of syndecans in relation to EC biology and angiogenesis. The specific purpose of this work was not only to increase the understanding of the complex process of new blood vessel formation but also to test the potential of syndecans as substrates and/or targets for anti-angiogenic therapies.

To this end, this thesis will describe two projects that I have carried out during the course of my PhD:

Project 1 (sections 4.1 and 4.2)

Key background: Contained within syndecan ectodomains are adhesion-regulatory domains.

Aim 1: To establish whether the ectodomains of syndecan-1, -2, -3 and -4 can affect endothelial cell adhesion/migration and angiogenesis *in vitro*.

In addressing this aim, I observed that all 4 syndecan ectodomains possess anti-angiogenic properties. Because of time restrictions, I decided to only follow up one of the four members. I chose syndecan-2 because it is expressed in the vasculature; this formed the basis of aim 2.

Aim 2: To investigate the anti-angiogenic properties of syndecan-2 ectodomain, aiming to characterise its mechanism of action and test its potential as an anti-angiogenic molecule in pathological models of angiogenesis *in vivo*.

Project 2 (section 4.3)

Key background: Syndecan-4 deficient mouse is viable, fertile and with no abnormalities; however, it develops a phenotype in certain pathologies characterised by an angiogenic response.

Aim: Determine if the full-length syndecan-4 has a role in the angiogenic process.

3. Materials and methods

3.1. Reagents

3.1.1. Antibodies

Reactivity	Host - Isotype	Target	Stock Conc.	Dilution / Fig.	Company	Catalogue number
12 aa HA tag	Mou IgG1	**HA tag**	1 ug/ul	1:1000 / Fig. 4.13 Fig. 4.21	Covance	MMS-101P
Human (h)/ Mouse (m)/ Rat (r)	poly Goat IgG	**CD148**	0.5 ug/ul	1:200 / Fig. 4.33 Fig. 4.34	R&D	AF1934
h/m/r	Mou IgG1	**β tubulin**	Unknown	1:1000 / Fig. 4.33 Fig. 4.63	Sigma	T4026
m	Rat IgG2a,κ	**CD29 - β1 integrin (9EG7)**	0.5 ug/ul	1:200 / Fig. 4.36 Fig. 4.37 Fig. 4.38	BD	553715
h	Rat IgG2a,κ	**CD29 - β1 integrin (Mab13)**	0.5 ug/ul	1:200 / Fig. 4.36	BD	552828
h/r	Mou IgG2b	**CD29 - β1 integrin (HUTS4)**	0.5 ug/ul	1:300 / Fig. 4.39	Millipore	MAB2079Z
m	Rat IgG2a, κ	**CD31 - PECAM-1 (390)**	0.5 ug/ul	1:100 / Fig. 4.18 Fig. 4.25 Fig. 4.53 1:400 / Fig. 4.27	eBioscience	11-0311
h/m/r	Mou IgG2a	**α-SMA (1A4)**	15 - 55 mg/ml	1:200 / Fig. 4.43 Fig. 4.44 Fig. 4.48 Fig. 4.49	Sigma	A2547
m	Rat IgG1κ		0.5 ug/ul		eBioscience	14-1441

		VE-Cadherin (BV13)		1:200 / Fig. 4.43 Fig. 4.44 1:100 / Fig. 4.68		
m	Rat IgG2a,k	**syndecan-4 (KY/8.2)**	0.5 ug/ul	1:200 / Fig. 4.48 Fig. 4.49 Fig. 4.62 1:1000 / Fig. 4.62	BD	550350
m	Rat IgG2a,κ	**Isotype control**	0.5 ug/ul	1: 200 / Fig. 4.49	BD	553927
h	Poly Rab IgG	**syndecan-4 (H-140)**	0.5 ug/ul	1:400 / Fig. 4.64 Fig. 4.66	Santa Cruz	15350
m	Poly Rab IgG	**syndecan-2 N-term**	1 ug/ul	1:800 / Fig. 4.66	Santa Cruz	15348
h/m	Rab IgG	**VEGFR2**	Unknown	1:1000 / Fig. 4.63 Fig. 4.67	Cell Signalling	9698
h/m	Rab IgG	**VEGFR2 pY1059**	Unknown	1:1000 / Fig. 4.63 Fig. 4.67	Cell Signalling	3817
h/m	Rab IgG	**VEGFR2 pY1175**	Unknown	1:1000 / Fig. 4.67	Cell Signalling	3770
m	poly Goat IgG	**VEGFR2 - N-term**	0.5 ug/ul	1:400 / Fig. 4.64 Fig. 4.66	R&D	AF644

Table 3 **Antibodies.**

3.1.2. Stimuli

Stimulus	Details and Company

Tumor necrosis factor-α (TNF-α)	Mouse TNF-α, R&D Systems, 401-ML-010/CF
Vascular endothelial growth factor A (VEGF-A)	Recombinant Mouse VEGF 164 R&D Systems, 493-MV-025
Phorbol 12-myristate 13-acetate (PMA)	Sigma, P8139
Angiopoietin-2	Recombinant human angiopoietin-2 R&D Systems 623-AN-025
Basic Fibroblast growth factor (FGF-2 or bFGF)	Invitrogen, PHG0026

Table 4 **Stimuli.**

3.1.3. General reagents

Reagent	Details and Company
7-Aminoactinomycin D (7-AAD)	Approximately 97%, Sigma (Poole, Dorset, UK)
Agarose	Invitrogen (Paisley, UK)
BS1-Isolectin	I21412 Invitrogen (Paisley, UK)
Bovine serum albumin (BSA)	New England Biolabs (Hitchin, UK)
Calcein	C3100MP Invitrogen (Paisley, UK)
Dapi	D9542 Sigma-Aldrich (Poole, Dorset, UK)
Deoxynucleotide triphosphates (dNTPs)	Bioline Reagents Ltd. (London, UK)
DNA Ladder	SmartLadder SF, Eurogentec (Southampton, UK)
Draq5	Draq5TM nuclear dye, c= 5 mM, Biostatus limited (Shepshed, UK)

EDTA	Sigma, E5134-100G
Ethanol	VWR (Soulbury, UK)
Evans Blue dye	VWR (Soulbury, UK)
Phalloidin	A12380 Invitrogen (Paisley, UK)
Formamide	VWR (Soulbury, UK)
GelRed	Biotum, via Cambridge BioScience (Cambridge UK)
Goat serum (GS)	Normal GS, AbD Serotec (Kidlingdon, UK)
Magnesium chloride (MgCl2)	Bioline Reagents Ltd. (London, UK)
Methanol	VWR (Soulbury, UK)
Paraformaldehyde (PFA)	VWR (Soulbury, UK)
Sodium Chloride (NaCl)	Fluka BioChemica, Sigma-Aldrich (Poole, Dorset, UK)
Sodium dodecyl sulphate (SDS)	10% SDS solution, Severn Biotech Ltd. (Kidderminister, UK)
Tris-Acetate-EDTA (TAE) buffer	UltraPure™ 10x TAE buffer Invitrogen (Paisley, UK)
Tris-HCl	1 M Tris-HCl solution, pH 8.5, Severn Biotech Ltd. (Kidderminister, UK)
Triton X-100	Sigma-Aldrich (Poole, Dorset, UK)

Table 5 **General reagents.**

3.1.4. Microscopes

Zeiss LSM 5 PASCAL confocal laser-scanning microscope (Carl Zeiss Ltd, Welwyn Garden City, UK) and a 10X Plan-Neofluar objective (numerical aperture 0.30) or a 63X oil-dipping Plan-apochromat objective (numerical aperture 1.4).

Olympus IX81 motorised inverted microscope (Olympus Medical, Southend-on-Sea, UK).

3.2. *In vitro* methods

3.2.1. RNA isolation

RNA was isolated from adherent cells using a RNeasy micro kit (QIAGEN). The RNeasy Micro Kit is designed for isolation of total RNA from small samples and comes with a series of buffers. Initially samples are lysed by addition of the buffer on the cell mono-layer and then homogenized. Ethanol is added to the lysate to provide ideal binding conditions. The lysate is then loaded onto the RNeasy MinElute spin column and RNA binds to the silica membrane. Rnase-free Dnase, provided in the RNeasy Micro Kit, enables simple and efficient on-column digestion of genomic DNA for sensitive applications. Then Dnase and any contaminants are efficiently washed away, and pure, concentrated RNA is eluted in 14 µl water. Following the isolation steps, RNA concentration and purity was measured using Nanodrop apparatus (Thermo Scientific). Concentrations varied within the range of 0.1-1 µg/µl and samples were considered pure from DNA contamination or other contaminants when with a A260/A230 ratio around 2 and a A260/A290 ratio between 2.0-2.2, respectively. Samples were then stored at -80°C.

3.2.2. cDNA synthesis

cDNA Synthesis from mRNA was performed using the iSCRIPT Kit (BioRad). Briefly, X volume of RNA solution, corresponding to 1 µg of RNA sample, was mixed with the 5X iSCRIPT reaction mix containing oligo (dT) and random exomers, the 20X iSCRIPT reverse transcriptase and brought to a volume of 20 µl with nuclease-free water.

Reagents	**Volume (µl)**
5x iSCRIPT reaction mix	4
iSCRIPT reverse transcriptase	1
Nuclease-free water	15-x
RNA (1 µg)	x
TOT	20

The samples were then processed in a thermocycler (DNAengine, Bio Rad) and the programme set as below:

Reagents	Temperature	Time
iSCRIPT activation	25°C	5’
Annealing	42°C	30’
Extension	85°C	5’
	4°C	∞

3.2.3. RT-PCR

To analyse the expression of syndecan-4 and GAPDH, cDNA samples were then diluted 1:5 with nuclease-free water and 5 µl were used to perform RT-PCR using reagents provided by the KOD PCR kit (Novagen). Primer sequences were designed to anneal to two adjacent exons.

Primers			Annealing T
syndecan-4 forward	5'-3'	GGT CTT GGC AGC TCT GAT C	55.6
syndecan-4 reverse	5'-3'	CAC CAG AAA GGT GAC TAG AG	52.1
product length	299 bp		

Primers			Annealing T
GAPDH forward	5'-3'	TCG TGGA TCT GAC GTG CCG CCT G	75
GAPDH reverse	5'-3'	CAC CAC CCT GTT GCT GTA GCC GTA	72
Product length	251 bp		

Reaction was set as follows:

Reagents	Volume (µl)

10x KOD buffer	5
25mM MgSO4	3
dNTPs	5
Forward primer (5μM)	1.5
Reverse primer (5 μM)	1.5
KOD polymerase	1
cDNA	5
Water	28
TOT	50

The samples were then processed in a thermocycler (DNAengine, Bio Rad) with the programme set as below:

Step	**Reagents**	**Temperature**	**Time**
1	KOD pol activation	95°C	2'
2	denaturing	95°C	20"
3	annealing	Ta	10"
4	extension	70°C	3’
5	Step 2 to 4		28 times
6		4°C	∞

3.2.4. qPCR

cDNA was synthesized from 10ng total RNA using the iScript cDNA synthesis kit (Biorad) and quantitative real time PCR was performed on an ABI7900HT (Applied Biosystems) real time PCR machine and reactions were prepared using the iQ Sybr green supermix (Biorad). Primers used in this study are described in 3.2.3.

Values were expressed as Increase relative to UT ($2^{\Delta\Delta Ct}$), according to the following formula:

$2^{\Delta\Delta Ct}$ where $\Delta\Delta Ct$ = (Ct S4 UT – Ct HK UT) – (Ct S4 T – Ct HK T)

UT= untreated T=treated HK=house-keeping gene S4=syndecan-4 gene

3.2.5. Gel electrophoresis

After amplification, blue agarose gel electrophoresis loading buffer (1:6) was added to the samples and 10 µl were run on a 3 % (w/v) agarose gel (in TAE buffer) supplemented with 2 µl GelRed. A 100 – 1,000 bp DNA ladder was used as a marker. Gels were left running in an electrophoresis chamber (Mupid®-One electrophoresis system, Eurogentec, Southampton, UK) for approximately 45' at 90 V. Subsequently, gel pictures were taken under ultraviolet light on a UV White Darkroom BioImaging system (UVP, Cambridge, UK).

3.2.6. Protein analysis

3.2.6.1. Sodium dodecyl sulfate-polyacrylamide gel electrophoresis (SDS-PAGE)

All samples were boiled at 100°C for 5' in SDS-sample buffer, syringed with a 23.5 gauge needle to decrease viscosity, and loaded on a 7.5% polyacrylamide gel with 1x TGS running buffer. Precision Plus protein marker (Biorad, Hertfordshire, UK) was used as molecular weight standard and samples were run at 100 V for approximately 1h30'.

3.2.6.2. Western Blotting

Following SDS-PAGE separation, gels were equilibrated in cathode buffer (1,5 g Tris Base (Fisher BP152-1), 3 g Glycine (Sigma G8898), 10% Methanol, deionized water for at least 10' and proteins were transferred to nitrocellulose membranes (Immobilon-P, Millipore), using a Biorad Trans Blot Cell apparatus. Prior to transfer, membranes were activated in 100% methanol for 30'', washes in milliQ water for 3' and equilibrated in anode buffer II (1,5 g Tris

Base (Fisher BP152-1), 10% Methanol, deionized water). The transfer sandwich was then set up as shown below (anode buffer I is composed of 18,5 g Tris Base (Fisher BP152-1), 10% Methanol, deionized water):

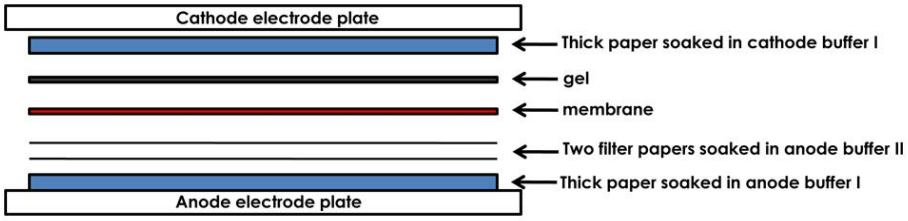

Semi-dry transfer was run at 0.5 mA for 1h45'. Membranes were then blocked for 1h in blocking buffer (5% BSA in TBST or 3% milk and 1% BSA in TBST for β-tubulin). Subsequently, membranes were washed once in TBST and incubated overnight at 4°C with primary Ab in blocking buffer. Then membranes were washed 3 times in TBST and incubated for 1-2 hrs in secondary Ab conjugated to HRP in blocking buffer. After 3 washes in TBST, membranes were incubated 1' in SuperSignal solution, as per the manufacturer's instructions, and developed using an SRX-101A medical film processor (Konica Minolta, Tokyo, Japan).

3.2.6.3. Immunoprecipitation

Medium was removed and adherent cells were gently washed with PBS. 1 ml of lysis buffer (1% Triton, Protease and Phosphatase Inhibitor 1X in PBS) was added to the plate and cells detached from the plate with a cell-scraper and collected in a 1.5 ml tube. Samples were then centrifuged at max speed for 10' and supernatant moved to a new 1.5 ml tube. In the meantime, affinity bead (EZ view red protein G affinity gel, SIGMA) equilibration was carried out. 10 µl of bead solution (2/sample) were pipetted into a 1.5 ml tube and 1 ml of dH_2O was added, samples were pulsed in the centrifuge for 10'', supernatant discarded and beads resupended in 1 ml of PBS and centrifuged again for 10'' (wash in PBS was performed twice). One bead solution was resuspended in 50 µl of 1% triton in PBS, added to each supernatant and left on a rotator for 1 hour. The solution was then centrifuged for 10'' and supernatant moved to a new 1.5 ml tube. The second bead solution was resuspended in 1 ml of PBS containing 5 µg of anti-HAtag Ab (Covance) and put on a rotator for 1 hour. Solution was then centrifuged for 10'' and resuspended in 50 µl of 1% triton. The Ab-coated beads were then added to the supernatant containing tubes and left over-night on a rotator at 4 °C. Tubes were then centrifuged at full speed for 3' and the pellet washed in PBS and resuspended in 20 µl of SDS

loading buffer. Supernatant was kept for β-tubulin analysis. Samples were then boiled at 100 °C and loaded on a 7.5% poly-acrylamide gel. Subsequently, gel electrophoresis and semi-dry transfer were carried out (see protocols above).

3.2.6.4. Dot blotting

Samples were diluted in blotting buffer (0.15 M NaCl buffered to pH 4.5 with 50 mM sodium acetate, and with 0.1% Triton X-100) and applied under vacuum to cationic nylon membranes (GE; Amersham Hybond™-N+) inserted into a slot blot apparatus (Hoefer PR648). Membranes were washed three times with blotting buffer, blocked for 1 h in blocking buffer (3% milk, 0.5% BSA, 0.15 M NaCl in 10 mM TRIS, pH 7.4), incubated over night with 1 ug/ml of mAb syndecan-2 (R&D) in blocking buffer plus 0.3 % Tween-20, washed with TBST three times (0.3% Tween-20), incubated for 2 hrs with HRP-conjugated anti-Rat IgG at 1:5000 dilution (Invitrogen) in blocking buffer plus 0.3 % Tween-20, washed with TBST three times (0.3% Tween-20). Signals were detected after addition of ECL substrate (Thermo Scientific) according to manufacturer instructions. Quantification of the signal intensity was performed using ImageJ software (http://rsbweb.nih.gov/ij/index.html).

3.3. Cell-based methods

3.3.1. Cell culture

Brain ECs (bEND3.1) and skin ECs (sEND) were obtained from Health Protection Agency (HPA) UK and were grown in DMEM (PAA, GE Healthcare) supplemented with 10% FBS, 2 mM l-glutamine, 1% non-essential amino acids, 1% Penicillin (10,000 u/ml)/ Streptomycin (10 mg/ml), 1 mM sodium pyruvate and 5 μM β-mercaptoethanol (all Invitrogen), at 37°C, 10% CO2.

HEK293T were purchased from HPA culture collection and grown in DMEM, as above.

Human umbilical vein ECs (HUVEC) were obtained from HPA laboratories and were grown in in-house made medium (MLEC medium) which contained:

- 40% ml Modified Eagles Medium low glucose (ref. 21885 Invitrogen)
- 40% ml Hams F-12 medium (ref. 31765 Invitrogen)
- 20% ml heat-inactivated Fetal Bovine Serum
- 100 mg/l Heparin (sls, H3149-100KU)
- 1% Penicillin (10,000 u/ml)/ Streptomycin (10 mg/ml).
- 50mg/l EC growth supplement (Sigma, E2759)

Opti-MEM® I Reduced Serum Medium (Invitrogen, 31985-054) was also used during cell treatments and for aortic ring and choroid explant assay.

3.3.2. Expression of syndecan ectodomain GST-fusion proteins

These constructs were designed, transformed into *E. coli* and purified by Dr. James Whiteford.

The ectodomain sequences were amplified using the primer pairs indicated. Subsequently, PCR products were kinased and digested with indicated restriction enzymes prior to ligation into the bacterial expression vector pET-41 (Novagen).

Gene	Primers	Restriction enzymes
hsyndecan-1	FOR ttaaggatcccagccggccctgccgc REV ttatataagcttctagaggaggccctgtgagg	HindIII and Bam HI
msyndecan-2	FOR ggagacgagaacagagctga REV tatatgaattcttaaaacagattgtctgaatgtttct	EcoRi and PshA1
hsyndecan-3	FOR ttaattgaattcgctcaacgctggcgcaatg REV ttaattaagcttctacagtatgctcttctgaggga	EcoRI and HIndIII
hsyndecan-4	FOR agagtcgatcccgagagactg REV taataaggatccaaagatgttgctgccctgca	BamHI AND PshA1

Human syndecan-1 (cDNA, ectodomain)

```
>human SYNDECAN-1 cDNA 933 bp
ATGAGGCGCGCGGCGCTCTGGCTCTGGCTGTGCGCGCTGGCGCTGAGCCTGCAGCCGGCCCTGCCGCAAA
TTGTGGCTACTAATTTGCCCCCTGAAGATCAAGATGGCTCTGGGGATGACTCTGACAACTTCTCCGGCTC
AGGTGCAGGTGCTTTGCAAGATATCACCTTGTCACAGCAGACCCCCTCCACTTGGAAGGACACGCAGCTC
CTGACGGCTATTCCCACGTCTCCAGAACCCACCGGCCTGGAGGCTACAGCTGCCTCCACCTCCACCCTGC
CGGCTGGAGAGGGGCCCAAGGAGGGAGAGGCTGTAGTCCTGCCAGAAGTGGAGCCTGGCCTCACCGCCCG
GGAGCAGGAGGCCACCCCCCGACCCAGGGAGACCACACAGCTCCCGACCACTCATCTGGCCTCAACGACC
ACAGCCACCACGGCCCAGGAGCCCGCCACCTCCCACCCCCACAGGGACATGCAGCCTGGCCACCATGAGA
CCTCAACCCCTGCAGGACCCAGCCAAGCTGACCTTCACACTCCCCACACAGAGGATGGAGGTCCTTCTGC
CACCGAGAGGGCTGCTGAGGATGGAGCCTCCAGTCAGCTCCCAGCAGCAGAGGGCTCTGGGGAGCAGGAC
TTCACCTTTGAAACCTCGGGGGAGAATACGGCTGTAGTGGCCGTGGAGCCTGACCGCCGGAACCAGTCCC
CAGTGGATCAGGGGGCCACGGGGGCCTCACAGGGCCTCCTGGACAGGAAAGAGGTGCTGGGAGGGGTCAT
TGCCGGAGGCCTCGTGGGGCTCATCTTTGCTGTGTGCCTGGTGGGTTTCATGCTGTACCGCATGAAGAAG
AAGGACGAAGGCAGCTACTCCTTGGAGGAGCCGAAACAAGCCAACGGCGGGGCCTACCAGAAGCCCACCA
AACAGGAGGAATTCTATGCCTGA
```

Human syndecan-1 (protein sequence, ectodomain)

```
>human syndecan-1 311 aa
  1 mrraalwlwl calalslqpa lpqivatnlp pedqdgsgdd sdnfsgsgag alqditlsqq
 61 tpstwkdtql ltaiptspep tgleataast stlpagegpk egeavvlpev epgltareqe
121 atprprettq lptthqastt tattaqepat shphrdmqpg hhetstpagp sqadlhtpht
181 edggpsater aaedgassql paaegsgeqd ftfetsgent avvavepdrr nqspvdqgat
241 gasqglldrk evlggviagg lvglifavcl vgfmlyrmkk kdegsyslee pkqanggayq
301 kptkqeefya
```

Murine syndecan-2 (cDNA, ectodomain)

>murine SYNDECAN-2 609 bp
ATGCAGCGCGCGTGGATCCTGCTCACCTTGGGCTTGATGGCCTGTGTGTCCGCAGAGACG
AGAACAGAGCTGACATCCGATAAGGATATGTACCTTGACAATAGCTCCATTGAGGAAGCT
TCAGGAGTATATCCTATTGATGATGATGACTATTCTTCTGCCTCAGGCTCAGGAGCTGAT
GAAGACATAGAGAGTCCAGTTCTGACAACATCCCAACTGATTCCAAGAATCCCACTCACT
AGTGCTGCTTCCCCCAAAGTGGAAACCATGACGTTGAAGACACAAAGCATTACACCTGCT
CAGACTGAGTCACCTGAAGAAACTGACAAGGAGGAAGTTGACATTTCTGAGGCAGAAGAG
AAGCTGGGCCCTGCTATAAAAAGCACAGATGTGTACACGGAGAAACATTCAGACAATCTG
TTTAAACGGACAGAAGTTCTAGCAGCCGTCATTGCTGGTGGTGTGATCGGCTTTCTCTTT
GCCATTTTCCTCATCCTGCTATTGGTGTACCGCATGCGGAAGAAAGATGAAGGAAGCTAC
GACCTTGGAGAACGCAAACCATCCAGCGCAGCTTACCAGAAGGCACCCACTAAGGAGTTT
TATGCATAA

Murine syndecan-2 (protein sequence, ectodomain, adhesion regulatory domain)

>murine syndecan-2 204 aa
  1 mqrawilltl glmacvsa**et rteltsdkdm yldnssieea sgvypidddd yssasgsgad**
 61 ediespvltt sqlipriplt saaspkvetm tlktqsitpa qtespeetdk eevdiseaee
121 klgpaikstd vytekhsdnl fkrtevlaav iaggvigflf aiflilllvy rmrkkdegsy
181 dlgerkpssa ayqkaptkef ya

>S2ED
etrteltsdkdmyldnssieeasgvypiddddyssasgsgadediespvlttsqliprip
ltsaaspkvetmtlktqsitpaqtespeetdkeevdiseaeeklgpaikstdvytekhsd
nlf

>S2EDΔP124-F141
etrteltsdkdmyldnssieeasgvypiddddyssasgsgadediespvlttsqliprip
ltsaaspkvetmtlktqsitpaqtespeetdkeevdiseaeeklg

>S2EDΔL73-G123
etrteltsdkdmyldnssieeasgvypiddddyssasgsgadediespvlttsqpaikst
dvytekhsdnlf

Human syndecan-3 (cDNA, ectodomain)

>human syndecan-3 cDNA 1329 bp
ATGAAGCCCGGGCCGCCGCGCCGCGGGACCGCACAGGGGCAGCGCGTGGACACCGCCACC
CATGCGCCCGGGGCCCGCGGGCTGTTGCTGCCACCGCTGCTGCTGCTGCTGCTGGCCGGC
CGCGCCGCGGGGGCTCAACGCTGGCGCAATGAGAACTTCGAGAGGCCGGTGGATCTTGAG
GGCTCAGGGGATGACGACTCGTTTCCTGATGATGAACTAGACGACCTCTACTCGGGGTCA
GGCTCTGGCTACTTCGAGCAGGAGTCCGGCCTTGAGACGGCCATGCGGTTCATCCCTGAT
ATGGCCCTGGCTGCGCCCACTGCACCTGCCATGCTACCCACAACCGTTATCCAGCCCGTG
GACACCCCATTTGAGGAACTCCTTTCTGAGCACCCCAGCCCTGAACCAGTCACCAGTCCC
CCGCTGGTGACAGAGGTGACAGAGGTCGTAGAAGAGTCCAGCCAGAAAGCTACCACCATC
TCTACCACCACATCTACCACCGCGGCCACCACCACAGGGGCCCCAACTATGGCCACAGCA
CCTGCCACAGCAGCCACCACTGCCCCTAGCACTCCCGAGGCGCCCCCTGCCACGGCTACC
GTGGCTGACGTAAGGACCACCGGCATACAGGGGATGCTGCCTCTTCCCCTGACCACAGCT
GCCACAGCCAAGATCACTACCCCAGCAGCACCCTCACCACCCACTACTGTGGCTACCTTG
GACACAGAGGCCCCGACACCTAGGCTGGTCAACACAGCTACCTCGAGGCCACGAGCCCTT
CCTCGGCCAGTCACCACCCAGGAGCCTGATGTTGCTGAGAGGAGTACCCTGCCGTTGGGG
ACCACGGCTCCTGGACCCACGGAGATGGCTCAGACCCCAACTCCAGAGTCCCTTCTGACC

ACCATCCAGGATGAGCCAGAGGTGCCAGTAAGTGGGGGGCCCAGCGGGGACTTTGAGCTT
CAAGAAGAGACCACGCAGCCGGACACGGCCAATGAGGTGGTGGCTGTGGAAGGAGCCGCG
GCCAAGCCGTCACCTCCACTGGGGACACTGCCCAAGGGTGCCCGCCCAGGCCCTGGCCTC
CACGACAATGCCATCGATTCGGGCAGCTCGGCCGCCCAGCTCCCTCAGAAGAGCATACTG
GAGCGGAAGGAGGTGCTCGTAGCCGTGATCGTGGGTGGGGTGGTGGGCGCCCTCTTCGCT
GCCTTCCTGGTCACGCTGCTCATCTACCGCATGAAGAAGAAGGACGAAGGCAGCTACACC
TTGGAAGAACCCAAGCAGGCAAGCGTCACGTACCAGAAACCTGACAAGCAGGAGGAGTTC
TACGCTTAG

Human syndecan-3 (protein sequence, ectodomain)

```
>human syndecan-3 442 aa
  1 mkpgpphrag aahgagagag aaagpgargl llppllllll agraagaqrw rsenferpvd
 61 legsgdddsf pddelddlys gsgsgyfeqe sgietamrfs pdvalavstt pavlpttniq
121 pvgtpfeelp serptlepat splvvtevpe epsqrattvs ttmattaats tgdptvatvp
181 atvatatpst paappftatt avirttgvrr llplplttva tarattpeap sppttaavld
241 teaptprlvs tatsrpralp rpattqepdi perstlplgt tapgptevaq tptpetfltt
301 irdepevpvs ggpsgdfelp eeettqpdta nevvavggaa akasppgtl pkgarpgpgl
361 ldnaidsgss aaqlpqksil erkevlvavi vggvvgalfa aflvtlliyr mkkkdegsyt
421 leepkqasvt yqkpdkqeef ya
```

Murine syndecan-4 (cDNA, ectodomain)

```
>murine syndecan-4 cDNA 597 bp
ATGGCCCCCGCCCGTCTGTTCGCGCTGCTGCTGTTCTTCGTAGGCGGAGTCGCCGAGTCGATCCGAGAGA
CTGAGGTCATCGACCCCCAGGACCTCCTAGAAGGCCGATACTTCTCCGGAGCCCTACCAGACGATGAGGA
TGTAGTGGGGCCCGGGCAGGAATCTGATGACTTTGAGCTGTCTGGCTCTGGAGATCTGGATGACTTGGAA
GACTCCATGATCGGCCCTGAAGTTGTCCATCCCTTGGTGCCTCTAGATAACCATATCCCTGAGAGGGCAG
GGTCTGGGAGCCAAGTCCCCACCGAACCCAAGAAACTAGAGGAGAATGAGGTTATCCCCAAGAGAATCTC
ACCCGTTGAAGAGAGTGAGGATGTGTCCAACAAGGTGTCAATGTCCAGCACTGTGCAGGGCAGCAACATC
TTTGAGAGAACGGAGGTCCTGGCAGCTCTGATTGTGGGTGGCATCGTGGGCATCCTCTTTGCCGTCTTCC
TGATCCTACTGCTCATGTACCGTATGAAGAAGAAGGATGAAGGCAGCTATGACCTGGGCAAGAAACCCAT
CTACAAGAAAGCCCCCACCAATGAGTTCTACGCGTGA
```

Murine syndecan-4 (protein sequence, ectodomain)

```
>Murine syndecan-4 198 aa
  1 maparlfall lffvggvaes iretevidpq dllegryfsg alpddedvvg pgqesddfel
 61 sgsgdlddle dsmigpevvh plvpldnhip eragsgsqvp tepkkleene vipkrispve
121 esedvsnkvs msstvqgsni fertevlaal ivggivgilf avflilllmy rmkkkdegsy
181 dlgkkpiykk aptnefya
```

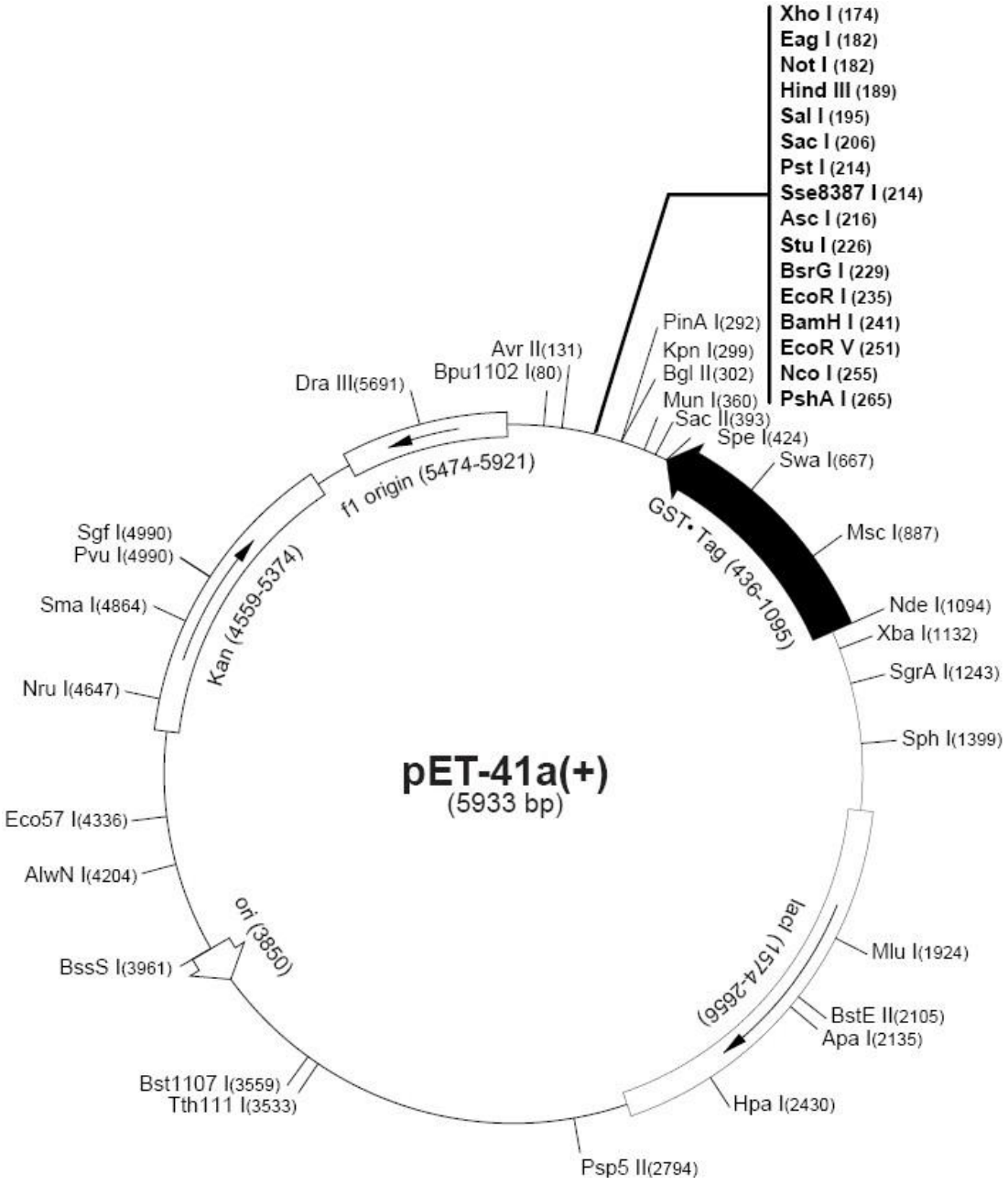

Fig. 3.1 **pET-41 plasmid for bacterial expression of syndecan ectodomains.**

Plasmids were then transformed into the Escherichia coli BL21 strain (Promega), and the bacteria were grown to an A600 of 0.6 at 37 °C prior to the addition of 0.25 ml/liter 1 M isopropyl 1-thio-β-D-galactopyranoside (Calbiochem) followed by a further 3 hours incubation. Bacteria were resuspended in phosphate buffered saline (PBS), lysed in a

sonicator, and GST syndecan ectodomain fusion proteins were purified on columns of glutathione-Sepharose 4B (GE Healthcare) as described in the manufacturer's protocol.

Fusion proteins were then run in a SDS-Page to verify the correct expression and molecular size (Fig. 3.2).

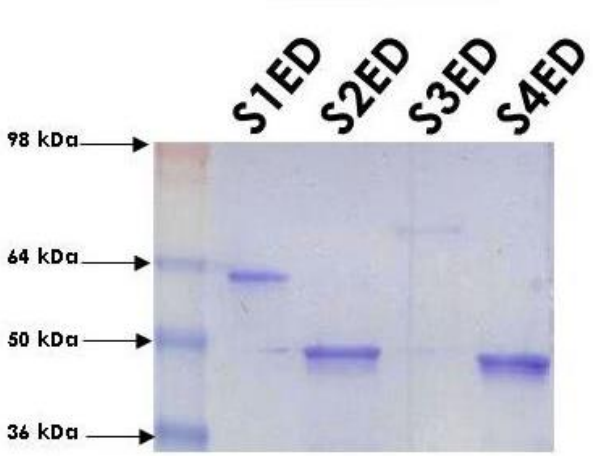

Fig. 3.2 **Syndecan ectodomains N-terminally fused to GST were produced in E.coli.** Diagram shows the structure of the proteins used in the experiments. All 4 syndecan extracellular core proteins were expressed and purified from E.coli and possess a Glutathione S-transferase (GST) fused to their N-terminus. SDS-PAGE was used to verify the correct molecular weight of the proteins.

3.3.3. Lentiviral transduction

This constructs were designed and transfected into HEK293T cells by Dr. James Whiteford.

Gene synthesis of the complete murine syndecan-2 cDNA and the cDNA encoding only the syndecan-2 ectodomain coding sequence was performed by GeneArt (Invitrogen). Both full-length and truncated syndecan-2 cDNAs were mutated such that the HA epitope was inserted between D^{27} and K^{28}. BamHI sites were also incorporated at the N and C end of the two synthetic genes. The cDNAs were cloned into the BamHI site of the lentiviral vector pLNTSFFV-MCS-EGFP (provided by Dr. Tristan MacKay, St. George's University of London). Lentiviruses were produced in HEK293T cells and packaged into a VSVG coat using conventional procedures. HEK293T cells were transfected using the supernatant transfer method. Cells expressing high levels of eGFP were sorted by flow cytometry and these were cultured in DMEM as described above.

>murine syndecan-2 221 aa

```
1   mqrawilltl glmacvsae19t  rteltsd27ypy  dvpdyak28dmy ldnssieeas gvypiddddy
61  ssasgsgade diespvl73tts  qlipriplts   aaspkvetmt   lktqsitpaq tespeetdke
121 evdiseaeek lgp124aikstdv ytekhsdnlf141* krtevlaavi  aggvigflfa iflilllvyr
181 mrkkdegsyd lgerkpssaa   yqkaptkefy    a*
```

Full length msyndecan-2

HA tag

mS2ED

18 aa peptide

stop codon *

signal peptide

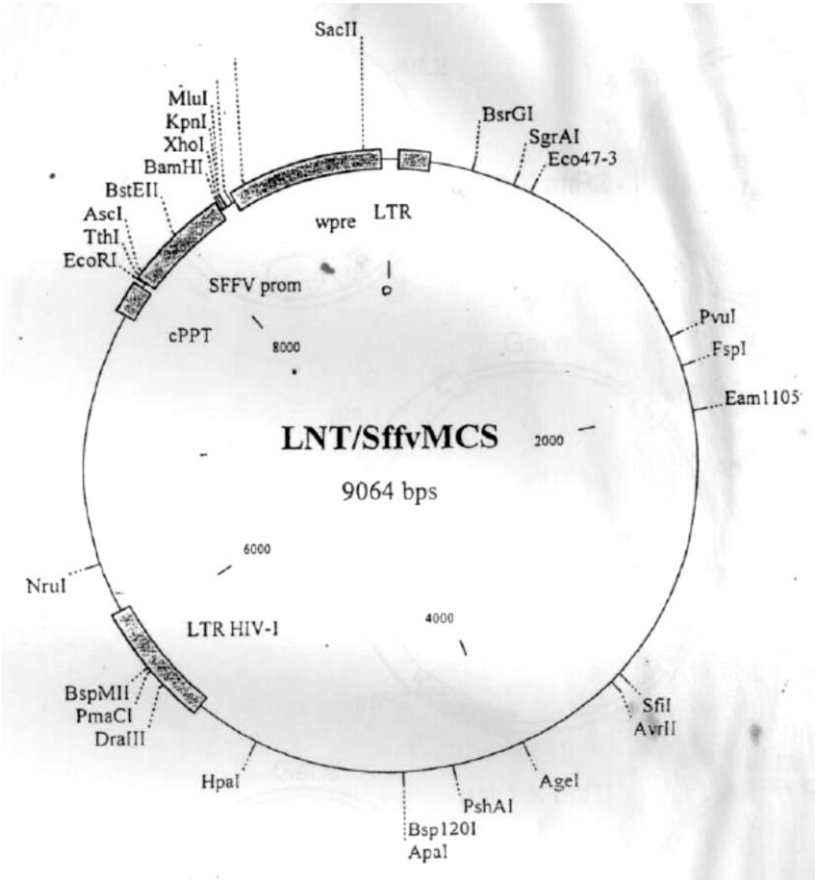

Fig. 3.3 **pLNTSFFV-MCS-EGFP lentiviral vector for expression of Syndecan-2 constructs in eukaryotic system.**

3.3.4. Scratch wound assay

ECs (primary or cell lines) were plated in a 6-well tissue culture plate. When cells reached complete confluence, a 200 µl pipette tip was used to scratch a thin line along one direction of the well. Medium was then removed, cells washed once with PBS and fresh medium containing treatments was added. The plate was then placed inside the incubator chamber of an Olympus IX81 inverted microscope connected to the computer. The software Cell^m was set to take one picture every 30' for 9 hrs of 2 spots per condition. At the end of the experiment, pictures were saved and analysed using Adobe Photoshop CS5. The gap area between the two cell fronts at time 0, 3, 6 and 9 hrs was selected and measured in pixels. The percentage of wound closure was calculated with the following formula:

$$\% \text{ wound closure at time x} = \frac{gap\ area\ time\ 0}{gap\ area\ time\ 0 - gap\ area\ time\ x}\%$$

Cell speed was quantified by manually measuring the track of individual cells migrated for 9 hours (20 cells per condition) using Adobe Photoshop, track lengths were then divided by the time to obtain cell speed.

3.3.5. Tube formation assay

The ability of ECs to associate into tubules was assessed using the V2A Kit (Cellworks), according to manufacturer instructions. In brief, human ECs were co-cultured with other human cells in a 24-well plate in a specially designed medium and kept at 37°C in 5% CO_2. The Kit provides positive control treatment (VEGF 2 ug/ml) and negative (Suramin 1 mM), together with medium, cells, plate, anti-CD45 Ab, secondary Ab conjugated to alkaline phosphatase and its substrate. Medium was changed every second day and at day 14 ECs were stained for CD31 to assess the formation of tubes. Pictures were taken on an Olympus IX81 inverted microscope (10x objectives), tube length and branching points were quantified using Photoshop (Adobe).

3.3.6. Invasion assay

EC invasion assay through collagen matrix was performed in 24-well plates with trans-well inserts (Millipore; 8 µm pore size, polyester (PET) membrane). Membranes were coated with 10 µl of Collagen Type I mixture (Millipore; 1 mg/ml in E4 medium) containing 0.5 µM GST

or syndecan ectodomains. sEND cells were seeded on the gel in a homogenous single cell suspension of $5x10^3$ cells/ insert in 200 µl of DMEM + 10% FBS; 1 ml of the same medium was added to the bottom well. Invasion was measured at 6 hours after which time gels were removed with a cotton swab, the filter washed in PBS and stained with Calcein (Invitrogen) and the number of cells attached to the filter was counted.

3.3.7. Proliferation assay

Cell proliferation was measured using the CellTiter 96 AQueous Cell proliferation assay kit as described by the manufacturer (Promega). This method is based on the ability of viable cells to reduce a tetrazolium compound (MTS) into a formazan product which is soluble in tissue culture medium and whose absorbance at 490 nm can be measured directly from a 96-well plate without additional processing. The amount of 490 nm absorbance is directly proportional to the number of living cells in culture. 5000 cells in 100 µl of complete medium were seeded in each well of a 96-well plate (Corning). At the desired time point 20 µl of MTS was added to each well and plate incubated for 1-4 hours at 37°C and 5% CO_2. The absorbance at 490 nm was then measured using an ELISA reader.

3.3.8. VE-Cadherin internalization assay

VE-cadherin internalization *in vitro* was performed as described previously (Xiao et al. 2003) with some modifications. Cells were plated on glass slides and experiments were started once cells reached complete confluence. Cells were then washed with PBS and anti-VE-Cadherin Ab (BV13 clone) was incubated with cells at 4°C for 1h in medium containing 20 mM HEPES and 3% BSA. Unbound Ab was then rinsed with ice-cold medium and cells were incubated with 30 ng/ml of VEGF-A in serum-free medium or serum-free medium alone at 37°C for 5' to allow the internalization of VE-Cadherin. An acid wash was then used to remove the Ab bound to cell-surface VE-Cadherin, this wash contained 25 mM glycine, 3% BSA in PBS (pH 2.7). Slides were then fixed in MeOH for 5' at -20°C, washed in PBS containing Draq5 (1:5000) and mounted with prolong fixative (Life Technologies).

3.3.9. Proximity ligation assay

Proximity ligation assay or PLA is a technique that allows the identification *in situ* of spots in which 2 proteins are in close proximity (less than 40 μm). The protocol requires the use of 2 primary Abs raised in different species which recognize the target antigen or antigens of interest. Species-specific secondary Abs, called PLA probes, each with a unique short DNA strand attached to it, bind to the primary Abs. When the PLA probes are in close proximity, the DNA strands can interact through a subsequent addition of two other circle-forming DNA oligonucleotides. After joining of the two added oligonucleotides by enzymatic ligation, they are amplified via rolling circle amplification using a polymerase. After the amplification reaction, several-hundred fold replication of the DNA circle has occurred, and labelled complementary oligonucleotide probes highlight the product. The resulting high concentration of fluorescence in each single-molecule amplification product is easily visible as a distinct bright spot when viewed with a fluorescence microscope.

Cells tested in the proximity ligation assay were treated as indicated in the results section. Following treatments, medium was taken off, cells washed in PBS at RT, fixed in 4% PFA for 15' at RT. After a 5' wash in PBS, PFA was quenched by incubating cells with 0.1M NH4CL for 10' at RT. Cells were then permeabilised in 0.1% triton x100 in PBS for 10 mins at RT.

The PLA experiments were performed as per manufacturer's instructions (Duolink, Sigma Aldrich).

3.3.10. Flow cytometry

Cells were washed twice with PBS, 3 ml of PBS-based dissociation buffer was added to a T75 tissue culture flask and incubated at 37°C for 3-5' until cells are detached. The cell-containing solution was then moved to a 50 ml tube and centrifuged at 1000 rpm for 3' at RT. Pellets were then resuspended in 3-5 ml of ice-cold FACS buffer (PBS with 1% NGS [normal goat serum]). Cells were then counted with a Haemocytometer and plated at a concentration of $5x10^4$ cells/well in a 96-well round bottom plate. Plates were then left on ice for 10', after which it was centrifuged at 1000 rpm for 3' at RT. Supernatant was discarded and cells resuspended in 200 μl of FACS buffer containing the appropriate dilutions of the primary Ab. Plates were then left on ice for 20' and then centrifuged at 1000 rpm for 3' at RT. The supernatant was discarded and cells resuspended in 200 μl of FACS buffer containing the appropriate dilutions of the secondary Ab. Plates were then left on ice for 20' and then centrifuged at 1000 rpm for 3' at RT. Cells were then washed to remove unbound Ab by three

washes with FACS buffer (discard supernatant, resuspend in 200 µl of FACS buffer, centrifuge at 1000 rpm for 3' at RT) after which, samples were transferred to FACS tubes, 10 µl of 7-ADD was added to the side of the tubes and samples were read using a BD FACS Calibur and CellQuest Pro software (BD).

3.3.11. β1 activation assay

Confluent bEND3.1 cells were trypsinised and the trypsin inactivated with 5% BSA. Cells were re-suspended in Hank's buffer (without Ca2+ and Mg2+) containing the treatments described (0.5 mM GST or S2ED) and incubated for 30' at 37°C. Cells were then fixed in 2% PFA prior to FACS analysis for both total and active β1 integrin and the percentage of cells expressing active β1 calculated. First cells were gated using side (SSC-H) and forward (FSC-H) scatter to exclude cell aggregates and debris, subsequently another gate was used to select the live cells based on the 7AAD staining (FL3-H). Cells were then analysed for their expression of β1 integrin (FL2-H) and active β1 integrin (FL1-H). Gates were made based on the isotype controls and this resulted into the distribution of cells in 4 quadrants: Q1 with cells negative for β1 positive for active β1 integrin, Q2 with cells double positive, Q3 with cells positive for β1 but negative for active β1 and Q4 with cells double negative.

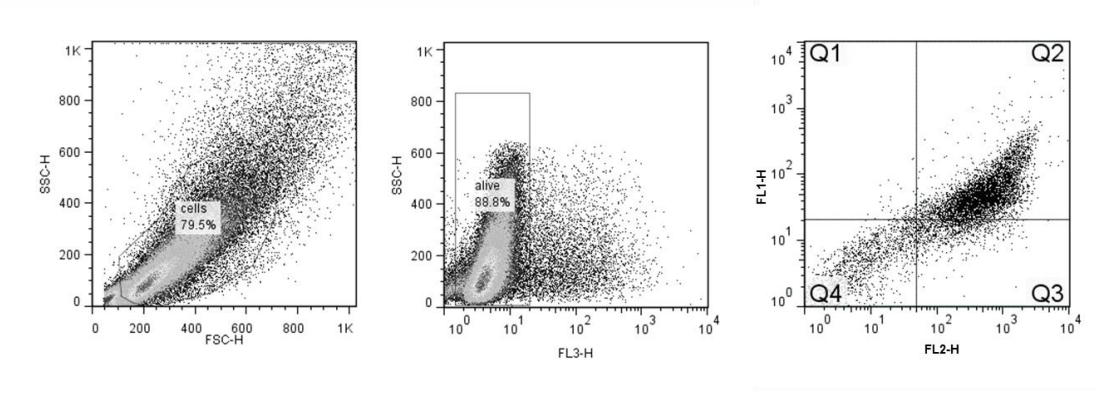

Fig. 3.4 **Flow cytometry gating strategy for active β1 integrin analysis on bEND3.1 cells.**

For immunofluorescence staining of active β1 integrin, confluent monolayers of sEND cells were grown on microscope slides and scratch wounds were made and either 0.5 µM GST or S2ED was added. After 30', cells were fixed with 4% PFA (Sigma) and permeabilized in 0.1% Triton X-100 (Sigma) in PBS. Samples were incubated with active β1-integrin-specific Ab 9EG7 in 1% normal goat serum in PBS overnight at 4°C. Slides were washed in PBS and

incubated in anti-rabbit-IgG Ab conjugated to Alexa Fluor 488 (Molecular Probes) and DAPI, and images were captured on an Olympus IX81 inverted microscope. Fluorescent intensity profiles from the resulting images were calculated using ImageJ. For higher resolution images, cells were imaged using a PASCAL laser-scanning confocal microscope (Carl Zeiss) with a 63X objective and the resulting stacks were processed using IMARIS software.

HUVECs were seeded on coverslips coated with fibronectin (10 mg/ml) and collagen I (30 mg/m) in 0.1% gelatin. Once 60% confluent, cells were washed with serum-free OptiMEM then treated either with or without 1 mM MnCl2 in the presence of either 0.5 mM GST or S2ED for 30'. Cells were then fixed in 2% PFA and stained using a monoclonal active b1-integrin specific Ab (clone HUTS4, at 1:300). After washing, cells were stained with an anti-mouse-IgG Ab conjugated to Alexa Fluor 594 (Molecular Probes). Cells were analysed by confocal microscopy as described above.

3.4. *In vivo* methods

3.4.1. Animals

Animals were housed and treated in Accordance with UK Home Office Regulations and all experiments were approved by the UK Home Office according to the Animals Scientific Procedures Act 1986 (ASPA).

C57BL/6 wild-type mice were purchased from Charles River.

SCID SHO mice were also purchased from Charles River. This animals were produced by inter-crossing the Crl:HA-Prkdc^{scid} and Crl:SKH1-Hr^{hr} stocks. They are homozygous for the Prkdc^{scid} and the Hr^{hr} mutations and thus exhibit the severe combined immunodeficiency phenotype characteristic of SCID mice and are also hairless.

Syndecan-4 -/- (S4KO) mice were obtained from the Centre for Animal Resources and Development (CARD, Kunamoto University, Japan) with the kind permission of Professor Tetsuhito Kojima (Nagoya University, Japan).

All mice were used at an age between 5-8 weeks at an average weight of 25g. As appropriate, age-matched control mice were litter mates or commercially purchased C57BL/6 wild-type mice.

Wistar rats were purchased from Harlan Laboratories and used at 6-8 weeks of age (≈200 g).

3.4.2. Cremaster muscle dissection

The cremaster muscle is a thin layer of striated muscle that surrounds the testicle. To isolate this tissue, a midline incision was made in the scrotum making sure not to damage the underlying tissues and testis. The testicles were gently drawn out by separating the underlying connective tissue from the cremaster muscle. The distal end of the cremaster muscle was pinned to the viewing column of the microscope stage to keep the cremaster muscle exteriorised. An incision was made along the centre of the muscle, ensuring that the main artery and venule going into and out of the tissue was kept intact. The cremaster muscle was then opened and pinned flat over the viewing window. The connective tissue attaching the testis to the cremaster muscle was then cut to enable the testes to be laid toward the side so that the entire cremaster muscle microvasculature could be clearly observed.

3.4.3. Primary murine lung EC isolation

This protocol was optimized to obtain a confluent T75 tissue culture flask of primary lung ECs (MLEC) from three mice in around 2-3 week time.

Day 1 – Lung dissection and digestion - 6-8 week old mice were sacrificed by cervical dislocation. Fur was sprayed with 70% EtOH and a longitudinal incision was made along the chest area using a scalpel. Skin was peeled back and pinned down to reveal the rib cage. Fresh forceps and scissors were used to open the chest cavity and dissect out the lungs. Lungs were immediately put into a 50 ml tube containing Hams F12 medium and kept on ice for no longer than 6 hrs. At this point, procedures were carried out under a fume hood to decrease bacterial contamination. Lungs were removed from the tube using sterile forceps, sprayed with 70% EtOH and immediately put in MLEC medium. Subsequently, lungs were placed on the inverted lid of a petri dish and minced using a sterile scalpel for no longer than 5' to produce a homogenized. Minced lungs were transferred into a sterile 50 ml tube containing 10 ml of 0.1% Type I Collagenase and placed in an incubator at 37 °C for 1 h, swirling tube occasionally. Later, 10 ml of MLEC medium were added to the solution which was then poured in a petri dish. A 20 ml syringe was used to draw up the digested lungs, a 19.5 gauge needle was then placed on the syringe and the solution was forced through the needle 4 times. The solution was then passed through a 70 µm cell strainer into a 50 ml tube containing 20 ml of MLEC medium and centrifuges for 5' at 1200 rpm. Supernatant was then removed, cells-containing pellet resuspended in 10 ml of fresh MLEC medium and the solution transferred into a 75 cm^2 pre-coated with 0.1% Gelatin, 300 µg/ml of Vitrogen (Nutacon) and human plasma Fibronectin (Millipore) and incubated at 37 °C, 10% CO_2 for 24 hrs.

Day 2 – Negative sort against macrophages - Medium was removed from the flask and replaced with 5 ml of fresh MLEC medium. The flask was then incubated at 4°C for 20'. Medium was then replaced with 5 ml of PBS containing 5 µl of rat anti-mouse CD16/CD32 Ab (BD 553142) and the flask was incubated at 4°C for 30'. The Ab solution was then removed, the flask was washed once with PBS and re-incubated at 4°C for 30' with 5 ml of MLEC containing 25 µl of sheep anti-rat Dynabeads (Dynal DB M450). The bead-containing solution was then removed and flask washed three times with PBS. Cells were then detached from the flask by adding 2.5 ml of 0.25% Trypsin/EDTA and incubating at 37°C for approximately 5'. 9.5 ml of MLEC medium was then added and cells resuspended. The solution was then moved into a 15 ml tube inserted into a magnetic holder and left there for 5' to allow the beads to attach to the side of the tube. The solution was then carefully moved from

the tube into a new pre-coated tissue culture flask, avoiding touching the tube. Medium was changed every 2 days until colonies of approximately 20 cells are apparent.

Positive sort for ECs - Once colonies of approximately 20 cells appeared, medium was removed from the flask and replaced with 5 ml of fresh MLEC medium. The flask was then incubated at 4°C for 20'. Medium was then replace with 5 ml of PBS containing 5 µl of rat anti-mouse CD102 Ab (BD 553325) and the flask was incubated at 4°C for 30'. The Ab solution was then removed, the flask was washed once with PBS and re-incubated at 4°C for 30' with 5 ml of MLEC containing 15 µl of sheep anti-rat Dynabeads. The bead-containing solution was then removed and the flask washed three times with PBS. Cells were then detached from the flask by adding 2.5 ml of 0.25% Trypsin/EDTA and incubating at 37°C for approximately 5'. 9.5 ml of MLEC medium was then added and cells resuspended. The solution was then moved into a 15 ml tube inserted into a magnetic holder and left for 5' to allow the beads to attach to the side of the tube. The solution was then carefully moved from the tube and discarded, ECs, attached to the beads, were then resuspended in 10 ml of fresh MLEC medium and plated on pre-coated tissue culture flask. Medium was changed every 2 days.

3.4.4. Aortic ring assay

Angiogenic sprouts were induced from mouse or rat thoracic aortas according to the method of Nicosia and Ottinetti (Nicosia and Ottinetti, 1990a, b). 6-8 week old male mice or 180–200 g male Wistar rats (Harlan Laboratories) were sacrificed by cervical dislocation. Fur was sprayed with 70% EtOH and a longitudinal incision was made along the chest area using a scalpel. Skin was peeled back and pinned down with scissors and forceps to reveal the rib cage. Aortas were then dissected using forceps and micro-scissors and put in a 50 ml pot with ice-cold PBS on ice. After a first wash in PBS to wash off the blood, the aorta was transferred into a petri-dish containing fresh PBS, here fat was carefully removed using forceps avoiding stretching the aorta, the long branches protruding from the aorta were also cut off using a scalpel. The aorta was then moved to a new petri-dish containing ice-cold serum-free Opti-MEM (containing P/S) and cut into rings of 1-mm of diameter using a scalpel. Under a tissue culture hood, rings were moved into a fresh petri-dish and incubated overnight in serum-free Opti-MEM (containing P/S) at 37°C. On the next day, a coating gel was made by mixing type I collagen (1 mg/ml), 10% v/v E4 media (Invitrogen) in water. 150 µl of the gel was pipetted in each well of a 48-well plate (Corning). Rings were then quickly dried on the lid of the petri-dish and carefully positioned in the middle of the well containing collagen. The plate was then

incubated at 37°C for 30' to allow the Collagen to polymerize, after which time wells were supplemented with Opti-MEM with 1% FBS and VEGF (30 ng/ml for mouse rings, 10 ng/ml for rat rings) and incubated at 37°C, 10% CO^2. Medium was changed every third day. Angiogenic sprouts from aortas were counted after 1 week and results were expressed as the number of sprouts per ring.

3.4.5. Choroid explant neo-vascularisation assay

Mice, 19 to 21 days old, were euthanized by cervical dislocation and eyes collected with curved forceps and transferred to PBS to wash away residual blood. Subsequently, eyes were fixed for 5' in 4% PFA on ice and transferred again in new PBS were they can be stored for up to 1 month in the fridge. For choroid/RPE tissue isolation, the eye is punctured with a 19 G needle below the iris so to facilitate the entrance of the forceps. A 1 mm incision is then made below the iris so that the periphery will be around 1 mm thick and using scissors cut around at that level. Iris/cornea/lens/retina are removed. Separate limbus from peripheral 1 mm strip. Flatten the tissue along so that it's easier to cut little 1 mm pieces. Cut choroid/sclera into approximately 1 mm×1 mm (~ 4 for central (quarters); 6 for peripheral). Around 6-8 squares result from one eye, these can be transferred into sterile Optimem (with P/S) overnight. Then proceed as per Aortic ring assay.

3.4.6. Miles assay for permeability

Vascular permeability was assessed by measuring the accumulation of Albumin-bound Evans Blue dye in the dorsal skin of mice stimulated with locally injected permeability factors or PBS alone. 6-8 week mice were anesthetized by i.m. injection of 1 ml/kg ketamine (40 mg) and xylazine (2 mg) in saline solution. The back skin was shaved using an electric razor. Mice then received Evans Blue dye (0.5% in PBS, 5 µl per g bodyweight) i.v. through the tail vein. Afterwards, 50 ul of PBS containing either 100 ng of VEGF-A or 100 µg of Bradykinin or PBS alone were injected s.c. in the mouse dorsal skin. After 1h30' animals were sacrificed by cervical dislocation. Dorsal skin was removed and injected sites were cut out as circular patches using a metal puncher (~8 mm in diameter). Samples were then incubated in 250 µl of formamide at 56°C for 24 h to extract Evans Blue dye from the tissues. The amount of accumulated Evans Blue dye was quantified by spectroscopy at 620 nm using a Spectra MR spectrometer (Dynex technologies Ltd., West Sussex, UK). Results are presented as the optical density at 620 nm (OD620) per mg tissue and per mouse.

3.4.7. Matrigel plug assay

The matrigel plug assay is considered one of the gold-standard methods to test angiogenesis *in vivo*. On day 1, 400 µl of matrigel (BD Biosciences) was thawed on ice and mixed with 100 µl PBS containing growth factors (100 ng/ml VEGF-A, 100 ng/ml bFGF) and 20 U/ml of Heparin to obtain a solution with a concentration of matrigel of ≈7.5 mg/ml.

6-8 weeks old mice were anesthetized by i.m. injection of 1 ml/kg of body weight of ketamine (40 mg) and xylazine (2 mg) in saline solution. 500 µl of the matrigel solution was aspired using a 1 ml syringe without the needle, a 27 gauge needle was then added to the syringe and the solution was injected sub-cutaneously into the flank of the animal, roughly between the rib cage and the posterior leg. After 5 days, mice were sacrificed by cervical dislocation. A longitudinal incision was made from the chest to the genital area, skin was peeled and pinned down and plugs were revealed. Photographs were taken with a digital camera and plugs excised using scalpel and tweezers. Plugs were then weighed on a precision balance and incubated overnight at 4°C with 500 µl of dH_2O. On the next day the amount of haemoglobin released from the plugs was measured using the Drabkin reagent kit (Sigma). 100 µl of samples was mixed with 100 µl of Drabkin solution and allowed to stand for 15' at RT. A calibration curve using known concentrations of Haemoglobin was also used. Absorbance at 540 nm was read using a spectrophotometer and results were expressed as the concentration of haemoglobin per gram of plug (HG mg/ml/g).

3.4.8. Xenograft HEK293T tumor-like model in SCID mice

HEK293T cells stably expressing either the empty vector or S2ED were grown in complete medium (DMEM+10%FBS) until 70-80% confluent. 3-4 hrs before harvesting, medium was replaced with fresh one to remove dead and detached cells. Subsequently medium was removed and cells washed with PBS and detached from the plate with a minimum amount of trypsin-EDTA (enough to cover the cell whole plate). A single cell suspension was then made by adding fresh complete medium to the trypsin-EDTA solution (10:1). Cell suspension was then centrifuged at 1000 rpm for 3', washed twice with PBS and stored on ice. Dilution was made appropriately to obtain a concentration of 3×10^7 cells/ml.

6 week old SCID SHO mice (Charles River) were anesthetized by i.m. injection of 1 ml/kg of body weight of ketamine (40 mg) and xylazine (2 mg) in saline solution. Injection area (left flank, ribcage area) was cleaned and sterilized with ethanol and 100 µl of cell suspension was injected s.c. using a 27g needle and a 1 ml syringe. Mice were left for 21 days prior to sacrifice

by cervical dislocation. A longitudinal incision was made from the chest to the genital area, skin was peeled and pinned down and plugs were revealed. Photographs were taken with a digital camera and tumors excised using scalpel and tweezers. Samples were then weighed on a precision balance and diameter measured using a ruler. Samples were then snap frozen in liquid nitrogen and stored at -80°C.

3.4.9. B16F1 tumor model in Wild-type and syndecan-4 KO mouse

B16F1 mouse melanoma cells were grown in complete medium (DMEM+10%FBS) until 70-80% confluent. 3-4 hrs before harvesting, medium was replaced with fresh to remove dead and detached cells. Subsequently medium was removed and cells washed with PBS and detached from the plate with a minimum amount of trypsin-EDTA (enough to cover the cell whole plate). A single cell suspension was then made by adding fresh complete medium to the trypsin-EDTA solution (10:1). Cell suspensions were then centrifuged at 1000 rpm for 3', washed twice with PBS and stored on ice. Dilutions were made appropriately to obtain a concentration of 5 x 10^7 cells/ml.

6 week old wild-type and syndecan-4 KO mice were anesthetized by i.m. injection of 1 ml/kg of body weight of ketamine (40 mg) and xylazine (2 mg) in saline solution. Injection area (left flank, ribcage area) was cleaned and sterilized with ethanol and 100 µl of cell suspension was injected s.c. using a 27g needle and a 1 ml syringe. Mice were left for 7 days prior to sacrifice by cervical dislocation. A longitudinal incision was made from the chest to the genital area, skin was peeled and pinned down and plugs were revealed. Photographs were taken with a digital camera and tumors excised using scalpel and tweezers. Samples were then weighed on a precision balance and diameter measured using a ruler. Samples were then snap frozen in liquid nitrogen and stored at -80°C.

3.4.10. Immunohistochemical staining

3.4.10.1. Whole mount cremaster muscle and ear staining

Cremaster muscles were dissected from the mouse and pinned out on a piece of wax. In some experiments the vasculature of the ear was also used. Tissues (cremaster and ear) were fixed in 4% PFA for 30 mins at 4°C. Immunofluorescent staining of whole mounted tissues was then performed. Tissues were permeabilized after fixation with blocking buffer (0.5 % Triton X-100 and 10 % foetal calf serum and 10 % goat serum in PBS) for 2 hours, at room

temperature on a gentle rotator. Tissues were then incubated with appropriate primary mAb overnight in cold room. Tissues were washed 3 times with PBST (PBS+0.1% Tween20) on a shaker and re-blocked in PBS containing 20% serum with appropriate secondary Ab for 2 hour. Tissues were washed 3 times with PBST before a final wash in PBS, the tissues were then positioned on glass slides and viewed under the PASCAL laser-scanning confocal microscope (Carl Zeiss) with a 63X or 10X objective and the resulting stacks were processed using IMARIS software (Bitplane, Zurich, Switzerland).

3.4.10.2. Quantification of vascular morphology parameters

Vessel density was measured by drawing 2 orthogonal lines in the middle of each images and counting the number of vessels crossing the lines and dividing that value by the length of the line. The average of the horizontal and vertical density was calculated and average with that of at least 5 images per group.

Percentage of capillaries (diameter <10 μm), arterioles and venules (diameter between 10-40 μm) and arteries and veins (diameter >40 μm) was measured using Imaris (Bitplane, Zurich, Switzerland) 3D analysis software. Vessels were divided into 3 groups accordingly and their respective percentages were calculated.

Pericyte coverage index was quantified as the percentage of vessel area covered by αSMA in both venules (10<40 μm) and veins (>40 μm) using ImageJ (National Institute of Health, Bethesda, Maryland, USA).

3.4.10.3. Whole mount aortic ring and choroid explant staining

Medium was removed from the wells; explants were washed 3 times in PBS and fixed in 100% Methanol for 30 mins at -20°C. Washed in PBS and blocked in PBS and 3% BSA for 1 hour. Tissues were then incubated with appropriate primary mAb overnight in a cold room at 4°C. Tissues were washed 3 times with PBST (PBS + 0.1% Tween20) on a shaker and re-blocked in PBS containing 3% BSA with appropriate secondary Ab for 2 hour. Tissues were washed 3 times with PBST before a final wash in PBS, the tissues were then positioned on glass slides and viewed under a confocal microscope. Analysis of the staining was carried out using Imaris (Bitplane, Zurich, Switzerland) 3D analysis software.

3.4.10.4. HEK293T tumors, B16F1 tumors, Matrigel plugs sectioning and staining

The specimen (tumor or Matrigel plug) is placed on a metal tissue disc which is then secured in a chuck and frozen rapidly to about –20 to –30 °C. The specimen is embedded in a gel like medium called OCT and consisting of poly ethylene glycol and polyvinyl alcohol; this compound when frozen has the same density as frozen tissue. At this temperature, most tissues become rock-hard. Subsequently, sample is cut frozen with the microtome portion of the cryostat, the section is picked up on a poly-lysine glass slide. Section thickness was 60, 50 and 20 µm for HEK293T tumors, Matrigel plugs and B16F1 tumors, respectively. Slides were then fixed in 100% Methanol for 20' at -20°C, blocked and permeabilized in 20% normal goat serum and 0.5% Triton in PBS for 1h in a humid chamber. Incubated with primary Ab solution over-night at -4°C, washed in PBS 3 times for 10', incubated with secondary Ab solution for 1h, washed in PBS 3 times for 10', let to dry and finally mounted with ProLong Gold Anti-fade fixative (Life technologies).

4. Results

4.1. Syndecan extracellular core proteins have anti-angiogenic properties

4.1.1. Introduction

During the angiogenic process, ECs collectively move and change their reciprocal positions as a response to both soluble stimuli (growth factors and cytokines) and the extracellular microenvironment. Cell motility is in fact a highly coordinated process that strongly relies on cell adhesion to the ECM components (Lamalice et al., 2007). Integrins belong to a large group of structurally related receptors for ECM components and immunoglobulin superfamily molecules. They are divalent cation-dependent heterodimeric membrane glycoproteins comprised of non-covalently associated α and β subunits, each subunit has an extracellular domain, a single transmembrane domain and a short cytoplasmic region. 18 α and 8 β subunits can combine into 24 heterodimers with distinct yet often overlapping substrate affinity (Hynes, 2002). Central to integrin function in cell adhesion is their clustering on the cell surface which depends on (i) close proximity or periodicity of integrin-binding motifs within ECM components, (ii) lateral association of integrins and (iii) interactions of integrins cytoplasmic domains with adaptor molecules (Ziegler et al., 2008). In turn, the type of adaptors and enzyme recruited at the intracellular side of the clustered integrins will determine the signalling events and thereby cell-fate decisions (Burridge et al., 1992; Legate et al., 2006; Mitra and Schlaepfer, 2006). In ECs α4β1, α5β1, αVβ3 and αVβ5 are most commonly expressed (DeHahn et al., 2004; van der Flier et al., 2010). Since cell adhesion through integrins mediates migratory, adhesive and survival responses in ECs, it is unsurprising that integrins have key roles in angiogenesis. Several experimental approaches, for example, indicate that αVβ3 (a fibronectin and vitronectin receptor) and αVβ5 (a vitronectin receptor) have key roles in EC survival and migration during new blood vessel formation (Brooks et al., 1994); indeed, antagonists for these two integrins inhibit angiogenesis in cancer (Scaringi et al., 2012) and ischemic retinopathy (Hammes et al., 1996). However, whilst gene ablation of the αV subunit allows developmental vasculogenesis to proceed normally until E9.5 (Bader et al., 1998) after which it causes 100% lethality, mice lacking β3 and/or β5 reach adulthood but have enhanced tumor growth and angiogenesis, which would suggest that β3 and β5 play a negative role in pathological angiogenesis but not during development (Reynolds et al., 2002). Moreover, genetic experiments showed that successful vasculogenesis and angiogenesis depend on Fibronectin (George et al., 1993) and its main receptor α5β1(Francis et al., 2002) and interestingly this integrin is found overexpressed in blood vessels of human and mouse tumors

(Kim et al., 2000b). The importance of integrins in angiogenesis has made them an attractive target for anti-angiogenic therapy; drugs such as Voloxicimab (Ng et al., 2010) (targeting α5β1 integrin), Cilengitide (Reardon et al., 2008) (targeting RGD integrins) and Intetimumab (O'Day et al., 2012) (αV antagonist) are already in clinical trials.

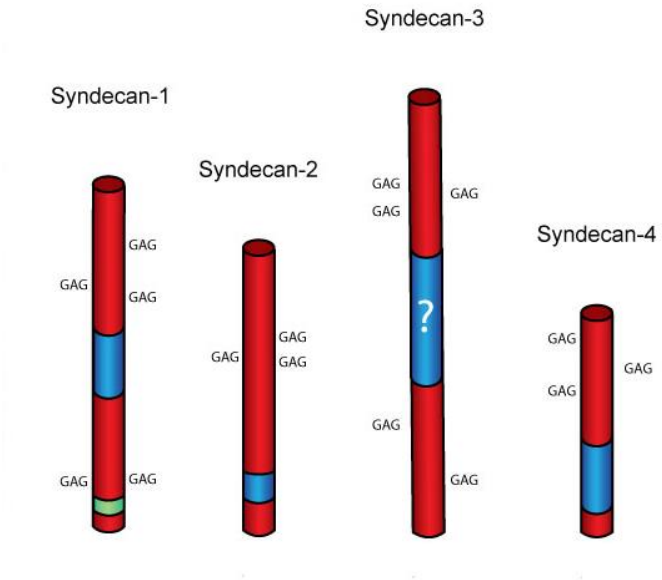

Fig. 4.1 **Syndecan ectodomains possess adhesion-regulatory sites.** Diagram shows the 4 syndecan ectodomains, the sites of glycosaminoglycan substitutions (GAG) and their respective adhesion-regulatory sites (blue) and invasion-regulatory site (green). To note, no adhesion-regulatory site has been described for syndecan-3.

As reviewed in 1.1.7 evidence suggests that syndecan extra-cellular core proteins can regulate cell adhesion in an integrin-dependent fashion (Fig. 4.1). The works of Beauvais (Beauvais et al., 2004) and Mcquade (McQuade et al., 2006) showed how the direct interaction between syndecan-1 ectodomain and αVβ3 and αVβ5 integrin leads to spreading of human breast tumor cells (MDA-MB-231) and fibroblasts, respectively. Similarly, the ectodomain of syndecan-2 and -4 possess an adhesion regulatory sequence which when expressed as glutathione S-transferase (GST) fusion protein can promote attachment and spreading of mesenchymal cells. This is, again, dependent on integrins, specifically the β1 subfamily, but unlike in the case of S1ED, there is no direct interaction between S2ED or S4ED and β1integrins. Interestingly, this adhesive effect is cell specific as it is restricted to cells of mesenchymal origin. Moreover, S2ED and S4ED pathways are in some way distinct because addition of the alternate ED as a competitor in adhesion assays showed no effect suggesting the presence of different intermediates (Whiteford et al., 2007). Also in accordance with this hypothesis is the finding that S4ED requires the NXIP motif contained in its C-terminus for its adhesive effect which

is not present in the syndecan-2 extracellular core protein (Whiteford and Couchman, 2006). An intermediate for the S4ED and β1 integrin interaction has yet to be found, while in the case of S2ED the tyrosine phosphatase receptor CD148 appears to have a role in mediating β1 integrin-driven cell responses to S2ED. This work also revealed that the amino acids residing between P^{124} and F^{141} of murine syndecan-2 are important for fibroblast responses to S2ED (Whiteford et al., 2011).

4.1.2. Aims

On the basis of the work described above, it is clear that regulatory sequences contained within syndecan ectodomains can influence cell behaviour through integrins. However, relatively little is known about how these sequences affect ECs and EC-dependent processes such as angiogenesis.

The aims of the experiments which will be described in this first section of the thesis are as follows:

1. Establish whether the ectodomains of syndecan-1, -2, -3 and -4 affect angiogenesis.
2. Determine their associated mechanisms of action on ECs.

4.1.3. Results

4.1.3.1. Syndecan ectodomains dose-dependently inhibit angiogenesis in the aortic ring model

To establish whether syndecan ectodomains were able to influence EC processes, we used GST fusion proteins consisting of GST N-terminally fused to the extracellular core proteins of syndecan-1, -2, -3 and -4 in angiogenesis assays. The fusion proteins were expressed and purified from bacterial lysates. Despite many efforts to purify syndecan ectodomains in isolation, this has proved impossible due to solubility issues, for this reason we adopted the GST fusion approach.

The aortic ring assay is an *ex vivo* model of angiogenesis which is widely used in the field; here, rat aortas are dissected from the animal and cut into small rings (*ca.* 1 mm width) which are then embedded in a thin layer of Collagen I and fed every 3 days with medium containing serum and VEGF-A as a pro-angiogenic factor. In a week's time angiogenic sprouts develop from the rings and the number of those is considered directly proportional to the extent of the angiogenic response (Fig. 4.2).

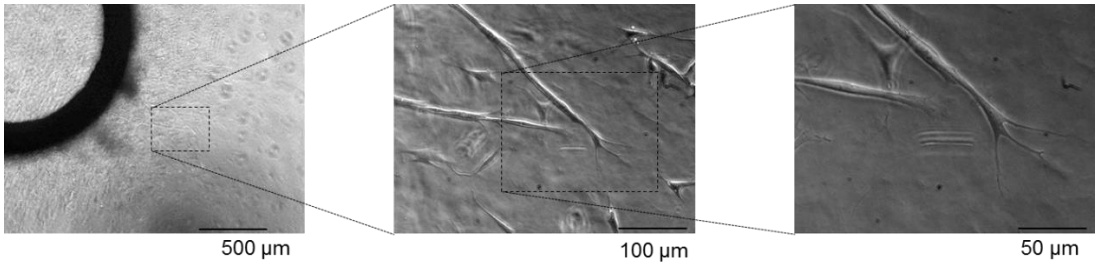

Fig. 4.2 **Rat aortic ring assay.** Rat thoracic aortas were cut into rings which were embedded in 150 µl of Collagen type I (1 mg/ml) and 200 µl of OPTIMEM containing 10ng/ml of VEGF-A. The number of sprouts was measured 7 days after embedding. Micrographs taken under a phase contrast microscope show an example of aortic ring at different magnifications, notably the tip cell extending 3 filopodia.

To address the project's objectives, a range of concentrations (0-0.5 µM) of murine syndecan ectodomains fused to GST or GST alone were embedded in collagen and sprout growth was measured after 7 days. It should be noted that GST unconjugated was bacterially-expressed and purified following the same protocols of the fusion proteins and was used as a control for endotoxin-dependent side effects in every experiment.

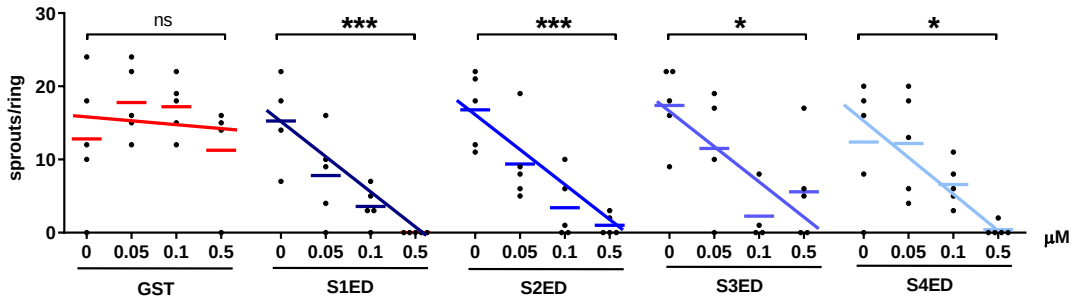

Fig. 4.3 **Dose-dependent effect of syndecan ectodomains on angiogenic sprouting.** Rat thoracic aortas were cut into rings which were embedded in 150 µl of Collagen type I (1 mg/ml) containing the syndecan core proteins (S1ED, S2ED, S3ED and S4ED) or GST control at the concentration indicated in 200 µl of OPTIMEM containing 10ng/ml of VEGF-A. The number of sprouts was measured 7 days after embedding. Each dot represents the number of sprouts of one ring, the short lines represent the mean number of sprouts at the concentration indicated and the long lines show the linear trend of the treatment dose-dependent effect. Significant differences between untreated control (0 µM) group and groups treated with the highest dose of each substrate (0.5 µM) were determined using one-way Anova with Bonferroni correction for multiple comparisons. *P<0.05, ***P<0.001.

An almost complete ablation of angiogenic sprout development was observed with 0.5 µM of all four syndecan ectodomains. Furthermore, lowering the dose of the proteins resulted in a progressive restoration of the angiogenic response, unlike the GST control for which a consistent strong angiogenic response was detected at all concentrations (Fig. 4.3).

These results suggested a dose-dependent anti-angiogenic effect of all four syndecan ectodomains with the concentration of 0.5 µM of protein as the one with the maximum efficacy. Syndecan ectodomains were therefore used at the concentration of 0.5 µM in the following experiments.

4.1.3.2. Syndecan ectodomains inhibit EC network formation

The aortic ring model previously used to establish the effect of syndecan ectodomains on angiogenesis is an *ex vivo* model and importantly it is characterized by the participation of several cell types: ECs, smooth muscle cells, pericytes and often fat cells and blood cells which escape the dissection steps. A change in the number of sprouts could therefore be the result of an effect on one or more of these cell types, not necessarily ECs. To investigate whether the anti-angiogenic properties of syndecan ectodomains observed in the aortic ring model were the result of a direct effect on ECs, we tested these proteins in a tubule formation assay. Skin

ECs were seeded on a thin layer of Matrigel and left in complete medium containing syndecan ectodomains or GST for 24 hrs to allow them to organize into a spontaneous network of tubules.

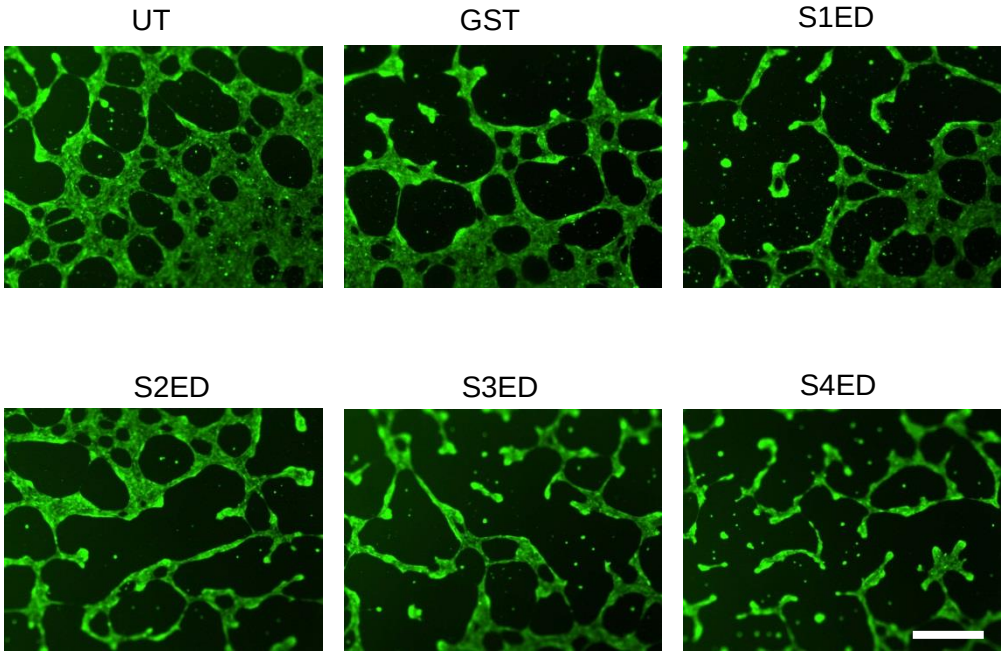

Fig. 4.4 **Effect of syndecan ectodomains on EC tubule formation.** 10000 Skin ECs (sEND) were seeded in a 24-well plate coated with 150 µl of Matrigel in complete medium containing the syndecan core proteins or GST at a concentration of 0.5 µM. After 24 hours Calcein was added to the medium to visualize cell (green) tubule network. Analysis was carried out on Photoshop (Adobe). Photographs were taken using a fluorescence microscope. Pictures are representative of 3 experiments were 4 pictures were analysed for each condition. Scale bar represents 500 µm.

While the untreated and the GST control samples were capable of developing a tubule network during the time frame used, ECs grown in the presence of syndecan ectodomains failed to do so. This effect is clear both from the pictures showing much less articulated tubules in the treated groups but also from the derived quantification which highlights how tubules are shorter when ECs were in the presence of syndecan ectodomains (Fig. 4.4 and Fig. 4.5).

This result suggested that syndecan ectodomains anti-angiogenic properties could be partially due to a direct effect on ECs, in particular to a negative regulation of their ability to migrate and organize into tubules.

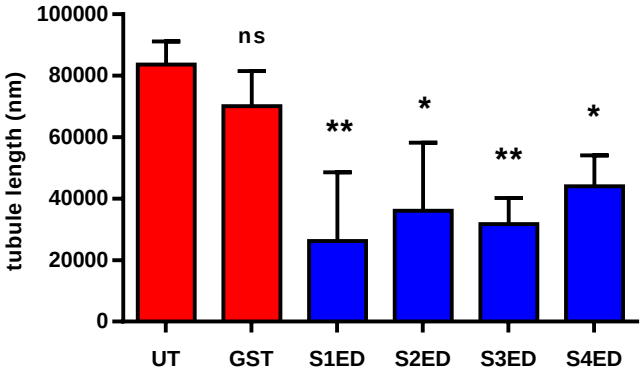

Fig. 4.5 **Effect of syndecan ectodomains on EC tubule formation.** Pictures from the previous experiments, where sENDs were allowed to form tubules in the presence of 0.5 µM of GST or syndecan ectodomains, analysed on Photoshop (Adobe) where tubule length was measured. Bars show the mean and standard deviation of 3 experiments where 4 pictures per condition were analysed. Significant differences between untreated control (UT) and treated groups were determined using one-way Anova with Bonferroni correction for multiple comparisons. *P<0.05, **P<0.01.

4.1.3.3. Syndecan ectodomains inhibit EC migration

To develop a tubule network similar to that seen in the previous set of experiments, ECs need to both proliferate and migrate. Having established that syndecan ectodomains affect EC tubule formation, possible effects on EC migration and proliferation were investigated. A scratch wound assay is an easy way to measure cell migration *in vitro*. Here, ECs plated in a 6-well plate are left to grow until confluence is reached. A scratch is then made in the centre of the well and cells are left to migrate for 9 hours. As previously, syndecan ectodomains or GST were added to the medium at the concentration of 0.5 µM right after the scratch was made.

After 9 hours ECs left untreated or treated with GST completely "repaired" the scratch wound by migrating into the empty space, while cells treated with syndecan ectodomains failed to do so as evident by comparing the micrographs taken at time 0 and 9 hours (Fig. 4.6). Quantification of the percentage of wound area at 0, 3, 6 and 9 hours highlights a strong anti-migratory effect of all syndecan ectodomains with that of S4ED being consistently higher at every time point (Fig. 4.7). To confirm these results, single cells were also analysed and their speed quantified. Cells migrating in the presence of syndecan ectodomains in the medium are slower than when treated with GST or left untreated (Fig. 4.8).

To avoid disturbing any of EC functions during migration, proliferation was not chemically inhibited by the addition of drugs (such as mytomycin C) in the experiments described above. Hence, to exclude that the effect seen in the scratch wound assay was due to syndecan ectodomains influencing EC mytogenic potential, a proliferation assay was carried out. Here, no statistically significant effect of syndecan ectodomains on EC proliferation at 9 hours was detected (Fig. 4.9), which suggested that the delay in the wound closure was due to inhibition of EC migration when in contact with syndecan ectodomains rather than to them being less proliferative.

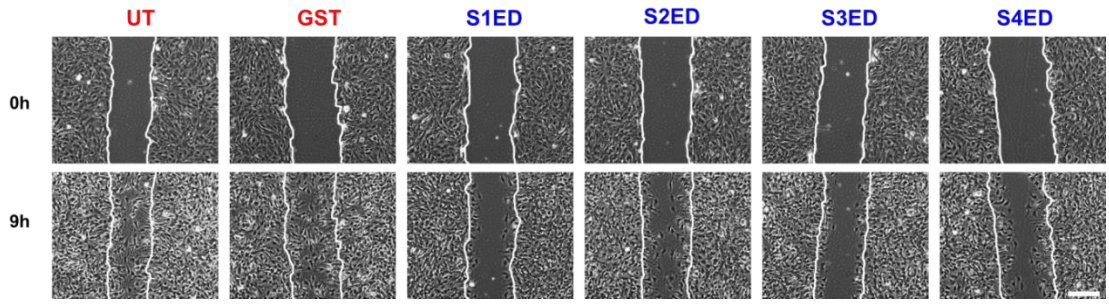

Fig. 4.6 **Effect of syndecan ectodomains on EC migration.** Confluent skin ECs (sEND) were scratched with a pipette tip in the middle of the well, washed in PBS and fresh medium containing 0.5 µM of the indicated proteins was added. Photographs of the same spot were taken on an inverted microscope straight after the addition of the treatment (0h) and after 9 hours (9h). White lines were drawn to cover the initial scratch margins to better visualize cell migration at the final time point. Pictures are representative of 3 experiments where at least 2 spots per condition were analysed. Scale bar represents 500 µm.

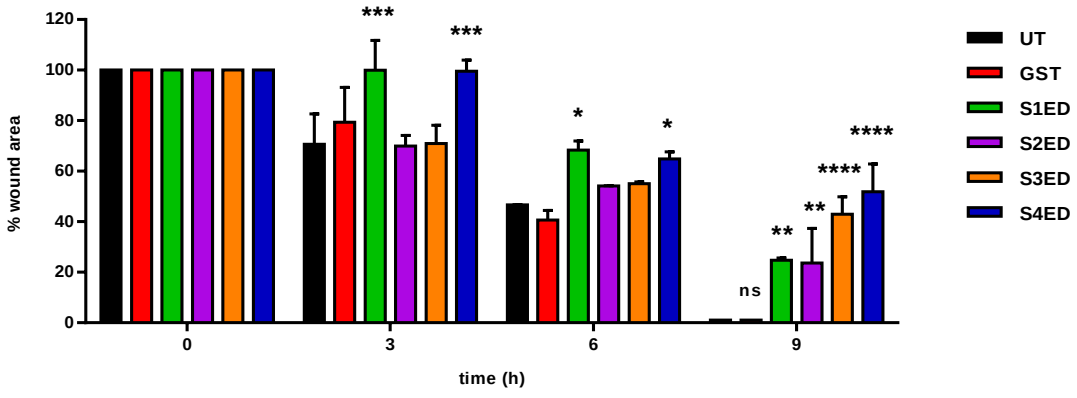

Fig. 4.7 **Effect of syndecan ectodomains on EC migration.** Confluent skin ECs (sEND) were scratched with a pipette tip in the middle of the well, washed in PBS and fresh medium containing 0.5 µM of the indicated proteins was added. Photographs of the same spot were taken on an inverted microscope straight after the addition of the treatment (0h) and after 3, 6 and 9 hours. Wound area was calculated at each time point and expressed as percentage, with 100% being the wound area at time 0h. Bars show the mean and standard deviation of 3

experiments where at least 2 spots per condition were analysed. Significant differences between untreated control (UT) and treated groups at each time point were determined using one-way Anova with Bonferroni correction for multiple comparisons. *P<0.05, ** P<0.01, ***P<0.001, ****P<0.0001.

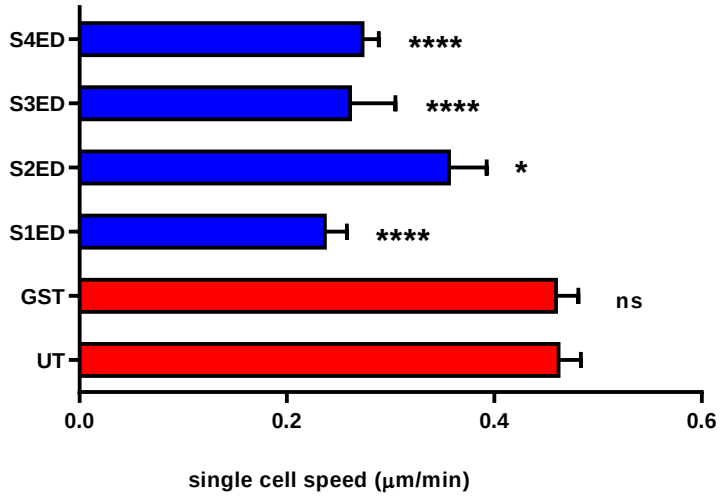

Fig. 4.8 **Effect of syndecan ectodomains on EC migration speed.** Single cell movements from previous experiments, where sENDs were allowed to migrate in the presence of 0.5 μM of GST or syndecan ectodomains, were tracked using Photoshop (Adobe) and single cell speed was calculated by dividing the length of the movement by 540 minutes to obtain cell speed. Bars show the mean and standard error of the mean of 3 experiments where at least 10 cells per condition were analysed. Significant differences between untreated control (UT) and treated groups were determined using one-way Anova with Bonferroni correction for multiple comparisons. *P<0.05, ****P<0.0001.

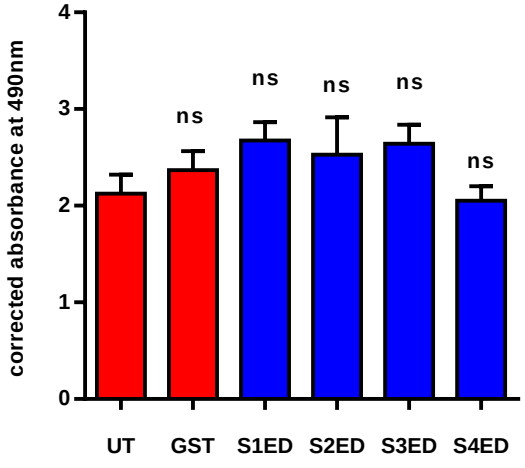

Fig. 4.9 **The effect syndecan ectodomains on EC proliferation.** EC proliferation was measured by using the Cell Titer 96 AQueous Cell proliferation assay kit. 5000 skin ECs (sEND) were seeded in 100 μl of complete medium containing 0.5 μM of the indicated protein in a 96-well plate. After 9 hours absorbance was read in an Elisa reader. Bars show the average corrected absorbance at 490 nm (final value/initial value) and its standard deviation from 2 experiments. No significant differences between untreated control (UT) and treated groups were determined using one-way Anova with Bonferroni correction for multiple comparisons.

4.1.3.4. Syndecan ectodomains inhibit EC invasion into collagen I

To evaluate the impact of the anti-migratory effect of syndecan ectodomains on ECs in a tri-dimensional situation, an invasion assay was carried out. In this set of experiments ECs were left to invade a thin layer of collagen I for 24 hours, after which the cells which had migrated through the collagen were counted.

Syndecan ectodomains were added to the collagen to establish whether their presence could exert the same anti-migratory effect noticed in the scratch wound model.

Far fewer ECs reached the bottom of the gel when syndecan ectodomains were added to the matrix compared to untreated or GST control, confirming that syndecan ectodomains are indeed able to inhibit EC migration both in a 2D (scratch wound assay) and a 3D system (invasion assay) (Fig. 4.10 and Fig. 4.11).

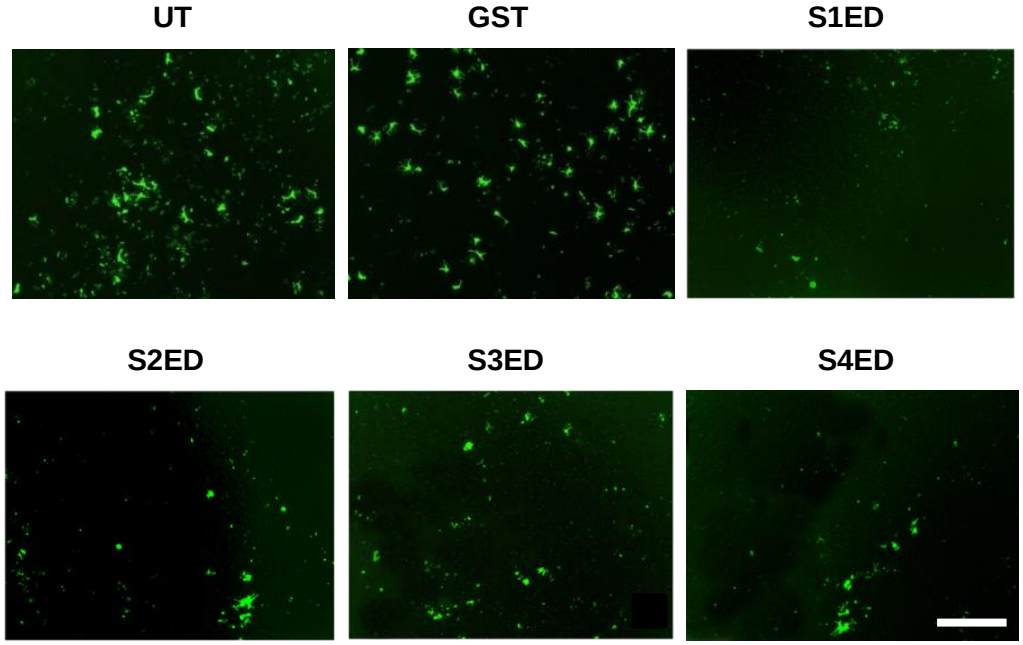

Fig. 4.10 **Effect of syndecan ectodomains on EC invasion into Collagen I.** Skin ECs (sEND) were seeded on top of membranes previously coated with 10 µl of a Collagen Type I mixture (1 mg/ml) containing the syndecan core proteins or GST at a concentration of 0.5 µM. After 24 hours, Collagen was removed, Calcein was added to the medium to visualize cells (green) which reached the filter. Photographs were taken using a fluorescence microscope. Pictures are representative of 3 experiments where each condition was performed in triplicate. Scale bar represents 500 µm.

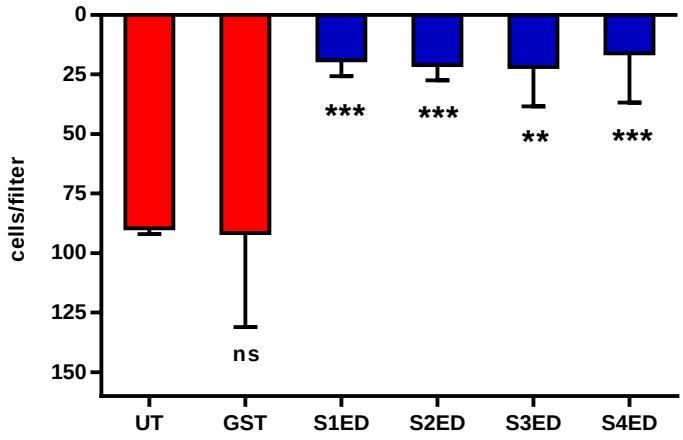

Fig. 4.11 **Effect of syndecan ectodomains on EC invasion into Collagen I.** Pictures from previous experiment, where sENDs were allowed to invade a collagen gel in the presence of 0.5 µM of GST or syndecan ectodomains, were analysed on Photoshop (Adobe) and cells counted. Bars show the mean and standard deviation of 3 experiments where 3 filters per condition were analysed. Significant differences between untreated control (UT) and treated groups were determined using one-way Anova with Bonferroni correction for multiple comparisons. **P<0.01, ***P<0.001.

4.1.4. Discussion

The aim of the experiments described in this section was to investigate whether soluble forms of syndecan ectodomains could affect EC behaviour during angiogenesis. From the results obtained we can conclude that all four syndecan extracellular core proteins are able to inhibit angiogenesis in the *ex vivo* model of the aortic ring assay and strongly negatively regulate EC migration, invasion and tube formation *in vitro*. One of the most striking observations is that all four syndecan ectodomains have anti-angiogenic effects despite their lack of sequence homology.

Previous works (Beauvais et al., 2004; McQuade et al., 2006; Whiteford et al., 2007; Whiteford et al., 2011) showed that the ectodomains of syndecan-1, -2 and -4 possess an adhesion-regulatory sequence which allow them to promote cell attachment when they are either immobilized on a plate or engaged by Ab. Interestingly, the adhesion-regulatory sites which have been identified in syndecan-1, -2 and -4 are unique to each syndecan. These studies also elucidated a requirement for integrins in these pathways, in particular αVβ3, αVβ5 for syndecan-1 and β1 families for syndecan-2 and -4. We also noticed an unanticipated anti-angiogenic effect of S3ED, a protein which has never been assessed in adhesion studies; because syndecan-3 is structurally similar to syndecan-1, one could speculate it could mediate the same αVβ3 and αVβ5-dependent adhesion pathway. As discussed in the introduction to this section, integrins αVβ3, αVβ5 and β1 have key roles in angiogenesis and this is because their interactions with the ECM can regulate EC survival, migration and proliferation (Avraamides et al., 2008): integrins αVβ3 (a Fibronectin and Vitronectin receptor) and αVβ5 (a Vitronectin receptor) antagonists have shown promising results in cancer, arthritis and ischemic retinopathy treatments and Fibronectin main receptor α5β1(Francis et al., 2002) is found overexpressed in blood vessels of human and mouse tumors (Kim et al., 2000b). So it is likely that syndecan ectodomain anti-angiogenic effects are caused by an increase in integrin-mediated EC adhesion which in turn slows down cell migration.

The experiments described in this section are based on the use of soluble syndecan ectodomains; it would be therefore interesting to know whether the same pathways would be triggered in *cis.* Syndecans are in fact expressed on ECs, with syndecan-2 being the most abundant, and some evidence suggests that their expression can be regulated by angiogenic factors: TNF-α for example, which is a potent angiogenic factor *in vitro* and *in vivo* (Montrucchio et al., 1994; Norrby, 1996), increases syndecan-4 expression on ECs while suppresses that of syndecan-1 (Zhang et al., 1999); syndecan-4, in addition, is found upregulated *in vivo* in a range of inflammatory conditions characterized by an angiogenic

response like ischaemic myocardial injury (Cizmeci-Smith et al., 1997) and dermal wound healing (Gallo et al., 1996b). It is therefore tempting to speculate that syndecan ectodomains could be interacting *in cis* with binding partners on the EC surface, leading to a modulation of integrins activity thus affecting EC adhesion and migration; however, it is important to bear in mind that in this scenario the full length syndecan molecule will be substituted by large and heavily charged HS chains and this will likely make its adhesion-regulatory site inaccessible. There is however no experimental evidence to prove that this is the case.

On the other hand, cell surface receptor cleavage is a common feature of many physiological and pathological processes and shed syndecans are often found in pathological fluids: elevated levels of syndecan-1 ectodomain are present in dermal wound fluid and in serum of patients with acute graft-vs-host disease (Seidel et al., 2003) and increased shed syndecan-1 in the sera of myeloma patients is indeed considered a marker of poor prognosis (Bayer-Garner et al., 2001; Seidel et al., 2000b), syndecan-4 shedding can also increase in situations of chronic inflammation such as asthma (Brightling et al., 2005) and wound healing (Subramanian et al., 1997) and syndecan-2 is readily shed from human colon cancer cells by MMP-7 (Choi et al., 2012). So, conditions such as chronic inflammation, wound healing and cancer growth are characterized by both an angiogenic response and syndecan shedding. This could seem in disagreement with the results described in this section, showing that syndecan extra-cellular proteins effectively inhibit angiogenesis; however, it is key to point out that new blood vessel formation results from a highly coordinated balance of pro- and anti-angiogenic signals. In this scenario, shedding of syndecans from specific cell types, at a precise time and place, would result in ectodomain moieties anchored to the ECM (via HS-ECM interactions) which would then function as "stop" signal to guide ECs to the site of tissue injury.

Another interesting point which would require further investigation to address is the characterization of the proteases able to cleave syndecan ectodomains. An increased accumulation of extracellular proteases such as MMPs, ADAMs and ADAMTs is associated with physiological angiogenesis but also to those pathologies which include an angiogenic response (e.g. chronic inflammation and cancer). However, given the little sequence homology between syndecan ectodomains, it is very unlikely that the same protease/s would be able to shed all four. In addition, the adhesion-regulatory sites which have been identified in syndecan-1, -2 and -4 (Fig. 4.1) are all encoded in the very C-terminus of the respective extracellular core protein, hence, depending on the cleavage site, they could be either released together with the N-terminal domain, retained as a truncated extracellular domain on the cell membrane or cut in half if the cleavage site is contained within its sequence. This raises the

question as to whether physiological or pathological shedding can regulate the anti-angiogenic properties of syndecan ectodomains.

The use of bacterially-derived syndecan ectodomains, which therefore lack glycosaminoglycan chains, allowed the identification of effects which are specific to the proteic domain, but was also a limitation. Syndecans are in fact likely to still be fully substituted by GAG chains once shed, so a question which is left unanswered is whether the presence of these substitutions would be inhibitory to the protein interactions. Moreover, murine sequences were used in the experiments to match the experimental design which took advantage of the rodents systems (rat aortic rings and murine cells in all the *in vitro* experiments), it would be therefore interesting to test whether human syndecan ectodomains would still retain the same activity we detected in the rodent counterpart. Notably, human and murine syndecan ectodomains share a sequence homology greater than 80%.

Moreover, in light of the strong anti-angiogenic capacity of these proteins, it would be exciting to test whether syndecan ectodomains could have potential as an anti-angiogenic therapy in diseases such as rheumatoid arthritis and cancer.

Further work is needed to answer these questions and more, but the data just presented represent a very encouraging starting point suggesting a novel regulatory role for syndecan ectodomains in angiogenesis.

In conclusion, in this first results section of the thesis it has been shown that:

1. All four syndecan ectodomains have anti-angiogenic properties.
2. This most likely occurs via an inhibition of EC migration.
3. We have identified adhesive function in the syndecan-3 ectodomain.

4.2. Shed syndecan-2 is a regulator of angiogenesis

4.2.1. Introduction

Syndecan-2, also called Fibroglycan, was originally described as the main HS proteoglycan expressed by human lung fibroblasts (Marynen et al., 1989) and later shown to be characteristic of cells of mesenchymal origin (David et al., 1993), neurons (Ethell and Yamaguchi, 1999) and some types of cancer cells (Gulyas and Hjerpe, 2003). Syndecan-2 participates in the formation of dendritic spines during hippocampal neuron differentiation (Ethell and Yamaguchi, 1999) and seems to mediate early decisions during development of left-right asymmetry in *Xenopus* (Kramer and Yost, 2002). Moreover, syndecan-2 was found to be up-regulated on colon cancer cells and is required for both cell cycle progression and cell-matrix interactions (Han et al., 2004). As described in 1.3.2, relatively few studies have associated syndecan-2 to angiogenesis. In the most notable work, syndecan-2 knocked down in zebrafish embryos was shown to dramatically impair angiogenic sprouting during vascular development. In both loss and gain of function experiments, syndecan-2 appeared to be required for VEGF-mediated signalling. The angiogenic function of syndecan-2 shown in zebrafish is likely conserved in mouse and human as its expression is similarly localized to the mesenchyme surrounding major vessels and human syndecan-2, when expressed in zebrafish ECs, could mimic the effect of the endogenous one. Notably to exert its function during new blood vessel formation syndecan-2 needs to be present as a full length molecule as its pro angiogenic effects were abolished when syndecan-2 was expressed as a cytoplasmically truncated form (Chen et al., 2004a).

In addition to its roles as a full length molecule, I described a novel function for the syndecan-2 extracellular core protein in angiogenesis (section 4.1). In my studies, when the murine syndecan-2 ectodomain, short of both its transmembrane and cytoplasmic domain and without GAG substitution, is expressed as a GST-fusion protein and added to the medium of ECs, it strongly inhibits cell migration, tubule formation and ultimately angiogenesis in the *ex vivo* model of aortic sprouting. Previously, it was shown that fibroblast attachment to S2ED promotes the formation of focal structures and this is mediated by the cell surface tyrosine-phosphatase CD148 and β1 integrins. Solid-phase binding assays showed that the extracellular domain of CD148 interacts with the last 18 aa of murine S2ED (P^{124} - F^{141}) and in particular the sequence DNLF seems to be key to this interaction. Interestingly, direct binding between β1 integrins and CD148 does not occur and cells failed to adhere to the CD148 extracellular domain when provided as a substrate in adhesion assays, suggesting an involvement of an intra-cellular signalling pathway that functionally connects CD148 to ß1 integrin. Analysis of

the possible intracellular substrates for CD148 revealed that ß1-mediated adhesion requires activated Src and PI3k-C2ß and there is evidence for the involvement of a de-phosphorylation step of the p85 subunit of PI3K (Whiteford et al., 2011).

CD148, also named DEP-1/PTPη, is a type III receptor protein tyrosine phosphatase that is composed of an extracellular domain containing 8 FN type III-like repeats, a transmembrane domain and a single cytoplasmic phosphatase domain (Ostman et al., 1994). The name DEP-1, density enhanced phosphatase-1, was given to this protein since it appeared upregulated on human foetal lung fibroblasts (WI38) cells when grown to high cell density. Further studies were supportive of a role for CD148 in inhibiting cell growth especially in cancer cells. Loss of CD148, for example, often correlates with a more malignant cancer cell phenotype (Keane et al., 1996; Zhang et al., 1997). Of particular interest to my project, CD148 is abundantly expressed in vascular ECs (Borges et al., 1996; Takahashi et al., 1999) and mutant mice lacking catalytic activity of CD148 die with vascular defects (increased EC proliferation and vessel growth) during gestation (Takahashi et al., 2003). Consistent with these findings, CD148 has been shown to inhibit signalling of growth factor receptors such as VEGFR-2 (Grazia Lampugnani et al., 2003) which is of paramount importance to angiogenesis. Notably, the CD148-null mice are viable and show no gross abnormalities (Takahashi et al., 2003a) suggesting the importance of the interaction between the CD148 ectodomain and its binding partners for its activity. In agreement with this hypothesis, engagement of CD148 extracellular domain with an agonistic Ab promotes its activation and suppresses EC growth in culture and angiogenesis in the cornea (Takahashi et al., 2006). Recently, thrombospondin-1 (TSP-1) has been identified as a CD148 agonistic ligand able to inhibit both epithelial and EC growth (Takahashi et al., 2012). In addition, further studies revealed that CD148 can play a role in inhibition of leukocyte cell migration (Zhu et al., 2011).

In light of the studies just mentioned, we hypothesized that S2ED-mediated inhibition of EC migration and angiogenesis described in the previous section requires the involvement of both CD148 and β1 integrins.

4.2.2. Aims

In the previous results section all four syndecan ectodomains were shown to directly affect EC migration and to strongly inhibit angiogenesis. The focus of this next section is one particular member of the family, syndecan-2, aiming to establish whether its anti-angiogenic properties are maintained *in vivo* and to explore in more detail the associated molecular mechanisms.

The specific aims of the experiments described here are therefore as follows:

1. Establish whether shed syndecan-2 can affect pathological angiogenesis *in vivo*.
2. Determine whether physiological shedding of syndecan-2 ectodomain produce a cleavage product which still retains anti-angiogenic properties.
3. Determine whether the heparan sulphate chains are important for shed syndecan-2 functions *in vivo* and *in vitro*.
4. Understand the mechanism of action; in particular, a possible involvement of CD148 and β1 integrins.

4.2.3. Results

4.2.3.1. Constitutively released syndecan-2 extracellular domain from HEK293T cells inhibits angiogenesis in a xenograft tumor model

To determine the effect of shed syndecan-2 on new blood vessel formation *in vivo*, a model of tumor angiogenesis was employed. A human embryonic kidney derived cell line (HEK293T) was lentivirally transfected with either an empty vector or a vector containing the sequence for the murine syndecan-2 extracellular domain with an HA-tag inserted (Fig. 4.12). Since this construct lacks the transmembrane domain (and the cytoplasmic domain) it is not retained in the plasma membrane but constitutively shed in the extracellular space. To confirm this rationale, conditioned medium was collected from either HEK293T transfected with the empty vector (EV) or the vector containing the syndecan-2 extracellular domain (eS2ED) sequence and dot-blotted for the presence of ectopic syndecan-2. Results confirmed that eukaryotic syndecan-2 extracellular domain is expressed and released in the conditioned medium of HEK293T transfected with the eS2ED vector while it is absent in the control medium (EV) (Fig. 4.13).

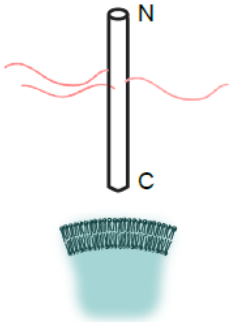

Fig. 4.12 **Syndecan-2 extracellular domain diagram.** The diagram shows the truncated form of syndecan-2 expressed in HEK293T cells. Notably, the protein is substituted by HS chains but lacks both the transmembrane and cytoplasmic domains hence it is not retained in the cell membrane but constitutively released in the extracellular space. (Figure from De Rossi et al., 2014).

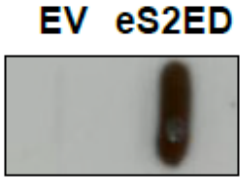

Fig. 4.13 **Syndecan-2 extracellular domain is expressed and released in the extracellular space.** After an overnight incubation in serum-free medium, conditioned medium from HEK293T cells transfected with the empty vector (EV) or the syndecan-2 extracellular core protein vector (eS2ED) (N-terminally fused to an HA tag) were run in a dot blot assay using an anti-HA tag Ab. A strong signal was detected in the eS2ED sample while no signal was present in the EV control, as expected. (Figure from De Rossi et al., 2014).

HEK293T cells were then injected sub-cutaneously in the flank of SCID mice and the xenograft tumors were allowed to develop. After 3 weeks, mice were culled and tumors excised. Notably, mice injected with HEK293T constitutively releasing eS2ED in the

surrounding cellular microenvironment grew far less than the control ones (Fig. 4.14). In fact tumors were significantly smaller both in size (Fig. 4.15) and in weight (Fig. 4.16) compared to the EV control. Interestingly, the decreased growth of those tumors constituted by HEK293T constitutively releasing eS2ED was unlikely due to a reduced proliferative potential of the tumor cells since the proliferation rate of those cells was tested *in vitro* and resulted similar to that of HEK293T transfected with empty vector (Fig. 4.17).

On the other hand, when tumors from the two groups were sectioned and stained for the EC marker CD31, far less CD31-positive structures were detected in the hek293t (eS2ED) tumors compared to the EV controls (Fig. 4.18 and Fig. 4.19).

These results showed that in a xenograft tumor model, the presence of syndecan-2 extracellular domain in the microenvironment has a strong inhibitory effect on tumor growth and on tumor derived angiogenesis. The fact that shed syndecan-2 had no effect on tumor cell proliferation *in vitro* would suggest that the reduced tumor growth is likely due to reduced angiogenesis which fails to provide tumor cells with enough nutrients and oxygen necessary for a higher growth rate.

Fig. 4.14 **Effect of syndecan-2 extracellular domain on tumor growth.** HEK293T cells previously transfected with either an empty vector (EV) or the constitutively released syndecan-2 extracellular domain (eS2ED) coding vector were injected s.c. into the flank of severe combined immuno-deficient (SCID) mice. Mice were culled after 3 weeks and the entire tumor excised and photographed. Image shows 5 tumors per group. Scale bar represents 1 cm. (Figure from De Rossi et al., 2014).

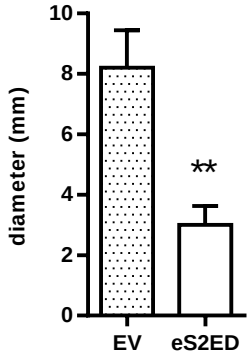

Fig. 4.15 **Effect of syndecan-2 extracellular domain on tumor size.** HEK293T cells previously transfected with either an empty vector (EV) or the constitutively released syndecan-2 extracellular domain (eS2ED) coding vector were injected s.c. into the flank of severe combined immuno-deficient (SCID) mice. Mice were culled after 3 weeks and the entire tumor excised and the diameter measured. Bars show the mean and standard error of the mean of 5 animals per group. Significant differences between control tumors (EV) and treated tumors (eS2ED) were determined using unpaired t-test. **P<0.01. (Figure from De Rossi et al., 2014).

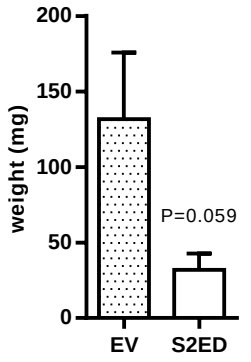

Fig. 4.16 **Effect of syndecan-2 extracellular domain on tumor weight.** HEK293T cells previously transfected with either an empty vector (EV) or the constitutively released syndecan-2 extracellular domain (eS2ED) coding vector were injected s.c. into the flank of severe combined immuno-deficient (SCID) mice. Mice were culled after 3 weeks and the entire tumor excised and the diameter measured. Bars show the mean and standard error of the mean of 5 animals per group. No significant differences between control tumors (EV) and treated tumors (eS2ED) were determined using unpaired t-test. (Figure from De Rossi et al., 2014).

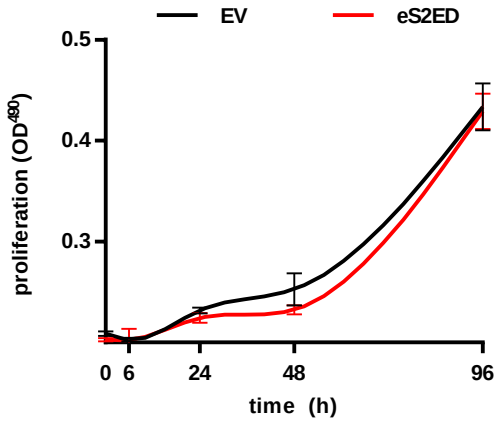

Fig. 4.17 **Effect of syndecan-2 extracellular domain on HEK293T cell proliferation.** Equal numbers of HEK293T cells previously transfected with either an empty vector (EV) or the constitutively released syndecan-2 extracellular domain (eS2ED) coding vector were cultured in a 96-well plate and their proliferation at 6, 24, 48 and 96 hours measured with the CellTiter 96 AQueous kit (Promega). Lines show the cubic spline generated from the data points. Error bars represent the standard deviation of the mean from 4 replicates per condition. No significant differences between control tumors (EV) and treated tumors (eS2ED) were determined using two-way Anova with Bonferroni correction for multiple comparisons. (Figure from De Rossi et al., 2014).

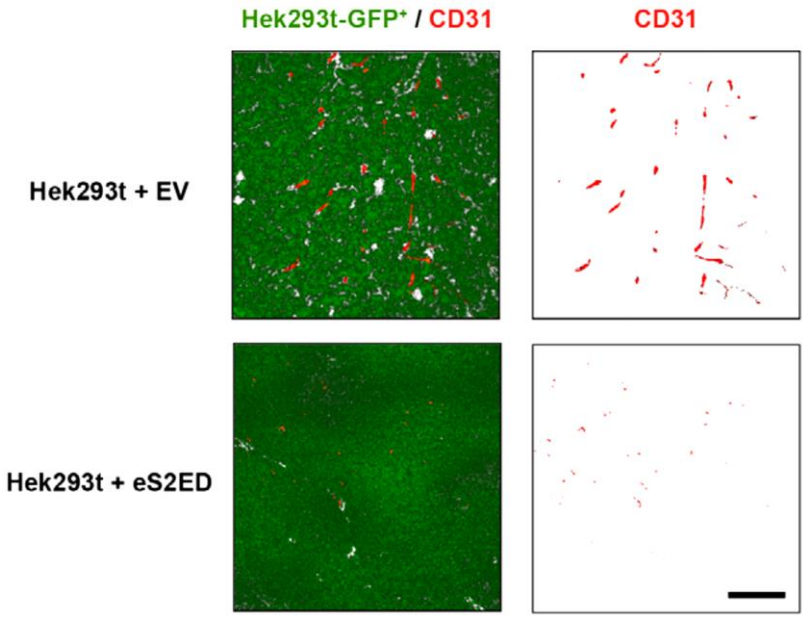

Fig. 4.18 **Effect of syndecan-2 extracellular domain on tumor angiogenesis.** HEK293T cells previously transfected with either an empty vector (EV) or the constitutively released syndecan-2 extracellular domain (eS2ED) coding vector were injected s.c. into the flank of severe combined immuno-deficient (SCID) mice. Mice were culled after 3 weeks and the entire tumor excised and immediately freezed in liquid nitrogen and stored at -80°C. Samples were then embedded in OCT and 60 µm sections were made using a cryotome. Sections were then fixed and blocked/permeabilized prior to staining with an anti-CD31 Ab (Red) to visualize ECs. HEK293T cells are GFP positive (green). Images are representative of 5 animals per group. Scale bar represents 100 µm. (Figure from De Rossi et al., 2014).

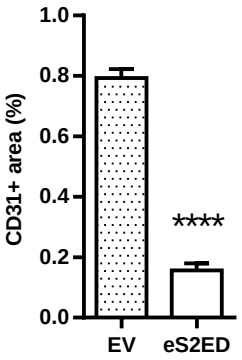

Fig. 4.19 **Effect of syndecan-2 extracellular domain on tumor angiogenesis.** Sections from the previous experiment were analysed to quantify new blood vessel formation. Image J was used to measure the area covered by CD31+ vessels and the value was then expressed as the percentage of CD31+ area over the whole image. Results are representative of 5 animals per group. Bars show the mean and standard error of the mean of 5 animals per group for which at least 4 images were analysed. Significant differences between control tumors (EV) and treated tumors (eS2ED) were determined using unpaired t-test. ****P<0.0001. (Figure from De Rossi et al., 2014).

4.2.3.2. Shed syndecan-2 from HEK293T cells has anti-angiogenic properties

Syndecans are often shed from the cell surface as a result of pathological conditions such as inflammation, cancer and wound healing; however, little is known about the proteases responsible for this phenomenon and/or their cutting sites. The next set of experiments were set to determine whether once syndecan-2 is shed in a physiological way (e.g. as a result of an inflammatory stimulation) it would still retain its anti-angiogenic properties.

The xenograft tumor model suggested an anti-angiogenic activity of the eS2ED molecule which was designed to contain the extracellular domain sequence of syndecan-2 in its entirety. To assess whether a physiologically shed form of syndecan-2 would retain the same properties, HEK293T cells were transfected with a vector containing the full-length murine syndecan-2 sequence (Fig. 4.20) and subsequently exposed to increasing doses of TNFα which is a known pro-inflammatory factor and can stimulate syndecan shedding *in vitro* (Brightling et al., 2005; Pruessmeyer et al., 2010; Tan et al., 2012). Conditioned medium was then collected and dot-blotted for the ectopic syndecan-2 using an Ab specific for the HA tag N-terminally fused to syndecan-2; HEK293T cells transfected with an empty vector showed no signal while HEK293T cells transfected with the full length syndecan-2 (eFLS2) secreted the molecule in a dose-dependent manner upon addition of TNFα in the medium (Fig. 4.21).

The rat aortic ring assay was then employed to determine the anti-angiogenic activity of the TNFα-induced shed form of syndecan-2. Conditioned media from HEK293T transfected with an empty vector and treated with TNFα, HEK293T transfected with full length syndecan-2 and treated with TNFα and HEK293T transfected with the constitutively shed syndecan-2 extracellular domain were collected and the proteoglycans contained within were purified via anion-exchange. Subsequently, 10 µg of each purification product were added to the collagen matrix in which the aortic rings were embedded and angiogenic sprout growth was measured after 7 days. A strong decrease in the number of angiogenic sprouts, hence in angiogenesis, occurred in the groups treated with induced or constitutively shed forms of syndecan-2 (eFLS2 and eS2ED, respectively) when compared to the control group (EV) (Fig. 4.22). Although the anion-exchange step only allowed the purification of a mix of proteoglycans not just syndecan-2, by using the purification product derived from the conditioned medium from HEK293T EV and treated with TNFα as a control, the anti-angiogenic effect of both eFLS2 and eS2ED groups was most likely due to the presence of the extra amount of ectopic syndecan-2 in the medium.

These results suggested that the anti-angiogenic properties of syndecan-2 extracellular domain seen in the xenograft tumor model are most likely retained when syndecan-2 is physiologically

shed. It is therefore reasonable to speculate that TNFα leads to syndecan-2 cleavage at its juxtamembrane region resulting in the release of the entirety of syndecan-2 extracellular domain.

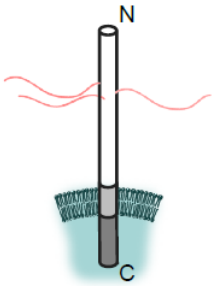

Fig. 4.20 **Full length syndecan-2 diagram.** The diagram shows the full length form of syndecan-2 expressed by HEK293T cells. The protein is substituted by HS chains in its extra-cellular domain and has transmembrane and cytoplasmic domains which anchor it to the cell membrane. (Figure from De Rossi et al., 2014).

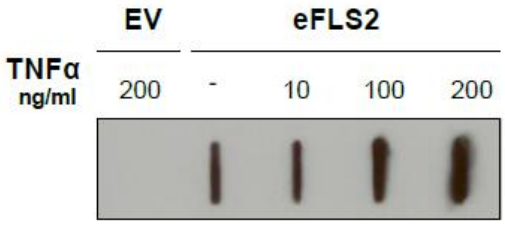

Fig. 4.21 **Full length syndecan-2 shedding in response to Tumor necrosis factor α (TNFα).** HEK293T cells expressing the empty vector (EV) or full length syndecan-2 (sFLS2) were incubated for 4 hours in serum-free medium with the indicated amount of TNFα. Conditioned media were then collected, run in a dot blot apparatus and probed with an anti-HA tag Ab. (Figure from De Rossi et al., 2014).

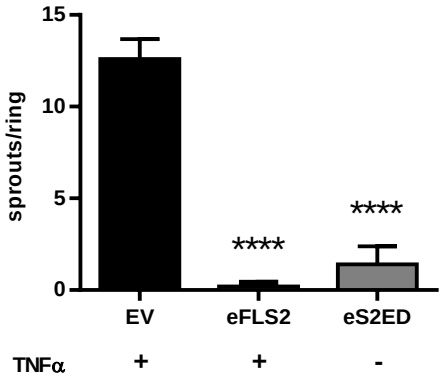

Fig. 4.22 **Effect of induced and constitutively shed syndecan-2 on angiogenic sprouting.** HEK293T cells expressing the empty vector (EV) or full length syndecan-2 (sFLS2) were incubated for 4 hours in serum-free medium with 200 ng/ml of TNFα while HEK293T expressing the constitutively shed eS2ED were left untreated in serum-free. Conditioned media were then collected, shed proteoglycans were purified via anion-exchange and 10 µg of each product were added into the collagen I layer of the rat aortic ring assay. Each bar represents the mean and standard deviation of 8 rings. Significant differences between control group (EV) and treated groups were determined using one-way Anova with Bonferroni correction for multiple comparisons. ****P<0.0001. (Figure from De Rossi et al., 2014).

4.2.3.3. The syndecan-2 extracellular core protein inhibits angiogenesis

Because syndecan-2 is a proteoglycan and as such is composed of a proteic backbone and sugar chains, we decided to establish whether the anti-angiogenic effect showed *in vivo* in the xenograft tumor model was mediated by the peptide alone (deprived of its HS chain substitutions) which had been previously shown to possess a cell adhesion regulatory domain(Whiteford et al., 2007) and to being able to inhibit angiogenesis *ex vivo* (4.1.3.1). To explore this hypothesis, we took advantage of the same substrates used in the previous section: syndecan-2 extracellular core protein N-terminally fused to GST and GST alone (Fig. 4.23).

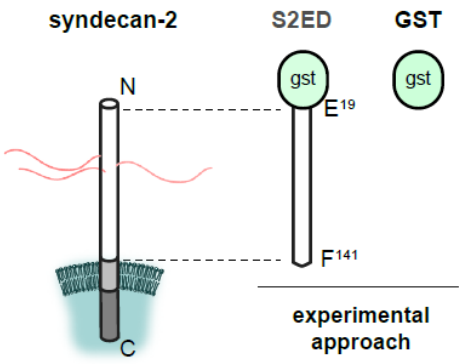

Fig. 4.23 **Experimental approach.** The diagram depicts the experimental approach used to assess if the anti-angiogenic properties of shed syndecan-2 are dependent on its proteic component. The extracellular core protein of syndecan-2 (aa E19 to F141) N-terminally fused to GST or GST alone were expressed in E.coli, subsequently purified using Sepharose columns and quantified via SDS-Page. (Figure from De Rossi et al., 2014).

These substrates were tested in an *in vivo* model of angiogenesis, namely the matrigel plug assay. Wild type mice were s.c. injected with Matrigel containing the same concentration of either GST or syndecan-2 ectodomain (S2ED) and the pro-angiogenic stimuli VEGF-A and bFGF. After 5 days mice were sacrificed, plugs were excised and incubated in deionized water over-night to extract the haemoglobin within them. It is clear from the photos that those plugs containing S2ED were far less red than the GST control group indicating the presence of a decreased amount of haemoglobin within them (Fig. 4.24). This suggested that less angiogenesis had happened in those plugs, in fact, when plugs were sectioned and stained for an EC marker (CD31) fewer ECs were detectable in the in the plugs containing S2ED (Fig. 4.25 and Fig. 4.26). This suggested that the anti-angiogenic activity of S2ED previously shown *ex vivo (4.1.3.1*) is still maintained *in vivo*.

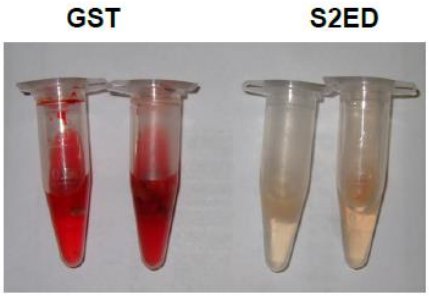

Fig. 4.24 **Effect of syndecan-2 extracellular core protein on angiogenesis *in vivo*.** 500 µl of 7.5 mg/ml matrigel in PBS containing 100 ng/ml of VEGF-A, 100 ng/ml of bFGF, 20 U/ml of Heparin and either 0.5 µM of GST or syndecan-2 extracellular core protein (S2ED) was injected s.c. in the flanks of 6-8 weeks old wild type mice. After 5 days mice were culled, plugs excised and left over-night in 500 µl of dH_2O to allow haemoglobin to be released from the matrigel. The image shows the two plugs from one animal per group after the over-night incubation in dH_2O and is representative of 4 animals per group. (Figure from De Rossi et al., 2014).

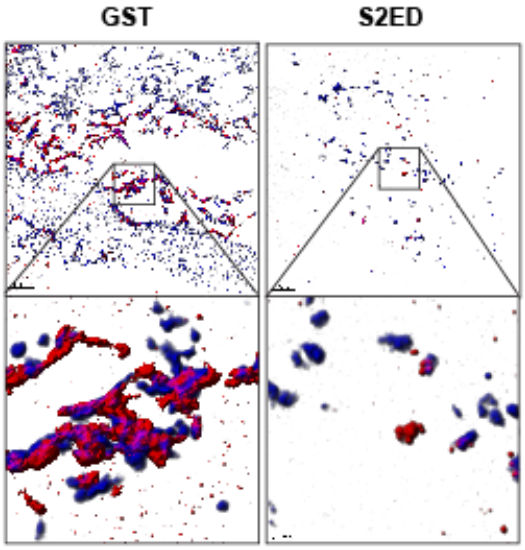

Fig. 4.25 **Effect of syndecan-2 extracellular core protein on EC migration into the matrigel plug *in vivo*.** 500 µl of 7.5 mg/ml matrigel in PBS containing 100 ng/ml of VEGF-A, 100 ng/ml of bFGF, 20 U/ml of Heparin and either 0.5 µM of GST or syndecan-2 extracellular core protein (S2ED) was injected s.c. in the flanks of 6-8 weeks old wild type mice. After 5 days mice were culled, plugs excised and frozen in liquid nitrogen. Plugs were then embedded in OCT and cryosections of 50 µm were cut. Sections were then fixed in 4% PFA, stained for ECs (PECAM-1, red) and nuclei (DRAQ5, blue) and photographed under a confocal microscope. Bottom images are magnifications of regions of interest from the top images, to highlight how in the control (GST) ECs (red) are already starting to organize into a tubule-like structure, while fewer cells and unorganized are present in the treated sample (S2ED). Scale bars represent 100 µm. Images are representative of 4 animals per group. (Figure from De Rossi et al., 2014).

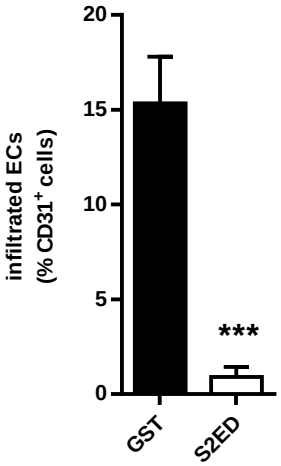

Fig. 4.26 **Effect of syndecan-2 extracellular core protein on EC migration into the matrigel plug *in vivo*.** Sections from the previous experiment were analysed to quantify EC infiltration into the matrigel plugs. Image J was used to count the number of cell nuclei present in the images (DRAQ5-positive) and the percentage of those nuclei which were also positive for PECAM (EC marker). Results are representative of 4 animals per group. Bars show the mean and standard error of the mean of 4 animals per group for which at least 4 images were analysed. Significant differences between control samples (GST) and treated sample (S2ED) were determined using unpaired t-test. ***P<0.001. (Figure from De Rossi et al., 2014).

To corroborate this finding, the effect of S2ED on tubule formation was established. Tubule formation is a widely used as an *in vitro* model of angiogenesis as it nicely resembles many important features which take place during the early steps of the angiogenic process *in vivo*, such as EC proliferation, migration and organization into a network of tubules. A tubule formation kit, commercially available, was used to test the effect of S2ED (at two concentrations) on this process. A co-culture of human dermal fibroblasts and ECs were seeded and grown for 2 weeks in the presence of different stimuli. The greatest tube formation response was unsurprisingly detected in the sample treated with VEGF-A which is a known pro-angiogenic factor and was therefore used as a positive control. Suramin instead, an angio-suppressive agent used as a negative control, completely inhibited tubule formation (Fig. 4.27). Interestingly, S2ED inhibited this process both in terms of number of branching points (Fig. 4.28) and tubule length (Fig. 4.29). This effect seemed to be dose dependent although the difference between the group treated with 0.1 μM of S2ED and the control group (medium only) was not statistically significant.

Altogether these results suggested that the anti-angiogenic properties of shed syndecan-2 reside in its proteic domain and that it likely to be a direct effect on ECs.

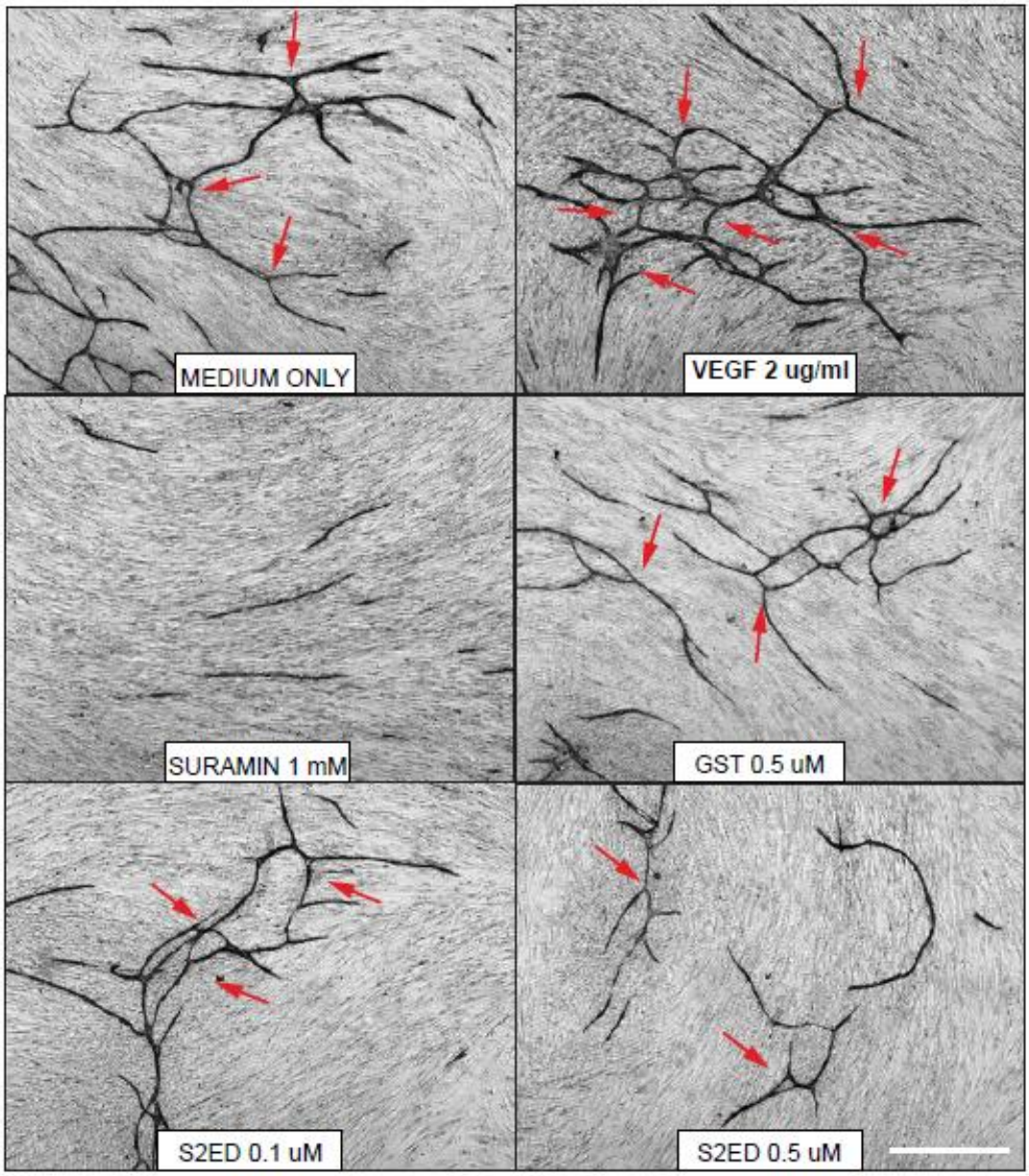

Fig. 4.27 **Effect of syndecan-2 extracellular core protein on tubule formation.** HUVECs and human dermal fibroblasts were co-cultured using the Cell Works V2a kit. Medium containing positive control compound VEGF, negative control compound Suramin, GST or S2ED at the concentrations indicated or medium only was changed every second day and at day 14 ECs were stained for PECAM-1 (black signal) to assess the tubule formation. Red arrows indicate examples of branching points. Imaging was performed using an inverted microscope. Images are representative of triplicates of which at least 3 pictures were taken. Scale bar represents 500 µm. (Figure from De Rossi et al., 2014).

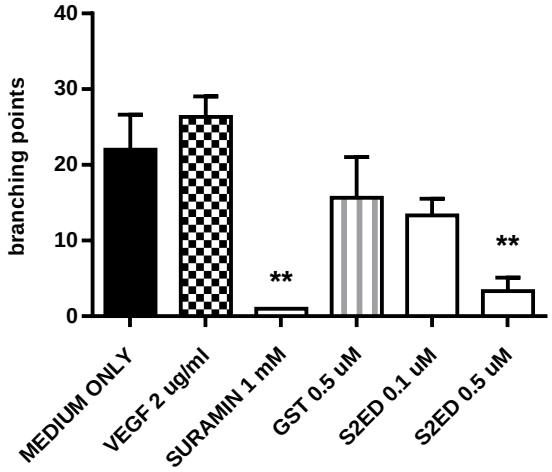

Fig. 4.28 **Effect of syndecan-2 extracellular core protein on tubule branching**. HUVECs and human dermal fibroblasts were co-cultured using the Cell Works V2a kit. Medium containing positive control compound VEGF, negative control compound Suramin, GST or S2ED at the concentrations indicated or medium only was changed every second day and at day 14 ECs were stained for PECAM-1 (black signal) to assess the tubule formation. Tubule branching was quantified using Photoshop (Adobe). A branch point was defined as the point at which two or more tubules met. Each bar represents the mean with standard error of the mean of triplicates. Significant differences between untreated control (MEDIUM ONLY) group and treated groups were determined using one-way Anova with Dunnett correction for multiple comparisons. **P<0.01. (Figure from De Rossi et al., 2014).

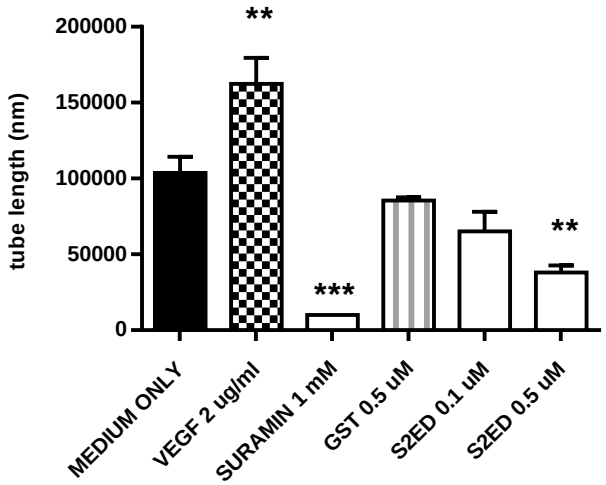

Fig. 4.29 **Effect of syndecan-2 extracellular core protein on tubule length.** HUVECs and human dermal fibroblasts were co-cultured using the Cell Works V2a kit. Medium containing positive control compound VEGF, negative control compound Suramin, GST or S2ED at the concentrations indicated or medium only was changed every second day and at day 14 ECs were stained for PECAM-1 (black signal) to assess the tubule formation. Tubule length was quantified using Photoshop (Adobe). A branch point was defined as the point at which two or

more tubules met, and the tubule length as the length of tubules between branch points. Each bar represents the mean with standard error of the mean of triplicates. Significant differences between untreated control (MEDIUM ONLY) group and treated groups were determined using one-way Anova with Dunnett correction for multiple comparisons. **P<0.01, ***P<0.001. (Figure from De Rossi et al., 2014).

4.2.3.4. The anti-angiogenic properties of S2ED are due to inhibition of EC migration and are mediated by amino acids P^{124}-F^{141}

Because syndecan-2 ectodomain had previously been shown to possess an adhesion-regulatory domain (ARD) at the C-terminus of its extracellular domain (aa P^{124}-F^{141}) (Fig. 4.30) which when engaged promotes cell adhesion in both fibroblasts and ECs (Whiteford et al., 2007), we hypothesized that the anti-migratory effect that syndecan-2 extracellular core protein exerts on ECs, shown in the previous section (4.1.3.3), is mediated by the ability of the ARD to promote EC switch from a migratory to a more adhesive state. To test this hypothesis, 2 mutant forms of S2ED were produced and purified from *E.coli*. S2EDΔP^{124}-F^{141} lacks the last 18 aa (the ARD) while S2EDΔL^{73}-G^{123} still possesses the ARD but lacks the region between the ARD and the HS chains substitution sites (Fig.4.30). Firstly, these constructs were tested in a rat aortic ring assay and interestingly only the construct containing the adhesion regulatory domain retained the S2ED anti-angiogenic effect while the one lacking those 18 aa had no effect on angiogenesis compared to both untreated and GST-treated controls (Fig. 4.31).

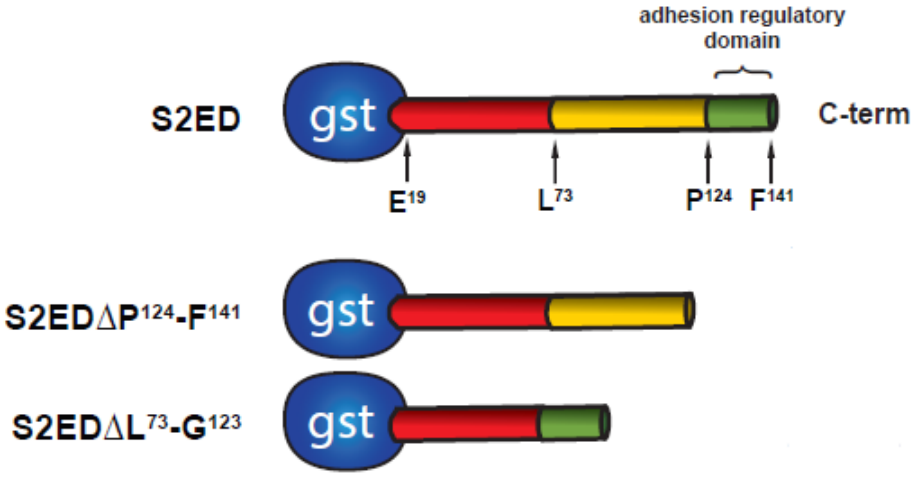

Fig. 4.30 **Syndecan-2 extra-cellular core protein mutants N-terminally fused to GST were produced in E.coli.** Diagram shows the structure of the proteins used in the experiments. Syndecan-2 extra-cellular core proteins were expressed and purified from E.coli and possess a Glutathione S-transferase (GST) fused to their N-terminus. The region coloured in green ranging from amino acid P^{124} to F^{141} has previously been described as the adhesion regulatory domain (ARD), the red region which comprises amino acid E^{19} to L^{73} is the region substituted by HS chains and it is separated from the ARD by the yellow region from L^{73} to P^{124}. However, since these peptides are produced in *E.coli*, they are not substituted by HS chains. (Figure from De Rossi et al., 2014).

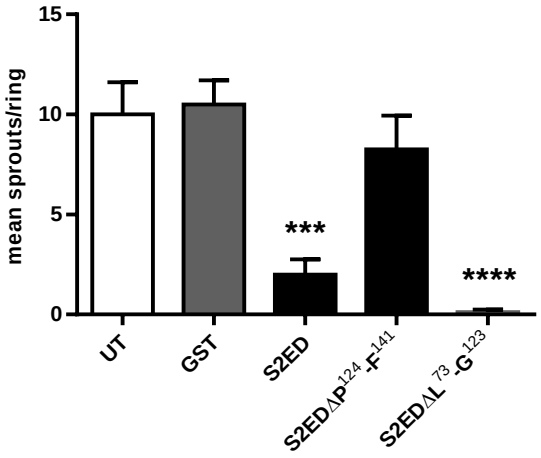

Fig. 4.31 **Effect of syndecan-2 adhesion regulatory domain on angiogenic sprouting.** Rat thoracic aortas were cut into rings which were embedded in 150 µl of Collagen type I (1 mg/ml) containing 0.5 µM of syndecan-2 extra-cellular core protein (S2ED), its truncated mutant forms (S2EDΔP^{124}-F^{141} and S2EDΔL^{73}-G^{123}) or GST control in 200 µl of OPTIMEM containing 10 ng/ml of VEGF-A. The number of sprouts was measured 7 days after embedding. Each bar represents the mean with standard deviation of 8 rings per group. Significant differences between untreated control (UT) group and treated groups were determined using one-way Anova with Dunnett correction for multiple comparisons. ***P<0.001, ****P<0.0001. (Figure from De Rossi et al., 2014).

Having established that the previously characterized ARD is necessary for S2ED anti-angiogenic effect, we further explored the aforementioned hypothesis that this was due to an effect on EC migration. We tested if skin endothelial (sEND) cells migratory potential was affected by the presence of the different S2ED mutant constructs in a scratch wound assay. After 9 hours control cells treated with GST or with S2EDΔP^{124}-F^{141} lacking the ARD migrated and refilled the empty space created by the scratch, while those treated with S2ED or the shorter form S2EDΔL^{73}-G^{123} which still possesses the ARD failed to do so (Fig. 4.32). These results showed that S2ED effect on EC migration is dependent on the ARD contained within its last 18 aa.

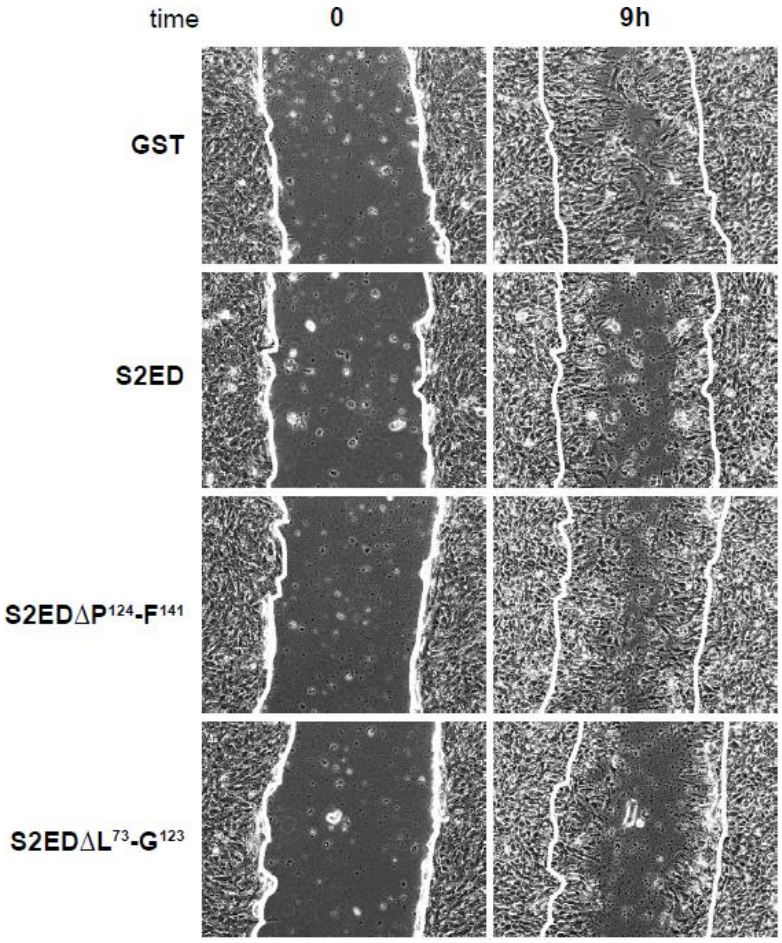

Fig. 4.32 **Effect of syndecan-2 adhesion regulatory domain on EC migration.** Confluent skin ECs (sEND) were scratched with a pipette tip in the middle of the well, washed in PBS and fresh medium containing 0.5 µM of the indicated proteins was added. Photographs of the same spot were taken on an inverted microscope straight after the addition of the treatment (0h) and after 9 hours (9h). White lines were drawn to over the initial scratch margins to better visualize cell migration at the final time point. Pictures are representative of 3 experiments where at least 2 spots per condition were analysed. Scale bar represents 500 µm. (Figure from De Rossi et al., 2014).

4.2.3.5. S2ED interacts with CD148, resulting in inhibition of angiogenesis

Previously it has been shown that S2ED is a novel ligand for the transmembrane tyrosine phosphatase CD148 in fibroblasts and the interaction between S2ED adhesion-regulatory domain and CD148 triggers fibroblast adhesion in a β1 integrin-dependent way (Whiteford et al., 2011). Since integrins are the main drivers of cell migration, we set to determine whether the pathway previously described for fibroblasts was also true for ECs.

First we determined whether ECs express CD148, to this purpose ECs from three different vascular beds (brain, lung and skin) were lysed and immuno-blotted with an anti-CD148 Ab, results showing the presence of the protein in ECs from all three origins (Fig. 4.33). Next, cell lysates from sENDs were incubated with beads coated with GST, S2ED, S2EDΔP^{124}–F^{141} or S2EDΔL^{73}–G^{123} and the precipitate was subsequently immuno-blotted with an anti-CD148 Ab. The western blot showed that CD148 from ECs binds the last 18 aa of S2ED (Fig. 4.34).

In light of these results, it was decided to test whether a soluble form of CD148 extracellular core protein could disrupt the interaction of the membrane-bound CD148 with S2ED and revert the anti-angiogenic effect. Surprisingly, when soluble CD148 alone was incorporated to the collagen in the rat aortic ring assay we noticed a strong anti-angiogenic effect which was further enhanced by the addition of S2ED (Fig. 4.35).

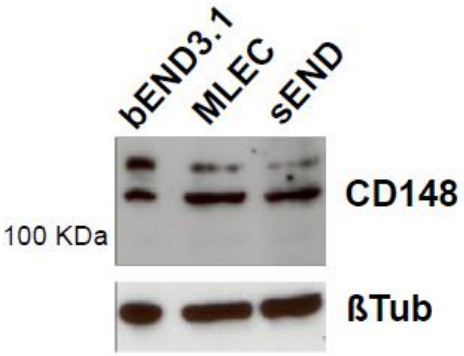

Fig. 4.33 **The expression of CD148 on ECs from different origins.** Western blot of lysates from EC lines from murine brain (bEND3.1) and skin (sEND) and primary murine lung ECs were probed with Abs against CD148 or β-tubulin. The blot is representative of 4 experiments. (Figure from De Rossi et al., 2014).

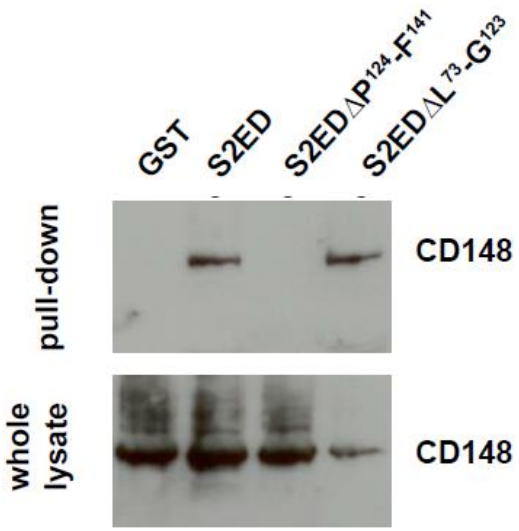

Fig. 4.34 **Binding of S2ED to CD148.** Cell lysates from sEND cells were incubated with beads coated with GST, S2ED, S2EDΔP^{124}–F^{141} or S2EDΔL^{73}–G^{123}. Precipitates were analysed by western blotting for the presence of CD148. The blot is representative of 4 experiments. (Figure from De Rossi et al., 2014).

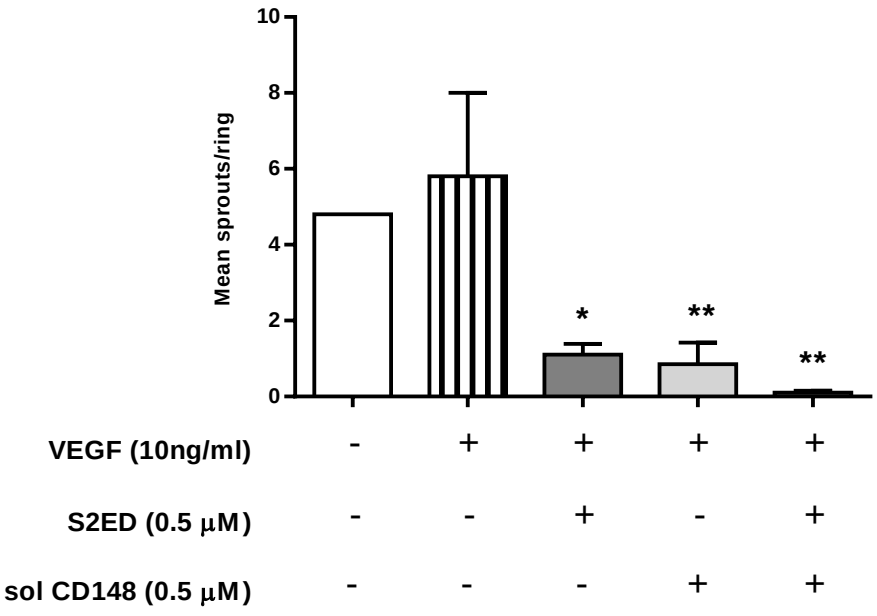

Fig. 4.35 **Effect of CD148 engagement on angiogenic sprouting.** Rat thoracic aortas were cut into rings which were embedded in 150 µl of Collagen type I (1 mg/ml) containing 0.5 µM of syndecan-2 extra-cellular core protein (S2ED), soluble CD148 or both in 200 µl of OPTIMEM containing 10 ng/ml of VEGF-A. The number of sprouts was measured 7 days after embedding. Each bar represents the mean with standard deviation of 4 experiments with at least 5 rings per group. Significant differences between positive control (striped bar) group and treated groups were determined using one-way Anova with Dunnett correction for multiple comparisons. *P<0.05, **P<0.01. (Figure from De Rossi et al., 2014).

4.2.3.6. Active β1 integrin expression is reduced on ECs in the presence of S2ED

In a previous work fibroblast adhesion to S2ED was shown to be dependent on β1 integrin since the use of a β1 integrin blocking Ab could ablate this process (Whiteford et al., 2011). The activation status of β1 integrins on ECs was therefore evaluated and, specifically, whether that was affected by S2ED. To this purpose, a suspension of brain endothelial (bEND) cells was treated with 0.5 μM of either GST or S2ED and analysed via FACS to evaluate the rate of activation of β1 integrins. The results showed that cells treated with S2ED had less active β1 compared to those treated with GST or left untreated (Fig. 4.36).

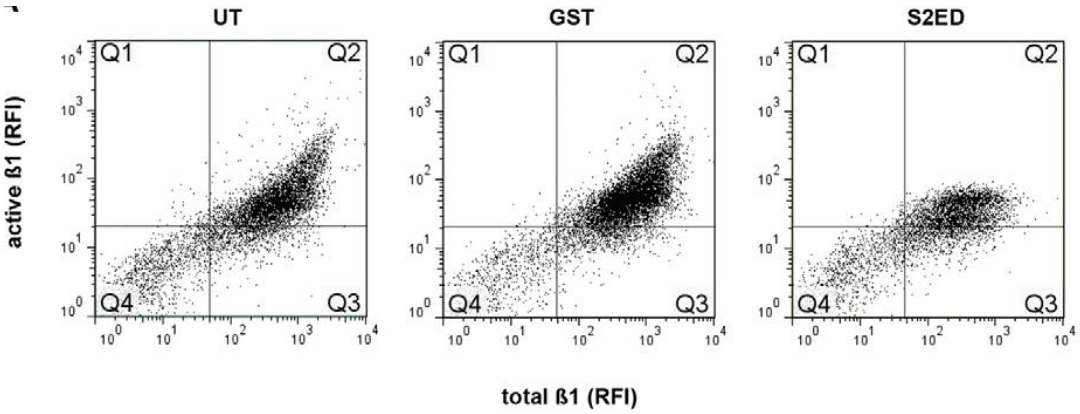

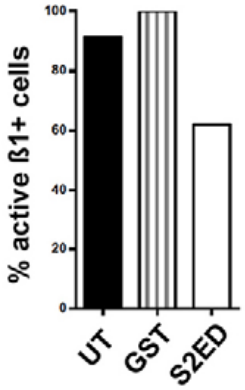

Fig. 4.36 **Effect of S2ED on β1 integrin activation – ECs in suspension.** bEND3.1 were suspended and treated with 0.5 μM of GST or S2ED for 30' at 37°C. Cells were then immunostained for both total and active β1 integrin (9EG7 Ab) and analysed by flow cytometry. Dot blots show the relative fluorescence intensity of active and total β1 integrin expression on ECs treated with the different proteins. Vertical and horizontal lines were drawn based on the fluorescence intensity of the isotype controls. The percentage of cells which are positive for active β1 integrin after each treatment is shown in the bar graph and was calculated using the following equation 100*Q2/(Q2+Q3). (Figure from De Rossi et al., 2014).

Next, the activation of β1 integrins when ECs are actively migrating was examined. A confluent monolayer of skin ECs was scratched and cell left to migrate for 30' in the presence of either GST or S2ED before being fixed and stained for active β1 integrins (9EG7 Ab). Untreated control (UT) showed a strong active β1 integrin staining across the all plate,

especially on the leading edges of the wound which was reflected in the staining signal intensity quantified across an arbitrary straight line ran horizontally on the micrograhs. Similar results were produced when cells were treated with GST, however cells treated with S2ED exhibited far less active β1 integrin staining (Fig. 4.37 and Fig. 4.38), which is in accordance to the previous FACS experiment.

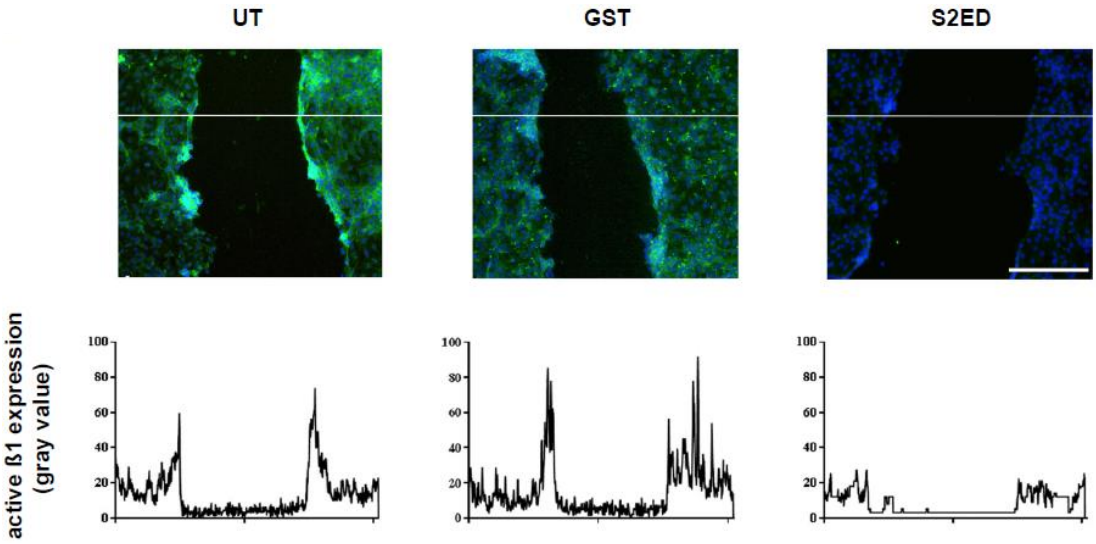

Fig. 4.37 **Effect of S2ED on β1 integrin activation – adherent ECs.** Confluent monolayers of sEND cells were grown in a 6-well plate and scratch wounds were made prior to the addition of either 0.5 mM GST or S2ED. After 30', cells were fixed, permeabilised and immunostained for active β1 expression (9EG7 clone, green) and cell nuclei (DAPI, blue). Images were captured on an Olympus IX81 inverted microscope. Fluorescent intensity profiles were calculated over an arbitrary horizontal line (white line) using ImageJ. Scale bar represents 200 µm. (Figure from De Rossi et al., 2014).

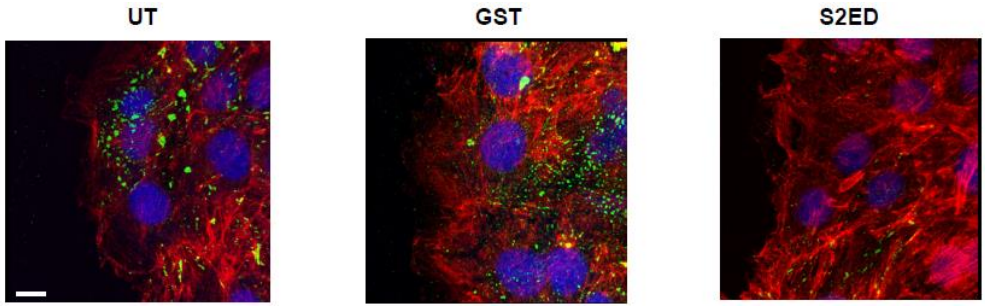

Fig. 4.38 **Effect of S2ED on β1 integrin activation – adherent ECs.** Confluent monolayers of sEND cells were grown on glass slides and scratch wounds were made prior to the addition of either 0.5 mM GST or S2ED. After 30', cells were fixed, permeabilised and immunostained for active β1 expression (green, 9EG7 clone), F-actin (red) and cell nuclei (DRAQ5, blue). Images captured on a Zeiss confocal microscope and processed on Imaris software are representative of at least 5 images per condition. Scale bar represents 20 µm. (Figure from De Rossi et al., 2014).

To gain more confidence over these results, we decided to use another EC line, namely HUVECs which is known to activate β1 integrins upon stimultation with Manganese. Again, the addition of S2ED in the medium, after stimulation with Manganese, resulted in a decrease in active β1 integrin compared to GST-treated or untreated control . Notably, these results were obtained using a different active β1-specific Ab (HUTS4) and nonetheless showed the same results seen previously with the 9EG7 Ab (Fig. 4.39).

This suggested that S2ED impairs the activation of β1 integrins on ECs both during migration and when that is triggered artificially with Manganese.

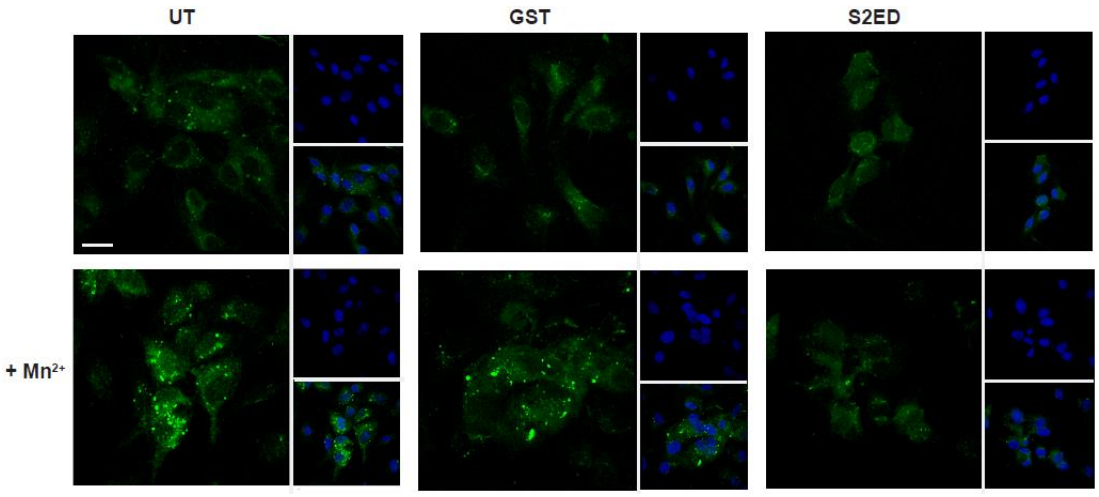

Fig. 4.39 **Effect of S2ED on β1 integrin activation – adherent ECs.** HUVECs were seeded on glass slides coated with fibronectin (10 µg/ml) and collagen I (30 µg/ml) in 0.1% gelatin. Cells were then treated with or without 1 mM MnCl2 in the presence of either 0.5 mM GST or S2ED for 30'. Cells were then fixed/permeabilised and immunostained for active β1 integrin (green, HUTS4 clone) and cell nuclei (DRAQ5, blue). Images were captured on a Zeiss confocal microscope and processed on Imaris software. Scale bar represents 20 µm. (Figure from De Rossi et al., 2014).

4.2.4. Discussion

In the first section of this thesis, I provided evidence to show that all four syndecan ectodomains are strong negative regulators of angiogenesis *in vitro*. The fact that the syndecan ectodomain sequences share very little homology would suggest that their anti-angiogenic effect is achieved through four different pathways and previous studies (Whiteford et al., 2007) would suggest these pathways involve integrins of the αVβ3, αVβ5 and β1 subfamily. For this reason, each syndecan ectodomain would deserve to be studied separately; unfortunately, due to the time limitation of a 3-year PhD program, I decided to focus on and follow up only syndecan-2 and explore in more detail not only the mechanistic of its anti-angiogenic properties but also the feasibility of its potential therapeutic application in anti-angiogenic therapies.

In this second section, I tried to answer experimentally the questions raised in the discussion to the previous section. For example, the anti-angiogenic effect of syndecan ectodomains was elucidated by using the aortic ring assay which is an *ex vivo* system at best, this obviously raised the question as to whether S2ED anti-angiogenic effect would hold true *in vivo*. Here we have shown that syndecan-2 ectodomain is a potent inhibitor of angiogenesis *in vivo* with extremely promising therapeutic potential in inhibiting tumor angiogenesis. We have in fact shown that when HEK293T cells are grown *in vivo* in the presence of syndecan-2 ectodomains they develop a tumor 40% smaller than control. The fact that these tumors are also less vascularised is in agreement with our hypothesis that syndecan-2 ectodomain inhibits the formation of new blood vessels.

In the previous section, it was discussed whether physiological shedding of syndecans would result in release of molecules with biological activity. This question was answered by over-expressing full length syndecan-2 in HEK293T and subsequently promoting its shedding via addition of TNF-α to the medium. The proteoglycans contained in the conditioned medium were then purified and the purification product, enriched of physiologically shed syndecan-2, was shown to be anti-angiogenic compared to control. This certainly represents one of the most interesting results I obtained during this part of the project. The fact that syndecan-2 is shed in response to an inflammatory stimulus such as TNFα does not come as a surprise as inflammation has been shown to trigger syndecan cleavage in many systems (Andrian et al., 2005; Pruessmeyer et al., 2010; Tan et al., 2012); syndecan shedding, however, has always been considered as a way to suppress syndecan functions on the cell surface and/or to release soluble competitors for ligand binding; here, for the first time, we showed that syndecan shedding has an additional consequence which has previously only been theorized and is that

of releasing in the extracellular space a biologically active molecule which is able to affect other cells behaviour in a paracrine way. Moreover, inflammation and angiogenesis are often intertwined in physiological and pathological conditions: for example, angiogenesis enables the exaggerated influx of leukocytes in the tissue during chronic inflammation and, on the other hand, an inflammatory response (innate immunity, for the most part) is associated with new blood vessel formation (e.g. during wound healing or cancer growth) (Imhof and Aurrand-Lions, 2006). It is therefore tempting to speculate that in these scenarios where inflammation and angiogenesis occur, shedding will release in the extracellular space shed syndecan-2 which will stay anchored to the ECM (via HS-ECM interactions) and would function as a "stop" signal to ECs. Where, when and from which cells syndecan-2 is shed, could potentially determine both spatial and temporal regulation of new blood vessel formation.

The use of HEK293T as an expression system for the production of syndecans was developed as part of my project for the first time and will represent an invaluable tool for future studies on syndecan biology in our lab. Studies on syndecan ectodomains have always taken advantage of bacterial expression systems and for this, syndecan ectodomains were studied as proteins lacking the HS-substitution. Our eukaryotic system enabled us to compare the effect on angiogenesis of syndecan-2 ectodomain (complete of its HS-substitutions), physiologically-shed syndecan-2 and bacterially-derived syndecan-2 ectodomain (without HS-substitutions) and led us to conclude that syndecan-2 ectodomain anti-angiogenic effect resides in its extracellular core protein, its independent of and unaffected by its HS chains.

The experiments I conducted confirmed the hypothesis that S2ED-mediated inhibition of EC migration and angiogenesis described in the previous section requires the involvement of both CD148 and β1 integrins (Fig. 4.40 a). We could show that for S2ED to exert its anti-angiogenic function the adhesion regulatory domain, previously (Whiteford et al., 2011) mapped to P^{124} to F^{141}, must be present. This sequence contains the domain which was shown to directly interact with CD148 on fibroblasts and we showed by immuno-precipitation that this is also the case for endothelial CD148. We've also been able to show that the anti-migratory effect of S2ED on ECs was also accompanied with a reduction in active β1 integrins. We haven't assessed whether other integrins might be activated or deactivated by S2ED, nor given direct evidence that deactivation of β1 integrins is what mediates S2ED anti-angiogenic effect. However, the fact that inhibition of EC migration by thrombospondin-1 type-1 repeats is mediated by β1 integrins (Short et al., 2005) and thrombospondin-1 (TSP-1) has identified as a CD148 agonistic ligand on ECs (Takahashi et al., 2012) are supportive of our hypothesis that S2ED engagement with CD148 may promote β1 integrin deactivation and lead to inhibition of EC migration and angiogenesis.

In Fig. 4.35, we came across a quite unexpected result when a soluble form of CD148, comprised of the N-terminal first five FN-like repeats, proved to be alone inhibitory of angiogenesis. With the information at hand, we can only hypothesize that soluble CD148 could form a dimer with the membrane bound CD148 on EC surface which activates the same signalling pathway that is activated by TSP-1 (Takahashi et al., 2012), S2ED (Whiteford et al., 2011) or anti-CD148 agonistic Ab (Takahashi et al., 2006) (Fig. 4.40 b).

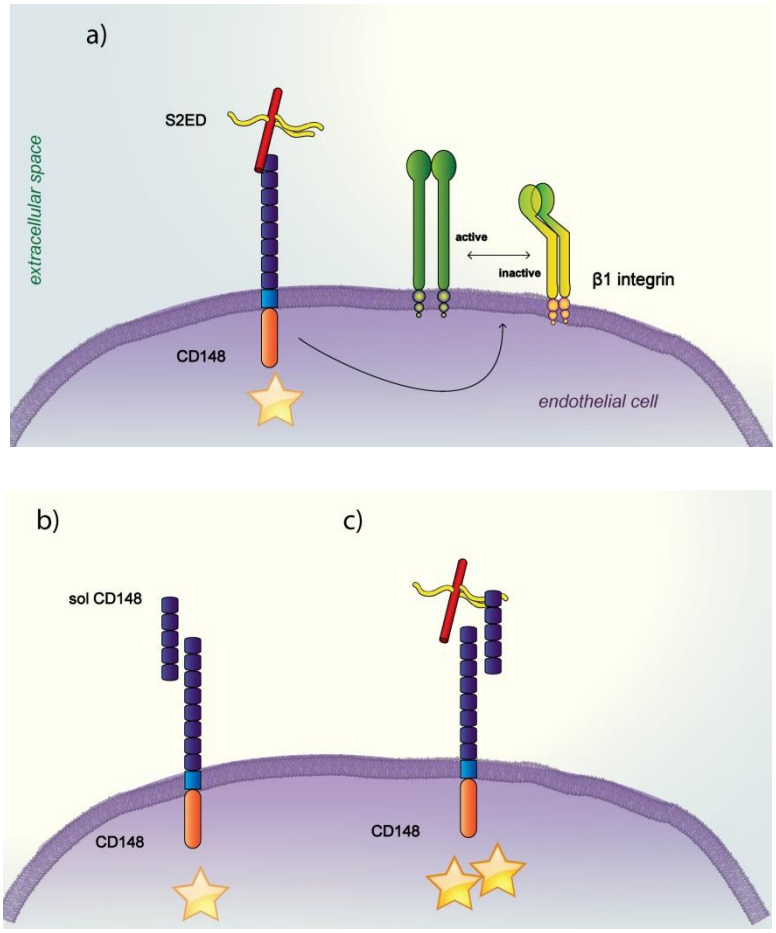

Fig. 4.40 **CD148 activation hypotheses.** a) Syndecan-2 ectodomain (S2ED) directly binds to the tyrosine phosphatase CD148, resulting in a decrease in the expression of active β1 integrins on the endothelial cell surface. b) Soluble CD148 (sol CD148) is also able to interact with its full length surface-bound counterpart and activate it. c) When both present in the medium, S2ED and sol CD148 act synergistically resulting in a stronger or wider activation of CD148.

Surprisingly, when we added to the medium both soluble CD148 and S2ED we noticed an additive effect in reducing angiogenic sprouting. Why that is we cannot explain but one could speculate that soluble CD148 has more affinity to cell surface CD148 than to S2ED and

therefore fails to bind S2ED in the extracellular space and disrupt its interaction with membrane CD148. This would result in a synergistic double activation of CD148 (Fig. 4.40 c) or in a single activation of more CD148 receptors by either S2ED or sol CD148.

In my experiments, the same concentration of S2ED and soluble CD148 (0.5 μM) inhibits angiogenesis to the same extent, it would be interesting to test how this compares to the other known agonist of CD148, TSP-1 and the anti-CD148 Ab. This is particularly interesting in the optic of a potential anti-angiogenic therapy targeting CD148. Anti-VEGF therapies, which represent the vast majority of the anti-angiogenic treatments, have been developed with partial success (Kiselyov et al., 2007). Some patients in fact fail to respond to anti-VEGF drugs, possibly because angiogenesis is a multi-factorial process and as such a one-target therapeutic approach is unlikely to meet with the expectations. Here we have identified a novel pathway for the reduction of angiogenesis which is independent to VEGF and also identified S2ED as an activator of this pathway which can be potentially used in anti-angiogenic therapies. For this reason, we are now carrying out preliminary experiments to determine whether a syndecan-2 derived peptide could be used as an alternative or in combination with anti-VEGF drugs and whether this could rapidly translate into a more successful anti-angiogenic therapy in cancer.

In conclusion, in this second results section of the thesis it has been shown that:

1. Syndecan-2 ectodomain inhibits tumor growth and tumor-angiogenesis *in vivo*.
2. Syndecan-2 is shed from HEK293T cells in response to TNFα.
3. Physiologically shed syndecan-2 retains its anti-angiogenic activity.
4. The anti-angiogenic and anti-migratory properties of syndecan-2 ectodomain reside in its core protein, specifically in the last 18 aa (P^{124} to F^{141}) corresponding to its adhesion-regulatory domain (ARD).
5. The tyrosine phosphatase CD148 is expressed on ECs from three different vascular beds (lungs, skin and brain).
6. The ARD of syndecan-2 can interact with EC CD148.
7. A soluble form of CD148 extracellular core protein is inhibitory of angiogenesis but is unable to compete with cell surface CD148 for S2ED binding.
8. Addition of S2ED to ECs (migrating or in suspension) results in a reduction of active β1 integrins.

These results can be summerized in a model whereby upon syndecan-2 shedding from the cell surface of various tissue cells (e.g. fibroblasts, tumor cells, leukocytes, depending on the scenario), its ectodomain is released in the extracellular space. Here, its adhesion regulatory

domain (last 18 amino acids of the C-terminus of S2ED) engages in an interaction with the extracellular region of the tyrosine-phosphatase CD148 which is expressed on the surface of ECs. The extracellular engagment of CD148 is enough to promote a decrease in the activation of β1 integrin which in turn results in a reduction of EC migration, tube formation and in turn angiogenesis (Fig. 4.41).

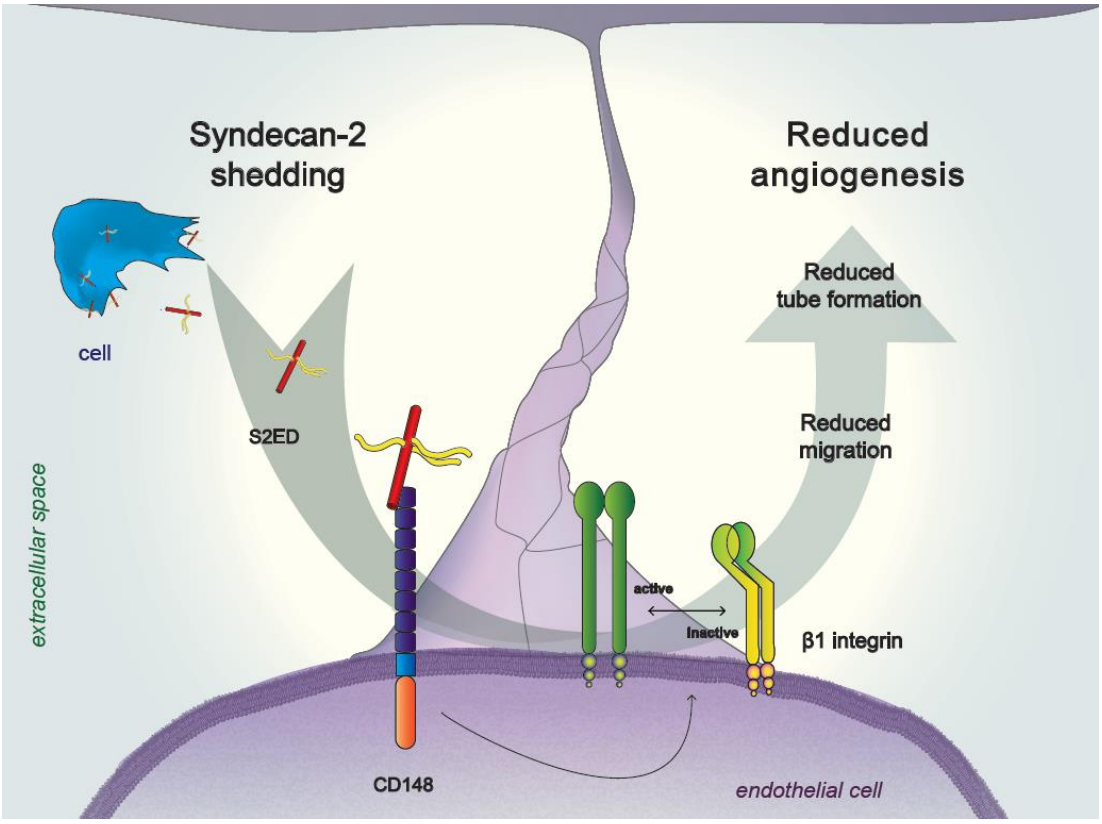

Fig. 4.41 **Schematic of the model whereby shed syndecan-2 reduces angiogenesis.** It is hypothesised that syndecan-2 is shed in inflammatory conditions from stromal cells (e.i. fibroblasts) and reaches the surface of endothelial cells on new blood vessels where it regulates β1 integrin activation via direct binding to CD148 tyrosine phosphatase. This modulation of β1 integrin activation status effectively suppresses endothelial cell migration, tube formation and angiogenesis (Figure from De Rossi et al., 2014).

4.3. Syndecan-4 is required for VEGF-A-induced angiogenesis

4.3.1. Introduction

Syndecan-4, also known as Ryudocan and Amphiglycan, is the smallest member of the syndecan family with a core protein of 22 kDa and 3 HS chains attached to it. It was initially isolated from rat microvascular ECs as a molecule capable of binding antithrombin (Kojima et al., 1992a; Kojima et al., 1992b) but since then additional biological functions have been described, the vast majority of which are dependent on syndecan-4's ability to interact with other adhesion receptors, ECM molecules and transferring these signals to the cytoskeleton via adaptor molecules (Woods and Couchman, 2001). Syndecan-4 is exceptional among the rest of the syndecan family in having a phosphatidylinositol-4,5-bisphosphate (PIP2) binding site that allows it to activate PKCα in the absence of changes in intracellular calcium levels (Horowitz et al., 1999; Horowitz and Simons, 1998; Oh et al., 1998). This activation of PKCα is key to several of syndecan-4 functions, including activation of RhoG and Rac1 and regulation of cell migration (Bass et al., 2007a) (Bass et al., 2011).

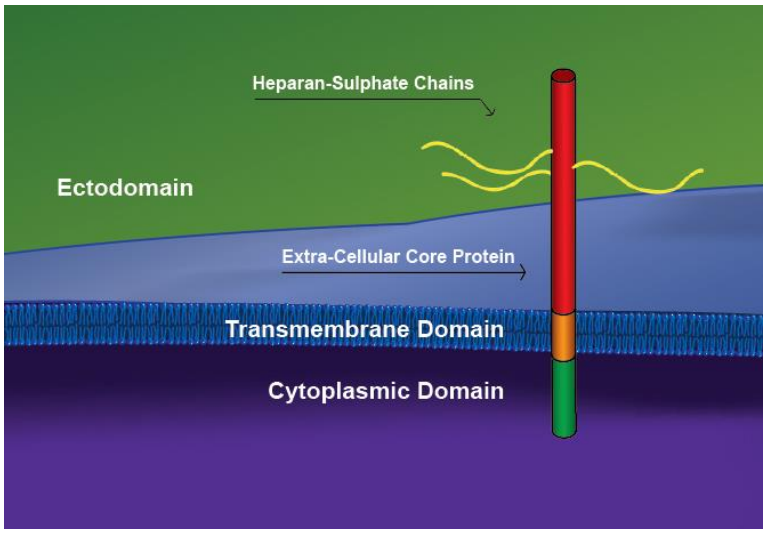

Fig. 4.42 **Syndecan-4 structural domains.** Syndecan-4 is a linear single-pass transmembrane proteoglycan. It possesses a short cytoplasmic domain (green), a transmembrane domain (orange) and a longer ectodomain which consists of an extra-cellular core protein (red) substituted by 3 HS chains (yellow). (Figure modified from De Rossi et al., 2013).

Syndecan-4 is ubiquitously expressed at very low level; however, its expression is highly inducible in certain situations. For example, it is found increased in the ischemic myocardium (Li et al., 1997), vascular tissues after injury (Nikkari et al., 1994) and in a variety of tumors

(Yoneda et al., 2012). Interestingly, the syndecan-4 Knock-Out (S4KO) mouse, which is viable, fertile and with no apparent abnormalities (Echtermeyer et al., 2001b), develops a more severe phenotype compared to wild-type littermates in those pathologies where angiogenesis is critical to the resolution phase of the disease; for example, these mice display delayed dermal wound healing associated with impaired angiogenesis and a cell migration defect (Echtermeyer et al., 2001b). The ability of syndecan-4 to regulate angiogenesis is also suggested by the observation of enhanced neovascularization in murine ischemic muscle following the combined delivery of basic Fibroblast growth factor and syndecan-4 (Jang et al., 2012), and also by the notion that lack of syndecan-4 leads to foetal vessel degeneration in the placenta (Ishiguro et al., 2000a). Moreover, the syndecan-4 knock-out mouse shows increased mortality post myocardial infarction which is, again, associated with reduced number of capillary vessels in the healing tissue (Matsui et al., 2011).

Quite recently syndecan-4 has been shown to participate in the signalling initiated by the inflammatory and pro-angiogenic molecule, Prostaglandin E_2 (PGE_2). The study revealed that in murine ECs lacking syndecan-4, PGE_2-mediated pro-angiogenic effects (i.e. EC migration and tube formation) were decreased. They also showed that syndecan-4 activation of PKCα is necessary for the phosphorylation of ERK following PGE_2 stimulation. This molecular mechanism was confirmed *in vivo* by showing a diminished angiogenic response to PGE_2 both in the syndecan-4 and in the PKCα knock-out mice compared to the wild type (Corti et al., 2013).

In vitro experiments on ECs have also revealed that syndecan-4 is a key player in FGF signalling (Murakami et al., 2002b; Volk et al., 1999). Interestingly, this is not just by facilitating the interaction between FGF2 and its receptor FGFR1, but syndecan-4 cytoplasmic domain seems to also have a key role, as chimeras and deletion mutants of this portion lacking the V or the C2 regions fail to promote an effective intracellular response to FGF2. In particular, lack of the C2 region (which contains the PDZ binding domain) prevents the binding of GIPC/Synectin which results in a failure to activate Rac1 and thus inhibits EC migration (Tkachenko et al., 2006; Tkachenko et al., 2004). In contrast with the potent angiogenic response elicited by exogenous FGF2 *in vitro*, the role of endogenous FGF2 remains uncertain. For one, fgf2 Knock-out mice are morphologically normal (Zhou et al., 1998) and do not even show impairment in neovascularization after injury (Tobe et al., 1998) or hypoxia (Ozaki et al., 1998). It is therefore unlikely that syndecan-4 contribution to FGF2 signalling can explain the dramatic angiogenic phenotype the syndecan-4 knock-out mice develop under pathological settings.

Moreover, syndecan-4 knock-out mouse is normal, viable and fertile; however, it develops a vascular phenotype in pathological settings, suggesting that either syndecan-4 is not expressed/needed during vascular development and only becomes fundamental during adulthood or that its function during vasculogenesis can be compensated by other molecules, possibly other syndecans.

These open questions led to the present work aiming at investigate the role of syndecan-4 in angiogenesis.

4.3.2. Aims

In this section of my thesis I'll describe the experiments I performed to determine the role of the EC heparan sulphate proteoglycan syndecan-4 during the angiogenic process.

The aims of the experiments are as follows:

1. Establish whether syndecan-4 knock-out mouse vasculature is normal; in other words, determine whether syndecan-4 has a role in vasculogenesis and/or vascular homeostasis.
2. Challenge the syndecan-4 knock-out mouse in a model of aggressive cancer which relies on angiogenesis for its fast growth to determine whether lack of syndecan-4 affects the pathology outcome.
3. Test the syndecan-4 knock-out in *in vivo* and *ex vivo* models of angiogenesis to establish whether syndecan-4 is required for angiogenesis, if its role is tissue-specific and if it is specifically required for the angiogenic response driven by one or more pro-angiogenic factors.
4. Look at the expression of syndecan-4 on ECs from homeostatic vasculature and angiogenic tissue.
5. Determine the role of syndecan-4 in EC responses during angiogenesis.

4.3.3. Results

4.3.3.1. Characterization of syndecan-4 knock-out mouse vasculature

Syndecan-4 knock-out mice do not present abnormalities at a glance and develop normally (Echtermeyer et al., 2001b). However, no detailed studies have been carried out to assess whether vasculogenesis in these animals occurs in such way to allow the formation of a vascular network comparable to that of wild-type littermates.

To establish whether the syndecan-4 knock-out mouse quiescent vasculature is normal, the cremaster muscle and ear skin vascular beds were stained and several parameters were analysed. The cremaster muscle was chosen as this tissue has been characterized in depth by members of my lab and its thinness of around 600 μm allows optimal confocal microscopy imaging without the need for sectioning. Cremaster muscles and ears were excised and stained for VE-Cadherin, an EC trans-membrane protein which localizes to intra-cellular junctions, and α Smooth muscle actin, which is expressed in the cytoskeleton of pericytes and smooth muscle cells. Staining for these two markers helps distinguishing the different types of vessels in the vasculature: smooth muscle cells on arterioles are uniformly shaped, circumferentially arranged, closely packed, and tightly associated with the endothelium while pericytes on capillaries have two thin major processes that are oriented longitudinally along the vessel from which multiple minor process extend surrounding the capillary, capillary pericytes cover only a small proportion of the endothelial surface while pericytes on venules exhibit an irregular shape and extend numerous major processes covering a great part of the endothelial surface; VE-cadherin, on the other hand, is specific to ECs and therefore its staining is consistent and uniform on the EC junctions throughout the whole vascular network.

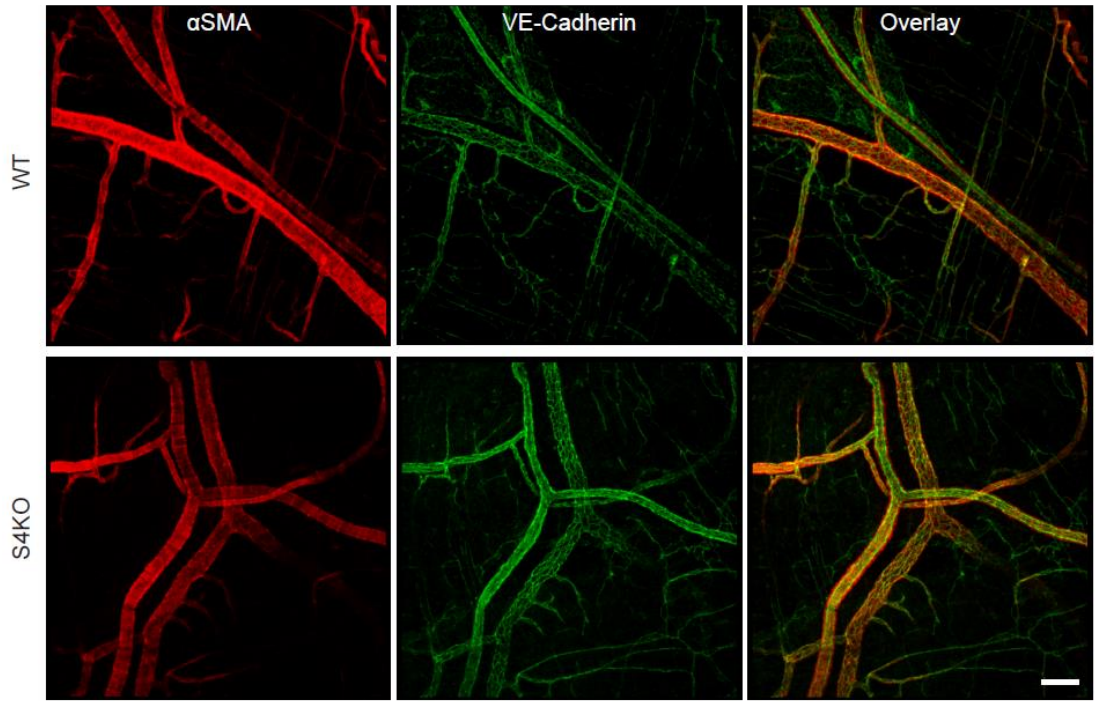

Fig. 4.43 **Characterization of cremaster muscle quiescent vasculature of wild-type and syndecan-4 knock out mice.** 6 Week old wild-type (WT) and syndecan-4 knock-out (S4KO) mice were culled and cremaster muscles excised, immediately fixed in 4% PFA, incubated for 2 hrs in perm/block solution prior to immune-fluorescent staining with anti-αSmooth muscle actin (αSMA, red) and anti-VE-Cadherin (green) Abs. αSMA is a pericyte marker and therefore is not found on capillaries while VE-Cadherin is specific to EC junctions. All images shown are representative of 3 animals per group. Scale bar represents 100 µm.

Confocal micrographs of wild-type and syndecan-4 knock-out cremaster muscle and skin vasculature (Fig. 4.43 and Fig. 4.44, respectively) show that no morphological differences can be detected by visual comparison; in addition, a more rigorous analysis of several parameters was carried out with the same result. Vessel density, vessel heterogeneity and pericyte coverage were evaluated (Fig. 4.45, Fig. 4.46 & Fig. 4.47) in both wild-type and syndecan-4 knock-out vasculatures and in all instances values were not significantly different.

In light of these results, we could conclude that syndecan-4 knock-out mice possess a morphologically normal vasculature, which would suggest that syndecan-4 does not play a major role in vascular development or that its role can be compensated, probably by other members of the syndecan family.

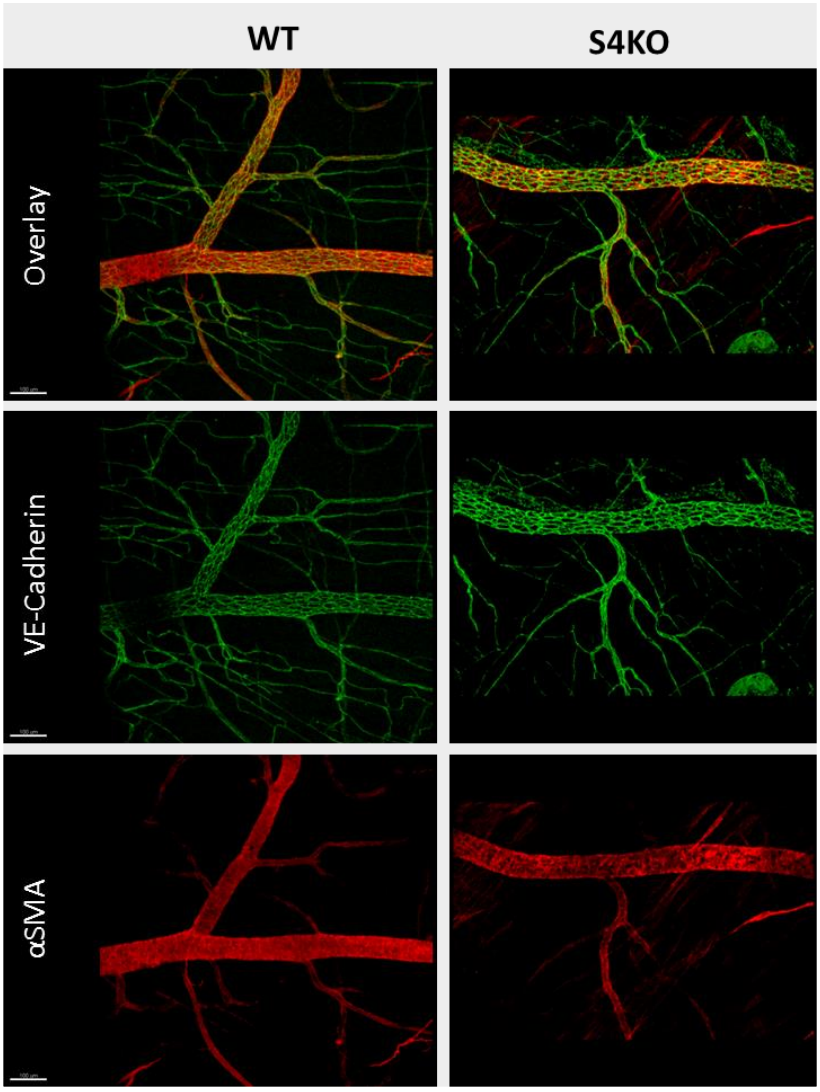

Fig. 4.44 **Characterization of skin quiescent vasculature of wild-type and syndecan-4 knock out mice.** 6 Week old wild-type (WT) and syndecan-4 knock-out (S4KO) mice were culled and ear excised, immediately fixed in 4% PFA, incubated for 2 hrs in perm/block solution prior to immune-fluorescent staining with anti-αsmooth muscle actin (αSMA, red) and anti-VE-Cadherin (green) Abs. αSMA is a pericyte marker and therefore is very low expressed on capillaries while VE-Cadherin is specific to EC junctions. All images shown are representative of 3 animals per group. Scale bar represents 100 µm.

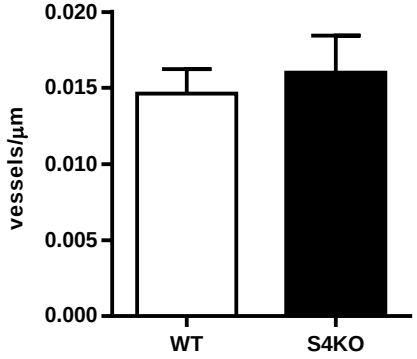

Fig. 4.45 **Comparison of vessel density in wild-type and syndecan-4 knock-out mouse vasculature.** An arbitrary line was drawn throughout the length of the micrographs (Fig. 4.43) and the number of vessels crossing that line counted and divided by the length of the line. At least 4 images per animal and 3 animals per group were analysed. No statistically significant differences were found between the 2 groups (WT vs. S4KO), according to Student's t-test.

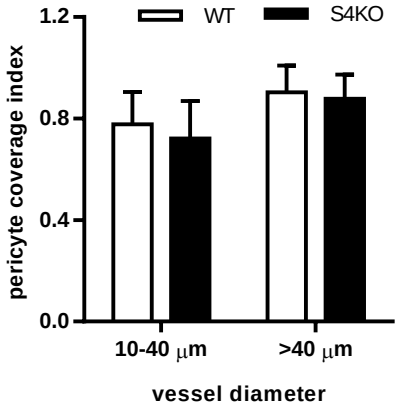

Fig. 4.46 **Comparison of vessel heterogeneity in wild-type and syndecan-4 knock-out mouse vasculature.** Micrographs from Fig. 4.43 were analysed to assess the percentage of capillaries (diameter <10 µm), arterioles and venules (diameter between 10-40 µm) and arteries and veins (diameter >40 µm). Vessel diameter was measured and vessels were divided into 3 groups accordingly and their respective percentages were calculated. At least 4 images per animal and 3 animals per group were analysed. No statistically significant differences were found between the 2 groups (WT vs. S4KO), according to Student's t-test.

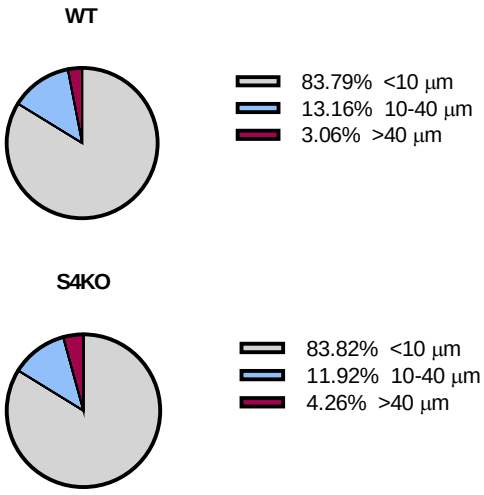

Fig. 4.47 **Comparison of pericyte coverage in wild-type and syndecan-4 knock-out mouse vasculature.** Micrographs from Fig. 4.43 were analysed to assess pericyte coverage index quantified as the percentage of vessel area covered by αSMA in both venules (10<40 µm) and veins (>40 µm). At least 4 images per animal and 3 animals per group were analysed. No statistically significant differences were found between the 2 groups (WT vs. S4KO), according to two-way Anova.

Next, the presence of syndecan-4 on quiescent vasculature was examined. Syndecan-4 was found to be expressed at very low levels in the endothelium, both on venules and arteries, while it's highly expressed on peri-vascular cells, possibly vessel-associated macrophages and fibroblasts (Fig. 4.48). Fig. 4.49 shows staining controls, left panel show a representative venule (top image) and artery (bottom image) stained with syndecan-4 Isotype control Ab (green), while red panel shows syndecan-4 knock out tissue stained with anti-syndecan-4 Ab.

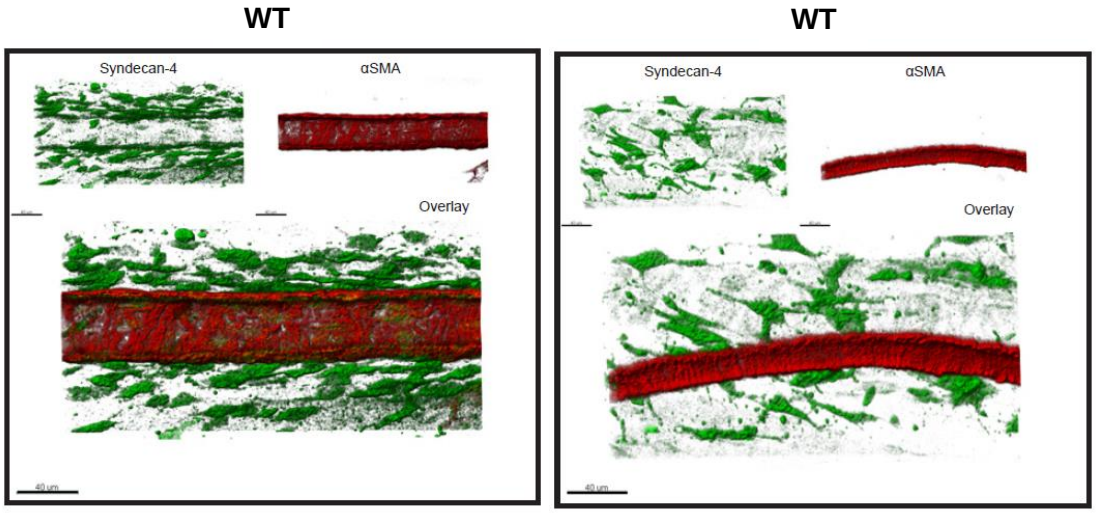

Fig. 4.48 **Characterization of cremaster muscle quiescent vasculature of wild-type and syndecan-4 knock out mice.** 6 Week old wild-type (WT) mice were culled and cremaster muscles excised, immediately fixed in 4% PFA, incubated for 2 hrs in perm/block solution prior to immune-fluorescent staining with anti-αsmooth muscle actin (αSMA, red) and anti-syndecan-4 (green) Abs. Left and right panels show a representative image of a venule and an artery, respectively. All images shown are representative of 3 animals per group. Scale bar represents 40 µm.

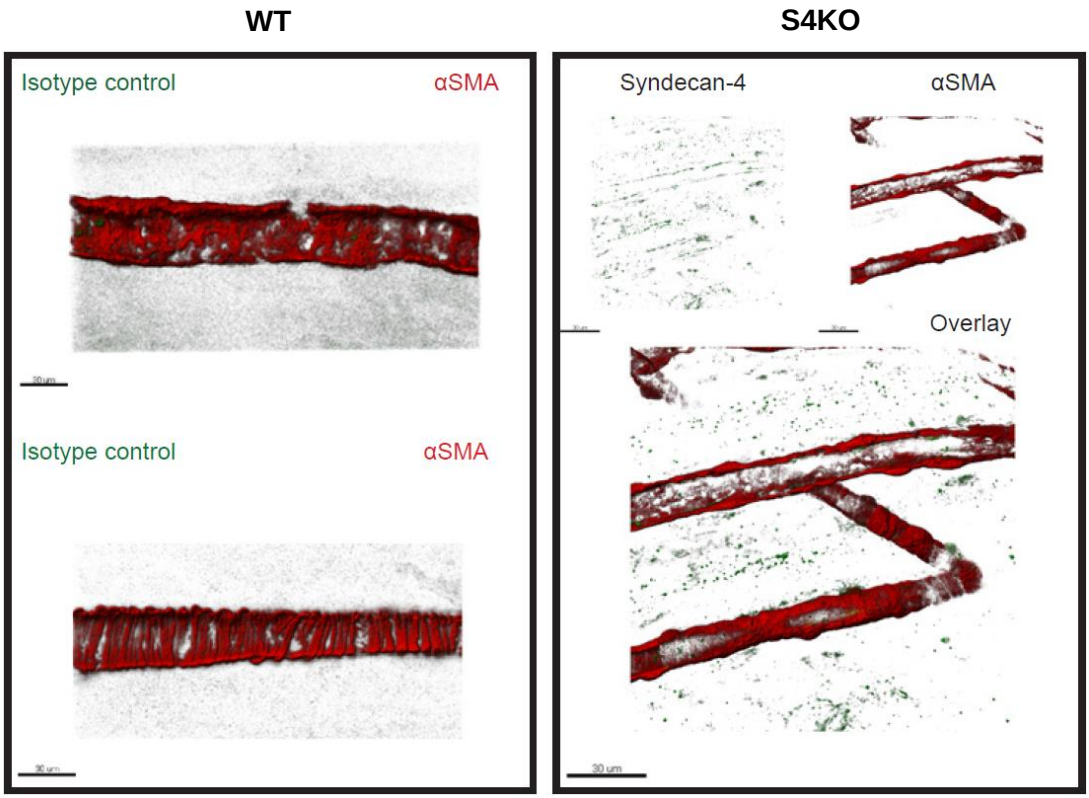

Fig. 4.49 **Characterization of cremaster muscle quiescent vasculature of wild-type and syndecan-4 knock out mice.** 6 Week old mice were culled and cremaster muscles excised, immediately fixed in 4% PFA, incubated for 2 hrs in perm/block solution prior to immune-fluorescent staining. Left panel show a representative image of a wild-type (WT) venule and artery, top and bottom images respectively, stained with anti-αsmooth muscle actin (αSMA, red) and syndecan-4 Isotype control (green) Abs. Right panel shows staining of syndecan-4 knock-out (S4KO) tissues with anti-αsmooth muscle actin (αSMA, red) and anti-syndecan-4 (green) Abs. All images shown are representative of 3 animals per group. Scale bar represents 30 µm.

We also looked at cutaneous vascular permeability in response to a known vasodilator (bradykinin) as a measure of vascular functionality and no significant difference between wild-type and syndecan-4 knock out animals was detected (Fig. 4.50).

These data suggest that syndecan-4 is dispensable for vasculogenesis and vascular homeostasis (Fig. 4.43, Fig. 4.45, Fig. 4.46, Fig. 4.47) and function (e.g. regulation of vascular permeability) (Fig. 4.50). This idea is also supported by the fact that the level of expression of syndecan-4 on the homeostatic endothelium is extremely low (Fig. 4.48). Because of this, the angiogenic response of syndecan-4 knock-out mice and wild-type littermates were compared, on the basis that an eventual phenotype would be ascribed to a defect in angiogenesis and not to the vasculature being already abnormal.

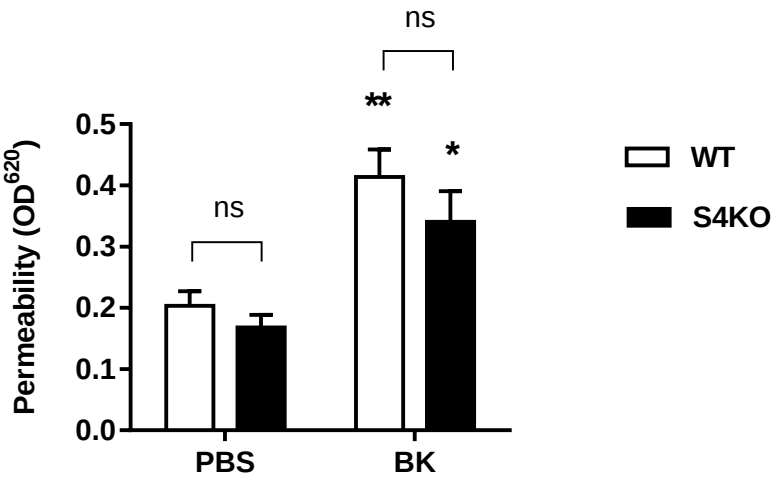

Fig. 4.50 **Vascular permeability in wild-type and syndecan-4 knock-out mice.** Vascular permeability was assessed by measuring the accumulation of Albumin-bound Evans Blue dye in the dorsal skin of mice. 6-8 week wild-type (WT) and syndecan-4 knock-out (S4KO) mice received Evans Blue dye (0.5% in PBS, 5 µl per g bodyweight) i.v. through the tail vein. Afterwards, 50 µl of PBS containing either 100 µg of Bradykinin (BK) in PBS or PBS alone were injected s.c. in the mouse dorsal skin. After 1h30' animals were sacrificed. Dorsal skin was then excised. Injected sites were cut out as circular patches using a metal puncher (~8 mm in diameter). Samples were then incubated in 250 µl of Formamide at 56°C for 24 h to extract Evans Blue dye from the tissue. The amount of accumulated Evans Blue dye was quantified by spectroscopy. Results are presented as the optical density at 620 nm (OD620) per mg tissue and per mouse. Values are expressed as mean ± s.e.m. of $5 \leq n \geq 7$ animals per group. Statistically significant differences between PBS control and BK within each group (WT and S4KO) are represented by asterisks while differences between WT and S4KO within each condition are not statistically significant. *P<0.05, **P<0.01 according to two-away Anova with Sidak correction for multiple comparisons.

4.3.3.2. Melanoma tumor growth is reduced in the syndecan-4 knock-out mice and correlates with decreased angiogenesis

As reviewed in 1.2.3, angiogenesis is a feature of numerous diseases including cancer. Skin cancer or Melanoma, is a form of aggressive cancer which strongly relies on angiogenesis. For this reason, melanomas were grown in syndecan-4 knock-out and wild-type mice to assess whether lack of syndecan-4 could impact the outcome of a pathology in which angiogenesis plays a key role.

Melanoma B16F1 cells, a murine cell line derived from spontaneous skin tumor of C57BL/6J mice, were injected into the flank of wild-type and syndecan-4 knock-out mice and tumors were allowed to grow for 1 and 2 weeks. At those time points mice were culled and tumors

photographed and measured. As clear from Fig. 4.51, tumors which developed in a syndecan-4-free micro-environment grew far less than those in wild-type animals; this observation was confirmed by both measuring tumor volume and weight (Fig. 4.52). Notably, when tumors were sectioned and stained for tumor-associated new blood vessels, while the wild-type presented vessel-like structures with, in many cases, a well-defined lumen (white arrows in Fig. 4.53), in the syndecan-4 knock-out mice-derived tumors, ECs failed to organize into tubules and appeared randomly sparse throughout the tumor (Fig. 4.53).

These results suggested that in a model of melanoma tumor, lack of syndecan-4 in the tumor microenvironment (to note that B16F1 cells are derived from wild-type animals) results in inhibition of tumor growth and is concomitant with impaired tumor angiogenesis.

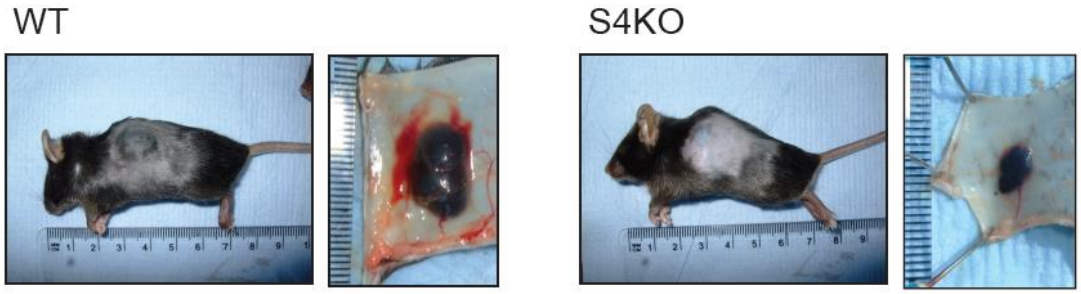

Fig. 4.51 **Tumor growth in wild-type and syndecan-4 knock-out mice.** 6 Week old Wild-type and syndecan-4 KO mice were anesthetized and 100 µl of B16F1 cell suspension (5 x 10^7 cells/ml in PBS) was injected s.c. into the mice flank. Mice were left for 7 days prior to sacrifice by cervical dislocation. Mice were shaved and pictures taken, skin was then excised and the tumor photographed. Images are representative of 6 mice per group.

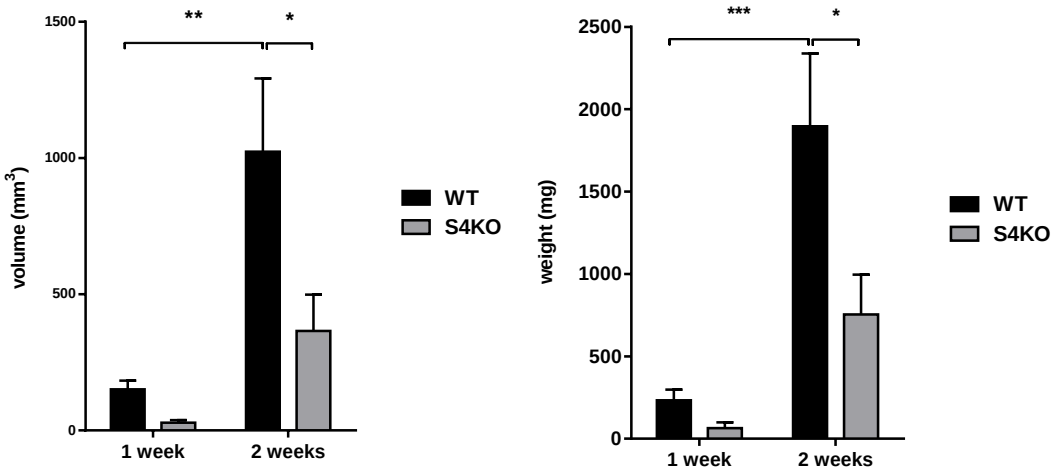

Fig. 4.52 **Quantification of tumor growth in wild-type and syndecan-4 knock-out mice.** 6 Week old Wild-type and syndecan-4 KO mice were anesthetized and 100 µl of B16F1 cell suspension (5 x 10^7 cells/ml in PBS) was injected s.c. into the mice flank. Mice were left for 1 or 2 weeks prior to sacrifice by cervical dislocation. Volume of the tumors was measured with a ruler and weight was measured with a precision balance. To note, given the softness of the tumors, skin was cut together with it to maintain integrity of the samples. Values are expressed as means with standard error of 6 animals per group. Statistically significant differences between groups were found according to two-away Anova with Holm-Sidak correction for multiple comparisons. *P<0.05, **P<0.01, ***P<0.001.

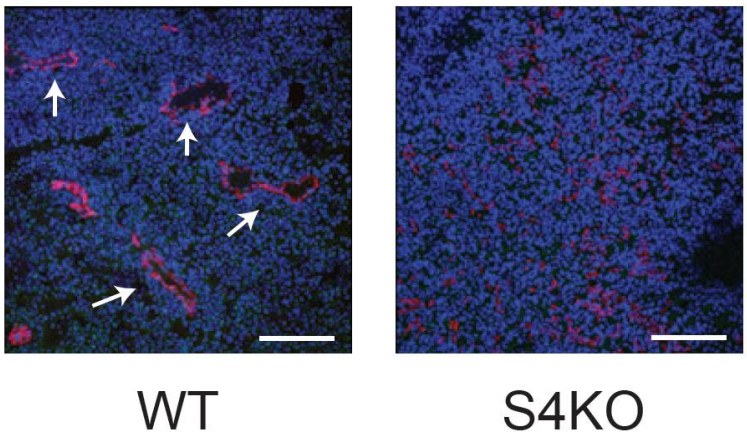

Fig. 4.53 **Tumor angiogenesis in wild-type and syndecan-4 knock-out mice.** 1-week tumors were snap frozen in liquid nitrogen and stored at -80°C. Subsequently, 20 µm-thick cryosections were cut, fixed in methanol and permabilized/blocked in normal goat serum prior to staining with an anti-CD31 Ab (red) and nuclei (draq5, blue). Arrows show the vessel lumen in the wild-type tumors. Scale bar represents 200 µm.

4.3.3.3. Syndecan-4 is required for VEGF-induced angiogenesis and its expression is increased by angiogenic stimuli

To assess whether diminished angiogenesis in the context of decreased tumor growth in the syndecan-4 knock-out mice was causation or just correlation, new blood vessel formation alone was evaluated in several well-established model of angiogenesis, namely, in the *in vivo* Matrigel plug assay and in the *ex vivo* Aortic ring and Choroid explant assays.

In the first set of experiments, both wild-type and syndecan-4 knock-out mice were injected with 500 µl of Matrigel containing PBS alone or with the angiogenic factors VEGF-A, bFGF or both. Because of the presence of the afore mentioned angiogenic factors, new blood vessels from the adjacent derma will respond to stimulus and invade the plug. After 5 days, all 3 conditions were able to trigger an angiogenic response in the wild-type, as evident from the blood content of the plugs, qualitatively reflected in the redness of the samples (Fig. 4.54) and quantified via measuring the haemoglobin concentration in the plug (Fig. 4.55). Interestingly, the syndecan-4 knock-out mice behaved similarly to wild-type in all conditions except when angiogenesis was induced by VEGF-A alone; here, the syndecan-4 knock-out showed a very modest angiogenic response, almost as low as that induced by the PBS negative control and certainly much reduced compared to the VEGF-driven angiogenic response of wild-type littermates.

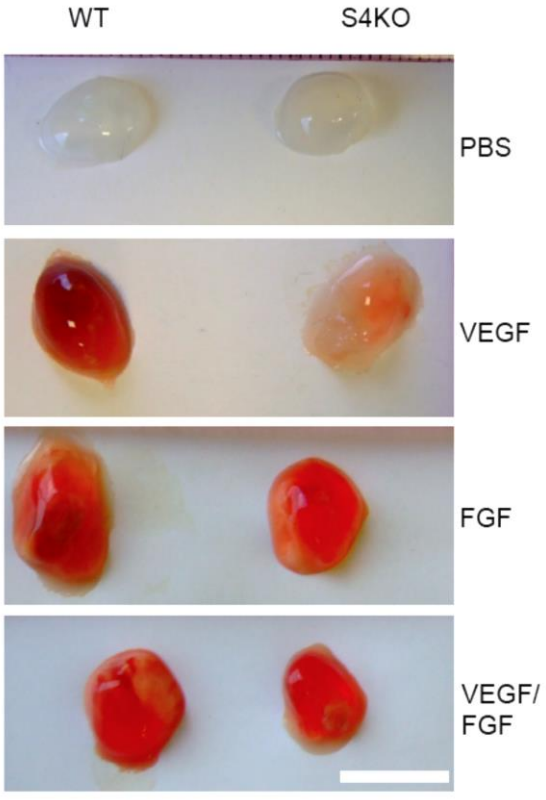

Fig. 4.54 ***In vivo* angiogenesis in wild-type and syndecan-4 knock-out mice.** Angiogenesis was measured *in vivo* in wild-type (WT) and syndecan-4 knock-out (S4KO) mice in the matrigel plug assay. 500 µl of matrigel (7.5 mg/ml in PBS) containing 20 U/ml of Heparin plus growth factors (100 ng/ml VEGF-A, 100 ng/ml bFGF) as indicated were injected s.c. into the flanks of 6 weeks old mice and plugs were excised after 5 days. Picture shows the excised plugs. All images shown are representative of n=5-9 animals per group. Scale bar represents 1 cm.

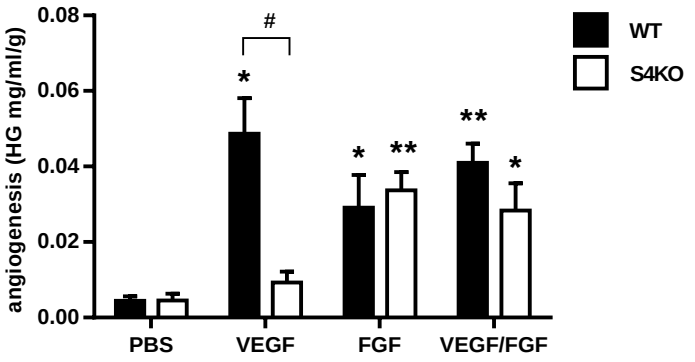

Fig. 4.55 **Quantification of angiogenesis in the Matrigel plug assay.** After 5 days from the Matrigel injections, plugs were excised, weighted and incubated overnight at 4°C in dH2O. On the next day the amount of haemoglobin released from the plugs was measured using the Drabkin reagent kit and a spectrophotometer. Results show the concentration of haemoglobin per gram of plug (HG mg/ml/g). Values are expressed as mean ± s.e.m. of $5 \leq n \geq 9$ animals per group. Statistically significant differences between PBS control and the different conditions within each group (WT and S4KO) are represented by asterisks while differences between the two groups within each condition are represented by hashtag. *P<0.05, **P<0.01, #P<0.001 according to two-away Anova with Sidak correction for multiple comparisons.

The results obtained in the dermal angiogenesis model were also observed in other models of angiogenesis in other tissues. These included the aortic ring assay, which takes advantage of the capacity of aortic grafts to develop an angiogenic response *in vitro*, in the form of aortic sprouts, when properly triggered by angiogenic factors. Similarly to dermal angiogenesis in the Matrigel plug, while the wild-type rings developed an angiogenic response when VEGF-A, bFGF or both were used, aortic rings derived from syndecan-4 knock-out tissue showed impaired angiogenesis only when it was triggered by VEGF-A (Fig. 4.56, Fig. 4.57).

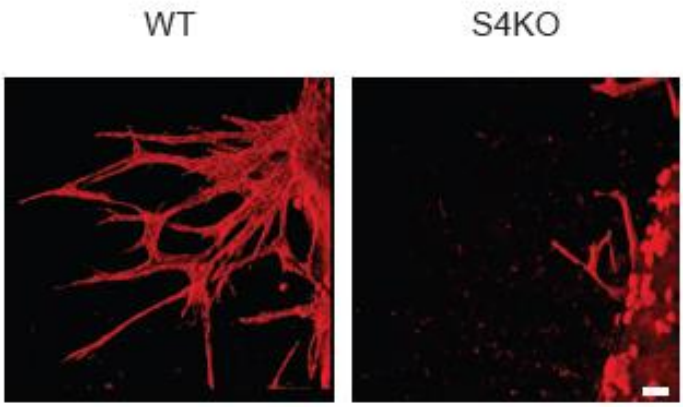

Fig. 4.56 ***Ex vivo*** **angiogenesis in wild-type and syndecan-4 knock-out mice.** Aortas from wild-type and syndecan-4 knock-out mice were cut into 1 mm rings and each ring singularly embedded into a thin layer of Collagen I containing the same conditions as for the Matrigel plug assay. Confocal micrographs of rings treated with VEGF-A showing angiogenesis reflected by the amount of angiogenic sprouts (ECs, BS1-Lectin-positive, red) growing from the aortic ring in 1 week time. Images shown are representative of n=3-7 animals per group.

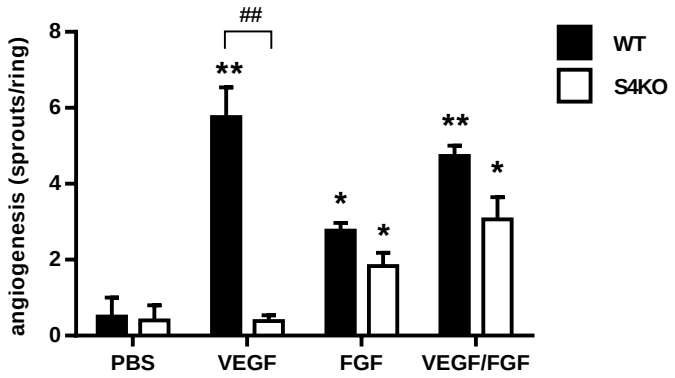

Fig. 4.57 **Quantification of angiogenesis in the aortic ring assay.** New blood vessel formation from the aortic ring experiments was quantified by counting the number of sprouts per ring 1 week from the embedding day. Values are expressed as mean ± s.e.m. of n=3-7 animals per group where at least 5 rings per condition were used. Statistically significant differences between PBS control and the different conditions within each group (WT and S4KO) are represented by asterisks while differences between WT and S4KO within each condition are represented by hashtag. *P<0.05, **P<0.01, ##P<0.0001 according to two-away Anova with Sidak correction for multiple comparisons.

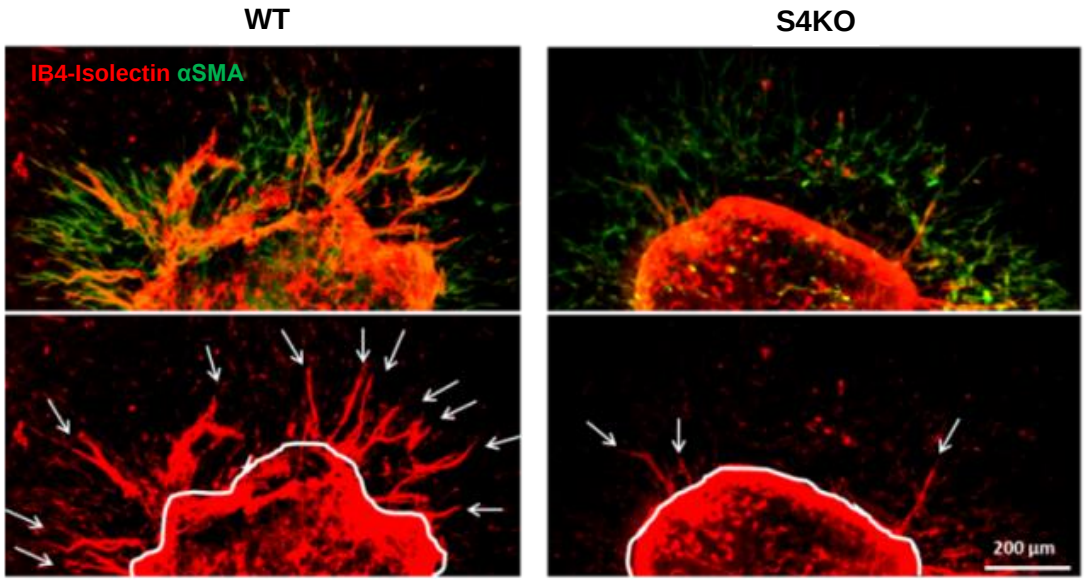

Fig. 4.58 ***Ex vivo* choroid explant neovascularisation assay.** Choroid explants from wild-type (WT) and syndecan-4 knock-out (S4KO) mice were cut into 1 mm^2 pieces and singularly embedded into a thin layer of Collagen I. Medium containing 1% FBS and 30 ng/ml of VEGF was added every 2 days. Confocal micrographs of choroid explants treated with VEGF-A showing angiogenesis reflected by the amount of angiogenic sprouts (ECs, BS1-Lectin-positive, red and pericytes and fibroblasts, αSMA positive, green) growing from the choroid explant in 1 week time. Images shown are representative of n=3-7 animals per group.

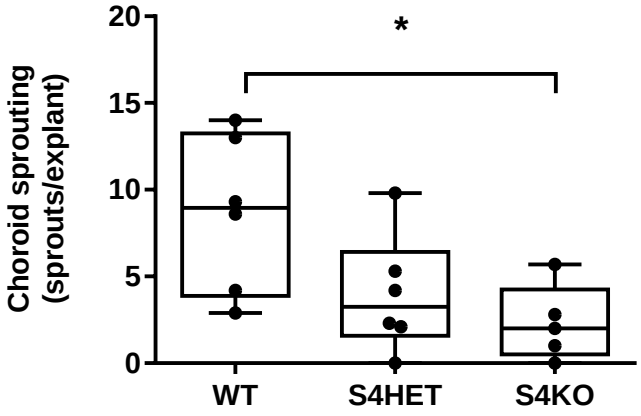

Fig. 4.59 **Quantification of angiogenesis in the choroid explant neovascularisation assay**. New blood vessel formation from the choroid explants was quantified by counting the number of sprouts per explant 1 week from the embedding day. Values are expressed as mean ± s.e.m. of $3 \leq n \geq 7$ animals per group where at least 6 explants per condition were used. Statistically significant differences between wild-type (WT) control and syndecan-4 het (S4HET) and knock-out (Syn4KO) are represented by asterisks. *$P<0.05$ According to one-away Anova with Dunnet correction for multiple comparisons.

These experiments have generated a number of novel findings: first, they showed that syndecan-4 could have a potential role in tumor angiogenesis and therefore on tumor development; secondly, that syndecan-4 requirement to initiate an angiogenic response is limited to VEGF-A-driven responses; lastly, results were similar in different organs (e.g. skin, aorta and eye), suggesting that syndecan-4's role in VEGF-A-induced angiogenesis is not tissue-specific.

4.3.3.4. Syndecan-4 expression during angiogenesis

Because an upturn in the biological activity of a molecule is often associated with its increased production, the expression of syndecan-4 during angiogenesis was next investigated.

Previous works showed that wild-type aortic rings develop angiogenic sprouts when treated with VEGF-A for 7 days (Fig. 4.57). Staining of this aortic explants with anti-syndecan-4 Ab showed that syndecan-4 is found highly expressed on both ECs (counter-stained with BS1-lectin) and stromal cells, possibly pericytes and smooth muscle cells. Notably, very low expression of syndecan-4 was observed in developed cremaster muscle ECs *in vivo* (Fig. 4.48) suggesting that syndecan-4 might be upregulated on ECs during angiogenesis.

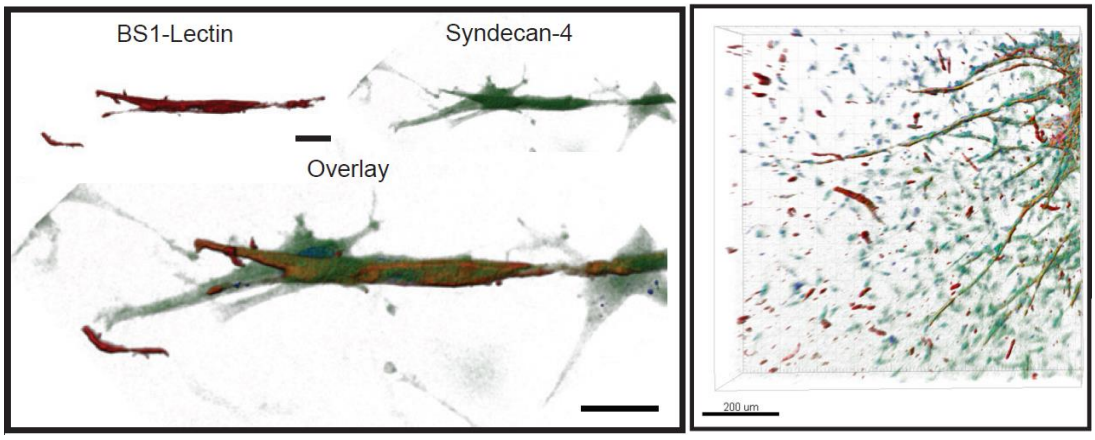

Fig. 4.60 **Syndecan-4 is highly expressed on angiogenic sprouts.** Wild-type aortic rings treated with VEGF-A for 7 days were fixed, permeabilized and subsequently stained with BS1-lectin (EC marker, red), Draq5 (nuclei, blue) and anti-syndecan-4 (green) Ab. Images shown are representative of 6 rings from 3 wild-type mice. Scale bar on the left is 40 µm and 200 µm on the right.

To investigate this possibility, isolated primary murine ECs were isolated from the lungs of wild-type mice, cultured for 3 passages and treated for 2 and 4 hours with angiogenic stimuli, namely VEGF-A, bFGF and Angiogepoietin-2 and analysed for syndecan-4 expression. Analysis of the messenger RNA via qPCR revealed a progressive time-dependent upregulation of syndecan-4 gene transcription in all 3 settings, suggestive that syndecan-4 expression can indeed be positively regulated by angiogenesis, at least at the messenger level (Fig. 4.61).

Concomitantly with increased syndecan-4 mRNA transcription, we also found, via FACS analysis, that upon VEGF-A treatment syndecan-4 is upregulated on EC surface. Notably, the increased presence of syndecan-4 on the cell membrane does not result in increased shedding, in fact no syndecan-4 is found in the conditioned media of ECs whether untreated or treated with VEGF-A, while shedding of syndecan-4 happens when cells are treated with a known shedding stimulator, Phorbol 12-myristate 13-acetate (PMA).

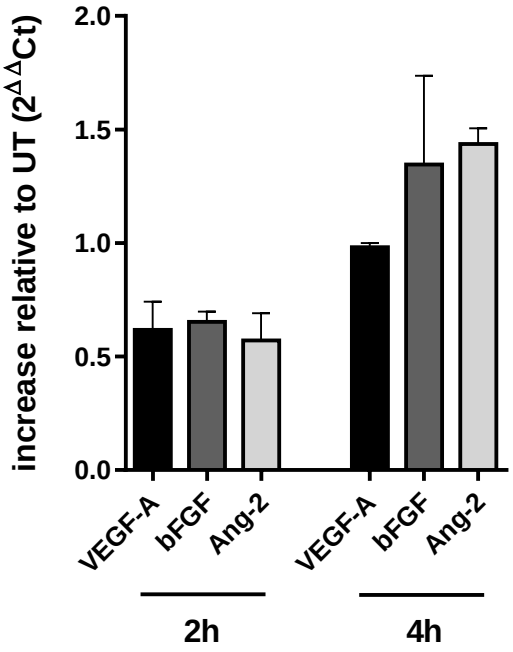

Fig. 4.61 **Syndecan-4 expression in ECs is increased *in vitro* by angiogenic factors.** Confluent wild-type primary lung ECs were treated for 2 and 4 hours with 20 ng/ml of VEGF-A, bFGF or Angiopoietin-2 in serum-free medium. Syndecan-4 expression was normalised over GAPDH expression and graphed as increase relative to untreated control. Results are representative of 2 experiments, overall P value is 0.04 according to one-way Anova.

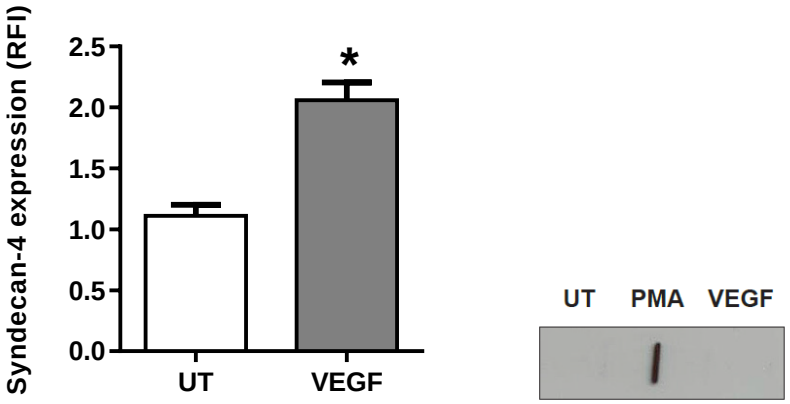

Fig. 4.62 **Syndecan-4 expression on the surface of ECs increases upon VEGF-A treatment and does not result in shedding.** Confluent wild-type primary mouse lung ECs were treated for 4 hours with 20 ng/ml of VEGF-A or PMA in serum-free medium. Cells were subsequently detached and analysed via FACS for syndecan-4 expression. Conditioned media was also collected prior to cell detachment and analysed for the presence of shed syndecan-4 via dot-blot. Results are representative of 3 experiments, significant differences between untreated and VEGF-treated cells were determined using unpaired t-test. *P<0.05.

These data provide strong indications that syndecan-4 is up-regulated on ECs during angiogenesis. This led us to investigate the role of syndecan-4 in EC responses during angiogenesis.

4.3.3.5. Syndecan-4 is a co-receptor for VEGFR2 and is required for VEGF-A induced phosphorylation

In the previous paragraph we have shown that syndecan-4 appears strongly up-regulated on ECs during angiogenesis and by angiogenic factors; in addition, we showed how the syndecan-4 knock-out mouse is unable to develop an angiogenic response in reaction to VEGF-A. Notably, VEGF-A acts solely on ECs, as its receptor, VEGFR2, is only expressed on this cell type; upon VEGF-A binding, several tyrosine residues in VEGFR-2 become phosphorylated and this ignites a number of signalling cascades which affect EC behaviour. We hypothesised that syndecan-4 could play a role in VEGF-A/VEGFR2 activity.

To test this hypothesis, primary lung ECs were isolated from wild-type and syndecan-4 knock-out mice and grown to confluence in complete medium. Cells were then serum-starved for 6 hours and treated with 30 ng/ml of VEGF-A for 5'. This time point and dose were chosen after several optimizations and literature research as they are able to induce the phosphorylation of

VEGFR2 upon addition of VEGF-A in wild-type primary lung ECs of murine origin. However, when the same dose of VEGF-A and incubation time were applied to syndecan-4 knock-out ECs, these were found to be unable to produce the same response as their wild-type counter-parts, as evident from a representative Western blot film showing decreased phosphorylated (e.g. activated) VEGFR2 in syndecan-4 knock-out cells treated with VEGF-A (Fig. 4.63).

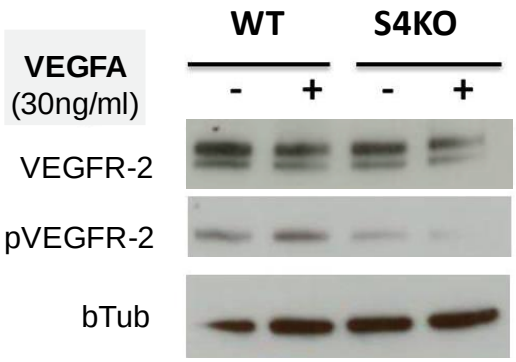

Fig. 4.63 **Endothelial syndecan-4 is required for VEGFR2 phosphorylation.** Confluent wild-type (WT) and syndecan-4 knock-out (S4KO) primary mouse lung ECs were serum-starved for 6 hours and then treated with 30 ng/ml of VEGF-A for 5'. Western blot of lysates from these cells were probed with Abs against total VEGFR-2 or phosphorylated VEGFR-2 (pVEGFR-2) or β-tubulin. The blot is representative of at least 4 experiments. Densitometry was performed on 4 blots and normalized against β-tubulin. Significant differences between untreated control and treated group were determined using two-way Anova with Tukey correction for multiple comparisons. *P<0.05.

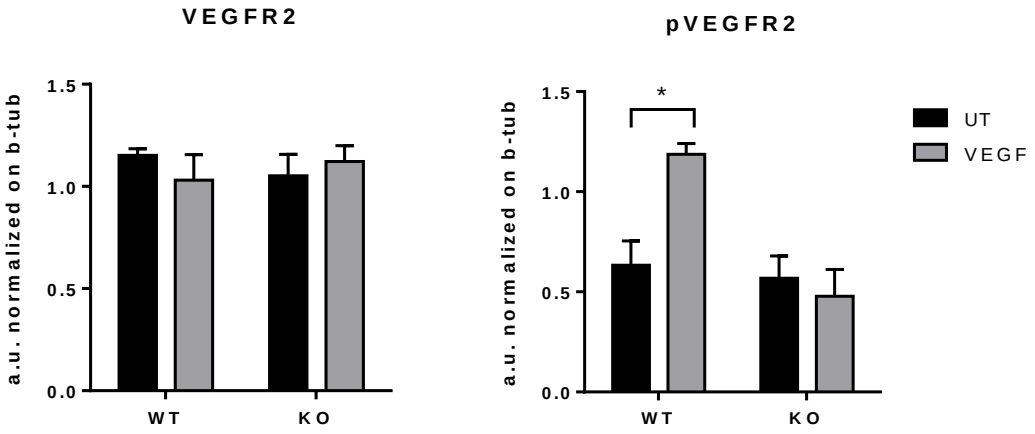

It is described in the literature that VEGF-A binds to HS with high affinity (Robinson et al., 2006b), and cells where HS has been enzymatically removed have abrogated VEGF-A signalling (Ashikari-Hada et al., 2005). In addition, VEGFR-2 also binds to HS, suggesting that HSPGs may play a role in facilitating the formation of an active signalling complex

between VEGF-A and VEGFR-2 (Nishiguchi et al., 2010). Collectively, these evidences led us to speculate that syndecan-4 could act as a co-receptor and facilitate the interaction of VEGF-A with its receptor VEGFR-2.

A proximity ligation assay was used to investigate whether syndecan-4 and VEGFR-2 associate in a complex in ECs upon VEGF-A treatment. This assay involves the use of two primary Abs raised in different species, species-specific secondary Abs, called PLA probes, each with a unique short DNA strand attached to it, bind to the primary Abs. When the PLA probes are in close proximity (< 40 μm), the DNA strands can interact through a subsequent addition of two other circle-forming DNA oligonucleotides. After joining of the two added oligonucleotides by enzymatic ligation, they are amplified via rolling circle amplification using a polymerase. After the amplification reaction, several hundred-fold replication of the DNA circle has occurred, and labelled complementary oligonucleotide probes highlight the product. The resulting high concentration of fluorescence in each single-molecule amplification product is easily visible as a distinct bright red spot when viewed with a fluorescence microscope. Confluent wild-type primary mouse lung ECs were serum-starved for 6 hours and then treated with 30 ng/ml of VEGF-A for 2' and 5'. Subsequently, the proximity ligation assay was performed, following manufacturer instructions, to investigate the formation of complexes between syndecan-4 and VEGFR-2. Results showed that within 2' of VEGF-A treatment, there is a high increase in the formation of syndecan-4/VEGFR2 complexes on ECs which then goes back to basal level at 5' (Fig. 4.64, Fig. 4.65).

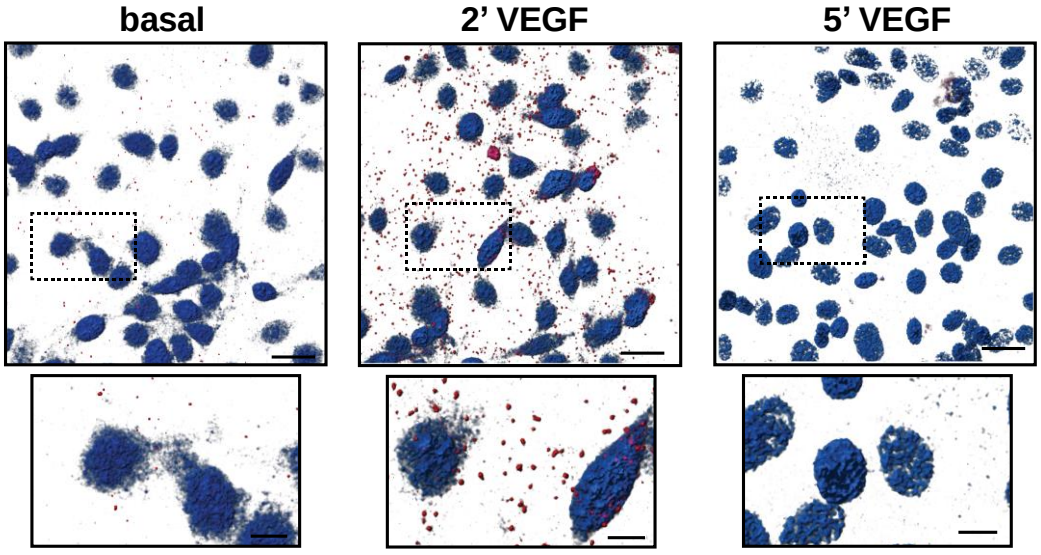

Fig. 4.64 **Syndecan-4 and VEGFR2 transiently go into close proximity upon VEGF stimulation in ECs.** Confluent wild-type primary mouse lung ECs were serum-starved for 6 hours and then treated with 30 ng/ml of VEGF-A for 2' and 5'. Subsequently, the proximity ligation assay was performed, following manufacturer instructions, using anti-syndecan-4 and

anti-VEGFR-2 Abs both specific for the N-terminal domain of the 2 molecules. Nuclei are stained with DRAQ5 (blue) while red dots (PLA dots) only appear when syndecan-4 and VEGFR-2 are in close proximity (< 40 μm). Images shown were captured on a Zeiss confocal microscope and processed on Imaris software and are representative of at least 5 images per condition. Scale bar 20 μm.

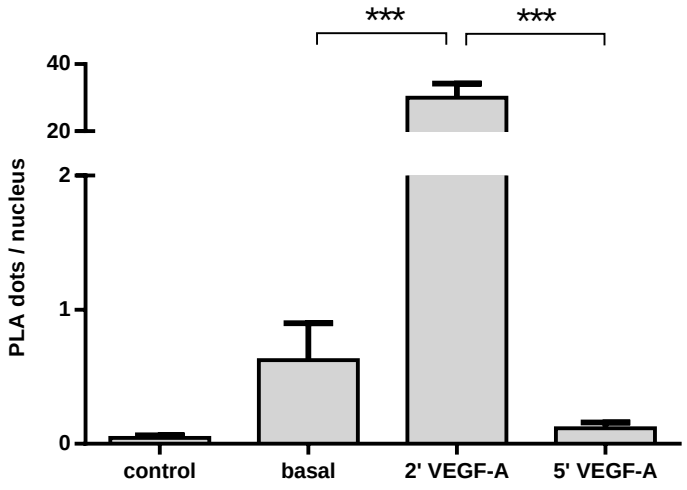

Fig. 4.65 **Syndecan-4 and VEGFR2 transiently go into close proximity upon VEGF stimulation in ECs.** Confluent wild-type primary mouse lung ECs were serum-starved for 6 hours and then treated with 30 ng/ml of VEGF-A for 2' and 5'. Subsequently, the proximity ligation assay was performed, following manufacturer instructions, using anti-syndecan-4 and anti-VEGFR-2 Abs both specific for the N-terminal domain of the 2 molecules. In control samples the protocol was conducted using only the anti-VEGFR2 Ab. PLA dots only appear when syndecan-4 and VEGFR-2 are in close proximity (< 40 μm). Images were captured on a Zeiss confocal microscope and PLA dots were counted on Imaris software. Data are representative of at least 5 images per condition. Significant differences were determined using one-way Anova with Tukey correction for multiple comparisons. ***P<0.001.

Having established that upon VEGF-A addition syndecan-4 and VEGFR2 go into close proximity, possibly forming a complex, in wild-type ECs, we set to determine what happens in the absence of syndecan-4. Critically, PLA experiments with syndecan-4 knock-out cells using anti-syndecan-2 Ab suggested a compensatory mechanism whereby, in the absence of syndecan-4, ECs can partially but not sufficiently compensate (note that the number of Syn2/VR2 in the syndecan-4 knock-out cells is much lower than that of Syn4/VR4 complexes in the wild-type cells) by using syndecan-2 as a co-receptor to VEGFR2 (Fig. 4.66).

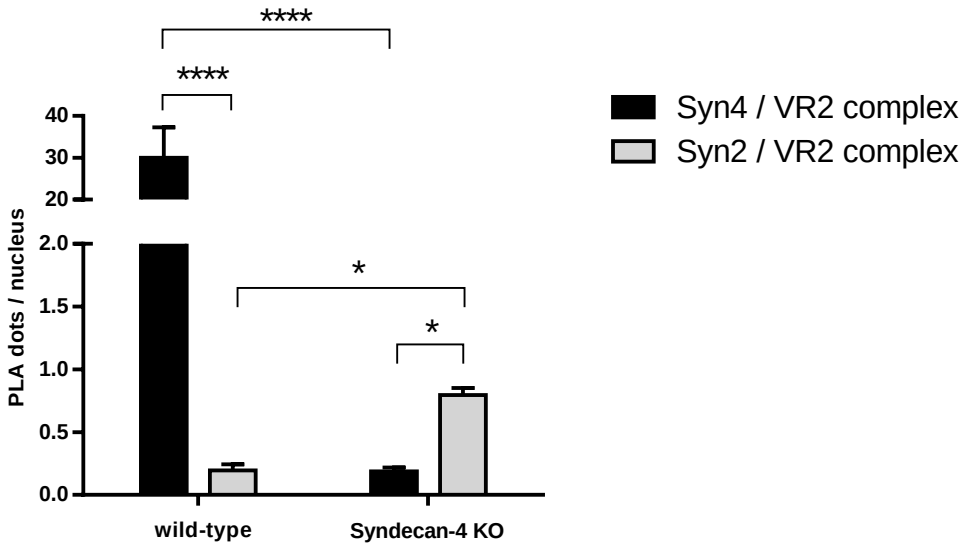

Fig. 4.66 **Syndecan-2 and VEGFR2 transiently go into close proximity upon VEGF stimulation in syndecan-4 knock-out ECs.** Confluent wild-type and syndecan-4 knock-out primary mouse lung ECs were serum-starved for 6 hours and then treated with 30 ng/ml of VEGF-A for 2'. Subsequently, the proximity ligation assay was performed, following manufacturer instructions, using anti-syndecan-4 or anti-syndecan-2 Ab in combination with anti-VEGFR-2 Ab, all three specific for the N-terminal domain of the molecules. PLA dots only appear when syndecan-4 or syndecan-2 and VEGFR-2 are in close proximity (< 40 μm). Images were captured on a Zeiss confocal microscope and PLA dots were counted on Imaris software. Data are representative of at least 5 images per condition. Significant differences were determined using two-way Anova with Sidak correction for multiple comparisons. *P<0.05, ****P<0.0001.

Collectively, the data presented in this paragraph showed that syndecan-4 is required for efficient VEGFR2 activation; moreover, proximity ligation assays gave strong indications that syndecan-4 is acting as a co-receptor facilitating the interaction between VEGF-A and VEGFR2. Also of note, syndecan-2 appears to be involved in a compensatory mechanism in syndecan-4-deficient EC to overcome the co-receptor role of syndecan-4.

4.3.3.6. Soluble competitor of syndecan-4 can reduce angiogenesis

Because our results suggest that VEGF-A-driven angiogenesis requires the formation of a tri-molecular complex including syndecan-4, VEGFR-2 and VEGF-A on the cell surface of ECs, we decided to test the effect of the addition of soluble syndecan-4 ectodomain to the medium of wild-type cells to compete in the syndecan-4 interactions and dismantle the complex.

Treatment of wild-type ECs with syndecan-4 extra-cellular domain (solS4ED) diminished the activation of VEGFR2 in response to VEGF-A, confirming that syndecan-4 interacts with VEGFR2 on the cell surface rather than intracellularly (Fig. 4.67). Moreover, this effect has functional implications to VEGFR2-dependent signalling pathways; for example, one of VEGF-A effects on ECs is the promotion of VE-Cadherin internalization which leads to dissociation of cell-cell contacts (Gavard and Gutkind, 2006). When confluent MLECs were treated with VEGF-A164, VE-Cadherin started to disappear from the cell junctions and got internalized into cytoplasmic vesicles, but when soluble S4ED was added to the medium, such process appeared prevented, with VE-Cadherin still retained in EC adherens junctions after VEGF-A164 addition and not much of it being found inside cell vesicles (Fig. 4.68, Fig. 4.69). Finally, we tested soluble S4ED in the *ex vivo* model of neo-vascularisation of the mouse aortic ring assay and, notably, we observed a strong reduction in the angiogenic response (Fig. 4.70).

Collectively, these results provide further evidence that syndecan-4 is indeed required on the EC surface using soluble syndecan-4 as a competitor of the membrane-bound form has the therapeutic potential of efficiently blocking VEGF-driven angiogenesis.

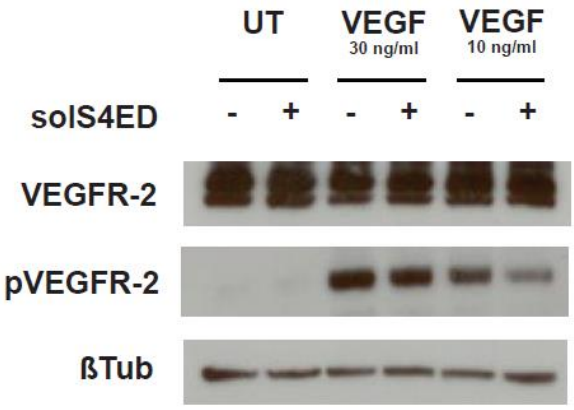

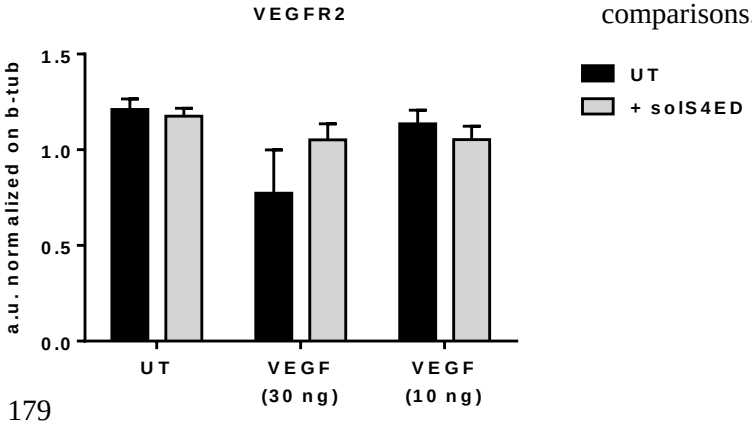

Fig. 4.67 **Soluble syndecan-4 ectodomain diminishes VEGFR2 phosphorylation.** Confluent wild-type (WT) primary mouse lung ECs were serum-starved for 6 hours and then treated with 30 or 10 ng/ml of VEGF-A for 5' in the absence or presence of soluble syndecan-4 ectodomain (solS4ED) 0.5 µM. Western blot of lysates from these cells were probed with Abs against total VEGFR-2 or phosphorylated VEGFR-2 (pVEGFR-2, tyrosine 1056). The blot is representative of at least 4 experiments. Densitometry was performed on 4 blots and normalized against β-tubulin. Significant differences between untreated control and treated group were determined using two-way Anova with Tukey correction for multiple comparisons. **P<0.01.

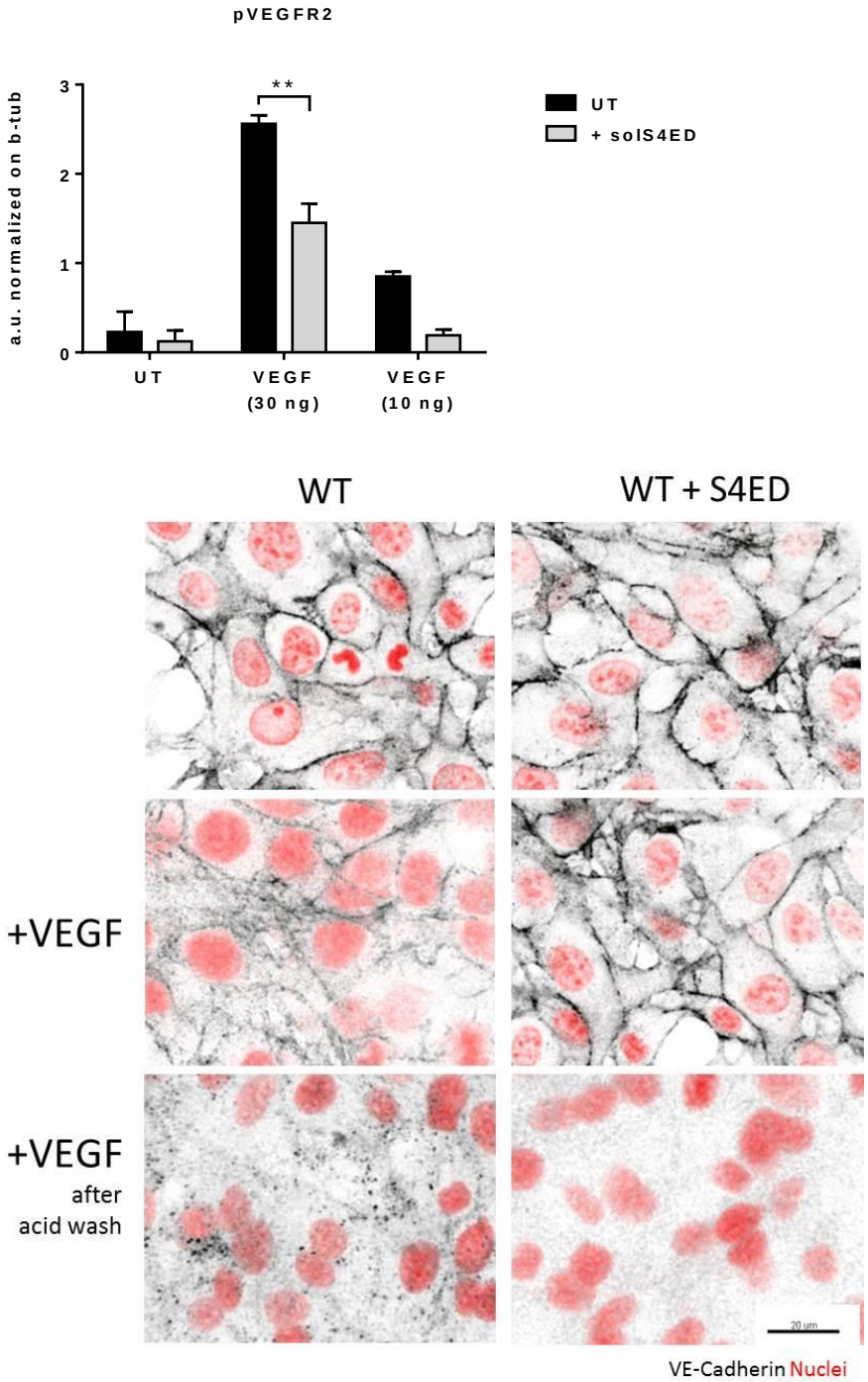

Fig. 4.68 **Effect of soluble syndecan-4 ectodomain on VEGF-induced VE-Cadherin internalization in ECs.** Primary mouse lung ECs were plated on glass slides; confluent cells were then washed with PBS and incubated with anti-VE-Cadherin Ab (BV13 clone) at 4°C for 1h in medium containing 20 mM HEPES and 3% BSA. Unbound Ab was then rinsed with ice-cold medium and cells were incubated with 30 ng/ml of VEGF-A in serum-free medium or serum-free medium alone at 37°C for 5' to allow the internalization of VE-Cadherin. An acid wash was then use to remove the Ab bound to cell-surface VE-Cadherin, this wash contained 25 mM glycine, 3% BSA in PBS (pH 2.7). To assess the effect of soluble syndecan-4, 0,5 µM of shed syndecan-4 was added in the VEGF-A incubation. Images shown were captured on a Zeiss confocal microscope and processed on Imaris software to show VE-

cadherin in black and nuclei in red and are representative of at least 5 images per condition. Scale bar represents 20 µm.

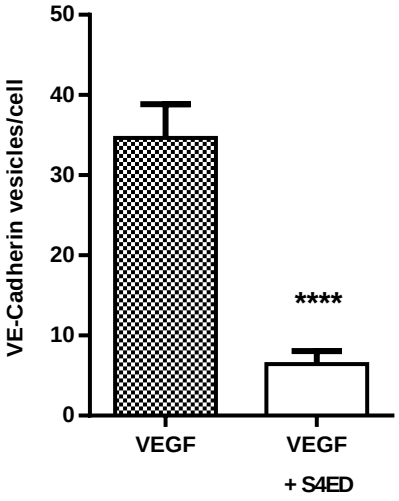

Fig. 4.69 **Quantification of VE-Cadherin internalization.** Images from previous experiments were analysed on Imaris software and black dots, indicative of VE-cadherin positive vesicles, were counted and divided by the amount of nuclei in the picture. At least 5 images per group were analysed. Statistically significant difference was found between cells treated with VEGF and those treated with VEGF in the presence of soluble syndecan-4. ****P<0.0001 according to Student's T-test.

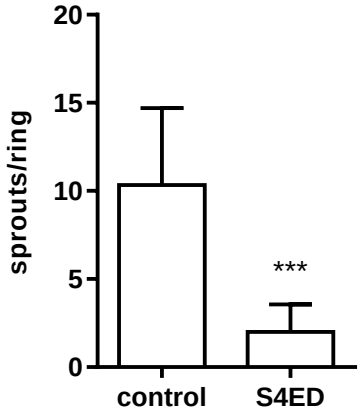

Fig. 4.70 **Soluble syndecan-4 ectodomain inhibits aortic sprouting.** Mouse thoracic aortas were cut into rings which were embedded in 150 µl of Collagen type I (1 mg/ml) containing 0.5 µM of syndecan-4 ectodomain (S4ED) or PBS in 200 µl of OPTIMEM containing 30 ng/ml of VEGF-A. The number of sprouts was measured 7 days after embedding. Each bar represents the mean with standard deviation of at least 9 rings per group. Significant differences between untreated control and treated group were determined using one-way Anova with Dunnett correction for multiple comparisons. ***P<0.001.

4.3.4. Discussion

This section describes experiments conducted to investigate the role of the HS proteoglycan syndecan-4 in angiogenesis.

Here, I have shown that:

1. Syndecan-4 does not affect vasculogenesis of muscle or skin vasculature
2. Syndecan-4 expression is low on the cremaster muscle homeostatic vasculature
3. Skin vascular permeability is not affected by lack of syndecan-4
4. Syndecan-4 knock-out mice develop smaller and less vascularised melanoma tumors
5. Lack of syndecan-4 impairs specifically VEGF-A-driven angiogenesis
6. Requirement for syndecan-4 for VEGF-A-driven angiogenesis is not tissue-specific
7. Syndecan-4 is expressed on ECs in angiogenic tissues
8. Syndecan-4 expression on ECs is increased by angiogenic stimuli both at messenger and protein level by angiogenic factors *in vitro*
9. Syndecan-4 is retained on EC surface and it is not shed upon VEGF-A treatment *in vitro*
10. Efficient VEGFR2 phosphorylation upon VEGF-A binding requires endothelial syndecan-4 *in vitro*
11. Syndecan-4 and VEGFR2 go into close proximity upon VEGF-A stimulation of ECs *in vitro*
12. Syndecan-2 could partially compensate for syndecan-4 in its absence as a VEGFR2 co-receptor
13. Addition of a soluble form of syndecan-4 ectodomain is effective in decreasing VEGFR2 phosphorylation, one of its downstream pathways and strongly inhibits angiogenesis *ex vivo*

In summary, I have identified syndecan-4 as a key regulator of adult neo-vascularisation but dispensable for vasculogenesis and vascular homeostasis. I have shown that syndecan-4 is expressed at very low level on homeostatic vasculature, whereas its expression is markedly increased on angiogenic vessels and following *in vitro* stimulation of ECs with angiogenic factors. The data suggest that syndecan-4 acts as a co-receptor to facilitate the interaction of VEGF-A with its receptor VEGFR2 during angiogenesis. Finally, I have revealed that the treatment of ECs with a soluble form of syndecan-4 blocks VEGF-A signalling and inhibits *ex vivo* neo-vascularisation.

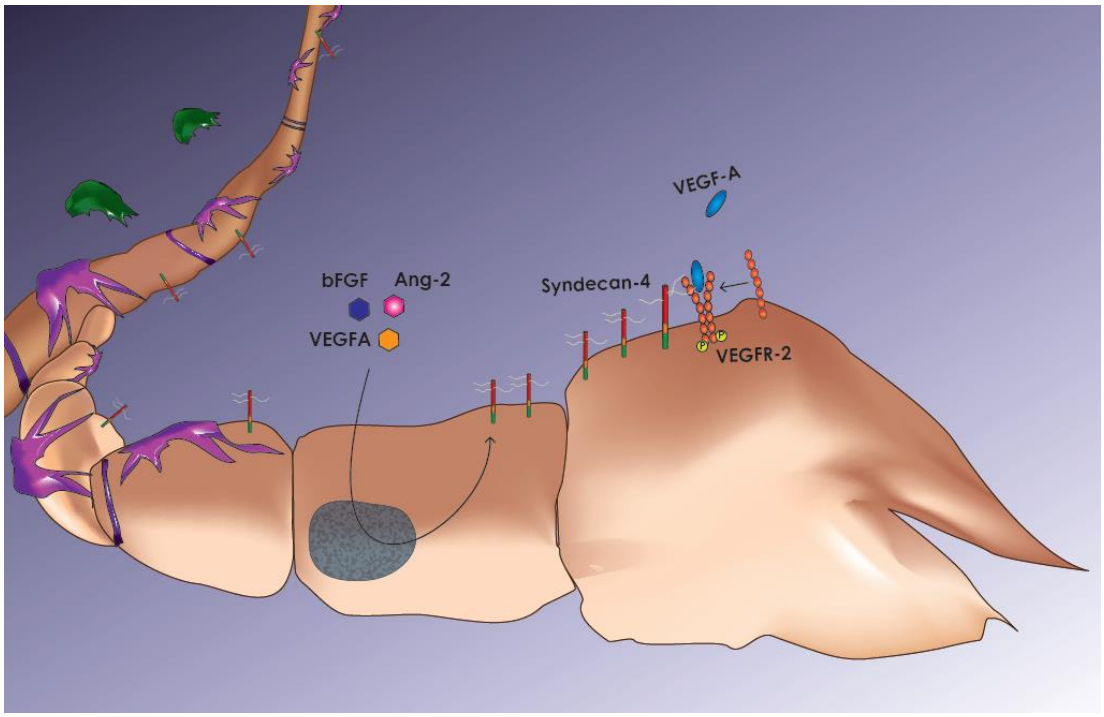

Fig. 4.71 **Schematic of the model whereby syndecan-4 is required for VEGF-A-induced angiogenesis.** Syndecan-4 is found very low expressed on the endothelium; during angiogenesis, however, syndecan-4 expression increases and its presence on the endothelial cell surface is required to facilitate the interaction of VEGF-A with its receptor VEGFR-2.

This model fits well with previous studies showing that syndecan-4 expression is found increased in pathologies featured by an angiogenic response, these include the ischemic myocardium (Li et al., 1997), vascular tissues after injury (Nikkari et al., 1994) and in a variety of tumors (Yoneda et al., 2012). Moreover, the syndecan-4 knock-out (S4KO) mouse develops a more severe phenotype compared to wild-type littermates in those pathologies where angiogenesis is critical to the resolution phase of the disease; for example, these mice display a delayed dermal wound healing associated with impaired angiogenesis and a cell migration defect (Echtermeyer et al., 2001b). The ability of syndecan-4 to regulate angiogenesis is also suggested by the observation of enhanced neovascularization in the ischemic muscle following the combined delivery of basic Fibroblast growth factor and syndecan-4 (Jang et al., 2012) and also by the notion that lack of syndecan-4 impairs foetal vessels in the placenta (Ishiguro et al., 2000a). Moreover, the syndecan-4 knock-out mouse shows increased mortality post myocardial infarction which is, again, associated with reduced number of capillary vessels in the healing tissue (Matsui et al., 2011). Because VEGF-A is the most potent pro-angiogenic factor (Larrivee and Karsan, 2000) and because syndecan-4 is necessary for VEGF-A activity,

it is not surprising that the syndecan-4 null mice develop a dramatic phenotype in those pathological settings where new blood vessel formation is required.

The VEGF-A gene is composed of 8 exons which by undergoing alternative splicing result in the generation of 4 different isoforms: VEGF-A121, VEGF-A165, VEGF-A189, VEGF-A206 (where the numbers are indicative of the amount of amino acids they retain after signal peptide cleavage) (Houck et al., 1991). In all my experiments I have used VEGF-A165 (164 for work on murine cells) as this is the predominant isoform. This isoform is a heparin-binding homodimeric glycoprotein of 45 kDa (Houck et al., 1992). Interestingly, when VEGF-A loses its heparin-binding properties, this reflects in loss of its mitogenic activity (Keyt et al., 1996). The importance of VEGF-A 165 became clear when it was shown to be the only isoform able to rescue a tumorigenic phenotype in mice lacking the VEGF gene (Grunstein et al., 2000), moreover, mice expressing only VEGF-A120 (an isoform which does not have the heparin-binding domain) die shortly after delivery, emphasizing the importance of the heparin-binding domain for VEGF-A properties. VEGF-A binds to HS with high affinity (Robinson et al., 2006b), and cells where HS has been enzymatically removed have abrogated VEGF-A signalling (Ashikari-Hada et al., 2005). VEGF-A receptor, VEGFR2, also binds to HS, suggesting that HSPGs may play a role in facilitating the formation of an active signalling complex between VEGF-A and VEGFR2 (Nishiguchi et al., 2010). HSPGs are in fact regulators of VEGF-A gradients. It was however unknown whether this activity was common to all HSPG or specific to one or more. The data I've just presented certainly suggest that syndecan-4 possesses the ability to complex with VEGFR2 and the fact that soluble syndecan-4 ectodomain is able to inhibit VEGF-A driven VEGFR2 phosphorylation would infer that the HS chains are important to this function (Fig. 4.64, Fig. 4.70). However, I do not possess at the moment solid data to conclusively say whether syndecan-4 HS chains actively interact with VEGF-A, VEGFR2 or both. It is tempting to speculate that they are all implicated in the formation of a tri-molecular complex.

Another important aspect of VEGFR2 activity is represented by the regulation of its endocytosis and trafficking (Simons, 2012). Upon entry into the cells, VEGFR2 continues to signal, first in early endosomes (APPL and Rab5 positive) and then transitions into endosomes which are positive for EEA1 (Santambrogio et al., 2011). $EEA1^{+}$endosomes containing VEGFR2 undergo intracellular trafficking utilising the complex Synectin/Myosin VI. VEGF signalling and *in vivo* angiogenesis are impaired in both synectin- and myosin VI-null mice (Dedkov et al., 2007; Paye et al., 2009). It is, however, unclear at the moment how VEGFR2 in the EEA1+ endosome interacts with synectin/myosin VI complex. Interestingly, synectin possesses a PDZ motif which is known to interact with a number of molecules including

syndecan-4. It would be therefore tempting to speculate that syndecan-4 is involved in VEGFR2 endocytosis and trafficking. An interesting approach to test this hypothesis would be to evaluate the effect of a syndecan-4 mutant lacking the PDZ binding domain on VEGF signalling and VEGFR2 trafficking.

Given the critical importance of the VEGF signalling system to vascular development and its exquisite sensitivity to the level of the ligand (even a 50% reduction in VEGF levels during development leads to embryonic lethality), it is quite surprising that the syndecan-4 null mouse develops normally. There are however several possible explanations to this. For example, as mentioned above, an important difference between VEGF-A165 and 121 isoforms is the absence of the heparin-binding domain in the latter. While VEGF-A165 has intermediate properties as it is secreted but some diffuse and some stay anchored to the cell surface or the ECM, the 121 isoform is freely diffusible (Houck et al., 1992; Park et al., 1993). It is likely that the isoforms of VEGF-A that do not possess a heparin binding domain, including VEGF-A-12, lack the capability to bind to syndecan-4 HS chains. This suggests that there may be syndecan-4 dependent and independent forms of VEGF signalling which in part may explain why developmentally the syndecan-4 knock-out mouse is normal.

In addition, because of the strong sequence homology in the cytoplasmic and transmembrane domains and in the sugar chains, especially between syndecan-1 and -3 and syndecan-2 and -4, it is commonly believed that syndecans have overlapping roles and can compensate for each other. A recent study, for instance, showed that syndecan-4 null mice have delayed bone fracture repair and, importantly, that, in the absence of syndecan-4, syndecan-2 gets upregulated in the developing cartilage (Bertrand et al., 2013). This situation could in many ways mirror what I'm seeing in the context of angiogenesis. An interesting question to address is whether syndecan-2 is upregulated during vasculogenesis since I saw a principle of compensatory mechanism when syndecan-4 null ECs formed syndecan-2/VEGFR2 complexes upon VEGF-A addition (Fig. 4.66). In cartilage and vasculature development, syndecan-2 might be structurally similar enough to syndecan-4 to compensate for its absence but in pathological settings, maybe because the quick response requires higher efficiency, is inadequate.

In vitro experiments on ECs have also shown that syndecan-4 is a key player in FGF2 signalling (Murakami et al., 2002b; Volk et al., 1999). However, in contrast with the potent angiogenic response elicited by exogenous FGF2 *in vitro*, fgf2 Knock-out mice are morphologically normal (Zhou et al., 1998) and do not even show impairment in neovascularization after injury (Tobe et al., 1998) or hypoxia (Ozaki et al., 1998). It is

therefore unlikely that syndecan-4 contribution to FGF2 signalling can explain the dramatic angiogenic phenotype the syndecan-4 knock-out mice develop under pathological settings. Challenging the syndecan-4 knock-out mouse both *in vivo* (Matrigel plug assay) and *ex vivo* (aortic ring assay) models of angiogenesis hasn't revealed any significant impairment in FGF-driven responses, which can be explained by the fact that FGF2 can also bind other HSPGs, including syndecan-1 (Filla et al., 1998).

Similarly to syndecan-4, syndecan-1 is also upregulated during skin wound healing (Gallo et al., 1996a), and lack of syndecan-1 results in delayed skin (Bernfield et al., 1999b) and corneal wound repair (Stepp et al., 2002). Again, likewise syndecan-4 null mice, syndecan-1 null mice are viable and fertile. The generation of a syndecan-1 and syndecan-4 double knock-out could shed light on whether these two HSPG provide complementary signalling pathways during wound healing.

Angiogenesis is a key feature of many diseases, many of which are life-threatening. Malignant tumors, for example, are composed of fast-growing highly-metabolic cells and without a good blood supply to bring nutrients and oxygen and remove waste products they wouldn't grow larger than 1 to 2 mm across. For this reason, tumor cells are known to produce and release pro-angiogenic factors which will stimulate neighbouring blood vessels to grow new capillaries within the tumor mass. Angiogenesis is also characteristic of chronic inflammatory conditions such as Rheumatoid Arthritis where the highly proliferative synovial cells increase the metabolic demand for oxygen and nutrients, but also cardiovascular diseases, blindness, complications of AIDS, diabetes, Alzheimer's disease and more than 70 other major health conditions affecting children and adults worldwide. The idea of blocking angiogenesis by targeting the VEGF-A/VEGFR2 pathway has led to the development of a number of drugs: targeting VEGF-A directly (e.g. the humanized monoclonal Ab Bevacizumab) or targeting VEGFR2 signalling pathways (mainly small tyrosine-kinase inhibitors such as Sunitinib and Sorafenib). Although this is the only form of effective therapy currently in clinical use, therapies that target VEGF directly are raising several concerns. One of which is that VEGF not only drives new vessel growth but increasing evidence is suggesting that it also has an important role for trophic maintenance of the healthy vasculature. Prolonged anti-VEGF therapy for cancer treatment is associated with a number of severe adverse effects associated with endothelial dysfunction including: hypertension, microangiopathy, proteinuria in the kidney; cardiac ischemia/infarct, thromboembolic events in the heart, and bleeding in the gastrointestinal system (Meadows and Hurwitz, 2012). Moreover, Kurihara et al. have recently described a dramatic and rapid loss of ECs of the choriocapillaries and severe vision loss in mice following genetic deletion of the VEGF gene from the retinal pigment epithelial cells,

with alerting implications for the anti-VEGF therapy which is currently in use for the treatment of Wet Age related macular degeneration. These data would in fact suggest that an indiscriminate suppression of VEGF signalling, an effect similar to that reached by the anti-VEGF therapies currently in use, might carry with it very dramatic side effects for the patients in the long run (Kurihara et al., 2012). This has highlighted the need to identify novel therapeutic targets to develop better therapies. In light of my results, it would be tempting to speculate that targeting syndecan-4 would still prove efficient in blocking VEGF signalling but unlike current anti-VEGF therapies, this effect would only be limited to the site of pathological neo-vascularisation with limited off-target side effects on the remaining healthy vasculature. This would represent an important translational advance for the treatment of angiogenesis-dependent diseases.

5. General discussion and Conclusions

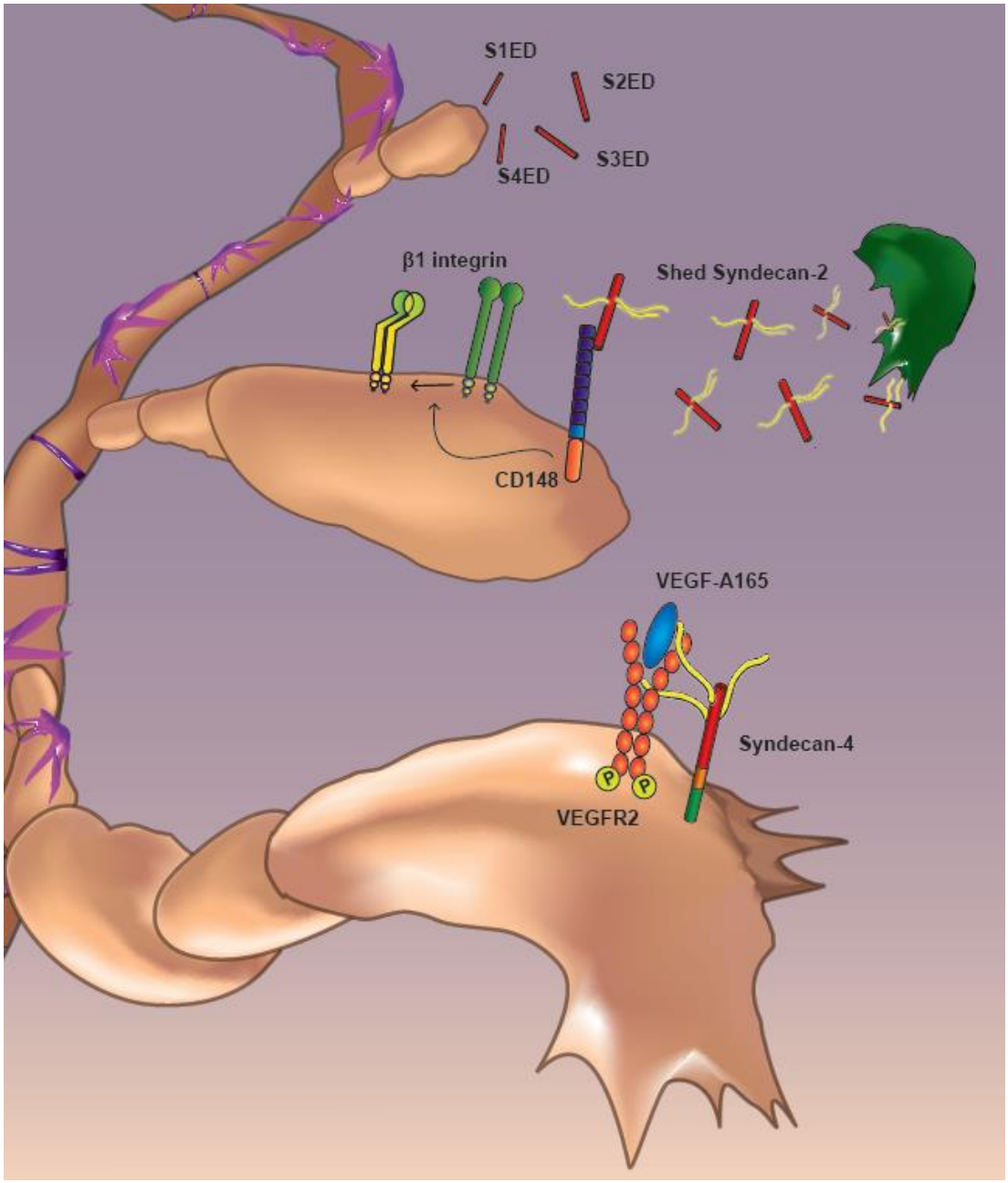

Fig. 5.1 **Diagram depicting the proposed modes of action of syndecan ectodomains, shed syndecan-2 and endothelial syndecan-4 during angiogenesis, based on the results obtained during this PhD.**

In the first part of my project, I investigated the effects of the extracellular core proteins of syndecan-1, -2, -3 and -4 on EC function, particularly with regard to angiogenesis, and revealed that all four syndecan extracellular core proteins are able to inhibit angiogenesis *ex vivo* and strongly negatively regulate EC migration, invasion and tube formation *in vitro* (Fig.

5.1). In the second part of my project, I further characterized the anti-angiogenic properties of one family member, namely syndecan-2, and showed that these reside in its ability to interact with the EC surface tyrosine phosphatase CD148. Upon binding of S2ED to CD148, we observed reduced active β1 integrins resulting into inhibition of EC migration. EC migration is of paramount importance in angiogenesis and the anti-migratory effect of S2ED greatly reduces new blood vessel formation both *in vitro* and *in vivo*. Remarkably, this is an entirely novel pathway for the reduction of angiogenesis, which doesn't directly act through VEGF (Fig. 5.1). Finally, since previous works suggested that syndecan-4-null mice may exhibit angiogenic defects I set out to determine the role of syndecan-4 in angiogenesis. Firstly, I observed an up-regulation of syndecan-4 on ECs upon stimulation with pro-angiogenic factors both *in vitro* and *in vivo;* then, by challenging syndecan-4 knock-out mice in *in vivo* models of angiogenesis, I revealed that these mice fail to respond specifically to VEGF-driven pro-angiogenic signals. This effect can partially be explained by an impaired phosphorylation (hence activation) of VEGFR2 that we revealed in syndecan-4-null ECs treated with VEGF. We therefore propose a model whereby syndecan-4 is the main HS proteoglycan to act as co-receptor for the VEGFR2/VEGF-A interaction (Fig. 5.1).

5.1 Shedding and the fate of syndecan ectodomains

Syndecan shedding is generally considered as a mechanism to promptly interrupt syndecan functions as co-receptor, chemo- and cytokine gradient regulator and adhesive receptor on the cell surface. Several proteinases, including MMPs and ADAMs, have been shown to being able to readily shed syndecans from a variety of cell types in specific conditions (e.g. tissue injury, inflammation, cancer). My work, and the work of others, has however highlighted that biological properties are contained within discrete regions of the syndecan ectodomains, properties which, depending on the reciprocal position of the active and the cleavage sites, can still be retained after syndecans are cleaved form the cell surface. Hence, shedding not only interrupts syndecan functions on the cell surface, but can also (or alternatively) release molecules in the extracellular space which are still bio-active and can interact with other cells in the surrounding tissue. It would therefore be interesting/necessary to re-evaluate all those studies which have looked at syndecan shedding only from a "loss of function" perspective. In mice, for example, shed syndecan-1 is often found in body fluids during inflammation. Syndecan-1 null mice show an exaggerated inflammatory response following allergen-exposure suggesting that syndecan-1 shedding is involved in the resolution phase of inflammation (Xu et al., 2005). Syndecan-1 seems to also have a protective role in LPS-

induced multi-organ injury and mortality. In particular, syndecan-1 shedding appears to be responsible for the clearance of KC and MIP-2 which regulates neutrophil infiltration (Hayashida et al., 2009). In this context would be interesting to investigate what the fate of shed syndecan-1 is: will it still stay in a complex with KC and MIP2 in the circulation? Can the sequestered chemokines interact with circulating leukocytes or with ECs? Could this mechanism promote off-site inflammation and distant organ damage? And what about cancer? Syndecans are expressed by most tumor cells and here they play important roles as adhesion receptors. It is therefore unsurprising that loss or increased expression of syndecans can affect both tumor cell adhesion and migration. However, not much is known about the autocrine effects of shed syndecans on tumor cells and even less about the paracrine effects of shed syndecans on the cells populating the tumor microenvironment. Recently, it has been shown that syndecan-2, shed from colon cancer cells, can act in an autocrine way to enhance cancer cell migration. We, on the other hand, have shown for the first time that shed syndecan-2 negatively affect EC migration and can impede tumor angiogenesis in an *in vivo* model of melanoma. I have also revealed that primary lung fibroblasts shed syndecan-2 in response to inflammatory stimuli (data not shown). Not only tumor cells but also stromal cells, like fibroblasts, can therefore be a source of shed syndecans in the tumor microenvironment. Cancer cells are able to promote the conversion of stromal fibroblasts to cancer-associated fibroblasts (CAFs). CAFs are attracting a lot of interest lately as they have been shown to switch tumors to a more aggressive/metastatic phenotype through various mechanisms. One such mechanism is the promotion of angiogenesis. It would be therefore tempting to speculate that while healthy fibroblasts retain syndecan-2, activated fibroblasts release anti-angiogenic syndecan-2 under inflammatory conditions (e.g. cancer), when they switch to the CAF phenotype, they stop doing so. Of interest would also be to investigate whether shed syndecans have effects on resident immune cells that populate the tumor microenvironment. Notably, B lymphocyte express the phosphotyrosine CD148, it would therefore be extremely relevant to test the effect of shed syndecan-2 (which we have shown being able to interact with CD148) on these cells and on lymphoma.

Further studies are critically needed to shed light on tumor syndecan shedding and how these moieties affect not only the tumor cells but also the surrounding cells; more thorough investigation would be needed especially to understand the temporal, spatial and dosage dependency of shed syndecan effects. On the basis of those results, development of anti-angiogenic syndecan-derived therapeutic would have to be approached with a lot of caution as they might have undesirable side-effects on tumor growth and motility, depending on the tumor type.

5.2 A peptide based on syndecan-2 shows therapeutic efficacy in a murine model of wet Age-related macular degeneration

The work I carried out to characterize the anti-angiogenic properties of syndecan-2 extracellular domain have revealed that these lay within the last 18 aa of the protein. A small peptide that is capable of reducing β1 integrin activation in endothelial cell upon binding to the phosphatase inhibitor CD148.

As β1 integrins have important roles in regulating angiogenesis, these integrins are an attractive target for anti-angiogenic therapies. Antagonists of one β1 integrin, α5β1, have undergone clinical testing. A chimeric mouse–human anti-α5β1 Ab, M200 (volociximab) has shown low toxicity in phase I studies. M200 was evaluated in phase II trials for metastatic melanoma, renal cell carcinoma and non-small cell lung cancer (Kuwada, 2007). Another drug in clinical trials, ATN-161, is a peptide inhibitor of integrin α5β1. In animal models of colon cancer, ATN-161 reduced metastases and improved survival when combined with chemotherapy (Stoeltzing et al., 2003). Thus, these two integrin α5β1-inhibiting drugs might offer future benefit to cancer patients.

What advantages would the use of syndecan-2-peptide give compared to using M200 or ARN-161 to inhibit angiogenesis? Although α5β1 integrin is found upregulated on ECs in the tumor vasculature, this integrin is widely expressed by many other cell types as it is the main receptor for the ECM molecule fibronectin. Thus targeting α5β1 integrin directly will carry with it unspecific side effects, due to the blocking of key functions on other cell types. Notably, the use of the syndecan-2-derived peptide will only block β1 integrins on those cells expressing CD148, which are endothelial cells and memory B-cells (according to our data and the literature). This will have the clear advantage of targeting the forming new blood vessels while sparing the remaining tissue.

This rationale led us to further investigate whether an anti-angiogenic peptide-based therapy could be possible. We received funding from Queen Mary Innovation Ltd, Queen Mary University technology transfer company, to further test the syndecan-2-based peptide, now called QM107, in a range of angiogenesis assays before the filing of a patent. These studies have confirmed the ability of QM107 to inhibit angiogenesis both *in vitro* and *ex vivo*, and, more importantly, a first preliminary round of pre-clinical studies in a mouse model of wet age-related macular degeneration has shown that as little as 1 μM of QM107, injected intra-vitreally, is able to attenuate choroidal neovascularisation by 30% with no visible side-effects. We are now looking forward to test higher doses and different times of injection to reach the

maximum efficacy possible for this potential therapeutic. Collectively, these data indicate that QM107 is a highly promising peptide-based anti-angiogenic therapeutic, which can be chemically synthesized and offer an alternative therapy to the current VEGF-based option. Furthermore, since it is a relatively small molecule compared to the existing Ab based therapeutics we envisage this could be administered in the form of eye drops as opposed to the current therapy which is administered via monthly injections into the eyes of patients.

5.3 The identification of syndecan-4 as the main HSPG involved in the VEGF-A/VEGFR2 pathway

There is a large body of evidence highlighting the importance of HS for an efficient VEGF-A165/VEGFR2 signalling. These studies however failed to identify a particular HS-bearing molecule and rather assign this function to all HSPG.

Importantly, growth factor binding to HSPG can serve four functions: (i) concentration of the growth factor at the cell surface and presentation to cell surface receptors, (ii) engagement of the HSPG in a co-receptor complex with altered binding or signalling properties compared to a minimal growth factor/receptor complex, (iii) control of growth factor diffusion to provide spatially restricted signalling cues and (iv) creation of a growth factor pool that can be released by shedding of either the HS chain or the growth factor (Iozzo, 2005).

The interaction of VEGF-A165 with HS is determined by the exons 6 and 7 which code for the heparin binding domain (HBD) located to the carboxy-terminal and was shown to depend on basic residues. Site-directed mutagenesis studies have identified arginine residues R123, R124 and R159 of VEGF-A165 as crucial residues for the interaction with HS (Krilleke et al., 2007). This finding is supported by the refined NMR structure of the HBD (Stauffer et al., 2002), where these residues are localized on a contiguous binding surface on one face of the domain. Together with K125, K140, R145, R149 and R156 they form an electropositive patch positioned to interact with negatively charged HS.

Several studies showed that both *N*-sulphation and 6-*O*-sulphation in the HS are crucial for VEGF-A165 binding, whereas 2-*O*-sulfate groups and carboxylate groups contribute to a lesser extent (Robinson et al., 2006a), a finding in agreement with earlier results obtained with heparin (Ono et al., 1999). VEGF-A binding to HS therefore differs from HGF and FGF-2 which strictly require 2-*O*-sulfation. Notably, different patterns of HS chains could therefore contribute to the tissue specificity of growth factor signalling.

Soluble extracellular domain of VEGFR-2 isolated from conditioned medium is retained by heparin sepharose, suggesting direct binding to HSPG (Chiang and Flanagan, 1995). Although the involvement of other factors present in the medium could not be excluded, this interaction was ascribed to a short basic stretch between Ig-like domains 6 and 7 (Dougher et al., 1997).

The importance of appropriately modified HS for cellular responses to VEGF-A165 has been well described. HUVEC cells treated with sodium chlorate, an inhibitor of HS sulphation, fail to proliferate in response to VEGF-A165 unless heparin (only sulphated forms) or sulphate is added back to the medium. Depletion of 6-*O*-sulfation by specific inactivation of the sulfotransferase HS6TS-2 results in abnormalities in branching morphogenesis of the caudal vein during embryogenesis in zebrafish (Ono et al., 1999). Interestingly, mammalian embryoid bodies derived from *Ndst1/2*$^{-/-}$ stem cells, lacking a sulphotransferase essential for HS biosynthesis, fail to respond to VEGF-A165 (Jakobsson et al., 2006) and the addition of exogenous HS could not substitute for the lack of correctly modified HSPG. Notably, co-culture with cells expressing wild-type HSPG, but not VEGFR-2, resulted in rescue of VEGF-A165 induced vascular development. Interestingly, VEGFR-2 activation was more persistent and this effect could not be elicited by binding of VEGF-A121. It's tempting to speculate that HSPGs could trap the VEGFR2 *in trans* and prevent internalization and degradation, explaining the prolonged signalling.

My studies would suggest that syndecan-4 is the main HSPG involved in VEGF-A165 signalling. Proximity ligation experiments implied the formation of a syndecan-4/VEGF-A165/VEGFR2 tri-molecular complex. Further work is however necessary to elucidate the exact interactions, of particular interest would be to understand what are the specific characteristic/modifications of syndecan-4 HS chains that make it such a strong VEGF co-receptor compared, for example, to syndecan-2, to which syndecan-4 is extremely structurally similar. Syndecan HS chains can range from 80-200 kDa in mass and undergo a great number of enzymatic modifications. The HS chains of syndecan-4 could therefore represent the most variable component in the VEGF/VEGFR2 signalling complex. On the basis of this hypothesis, differential expression of the enzymes involved in the sulphation pathways of syndecan-4 HS chains could determine an additional, never described before, level of regulation of VEGF-induced angiogenesis.

Ultimately, knowing which enzymes determine the optimal sulphation pattern on syndecan-4 could also be translated in the clinic. My data clearly showed the pivotal role of syndecan-4 in pathological angiogenesis (melanoma and choroidal neo-vascularisation) and the additional *ex vivo* and *in vitro* studies would suggest that syndecan-4 pro-angiogenic functions are not

limited to the skin and choroid. A gene-therapy approach aimed at silencing the target sulphotransferase, for example, could prove efficient in blocking VEGF-induced angiogenesis. Alternatively, blocking Abs targeting syndecan-4 ectodomain could prove efficient to spatially dislodge syndecan-4 from the tri-molecular complex with VEGF-A and VEGFR2 and limit the downstream signalling, ultimately preventive the angiogenic response.

5.4 Conclusions

Angiogenesis is feature of many diseases such as cancer, macular degeneration, cardiovascular diseases, blindness, complications of AIDS, diabetes, Alzheimer's disease and more than 70 other major health conditions affecting children and adults worldwide.

Like any biological process, angiogenesis is a complex process as it involves the participations of multiple cell types and molecules, working together to orchestrate the formation of a completely new blood vessel network. As part of its complexity, this process is tightly regulated and understanding how this is possible would allow us to switch it on and off when needed.

During my PhD, I revealed that syndecan ectodomains can inhibit angiogenesis and that syndecan-4 can enhance this process. These basic science discoveries could aid future research that can be translated to improve anti-angiogenic therapy for the treatment of over one billion people affected by angiogenesis-dependent diseases worldwide.

6. References

Adams, R.H., and Eichmann, A. (2010). Axon guidance molecules in vascular patterning. Cold Spring Harb Perspect Biol *2*, a001875.

Albert, J.M., Cao, C., Geng, L., Leavitt, L., Hallahan, D.E., and Lu, B. (2006). Integrin alpha v beta 3 antagonist Cilengitide enhances efficacy of radiotherapy in endothelial cell and non-small-cell lung cancer models. Int J Radiat Oncol Biol Phys *65*, 1536-1543.

Albuquerque, R.J., Hayashi, T., Cho, W.G., Kleinman, M.E., Dridi, S., Takeda, A., Baffi, J.Z., Yamada, K., Kaneko, H., Green, M.G., *et al.* (2009). Alternatively spliced vascular endothelial growth factor receptor-2 is an essential endogenous inhibitor of lymphatic vessel growth. Nat Med *15*, 1023-1030.

Altemeier, W.A., Schlesinger, S.Y., Buell, C.A., Brauer, R., Rapraeger, A.C., Parks, W.C., and Chen, P. (2012). The transmembrane and extracellular domains of syndecan-1 have distinct functions in regulating lung epithelial migration and adhesion. J Biol Chem.

Ambati, B.K., Nozaki, M., Singh, N., Takeda, A., Jani, P.D., Suthar, T., Albuquerque, R.J., Richter, E., Sakurai, E., Newcomb, M.T., *et al.* (2006). Corneal avascularity is due to soluble VEGF receptor-1. Nature *443*, 993-997.

Andersen, N.F., Standal, T., Nielsen, J.L., Heickendorff, L., Borset, M., Sorensen, F.B., and Abildgaard, N. (2005). Syndecan-1 and angiogenic cytokines in multiple myeloma: correlation with bone marrow angiogenesis and survival. Br J Haematol *128*, 210-217.

Andrian, E., Grenier, D., and Rouabhia, M. (2005). Porphyromonas gingivalis lipopolysaccharide induces shedding of syndecan-1 expressed by gingival epithelial cells. J Cell Physiol *204*, 178-183.

Arroyo, A.G., and Iruela-Arispe, M.L. (2010). Extracellular matrix, inflammation, and the angiogenic response. Cardiovasc Res *86*, 226-235.

Ashikari-Hada, S., Habuchi, H., Kariya, Y., and Kimata, K. (2005). Heparin regulates vascular endothelial growth factor165-dependent mitogenic activity, tube formation, and its receptor phosphorylation of human endothelial cells. Comparison of the effects of heparin and modified heparins. J Biol Chem *280*, 31508-31515.

Asundi, V.K., Erdman, R., Stahl, R.C., and Carey, D.J. (2003). Matrix metalloproteinase-dependent shedding of syndecan-3, a transmembrane heparan sulfate proteoglycan, in Schwann cells. J Neurosci Res *73*, 593-602.

Auguste, P., Gursel, D.B., Lemiere, S., Reimers, D., Cuevas, P., Carceller, F., Di Santo, J.P., and Bikfalvi, A. (2001). Inhibition of fibroblast growth factor/fibroblast growth factor receptor activity in glioma cells impedes tumor growth by both angiogenesis-dependent and -independent mechanisms. Cancer Res *61*, 1717-1726.

Augustin, H.G., Koh, G.Y., Thurston, G., and Alitalo, K. (2009). Control of vascular morphogenesis and homeostasis through the angiopoietin-Tie system. Nat Rev Mol Cell Biol *10*, 165-177.

Avraamides, C.J., Garmy-Susini, B., and Varner, J.A. (2008). Integrins in angiogenesis and lymphangiogenesis. Nature reviews Cancer *8*, 604-617.

Bachy, S., Letourneur, F., and Rousselle, P. (2008). Syndecan-1 interaction with the LG4/5 domain in laminin-332 is essential for keratinocyte migration. J Cell Physiol *214*, 238-249.

Baciu, P.C., and Goetinck, P.F. (1995). Protein kinase C regulates the recruitment of syndecan-4 into focal contacts. Mol Biol Cell *6*, 1503-1513.

Bader, B.L., Rayburn, H., Crowley, D., and Hynes, R.O. (1998). Extensive vasculogenesis, angiogenesis, and organogenesis precede lethality in mice lacking all alpha v integrins. Cell *95*, 507-519.

Baietti, M.F., Zhang, Z., Mortier, E., Melchior, A., Degeest, G., Geeraerts, A., Ivarsson, Y., Depoortere, F., Coomans, C., Vermeiren, E., *et al.* (2012). Syndecan-syntenin-ALIX regulates the biogenesis of exosomes. Nat Cell Biol *14*, 677-685.

Ballmer-Hofer, K., Andersson, A.E., Ratcliffe, L.E., and Berger, P. (2011). Neuropilin-1 promotes VEGFR-2 trafficking through Rab11 vesicles thereby specifying signal output. Blood *118*, 816-826.

Barbareschi, M., Maisonneuve, P., Aldovini, D., Cangi, M.G., Pecciarini, L., Angelo Mauri, F., Veronese, S., Caffo, O., Lucenti, A., Palma, P.D., *et al.* (2003). High syndecan-1 expression in breast carcinoma is related to an aggressive phenotype and to poorer prognosis. Cancer *98*, 474-483.

Barrett, P.J., Song, Y., Van Horn, W.D., Hustedt, E.J., Schafer, J.M., Hadziselimovic, A., Beel, A.J., and Sanders, C.R. (2012). The amyloid precursor protein has a flexible transmembrane domain and binds cholesterol. Science *336*, 1168-1171.

Barton, W.A., Tzvetkova-Robev, D., Miranda, E.P., Kolev, M.V., Rajashankar, K.R., Himanen, J.P., and Nikolov, D.B. (2006). Crystal structures of the Tie2 receptor ectodomain and the angiopoietin-2-Tie2 complex. Nat Struct Mol Biol *13*, 524-532.

Bass, M.D., Morgan, M.R., and Humphries, M.J. (2007a). Integrins and syndecan-4 make distinct, but critical, contributions to adhesion contact formation. Soft Matter *3*, 372-376.

Bass, M.D., Morgan, M.R., Roach, K.A., Settleman, J., Goryachev, A.B., and Humphries, M.J. (2008). p190RhoGAP is the convergence point of adhesion signals from alpha 5 beta 1 integrin and syndecan-4. J Cell Biol *181*, 1013-1026.

Bass, M.D., Roach, K.A., Morgan, M.R., Mostafavi-Pour, Z., Schoen, T., Muramatsu, T., Mayer, U., Ballestrem, C., Spatz, J.P., and Humphries, M.J. (2007b). Syndecan-4-dependent Rac1 regulation determines directional migration in response to the extracellular matrix. J Cell Biol *177*, 527-538.

Bass, M.D., Williamson, R.C., Nunan, R.D., Humphries, J.D., Byron, A., Morgan, M.R., Martin, P., and Humphries, M.J. (2011). A syndecan-4 hair trigger initiates wound healing through caveolin- and RhoG-regulated integrin endocytosis. Dev Cell *21*, 681-693.

Bastaki, M., Nelli, E.E., Dell'Era, P., Rusnati, M., Molinari-Tosatti, M.P., Parolini, S., Auerbach, R., Ruco, L.P., Possati, L., and Presta, M. (1997). Basic fibroblast growth factor-induced angiogenic phenotype in mouse endothelium. A study of aortic and microvascular endothelial cell lines. Arterioscler Thromb Vasc Biol *17*, 454-464.

Bax, D.V., Mahalingam, Y., Cain, S., Mellody, K., Freeman, L., Younger, K., Shuttleworth, C.A., Humphries, M.J., Couchman, J.R., and Kielty, C.M. (2007). Cell adhesion to fibrillin-1: identification of an Arg-Gly-Asp-dependent synergy region and a heparin-binding site that regulates focal adhesion formation. J Cell Sci *120*, 1383-1392.

Bayer-Garner, I.B., Sanderson, R.D., Dhodapkar, M.V., Owens, R.B., and Wilson, C.S. (2001). Syndecan-1 (CD138) immunoreactivity in bone marrow biopsies of multiple myeloma: shed syndecan-1 accumulates in fibrotic regions. Mod Pathol *14*, 1052-1058.

Beauvais, D.M., Burbach, B.J., and Rapraeger, A.C. (2004). The syndecan-1 ectodomain regulates alphavbeta3 integrin activity in human mammary carcinoma cells. J Cell Biol *167*, 171-181.

Beauvais, D.M., Ell, B.J., McWhorter, A.R., and Rapraeger, A.C. (2009). Syndecan-1 regulates alphavbeta3 and alphavbeta5 integrin activation during angiogenesis and is blocked by synstatin, a novel peptide inhibitor. J Exp Med *206*, 691-705.

Beauvais, D.M., and Rapraeger, A.C. (2003). Syndecan-1-mediated cell spreading requires signaling by alphavbeta3 integrins in human breast carcinoma cells. Exp Cell Res *286*, 219-232.

Beauvais, D.M., and Rapraeger, A.C. (2004). Syndecans in tumor cell adhesion and signaling. Reprod Biol Endocrinol *2*, 3.

Beauvais, D.M., and Rapraeger, A.C. (2010). Syndecan-1 couples the insulin-like growth factor-1 receptor to inside-out integrin activation. J Cell Sci *123*, 3796-3807.

Beekman, K.W., Colevas, A.D., Cooney, K., Dipaola, R., Dunn, R.L., Gross, M., Keller, E.T., Pienta, K.J., Ryan, C.J., Smith, D., *et al.* (2006). Phase II evaluations of cilengitide in asymptomatic patients with androgen-independent prostate cancer: scientific rationale and study design. Clin Genitourin Cancer *4*, 299-302.

Benjamin, L.E., Golijanin, D., Itin, A., Pode, D., and Keshet, E. (1999). Selective ablation of immature blood vessels in established human tumors follows vascular endothelial growth factor withdrawal. J Clin Invest *103*, 159-165.

Bernfield, M., Gotte, M., Park, P., Reizes, O., Fitzgerald, M., Lincecum, J., and Zako, M. (1999a). Functions of cell surface heparan sulfate proteoglycans. Annu Rev Biochem *68*, 729 - 777.

Bernfield, M., Gotte, M., Park, P.W., Reizes, O., Fitzgerald, M.L., Lincecum, J., and Zako, M. (1999b). Functions of cell surface heparan sulfate proteoglycans. Annu Rev Biochem *68*, 729-777.

Bertrand, J., Stange, R., Hidding, H., Echtermeyer, F., Nalesso, G., Godmann, L., Timmen, M., Bruckner, P., Dell'Accio, F., Raschke, M.J., *et al.* (2013). Syndecan 4 supports bone fracture repair, but not fetal skeletal development, in mice. Arthritis Rheum *65*, 743-752.

Bishop, J.R., Schuksz, M., and Esko, J.D. (2007). Heparan sulphate proteoglycans fine-tune mammalian physiology. Nature *446*, 1030-1037.

Blasi, F., and Carmeliet, P. (2002). uPAR: a versatile signalling orchestrator. Nat Rev Mol Cell Biol *3*, 932-943.

Bobardt, M., Saphire, A., Hung, H., Yu, X., Van der Schueren, B., Zhang, Z., David, G., and Gallay, P. (2003). Syndecan captures, protects, and transmits HIV to T lymphocytes. Immunity *1*, 27 - 39.

Borges, L.G., Seifert, R.A., Grant, F.J., Hart, C.E., Disteche, C.M., Edelhoff, S., Solca, F.F., Lieberman, M.A., Lindner, V., Fischer, E.H., *et al.* (1996). Cloning and characterization of rat density-enhanced phosphatase-1, a protein tyrosine phosphatase expressed by vascular cells. Circulation research *79*, 570-580.

Bradley, D.A., Daignault, S., Ryan, C.J., Dipaola, R.S., Cooney, K.A., Smith, D.C., Small, E., Mathew, P., Gross, M.E., Stein, M.N., *et al.* (2011). Cilengitide (EMD 121974, NSC 707544) in asymptomatic metastatic castration resistant prostate cancer patients: a randomized phase II trial by the prostate cancer clinical trials consortium. Invest New Drugs *29*, 1432-1440.

Brightling, C.E., Ammit, A.J., Kaur, D., Black, J.L., Wardlaw, A.J., Hughes, J.M., and Bradding, P. (2005). The CXCL10/CXCR3 axis mediates human lung mast cell migration to asthmatic airway smooth muscle. Am J Respir Crit Care Med *171*, 1103-1108.

Brkovic, A., Pelletier, M., Girard, D., and Sirois, M.G. (2007). Angiopoietin chemotactic activities on neutrophils are regulated by PI-3K activation. J Leukoc Biol *81*, 1093-1101.

Brooks, P., Clark, R., and Cheresh, D. (1994). Requirement of vascular integrin alpha v beta 3 for angiogenesis. Science *264*, 569-571.

Brooks, P.C., Klemke, R.L., Schon, S., Lewis, J.M., Schwartz, M.A., and Cheresh, D.A. (1997). Insulin-like growth factor receptor cooperates with integrin alpha v beta 5 to promote tumor cell dissemination in vivo. J Clin Invest *99*, 1390-1398.

Bullock, S.L., Fletcher, J.M., Beddington, R.S., and Wilson, V.A. (1998). Renal agenesis in mice homozygous for a gene trap mutation in the gene encoding heparan sulfate 2-sulfotransferase. Genes Dev *12*, 1894-1906.

Burbach, B.J., Friedl, A., Mundhenke, C., and Rapraeger, A.C. (2003). Syndecan-1 accumulates in lysosomes of poorly differentiated breast carcinoma cells. Matrix Biol *22*, 163-177.

Burbach, B.J., Ji, Y., and Rapraeger, A.C. (2004). Syndecan-1 ectodomain regulates matrix-dependent signaling in human breast carcinoma cells. Exp Cell Res *300*, 234-247.

Burri, P.H., Hlushchuk, R., and Djonov, V. (2004). Intussusceptive angiogenesis: its emergence, its characteristics, and its significance. Dev Dyn *231*, 474-488.

Burri, P.H., and Tarek, M.R. (1990). A novel mechanism of capillary growth in the rat pulmonary microcirculation. Anat Rec *228*, 35-45.

Burridge, K., Turner, C.E., and Romer, L.H. (1992). Tyrosine phosphorylation of paxillin and pp125FAK accompanies cell adhesion to extracellular matrix: a role in cytoskeletal assembly. J Cell Biol *119*, 893-903.

Burridge, K., and Wennerberg, K. (2004). Rho and Rac take center stage. Cell *116*, 167-179.
Caduff, J.H., Fischer, L.C., and Burri, P.H. (1986). Scanning electron microscope study of the developing microvasculature in the postnatal rat lung. Anat Rec *216*, 154-164.
Cao, R., Eriksson, A., Kubo, H., Alitalo, K., Cao, Y., and Thyberg, J. (2004). Comparative evaluation of FGF-2-, VEGF-A-, and VEGF-C-induced angiogenesis, lymphangiogenesis, vascular fenestrations, and permeability. Circulation research *94*, 664-670.
Carey, D.J. (1996). N-syndecan: structure and function of a transmembrane heparan sulfate proteoglycan. Perspect Dev Neurobiol *3*, 331-346.
Carmeliet, P., and Tessier-Lavigne, M. (2005). Common mechanisms of nerve and blood vessel wiring. Nature *436*, 193-200.
Castets, M., and Mehlen, P. (2010). Netrin-1 role in angiogenesis: to be or not to be a pro-angiogenic factor? Cell Cycle *9*, 1466-1471.
Chakravarti, R., and Adams, J. (2006). Comparative genomics of the syndecans defines an ancestral genomic context associated with matrilins in vertebrates. BMC Genomics *7*, 83.
Chaudhuri, P., Colles, S.M., Fox, P.L., and Graham, L.M. (2005). Protein kinase Cdelta-dependent phosphorylation of syndecan-4 regulates cell migration. Circ Res *97*, 674-681.
Chen, E., Hermanson, S., and Ekker, S. (2004a). Syndecan-2 is essential for angiogenic sprouting during zebrafish development. Blood *103*, 1710 - 1719.
Chen, E., Hermanson, S., and Ekker, S.C. (2004b). Syndecan-2 is essential for angiogenic sprouting during zebrafish development. Blood *103*, 1710-1719.
Chen, K., and Williams, K.J. (2013). Molecular mediators for raft-dependent endocytosis of syndecan-1, a highly conserved, multifunctional receptor. J Biol Chem *288*, 13988-13999.
Chen, L., Klass, C., and Woods, A. (2004c). Syndecan-2 regulates transforming growth factor-beta signaling. J Biol Chem *279*, 15715-15718.
Chen, Y., Gotte, M., Liu, J., and Park, P.W. (2008). Microbial subversion of heparan sulfate proteoglycans. Mol Cells *26*, 415-426.
Chiang, M.K., and Flanagan, J.G. (1995). Interactions between the Flk-1 receptor, vascular endothelial growth factor, and cell surface proteoglycan identified with a soluble receptor reagent. Growth Factors *12*, 1-10.
Choi, S., Kim, J.Y., Park, J.H., Lee, S.T., Han, I.O., and Oh, E.S. (2012). The matrix metalloproteinase-7 regulates the extracellular shedding of syndecan-2 from colon cancer cells. Biochem Biophys Res Commun *417*, 1260-1264.
Choi, Y., Kim, S., Lee, J., Ko, S.G., Lee, W., Han, I.O., Woods, A., and Oh, E.S. (2008). The oligomeric status of syndecan-4 regulates syndecan-4 interaction with alpha-actinin. Eur J Cell Biol *87*, 807-815.
Cianfrocca, M.E., Kimmel, K.A., Gallo, J., Cardoso, T., Brown, M.M., Hudes, G., Lewis, N., Weiner, L., Lam, G.N., Brown, S.C., *et al.* (2006). Phase 1 trial of the antiangiogenic peptide ATN-161 (Ac-PHSCN-NH(2)), a beta integrin antagonist, in patients with solid tumours. Br J Cancer *94*, 1621-1626.
Cizmeci-Smith, G., Langan, E., Youkey, J., Showalter, L., and Carey, D. (1997). Syndecan-4 is a primary-response gene induced by basic fibroblast growth factor and arterial injury in vascular smooth muscle cells. Arterioscler Thromb Vasc Biol *17*, 172 - 180.
Corti, F., Finetti, F., Ziche, M., and Simons, M. (2013). The syndecan-4/protein kinase Calpha pathway mediates prostaglandin E2-induced extracellular regulated kinase (ERK) activation in endothelial cells and angiogenesis in vivo. J Biol Chem *288*, 12712-12721.
Couchman, J.R. (2010). Transmembrane signaling proteoglycans. Annu Rev Cell Dev Biol *26*, 89-114.
Couchman, J.R., Hook, M., Rees, D.A., and Timpl, R. (1983). Adhesion, growth, and matrix production by fibroblasts on laminin substrates. J Cell Biol *96*, 177-183.
Couchman, J.R., and Woods, A. (1999). Syndecan-4 and integrins: combinatorial signaling in cell adhesion. J Cell Sci *112 (Pt 20)*, 3415-3420.
Crawford, Y., and Ferrara, N. (2009). Tumor and stromal pathways mediating refractoriness/resistance to anti-angiogenic therapies. Trends Pharmacol Sci *30*, 624-630.

Cross, M.J., and Claesson-Welsh, L. (2001). FGF and VEGF function in angiogenesis: signalling pathways, biological responses and therapeutic inhibition. Trends in Pharmacological Sciences *22*, 201-207.

David, G., Bai, X.M., Van der Schueren, B., Marynen, P., Cassiman, J.J., and Van den Berghe, H. (1993). Spatial and temporal changes in the expression of fibroglycan (syndecan-2) during mouse embryonic development. Development *119*, 841-854.

David, G., Danneels, A., Duerr, J., Grootjans, J., Mertens, G., Nackaerts, K., Romaris, M., Schrurs, B., Steinfeld, R., and Vekemans, S. (1995). Heparan sulfate proteoglycans. Essential co-factors in receptor-mediated processes with relevance to the biology of the vascular wall. Atherosclerosis *118 Suppl*, S57-67.

Daviet, I., Herbert, J.M., and Maffrand, J.P. (1990). Involvement of protein kinase C in the mitogenic and chemotaxis effects of basic fibroblast growth factor on bovine cerebral cortex capillary endothelial cells. FEBS Lett *259*, 315-317.

Davis, S., Aldrich, T.H., Jones, P.F., Acheson, A., Compton, D.L., Jain, V., Ryan, T.E., Bruno, J., Radziejewski, C., Maisonpierre, P.C., *et al.* (1996). Isolation of angiopoietin-1, a ligand for the TIE2 receptor, by secretion-trap expression cloning. Cell *87*, 1161-1169.

De Ceuninck, F., Allain, F., Caliez, A., Spik, G., and Vanhoutte, P.M. (2003). High binding capacity of cyclophilin B to chondrocyte heparan sulfate proteoglycans and its release from the cell surface by matrix metalloproteinases: possible role as a proinflammatory mediator in arthritis. Arthritis Rheum *48*, 2197-2206.

De Rossi, G., and Whiteford, J.R. (2013). A novel role for syndecan-3 in angiogenesis. F1000Res *2*, 270.

De Smet, F., Segura, I., De Bock, K., Hohensinner, P.J., and Carmeliet, P. (2009). Mechanisms of vessel branching: filopodia on endothelial tip cells lead the way. Arterioscler Thromb Vasc Biol *29*, 639-649.

Dedkov, E.I., Thomas, M.T., Sonka, M., Yang, F., Chittenden, T.W., Rhodes, J.M., Simons, M., Ritman, E.L., and Tomanek, R.J. (2007). Synectin/syndecan-4 regulate coronary arteriolar growth during development. Dev Dyn *236*, 2004-2010.

DeHahn, K.C., Gonzales, M., Gonzalez, A.M., Hopkinson, S.B., Chandel, N.S., Brunelle, J.K., and Jones, J.C. (2004). The alpha4 laminin subunit regulates endothelial cell survival. Exp Cell Res *294*, 281-289.

Dell'Era, P., Ronca, R., Coco, L., Nicoli, S., Metra, M., and Presta, M. (2003). Fibroblast growth factor receptor-1 is essential for in vitro cardiomyocyte development. Circ Res *93*, 414-420.

Denhez, F., Wilcox-Adelman, S.A., Baciu, P.C., Saoncella, S., Lee, S., French, B., Neveu, W., and Goetinck, P.F. (2002). Syndesmos, a syndecan-4 cytoplasmic domain interactor, binds to the focal adhesion adaptor proteins paxillin and Hic-5. J Biol Chem *277*, 12270-12274.

Derksen, P.W., Keehnen, R.M., Evers, L.M., van Oers, M.H., Spaargaren, M., and Pals, S.T. (2002). Cell surface proteoglycan syndecan-1 mediates hepatocyte growth factor binding and promotes Met signaling in multiple myeloma. Blood *99*, 1405-1410.

Dietrich, C.P., Nader, H.B., and Straus, A.H. (1983). Structural differences of heparan sulfates according to the tissue and species of origin. Biochem Biophys Res Commun *111*, 865-871.

Ding, K., Lopez-Burks, M., Sanchez-Duran, J.A., Korc, M., and Lander, A.D. (2005). Growth factor-induced shedding of syndecan-1 confers glypican-1 dependence on mitogenic responses of cancer cells. J Cell Biol *171*, 729-738.

Djonov, V., Baum, O., and Burri, P.H. (2003). Vascular remodeling by intussusceptive angiogenesis. Cell Tissue Res *314*, 107-117.

Djonov, V.G., Kurz, H., and Burri, P.H. (2002). Optimality in the developing vascular system: branching remodeling by means of intussusception as an efficient adaptation mechanism. Dev Dyn *224*, 391-402.

Do, M.K., Shimizu, N., Suzuki, T., Ohtsubo, H., Mizunoya, W., Nakamura, M., Sawano, S., Furuse, M., Ikeuchi, Y., Anderson, J.E., *et al.* (2015). Transmembrane proteoglycans

syndecan-2, 4, receptor candidates for the impact of HGF and FGF2 on semaphorin 3A expression in early-differentiated myoblasts. Physiol Rep *3*.

Dougher, A.M., Wasserstrom, H., Torley, L., Shridaran, L., Westdock, P., Hileman, R.E., Fromm, J.R., Anderberg, R., Lyman, S., Linhardt, R.J., *et al.* (1997). Identification of a heparin binding peptide on the extracellular domain of the KDR VEGF receptor. Growth Factors *14*, 257-268.

Dovas, A., and Couchman, J.R. (2005). RhoGDI: multiple functions in the regulation of Rho family GTPase activities. Biochem J *390*, 1-9.

Dumont, D.J., Jussila, L., Taipale, J., Lymboussaki, A., Mustonen, T., Pajusola, K., Breitman, M., and Alitalo, K. (1998). Cardiovascular failure in mouse embryos deficient in VEGF receptor-3. Science *282*, 946-949.

Dvorak, H.F., Harvey, V.S., Estrella, P., Brown, L.F., McDonagh, J., and Dvorak, A.M. (1987). Fibrin containing gels induce angiogenesis. Implications for tumor stroma generation and wound healing. Lab Invest *57*, 673-686.

Dyer, L.A., and Patterson, C. (2010). Development of the endothelium: an emphasis on heterogeneity. Semin Thromb Hemost *36*, 227-235.

Eble, J.A., and Niland, S. (2009). The extracellular matrix of blood vessels. Curr Pharm Des *15*, 1385-1400.

Echtermeyer, F., Baciu, P.C., Saoncella, S., Ge, Y., and Goetinck, P.F. (1999). Syndecan-4 core protein is sufficient for the assembly of focal adhesions and actin stress fibers. J Cell Sci *112 (Pt 20)*, 3433-3441.

Echtermeyer, F., Streit, M., Wilcox-Adelman, S., Saoncella, S., Denhez, F., Detmar, M., and Goetinck, P. (2001a). Delayed wound repair and impaired angiogenesis in mice lacking syndecan-4. J Clin Invest *107*, R9 - R14.

Echtermeyer, F., Streit, M., Wilcox-Adelman, S., Saoncella, S., Denhez, F., Detmar, M., and Goetinck, P. (2001b). Delayed wound repair and impaired angiogenesis in mice lacking syndecan-4. J Clin Invest *107*, R9-R14.

Eilken, H.M., and Adams, R.H. (2010). Dynamics of endothelial cell behavior in sprouting angiogenesis. Current opinion in cell biology *22*, 617-625.

Elfenbein, A., Rhodes, J.M., Meller, J., Schwartz, M.A., Matsuda, M., and Simons, M. (2009). Suppression of RhoG activity is mediated by a syndecan 4-synectin-RhoGDI1 complex and is reversed by PKCalpha in a Rac1 activation pathway. J Cell Biol *186*, 75-83.

Eliceiri, B.P., Paul, R., Schwartzberg, P.L., Hood, J.D., Leng, J., and Cheresh, D.A. (1999). Selective requirement for Src kinases during VEGF-induced angiogenesis and vascular permeability. Mol Cell *4*, 915-924.

Endo, K., Takino, T., Miyamori, H., Kinsen, H., Yoshizaki, T., Furukawa, M., and Sato, H. (2003). Cleavage of syndecan-1 by membrane type matrix metalloproteinase-1 stimulates cell migration. J Biol Chem *278*, 40764-40770.

Ethell, I.M., Hagihara, K., Miura, Y., Irie, F., and Yamaguchi, Y. (2000). Synbindin, A novel syndecan-2-binding protein in neuronal dendritic spines. J Cell Biol *151*, 53-68.

Ethell, I.M., and Yamaguchi, Y. (1999). Cell surface heparan sulfate proteoglycan syndecan-2 induces the maturation of dendritic spines in rat hippocampal neurons. J Cell Biol *144*, 575-586.

Fantin, A., Maden, C.H., and Ruhrberg, C. (2009). Neuropilin ligands in vascular and neuronal patterning. Biochem Soc Trans *37*, 1228-1232.

Fantin, A., Vieira, J.M., Gestri, G., Denti, L., Schwarz, Q., Prykhozhij, S., Peri, F., Wilson, S.W., and Ruhrberg, C. (2010). Tissue macrophages act as cellular chaperones for vascular anastomosis downstream of VEGF-mediated endothelial tip cell induction. Blood *116*, 829-840.

Faull, R.J., Kovach, N.L., Harlan, J.M., and Ginsberg, M.H. (1994). Stimulation of integrin-mediated adhesion of T lymphocytes and monocytes: two mechanisms with divergent biological consequences. J Exp Med *179*, 1307-1316.

Fears, C.Y., Gladson, C.L., and Woods, A. (2006). Syndecan-2 is expressed in the microvasculature of gliomas and regulates angiogenic processes in microvascular endothelial cells. J Biol Chem *281*, 14533-14536.

Ferrara, N., and Henzel, W.J. (1989). Pituitary follicular cells secrete a novel heparin-binding growth factor specific for vascular endothelial cells. Biochemical and Biophysical Research Communications *161*, 851-858.

Filla, M.S., Dam, P., and Rapraeger, A.C. (1998). The cell surface proteoglycan syndecan-1 mediates fibroblast growth factor-2 binding and activity. J Cell Physiol *174*, 310-321.

Fitzgerald, M.L., Wang, Z., Park, P.W., Murphy, G., and Bernfield, M. (2000). Shedding of syndecan-1 and -4 ectodomains is regulated by multiple signaling pathways and mediated by a TIMP-3-sensitive metalloproteinase. J Cell Biol *148*, 811-824.

Folkman, J. (1971). Tumor angiogenesis: therapeutic implications. N Engl J Med *285*, 1182-1186.

Fong, G.H., Rossant, J., Gertsenstein, M., and Breitman, M.L. (1995). Role of the Flt-1 receptor tyrosine kinase in regulating the assembly of vascular endothelium. Nature *376*, 66-70.

Foubert, P., and Varner, J.A. (2012). Integrins in tumor angiogenesis and lymphangiogenesis. Methods Mol Biol *757*, 471-486.

Francis, S.E., Goh, K.L., Hodivala-Dilke, K., Bader, B.L., Stark, M., Davidson, D., and Hynes, R.O. (2002). Central roles of alpha5beta1 integrin and fibronectin in vascular development in mouse embryos and embryoid bodies. Arterioscler Thromb Vasc Biol *22*, 927-933.

Freissler, E., Meyer auf der Heyde, A., David, G., Meyer, T.F., and Dehio, C. (2000). Syndecan-1 and syndecan-4 can mediate the invasion of OpaHSPG-expressing Neisseria gonorrhoeae into epithelial cells. Cell Microbiol *2*, 69-82.

Friess, H., Langrehr, J.M., Oettle, H., Raedle, J., Niedergethmann, M., Dittrich, C., Hossfeld, D.K., Stoger, H., Neyns, B., Herzog, P., *et al.* (2006). A randomized multi-center phase II trial of the angiogenesis inhibitor Cilengitide (EMD 121974) and gemcitabine compared with gemcitabine alone in advanced unresectable pancreatic cancer. BMC Cancer *6*, 285.

Gabler, C., Plath-Gabler, A., Killian, G.J., Berisha, B., and Schams, D. (2004). Expression pattern of fibroblast growth factor (FGF) and vascular endothelial growth factor (VEGF) system members in bovine corpus luteum endothelial cells during treatment with FGF-2, VEGF or oestradiol. Reprod Domest Anim *39*, 321-327.

Gaengel, K., Genove, G., Armulik, A., and Betsholtz, C. (2009). Endothelial-mural cell signaling in vascular development and angiogenesis. Arterioscler Thromb Vasc Biol *29*, 630-638.

Gallagher, J.T., Lyon, M., and Steward, W.P. (1986). Structure and function of heparan sulphate proteoglycans. Biochem J *236*, 313-325.

Gallagher, J.T., Turnbull, J.E., and Lyon, M. (1992). Patterns of sulphation in heparan sulphate: polymorphism based on a common structural theme. Int J Biochem *24*, 553-560.

Gallo, R., Kim, C., Kokenyesi, R., Adzick, N.S., and Bernfield, M. (1996a). Syndecans-1 and -4 are induced during wound repair of neonatal but not fetal skin. J Invest Dermatol *107*, 676-683.

Gallo, R., Kim, C., Kokenyesi, R., Adzick, N.S., and Bernfield, M. (1996b). Syndecans-1 and -4 are induced during wound repair of neonatal but not fetal skin. J Invest Dermatol *107*, 676-683.

Gamble, J.R., Drew, J., Trezise, L., Underwood, A., Parsons, M., Kasminkas, L., Rudge, J., Yancopoulos, G., and Vadas, M.A. (2000). Angiopoietin-1 is an antipermeability and anti-inflammatory agent in vitro and targets cell junctions. Circ Res *87*, 603-607.

Gao, Y., Li, M., Chen, W., and Simons, M. (2000). Synectin, syndecan-4 cytoplasmic domain binding PDZ protein, inhibits cell migration. J Cell Physiol *184*, 373-379.

George, E.L., Georges-Labouesse, E.N., Patel-King, R.S., Rayburn, H., and Hynes, R.O. (1993). Defects in mesoderm, neural tube and vascular development in mouse embryos lacking fibronectin. Development *119*, 1079-1091.

Gerber, H.P., Dixit, V., and Ferrara, N. (1998a). Vascular endothelial growth factor induces expression of the antiapoptotic proteins Bcl-2 and A1 in vascular endothelial cells. J Biol Chem *273*, 13313-13316.

Gerber, H.P., Hillan, K.J., Ryan, A.M., Kowalski, J., Keller, G.A., Rangell, L., Wright, B.D., Radtke, F., Aguet, M., and Ferrara, N. (1999). VEGF is required for growth and survival in neonatal mice. Development *126*, 1149-1159.

Gerber, H.P., McMurtrey, A., Kowalski, J., Yan, M., Keyt, B.A., Dixit, V., and Ferrara, N. (1998b). Vascular endothelial growth factor regulates endothelial cell survival through the phosphatidylinositol 3'-kinase/Akt signal transduction pathway. Requirement for Flk-1/KDR activation. J Biol Chem *273*, 30336-30343.

Gerhardt, H., Golding, M., Fruttiger, M., Ruhrberg, C., Lundkvist, A., Abramsson, A., Jeltsch, M., Mitchell, C., Alitalo, K., Shima, D., *et al.* (2003). VEGF guides angiogenic sprouting utilizing endothelial tip cell filopodia. J Cell Biol *161*, 1163-1177.

Gerhardt, H., Ruhrberg, C., Abramsson, A., Fujisawa, H., Shima, D., and Betsholtz, C. (2004). Neuropilin-1 is required for endothelial tip cell guidance in the developing central nervous system. Dev Dyn *231*, 503-509.

Ghossoub, R., Lembo, F., Rubio, A., Gaillard, C.B., Bouchet, J., Vitale, N., Slavik, J., Machala, M., and Zimmermann, P. (2014). Syntenin-ALIX exosome biogenesis and budding into multivesicular bodies are controlled by ARF6 and PLD2. Nature communications *5*, 3477.

Goel, S., Duda, D.G., Xu, L., Munn, L.L., Boucher, Y., Fukumura, D., and Jain, R.K. (2011). Normalization of the vasculature for treatment of cancer and other diseases. Physiol Rev *91*, 1071-1121.

Goger, B., Halden, Y., Rek, A., Mosl, R., Pye, D., Gallagher, J., and Kungl, A.J. (2002). Different affinities of glycosaminoglycan oligosaccharides for monomeric and dimeric interleukin-8: a model for chemokine regulation at inflammatory sites. Biochemistry *41*, 1640-1646.

Gopal, S., Bober, A., Whiteford, J.R., Multhaupt, H.A., Yoneda, A., and Couchman, J.R. (2010). Heparan sulfate chain valency controls syndecan-4 function in cell adhesion. J Biol Chem *285*, 14247-14258.

Gordts, P.L., and Esko, J.D. (2015). Heparan sulfate proteoglycans fine-tune macrophage inflammation via IFN-beta. Cytokine *72*, 118-119.

Gotte, M., Joussen, A.M., Klein, C., Andre, P., Wagner, D.D., Hinkes, M.T., Kirchhof, B., Adamis, A.P., and Bernfield, M. (2002). Role of syndecan-1 in leukocyte-endothelial interactions in the ocular vasculature. Invest Ophthalmol Vis Sci *43*, 1135-1141.

Grazia Lampugnani, M., Zanetti, A., Corada, M., Takahashi, T., Balconi, G., Breviario, F., Orsenigo, F., Cattelino, A., Kemler, R., Daniel, T.O., *et al.* (2003). Contact inhibition of VEGF-induced proliferation requires vascular endothelial cadherin, beta-catenin, and the phosphatase DEP-1/CD148. The Journal of cell biology *161*, 793-804.

Greene, D.K., Tumova, S., Couchman, J.R., and Woods, A. (2003). Syndecan-4 associates with alpha-actinin. J Biol Chem *278*, 7617-7623.

Gridley, T. (2010). Notch signaling in the vasculature. Curr Top Dev Biol *92*, 277-309.

Grootjans, J.J., Zimmermann, P., Reekmans, G., Smets, A., Degeest, G., Durr, J., and David, G. (1997). Syntenin, a PDZ protein that binds syndecan cytoplasmic domains. Proc Natl Acad Sci U S A *94*, 13683-13688.

Grunstein, J., Masbad, J.J., Hickey, R., Giordano, F., and Johnson, R.S. (2000). Isoforms of vascular endothelial growth factor act in a coordinate fashion To recruit and expand tumor vasculature. Molecular and cellular biology *20*, 7282-7291.

Guarani, V., Deflorian, G., Franco, C.A., Kruger, M., Phng, L.K., Bentley, K., Toussaint, L., Dequiedt, F., Mostoslavsky, R., Schmidt, M.H., *et al.* (2011). Acetylation-dependent regulation of endothelial Notch signalling by the SIRT1 deacetylase. Nature *473*, 234-238.

Guerrin, M., Moukadiri, H., Chollet, P., Moro, F., Dutt, K., Malecaze, F., and Plouet, J. (1995). Vasculotropin/vascular endothelial growth factor is an autocrine growth factor for human retinal pigment epithelial cells cultured in vitro. J Cell Physiol *164*, 385-394.

Gulyas, M., and Hjerpe, A. (2003). Proteoglycans and WT1 as markers for distinguishing adenocarcinoma, epithelioid mesothelioma, and benign mesothelium. The Journal of Pathology *199*, 479-487.

Gutheil, J.C., Campbell, T.N., Pierce, P.R., Watkins, J.D., Huse, W.D., Bodkin, D.J., and Cheresh, D.A. (2000). Targeted antiangiogenic therapy for cancer using Vitaxin: a humanized monoclonal antibody to the integrin alphavbeta3. Clin Cancer Res *6*, 3056-3061.

Halden, Y., Rek, A., Atzenhofer, W., Szilak, L., Wabnig, A., and Kungl, A.J. (2004). Interleukin-8 binds to syndecan-2 on human endothelial cells. Biochem J *377*, 533-538.

Hammes, H.P., Brownlee, M., Jonczyk, A., Sutter, A., and Preissner, K.T. (1996). Subcutaneous injection of a cyclic peptide antagonist of vitronectin receptor-type integrins inhibits retinal neovascularization. Nat Med *2*, 529-533.

Han, I., Park, H., and Oh, E.S. (2004). New insights into syndecan-2 expression and tumourigenic activity in colon carcinoma cells. J Mol Histol *35*, 319-326.

Hansen, T.M., Singh, H., Tahir, T.A., and Brindle, N.P. (2010). Effects of angiopoietins-1 and -2 on the receptor tyrosine kinase Tie2 are differentially regulated at the endothelial cell surface. Cell Signal *22*, 527-532.

Hayashida, K., Parks, W.C., and Park, P.W. (2009). Syndecan-1 shedding facilitates the resolution of neutrophilic inflammation by removing sequestered CXC chemokines. Blood *114*, 3033-3043.

Hayashida, K., Stahl, P.D., and Park, P.W. (2008). Syndecan-1 ectodomain shedding is regulated by the small GTPase Rab5. J Biol Chem *283*, 35435-35444.

Heier, J.S., Brown, D.M., Chong, V., Korobelnik, J.F., Kaiser, P.K., Nguyen, Q.D., Kirchhof, B., Ho, A., Ogura, Y., Yancopoulos, G.D., *et al.* (2012). Intravitreal aflibercept (VEGF trap-eye) in wet age-related macular degeneration. Ophthalmology. *119*, 2537-48

Hersey, P., Sosman, J., O'Day, S., Richards, J., Bedikian, A., Gonzalez, R., Sharfman, W., Weber, R., Logan, T., Buzoianu, M., *et al.* (2010). A randomized phase 2 study of etaracizumab, a monoclonal antibody against integrin alpha(v)beta(3), + or - dacarbazine in patients with stage IV metastatic melanoma. Cancer *116*, 1526-1534.

Hienola, A., Tumova, S., Kulesskiy, E., and Rauvala, H. (2006). N-syndecan deficiency impairs neural migration in brain. J Cell Biol *174*, 569-580.

Hilgard, P., and Stockert, R. (2000). Heparan sulfate proteoglycans initiate dengue virus infection of hepatocytes. Hepatology *32*, 1069-1077.

Hogan, B.L., and Kolodziej, P.A. (2002). Organogenesis: molecular mechanisms of tubulogenesis. Nature reviews Genetics *3*, 513-523.

Holen, I., Drury, N.L., Hargreaves, P.G., and Croucher, P.I. (2001). Evidence of a role for a non-matrix-type metalloproteinase activity in the shedding of syndecan-1 from human myeloma cells. Br J Haematol *114*, 414-421.

Hori, S., Ohtsuki, S., Hosoya, K., Nakashima, E., and Terasaki, T. (2004). A pericyte-derived angiopoietin-1 multimeric complex induces occludin gene expression in brain capillary endothelial cells through Tie-2 activation in vitro. J Neurochem *89*, 503-513.

Horowitz, A., Murakami, M., Gao, Y., and Simons, M. (1999). Phosphatidylinositol-4,5-bisphosphate mediates the interaction of syndecan-4 with protein kinase C. Biochemistry *38*, 15871-15877.

Horowitz, A., and Simons, M. (1998). Phosphorylation of the cytoplasmic tail of syndecan-4 regulates activation of protein kinase Calpha. J Biol Chem *273*, 25548-25551.

Houck, K.A., Ferrara, N., Winer, J., Cachianes, G., Li, B., and Leung, D.W. (1991). The vascular endothelial growth factor family: identification of a fourth molecular species and characterization of alternative splicing of RNA. Molecular endocrinology *5*, 1806-1814.

Houck, K.A., Leung, D.W., Rowland, A.M., Winer, J., and Ferrara, N. (1992). Dual regulation of vascular endothelial growth factor bioavailability by genetic and proteolytic mechanisms. J Biol Chem *267*, 26031-26037.

Huang, H., Bhat, A., Woodnutt, G., and Lappe, R. (2010). Targeting the ANGPT-TIE2 pathway in malignancy. Nat Rev Cancer *10*, 575-585.

Huang, J., Bae, J.O., Tsai, J.P., Kadenhe-Chiweshe, A., Papa, J., Lee, A., Zeng, S., Kornfeld, Z.N., Ullner, P., Zaghloul, N., *et al.* (2009). Angiopoietin-1/Tie-2 activation contributes to vascular survival and tumor growth during VEGF blockade. Int J Oncol *34*, 79-87.

Hynes, R.O. (2002). Integrins: bidirectional, allosteric signaling machines. Cell *110*, 673-687.

Imhof, B.A., and Aurrand-Lions, M. (2006). Angiogenesis and inflammation face off. Nature medicine *12*, 171-172.

Inki, P., Joensuu, H., Grenman, R., Klemi, P., and Jalkanen, M. (1994a). Association between syndecan-1 expression and clinical outcome in squamous cell carcinoma of the head and neck. Br J Cancer *70*, 319-323.

Inki, P., Larjava, H., Haapasalmi, K., Miettinen, H.M., Grenman, R., and Jalkanen, M. (1994b). Expression of syndecan-1 is induced by differentiation and suppressed by malignant transformation of human keratinocytes. Eur J Cell Biol *63*, 43-51.

Inki, P., Stenback, F., Grenman, S., and Jalkanen, M. (1994c). Immunohistochemical localization of syndecan-1 in normal and pathological human uterine cervix. J Pathol *172*, 349-355.

Iozzo, R.V. (2005). Basement membrane proteoglycans: from cellar to ceiling. Nat Rev Mol Cell Biol *6*, 646-656.

Iruela-Arispe, M.L., and Davis, G.E. (2009). Cellular and molecular mechanisms of vascular lumen formation. Dev Cell *16*, 222-231.

Ishiguro, K., Kadomatsu, K., Kojima, T., Muramatsu, H., Nakamura, E., Ito, M., Nagasaka, T., Kobayashi, H., Kusugami, K., Saito, H., *et al.* (2000a). Syndecan-4 deficiency impairs the fetal vessels in the placental labyrinth. Dev Dyn *219*, 539-544.

Ishiguro, K., Kadomatsu, K., Kojima, T., Muramatsu, H., Nakamura, E., Ito, M., Nagasaka, T., Kobayashi, H., Kusugami, K., Saito, H., *et al.* (2000b). Syndecan-4 deficiency impairs the fetal vessels in the placental labyrinth. Developmental dynamics : an official publication of the American Association of Anatomists *219*, 539-544.

Iurlaro, M., Scatena, M., Zhu, W.H., Fogel, E., Wieting, S.L., and Nicosia, R.F. (2003). Rat aorta-derived mural precursor cells express the Tie2 receptor and respond directly to stimulation by angiopoietins. J Cell Sci *116*, 3635-3643.

Jain, R.K. (2003). Molecular regulation of vessel maturation. Nat Med *9*, 685-693.

Jain, R.K. (2005). Normalization of tumor vasculature: an emerging concept in antiangiogenic therapy. Science *307*, 58-62.

Jakobsson, L., Franco, C.A., Bentley, K., Collins, R.T., Ponsioen, B., Aspalter, I.M., Rosewell, I., Busse, M., Thurston, G., Medvinsky, A., *et al.* (2010). Endothelial cells dynamically compete for the tip cell position during angiogenic sprouting. Nat Cell Biol *12*, 943-953.

Jakobsson, L., Kreuger, J., Holmborn, K., Lundin, L., Eriksson, I., Kjellen, L., and Claesson-Welsh, L. (2006). Heparan sulfate in trans potentiates VEGFR-mediated angiogenesis. Dev Cell *10*, 625-634.

Jang, E., Albadawi, H., Watkins, M.T., Edelman, E.R., and Baker, A.B. (2012). Syndecan-4 proteoliposomes enhance fibroblast growth factor-2 (FGF-2)-induced proliferation, migration, and neovascularization of ischemic muscle. Proc Natl Acad Sci U S A *109*, 1679-1684.

Javerzat, S., Auguste, P., and Bikfalvi, A. (2002). The role of fibroblast growth factors in vascular development. Trends Mol Med *8*, 483-489.

Jones, N., Chen, S.H., Sturk, C., Master, Z., Tran, J., Kerbel, R.S., and Dumont, D.J. (2003). A unique autophosphorylation site on Tie2/Tek mediates Dok-R phosphotyrosine binding domain binding and function. Mol Cell Biol *23*, 2658-2668.

Kaji, T., Yamamoto, C., Oh-i, M., Fujiwara, Y., Yamazaki, Y., Morita, T., Plaas, A.H., and Wight, T.N. (2006). The vascular endothelial growth factor VEGF165 induces perlecan synthesis via VEGF receptor-2 in cultured human brain microvascular endothelial cells. Biochim Biophys Acta *1760*, 1465-1474.

Kanno, S., Oda, N., Abe, M., Terai, Y., Ito, M., Shitara, K., Tabayashi, K., Shibuya, M., and Sato, Y. (2000). Roles of two VEGF receptors, Flt-1 and KDR, in the signal transduction of VEGF effects in human vascular endothelial cells. Oncogene *19*, 2138-2146.

Karar, J., and Maity, A. (2011). PI3K/AKT/mTOR Pathway in Angiogenesis. Front Mol Neurosci *4*, 51.

Kawamura, H., Li, X., Goishi, K., van Meeteren, L.A., Jakobsson, L., Cebe-Suarez, S., Shimizu, A., Edholm, D., Ballmer-Hofer, K., Kjellen, L., *et al.* (2008). Neuropilin-1 in regulation of VEGF-induced activation of p38MAPK and endothelial cell organization. Blood *112*, 3638-3649.

Kawasaki, T., Kitsukawa, T., Bekku, Y., Matsuda, Y., Sanbo, M., Yagi, T., and Fujisawa, H. (1999). A requirement for neuropilin-1 in embryonic vessel formation. Development *126*, 4895-4902.

Keane, M.M., Lowrey, G.A., Ettenberg, S.A., Dayton, M.A., and Lipkowitz, S. (1996). The protein tyrosine phosphatase DEP-1 is induced during differentiation and inhibits growth of breast cancer cells. Cancer Res *56*, 4236-4243.

Keck, P.J., Hauser, S.D., Krivi, G., Sanzo, K., Warren, T., Feder, J., and Connolly, D.T. (1989). Vascular permeability factor, an endothelial cell mitogen related to PDGF. Science *246*, 1309-1312.

Kehoe, O., Kalia, N., King, S., Eustace, A., Boyes, C., Reizes, O., Williams, A., Patterson, A., and Middleton, J. (2014). Syndecan-3 is selectively pro-inflammatory in the joint and contributes to antigen-induced arthritis in mice. Arthritis research & therapy *16*, R148.

Keum, E., Kim, Y., Kim, J., Kwon, S., Lim, Y., Han, I., and Oh, E.S. (2004). Syndecan-4 regulates localization, activity and stability of protein kinase C-alpha. Biochem J *378*, 1007-1014.

Keyt, B.A., Berleau, L.T., Nguyen, H.V., Chen, H., Heinsohn, H., Vandlen, R., and Ferrara, N. (1996). The carboxyl-terminal domain (111-165) of vascular endothelial growth factor is critical for its mitogenic potency. J Biol Chem *271*, 7788-7795.

Khaibullina, A.A., Rosenstein, J.M., and Krum, J.M. (2004). Vascular endothelial growth factor promotes neurite maturation in primary CNS neuronal cultures. Brain Res Dev Brain Res *148*, 59-68.

Kim, H.Z., Jung, K., Kim, H.M., Cheng, Y., and Koh, G.Y. (2009). A designed angiopoietin-2 variant, pentameric COMP-Ang2, strongly activates Tie2 receptor and stimulates angiogenesis. Biochim Biophys Acta *1793*, 772-780.

Kim, I., Kim, H.G., Moon, S.O., Chae, S.W., So, J.N., Koh, K.N., Ahn, B.C., and Koh, G.Y. (2000a). Angiopoietin-1 induces endothelial cell sprouting through the activation of focal adhesion kinase and plasmin secretion. Circ Res *86*, 952-959.

Kim, I., Moon, S.O., Park, S.K., Chae, S.W., and Koh, G.Y. (2001). Angiopoietin-1 reduces VEGF-stimulated leukocyte adhesion to endothelial cells by reducing ICAM-1, VCAM-1, and E-selectin expression. Circ Res *89*, 477-479.

Kim, J., Oh, W.J., Gaiano, N., Yoshida, Y., and Gu, C. (2011). Semaphorin 3E-Plexin-D1 signaling regulates VEGF function in developmental angiogenesis via a feedback mechanism. Genes Dev *25*, 1399-1411.

Kim, K.T., Choi, H.H., Steinmetz, M.O., Maco, B., Kammerer, R.A., Ahn, S.Y., Kim, H.Z., Lee, G.M., and Koh, G.Y. (2005). Oligomerization and multimerization are critical for angiopoietin-1 to bind and phosphorylate Tie2. J Biol Chem *280*, 20126-20131.

Kim, S., Bell, K., Mousa, S.A., and Varner, J.A. (2000b). Regulation of angiogenesis in vivo by ligation of integrin alpha5beta1 with the central cell-binding domain of fibronectin. Am J Pathol *156*, 1345-1362.

Kinnunen, T., Kaksonen, M., Saarinen, J., Kalkkinen, N., Peng, H.B., and Rauvala, H. (1998). Cortactin-Src kinase signaling pathway is involved in N-syndecan-dependent neurite outgrowth. J Biol Chem *273*, 10702-10708.

Kiselyov, A., Balakin, K.V., and Tkachenko, S.E. (2007). VEGF/VEGFR signalling as a target for inhibiting angiogenesis. Expert Opin Investig Drugs *16*, 83-107.

Kliment, C.R., Englert, J.M., Gochuico, B.R., Yu, G., Kaminski, N., Rosas, I., and Oury, T.D. (2009). Oxidative stress alters syndecan-1 distribution in lungs with pulmonary fibrosis. J Biol Chem *284*, 3537-3545.

Kliment, C.R., and Oury, T.D. (2011). Extracellular superoxide dismutase protects cardiovascular syndecan-1 from oxidative shedding. Free Radic Biol Med *50*, 1075-1080.

Koblizek, T.I., Weiss, C., Yancopoulos, G.D., Deutsch, U., and Risau, W. (1998). Angiopoietin-1 induces sprouting angiogenesis in vitro. Curr Biol *8*, 529-532.

Koch, A.W., Mathivet, T., Larrivee, B., Tong, R.K., Kowalski, J., Pibouin-Fragner, L., Bouvree, K., Stawicki, S., Nicholes, K., Rathore, N., *et al.* (2011). Robo4 maintains vessel integrity and inhibits angiogenesis by interacting with UNC5B. Dev Cell *20*, 33-46.

Kofler, N.M., Cuervo, H., Uh, M.K., Murtomaki, A., and Kitajewski, J. (2015). Combined deficiency of Notch1 and Notch3 causes pericyte dysfunction, models CADASIL, and results in arteriovenous malformations. Sci Rep *5*, 16449.

Kojima, T., Leone, C.W., Marchildon, G.A., Marcum, J.A., and Rosenberg, R.D. (1992a). Isolation and characterization of heparan sulfate proteoglycans produced by cloned rat microvascular endothelial cells. J Biol Chem *267*, 4859-4869.

Kojima, T., Shworak, N.W., and Rosenberg, R.D. (1992b). Molecular cloning and expression of two distinct cDNA-encoding heparan sulfate proteoglycan core proteins from a rat endothelial cell line. J Biol Chem *267*, 4870-4877.

Konisti, S., Kiriakidis, S., and Paleolog, E.M. (2012). Hypoxia--a key regulator of angiogenesis and inflammation in rheumatoid arthritis. Nat Rev Rheumatol *8*, 153-162.

Koo, B.K., Jung, Y.S., Shin, J., Han, I., Mortier, E., Zimmermann, P., Whiteford, J.R., Couchman, J.R., Oh, E.S., and Lee, W. (2006). Structural basis of syndecan-4 phosphorylation as a molecular switch to regulate signaling. J Mol Biol *355*, 651-663.

Kosacka, J., Figiel, M., Engele, J., Hilbig, H., Majewski, M., and Spanel-Borowski, K. (2005). Angiopoietin-1 promotes neurite outgrowth from dorsal root ganglion cells positive for Tie-2 receptor. Cell Tissue Res *320*, 11-19.

Kramer, K.L., and Yost, H.J. (2002). Ectodermal syndecan-2 mediates left-right axis formation in migrating mesoderm as a cell-nonautonomous Vg1 cofactor. Dev Cell *2*, 115-124.

Krilleke, D., DeErkenez, A., Schubert, W., Giri, I., Robinson, G.S., Ng, Y.S., and Shima, D.T. (2007). Molecular mapping and functional characterization of the VEGF164 heparin-binding domain. J Biol Chem *282*, 28045-28056.

Krueger, J., Liu, D., Scholz, K., Zimmer, A., Shi, Y., Klein, C., Siekmann, A., Schulte-Merker, S., Cudmore, M., Ahmed, A., *et al.* (2011). Flt1 acts as a negative regulator of tip cell formation and branching morphogenesis in the zebrafish embryo. Development *138*, 2111-2120.

Kurihara, T., Westenskow, P.D., Bravo, S., Aguilar, E., and Friedlander, M. (2012). Targeted deletion of Vegfa in adult mice induces vision loss. J Clin Invest *122*, 4213-4217.

Kurz, H., Burri, P.H., and Djonov, V.G. (2003). Angiogenesis and vascular remodeling by intussusception: from form to function. News Physiol Sci *18*, 65-70.

Kuwada, S.K. (2007). Drug evaluation: Volociximab, an angiogenesis-inhibiting chimeric monoclonal antibody. Curr Opin Mol Ther *9*, 92-98.

Kwak, H.J., Lee, S.J., Lee, Y.H., Ryu, C.H., Koh, K.N., Choi, H.Y., and Koh, G.Y. (2000). Angiopoietin-1 inhibits irradiation- and mannitol-induced apoptosis in endothelial cells. Circulation *101*, 2317-2324.

Lamalice, L., Le Boeuf, F., and Huot, J. (2007). Endothelial Cell Migration During Angiogenesis. Circ Res *100*, 782-794.

Landgren, E., Klint, P., Yokote, K., and Claesson-Welsh, L. (1998a). Fibroblast growth factor receptor-1 mediates chemotaxis independently of direct SH2-domain protein binding. Oncogene *17*, 283-291.

Landgren, E., Schiller, P., Cao, Y., and Claesson-Welsh, L. (1998b). Placenta growth factor stimulates MAP kinase and mitogenicity but not phospholipase C-gamma and migration of endothelial cells expressing Flt 1. Oncogene *16*, 359-367.

Langford, J.K., Yang, Y., Kieber-Emmons, T., and Sanderson, R.D. (2005). Identification of an invasion regulatory domain within the core protein of syndecan-1. J Biol Chem *280*, 3467-3473.

Larrivee, B., Freitas, C., Suchting, S., Brunet, I., and Eichmann, A. (2009). Guidance of vascular development: lessons from the nervous system. Circ Res *104*, 428-441.

Larrivee, B., and Karsan, A. (2000). Signaling pathways induced by vascular endothelial growth factor (review). Int J Mol Med *5*, 447-456.

Lebakken, C.S., and Rapraeger, A.C. (1996). Syndecan-1 mediates cell spreading in transfected human lymphoblastoid (Raji) cells. J Cell Biol *132*, 1209-1221.

Lee, P., Goishi, K., Davidson, A.J., Mannix, R., Zon, L., and Klagsbrun, M. (2002). Neuropilin-1 is required for vascular development and is a mediator of VEGF-dependent angiogenesis in zebrafish. Proc Natl Acad Sci U S A *99*, 10470-10475.

Lee, S.W., Kim, W.J., Jun, H.O., Choi, Y.K., and Kim, K.W. (2009). Angiopoietin-1 reduces vascular endothelial growth factor-induced brain endothelial permeability via upregulation of ZO-2. Int J Mol Med *23*, 279-284.

Legate, K.R., Montanez, E., Kudlacek, O., and Fassler, R. (2006). ILK, PINCH and parvin: the tIPP of integrin signalling. Nature reviews Molecular cell biology *7*, 20-31.

Leonova, E.I., and Galzitskaya, O.V. (2013). Structure and functions of syndecans in vertebrates. Biochemistry (Mosc) *78*, 1071-1085.

Leung, D.W., Cachianes, G., Kuang, W.J., Goeddel, D.V., and Ferrara, N. (1989). Vascular endothelial growth factor is a secreted angiogenic mitogen. Science *246*, 1306-1309.

Li, J., Brown, L.F., Laham, R.J., Volk, R., and Simons, M. (1997). Macrophage-dependent regulation of syndecan gene expression. Circ Res *81*, 785-796.

Li, Q., Park, P.W., Wilson, C.L., and Parks, W.C. (2002). Matrilysin shedding of syndecan-1 regulates chemokine mobilization and transepithelial efflux of neutrophils in acute lung injury. Cell *111*, 635-646.

Lim, S.T., Longley, R.L., Couchman, J.R., and Woods, A. (2003). Direct binding of syndecan-4 cytoplasmic domain to the catalytic domain of protein kinase C alpha (PKC alpha) increases focal adhesion localization of PKC alpha. J Biol Chem *278*, 13795-13802.

Lin, X., Wei, G., Shi, Z., Dryer, L., Esko, J.D., Wells, D.E., and Matzuk, M.M. (2000). Disruption of gastrulation and heparan sulfate biosynthesis in EXT1-deficient mice. Dev Biol *224*, 299-311.

Liu, W., Litwack, E.D., Stanley, M.J., Langford, J.K., Lander, A.D., and Sanderson, R.D. (1998). Heparan sulfate proteoglycans as adhesive and anti-invasive molecules. Syndecans and glypican have distinct functions. J Biol Chem *273*, 22825-22832.

London, N.R., Smith, M.C., and Li, D.Y. (2009). Emerging mechanisms of vascular stabilization. J Thromb Haemost *7 Suppl 1*, 57-60.

Lucke, S., and Levkau, B. (2010). Endothelial functions of sphingosine-1-phosphate. Cell Physiol Biochem *26*, 87-96.

Mahtouk, K., Cremer, F.W., Reme, T., Jourdan, M., Baudard, M., Moreaux, J., Requirand, G., Fiol, G., De Vos, J., Moos, M., *et al.* (2006). Heparan sulphate proteoglycans are essential for the myeloma cell growth activity of EGF-family ligands in multiple myeloma. Oncogene *25*, 7180-7191.

Mahtouk, K., Jourdan, M., De Vos, J., Hertogh, C., Fiol, G., Jourdan, E., Rossi, J.F., and Klein, B. (2004). An inhibitor of the EGF receptor family blocks myeloma cell growth factor activity of HB-EGF and potentiates dexamethasone or anti-IL-6 antibody-induced apoptosis. Blood *103*, 1829-1837.

Maisonpierre, P.C., Suri, C., Jones, P.F., Bartunkova, S., Wiegand, S.J., Radziejewski, C., Compton, D., McClain, J., Aldrich, T.H., Papadopoulos, N., *et al.* (1997). Angiopoietin-2, a natural antagonist for Tie2 that disrupts in vivo angiogenesis. Science *277*, 55-60.

Mali, M., Andtfolk, H., Miettinen, H.M., and Jalkanen, M. (1994). Suppression of tumor cell growth by syndecan-1 ectodomain. J Biol Chem *269*, 27795-27798.

Mandriota, S.J., and Pepper, M.S. (1998). Regulation of angiopoietin-2 mRNA levels in bovine microvascular endothelial cells by cytokines and hypoxia. Circ Res *83*, 852-859.

Manon-Jensen, T., Itoh, Y., and Couchman, J.R. (2010). Proteoglycans in health and disease: the multiple roles of syndecan shedding. FEBS J *277*, 3876-3889.

Marshall, L.J., Ramdin, L.S., Brooks, T., PC, D.P., and Shute, J.K. (2003). Plasminogen activator inhibitor-1 supports IL-8-mediated neutrophil transendothelial migration by inhibition of the constitutive shedding of endothelial IL-8/heparan sulfate/syndecan-1 complexes. J Immunol *171*, 2057-2065.

Martin, P.L., Jiao, Q., Cornacoff, J., Hall, W., Saville, B., Nemeth, J.A., Schantz, A., Mata, M., Jang, H., Fasanmade, A.A., *et al.* (2005). Absence of adverse effects in cynomolgus macaques treated with CNTO 95, a fully human anti-alphav integrin monoclonal antibody, despite widespread tissue binding. Clin Cancer Res *11*, 6959-6965.

Marynen, P., Zhang, J., Cassiman, J.J., Van den Berghe, H., and David, G. (1989). Partial primary structure of the 48- and 90-kilodalton core proteins of cell surface-associated heparan sulfate proteoglycans of lung fibroblasts. Prediction of an integral membrane domain and evidence for multiple distinct core proteins at the cell surface of human lung fibroblasts. J Biol Chem *264*, 7017-7024.

Matsuda, K., Maruyama, H., Guo, F., Kleeff, J., Itakura, J., Matsumoto, Y., Lander, A.D., and Korc, M. (2001). Glypican-1 is overexpressed in human breast cancer and modulates the mitogenic effects of multiple heparin-binding growth factors in breast cancer cells. Cancer Res *61*, 5562-5569.

Matsui, Y., Ikesue, M., Danzaki, K., Morimoto, J., Sato, M., Tanaka, S., Kojima, T., Tsutsui, H., and Uede, T. (2011). Syndecan-4 prevents cardiac rupture and dysfunction after myocardial infarction. Circ Res *108*, 1328-1339.

McFall, A.J., and Rapraeger, A.C. (1997). Identification of an adhesion site within the syndecan-4 extracellular protein domain. J Biol Chem *272*, 12901-12904.

McFall, A.J., and Rapraeger, A.C. (1998). Characterization of the high affinity cell-binding domain in the cell surface proteoglycan syndecan-4. J Biol Chem *273*, 28270-28276.

McNeel, D.G., Eickhoff, J., Lee, F.T., King, D.M., Alberti, D., Thomas, J.P., Friedl, A., Kolesar, J., Marnocha, R., Volkman, J., *et al.* (2005). Phase I trial of a monoclonal antibody specific for alphavbeta3 integrin (MEDI-522) in patients with advanced malignancies, including an assessment of effect on tumor perfusion. Clin Cancer Res *11*, 7851-7860.

McQuade, K.J., Beauvais, D.M., Burbach, B.J., and Rapraeger, A.C. (2006). Syndecan-1 regulates alphavbeta5 integrin activity in B82L fibroblasts. J Cell Sci *119*, 2445-2456.

Meadows, K.L., and Hurwitz, H.I. (2012). Anti-VEGF therapies in the clinic. Cold Spring Harb Perspect Med *2*.

Mesri, E.A., Federoff, H.J., and Brownlee, M. (1995). Expression of vascular endothelial growth factor from a defective herpes simplex virus type 1 amplicon vector induces angiogenesis in mice. Circulation research *76*, 161-167.

Mignatti, P., Tsuboi, R., Robbins, E., and Rifkin, D.B. (1989). In vitro angiogenesis on the human amniotic membrane: requirement for basic fibroblast growth factor-induced proteinases. J Cell Biol *108*, 671-682.

Miller, D.L., Ortega, S., Bashayan, O., Basch, R., and Basilico, C. (2000). Compensation by fibroblast growth factor 1 (FGF1) does not account for the mild phenotypic defects observed in FGF2 null mice. Mol Cell Biol *20*, 2260-2268.

Mitra, S.K., and Schlaepfer, D.D. (2006). Integrin-regulated FAK-Src signaling in normal and cancer cells. Current opinion in cell biology *18*, 516-523.

Modrowski, D., Basle, M., Lomri, A., and Marie, P.J. (2000). Syndecan-2 is involved in the mitogenic activity and signaling of granulocyte-macrophage colony-stimulating factor in osteoblasts. J Biol Chem *275*, 9178-9185.

Montrucchio, G., Lupia, E., Battaglia, E., Passerini, G., Bussolino, F., Emanuelli, G., and Camussi, G. (1994). Tumor necrosis factor alpha-induced angiogenesis depends on in situ platelet-activating factor biosynthesis. J Exp Med *180*, 377-382.

Morgan, M.R., Hamidi, H., Bass, M.D., Warwood, S., Ballestrem, C., and Humphries, M.J. (2013). Syndecan-4 phosphorylation is a control point for integrin recycling. Dev Cell *24*, 472-485.

Moya, I.M., Umans, L., Maas, E., Pereira, P.N., Beets, K., Francis, A., Sents, W., Robertson, E.J., Mummery, C.L., Huylebroeck, D., *et al.* (2012). Stalk cell phenotype depends on integration of Notch and Smad1/5 signaling cascades. Developmental cell *22*, 501-514.

Mullamitha, S.A., Ton, N.C., Parker, G.J., Jackson, A., Julyan, P.J., Roberts, C., Buonaccorsi, G.A., Watson, Y., Davies, K., Cheung, S., *et al.* (2007). Phase I evaluation of a fully human anti-alphav integrin monoclonal antibody (CNTO 95) in patients with advanced solid tumors. Clin Cancer Res *13*, 2128-2135.

Muller, Y.A., Li, B., Christinger, H.W., Wells, J.A., Cunningham, B.C., and de Vos, A.M. (1997). Vascular endothelial growth factor: crystal structure and functional mapping of the kinase domain receptor binding site. Proc Natl Acad Sci U S A *94*, 7192-7197.

Multhaupt, H.A., Yoneda, A., Whiteford, J.R., Oh, E.S., Lee, W., and Couchman, J.R. (2009). Syndecan signaling: when, where and why? J Physiol Pharmacol *60 Suppl 4*, 31-38.

Murakami, M., Horowitz, A., Tang, S., Ware, J.A., and Simons, M. (2002a). Protein kinase C (PKC) delta regulates PKCalpha activity in a Syndecan-4-dependent manner. J Biol Chem *277*, 20367-20371.

Murakami, M., Horowitz, A., Tang, S., Ware, J.A., and Simons, M. (2002b). Protein kinase C (PKC) delta regulates PKCalpha activity in a Syndecan-4-dependent manner. J Biol Chem *277*, 20367-20371.

Murphy, K.J., Merry, C.L., Lyon, M., Thompson, J.E., Roberts, I.S., and Gallagher, J.T. (2004). A new model for the domain structure of heparan sulfate based on the novel specificity of K5 lyase. J Biol Chem *279*, 27239-27245.

Nabors, L.B., Mikkelsen, T., Rosenfeld, S.S., Hochberg, F., Akella, N.S., Fisher, J.D., Cloud, G.A., Zhang, Y., Carson, K., Wittemer, S.M., *et al.* (2007). Phase I and correlative biology study of cilengitide in patients with recurrent malignant glioma. J Clin Oncol *25*, 1651-1657.

Nakayama, T., Hatachi, G., Wen, C.Y., Yoshizaki, A., Yamazumi, K., Niino, D., and Sekine, I. (2005). Expression and significance of Tie-1 and Tie-2 receptors, and angiopoietins-1, 2 and 4 in colorectal adenocarcinoma: Immunohistochemical analysis and correlation with clinicopathological factors. World J Gastroenterol *11*, 964-969.

Ng, C.M., Bai, S., Takimoto, C.H., Tang, M.T., and Tolcher, A.W. (2010). Mechanism-based receptor-binding model to describe the pharmacokinetic and pharmacodynamic of an anti-alpha5beta1 integrin monoclonal antibody (volociximab) in cancer patients. Cancer chemotherapy and pharmacology *65*, 207-217.

Nicoli, S., Standley, C., Walker, P., Hurlstone, A., Fogarty, K.E., and Lawson, N.D. (2010). MicroRNA-mediated integration of haemodynamics and Vegf signalling during angiogenesis. Nature *464*, 1196-1200.

Nicosia, R.F., Nicosia, S.V., and Smith, M. (1994). Vascular endothelial growth factor, platelet-derived growth factor, and insulin-like growth factor-1 promote rat aortic angiogenesis in vitro. Am J Pathol *145*, 1023-1029.

Nicosia, R.F., and Ottinetti, A. (1990a). Growth of microvessels in serum-free matrix culture of rat aorta. A quantitative assay of angiogenesis in vitro. Lab Invest *63*, 115-122.

Nicosia, R.F., and Ottinetti, A. (1990b). Modulation of microvascular growth and morphogenesis by reconstituted basement membrane gel in three-dimensional cultures of

rat aorta: a comparative study of angiogenesis in matrigel, collagen, fibrin, and plasma clot. In Vitro Cell Dev Biol *26*, 119-128.
Nikkari, S.T., Jarvelainen, H.T., Wight, T.N., Ferguson, M., and Clowes, A.W. (1994). Smooth muscle cell expression of extracellular matrix genes after arterial injury. Am J Pathol *144*, 1348-1356.
Nikolova, V., Koo, C.Y., Ibrahim, S.A., Wang, Z., Spillmann, D., Dreier, R., Kelsch, R., Fischgrabe, J., Smollich, M., Rossi, L.H., *et al.* (2009). Differential roles for membrane-bound and soluble syndecan-1 (CD138) in breast cancer progression. Carcinogenesis *30*, 397-407.
Nilsson, I., Bahram, F., Li, X., Gualandi, L., Koch, S., Jarvius, M., Soderberg, O., Anisimov, A., Kholova, I., Pytowski, B., *et al.* (2010). VEGF receptor 2/-3 heterodimers detected in situ by proximity ligation on angiogenic sprouts. EMBO J *29*, 1377-1388.
Nishiguchi, K.M., Kataoka, K., Kachi, S., Komeima, K., and Terasaki, H. (2010). Regulation of pathologic retinal angiogenesis in mice and inhibition of VEGF-VEGFR2 binding by soluble heparan sulfate. PLoS One *5*, e13493.
Noguer, O., Villena, J., Lorita, J., Vilaro, S., and Reina, M. (2009). Syndecan-2 downregulation impairs angiogenesis in human microvascular endothelial cells. Exp Cell Res *315*, 795-808.
Norrby, K. (1996). TNF-alpha and de novo mammalian angiogenesis. Microvascular research *52*, 79-83.
Nunes, S.S., Outeiro-Bernstein, M.A., Juliano, L., Vardiero, F., Nader, H.B., Woods, A., Legrand, C., and Morandi, V. (2008). Syndecan-4 contributes to endothelial tubulogenesis through interactions with two motifs inside the pro-angiogenic N-terminal domain of thrombospondin-1. J Cell Physiol *214*, 828-837.
Nyberg, P., Xie, L., and Kalluri, R. (2005). Endogenous inhibitors of angiogenesis. Cancer Res *65*, 3967-3979.
O'Day, S.J., Pavlick, A.C., Albertini, M.R., Hamid, O., Schalch, H., Lang, Z., Ling, J., Mata, M., Reddy, M., and Foster, B. (2012). Clinical and pharmacologic evaluation of two dose levels of intetumumab (CNTO 95) in patients with melanoma or angiosarcoma. Investigational new drugs *30*, 1074-1081.
O'Toole, T.E., Katagiri, Y., Faull, R.J., Peter, K., Tamura, R., Quaranta, V., Loftus, J.C., Shattil, S.J., and Ginsberg, M.H. (1994). Integrin cytoplasmic domains mediate inside-out signal transduction. J Cell Biol *124*, 1047-1059.
Ober, E.A., Olofsson, B., Makinen, T., Jin, S.W., Shoji, W., Koh, G.Y., Alitalo, K., and Stainier, D.Y. (2004). Vegfc is required for vascular development and endoderm morphogenesis in zebrafish. EMBO Rep *5*, 78-84.
Oberg-Welsh, C., Sandler, S., Andersson, A., and Welsh, M. (1997). Effects of vascular endothelial growth factor on pancreatic duct cell replication and the insulin production of fetal islet-like cell clusters in vitro. Molecular and cellular endocrinology *126*, 125-132.
Ogawa, S., Oku, A., Sawano, A., Yamaguchi, S., Yazaki, Y., and Shibuya, M. (1998). A novel type of vascular endothelial growth factor, VEGF-E (NZ-7 VEGF), preferentially utilizes KDR/Flk-1 receptor and carries a potent mitotic activity without heparin-binding domain. J Biol Chem *273*, 31273-31282.
Oh, E.S., Woods, A., and Couchman, J.R. (1997a). Multimerization of the cytoplasmic domain of syndecan-4 is required for its ability to activate protein kinase C. J Biol Chem *272*, 11805-11811.
Oh, E.S., Woods, A., and Couchman, J.R. (1997b). Syndecan-4 proteoglycan regulates the distribution and activity of protein kinase C. J Biol Chem *272*, 8133-8136.
Oh, E.S., Woods, A., Lim, S.T., Theibert, A.W., and Couchman, J.R. (1998). Syndecan-4 proteoglycan cytoplasmic domain and phosphatidylinositol 4,5-bisphosphate coordinately regulate protein kinase C activity. J Biol Chem *273*, 10624-10629.

Okina, E., Grossi, A., Gopal, S., Multhaupt, H.A., and Couchman, J.R. (2012). Alpha-actinin interactions with syndecan-4 are integral to fibroblast-matrix adhesion and regulate cytoskeletal architecture. Int J Biochem Cell Biol *44*, 2161-2174.

Okina, E., Manon-Jensen, T., Whiteford, J.R., and Couchman, J.R. (2009). Syndecan proteoglycan contributions to cytoskeletal organization and contractility. Scand J Med Sci Sports *19*, 479-489.

Olofsson, B., Korpelainen, E., Pepper, M.S., Mandriota, S.J., Aase, K., Kumar, V., Gunji, Y., Jeltsch, M.M., Shibuya, M., Alitalo, K., *et al.* (1998). Vascular endothelial growth factor B (VEGF-B) binds to VEGF receptor-1 and regulates plasminogen activator activity in endothelial cells. Proc Natl Acad Sci U S A *95*, 11709-11714.

Olsson, A.K., Dimberg, A., Kreuger, J., and Claesson-Welsh, L. (2006). VEGF receptor signalling - in control of vascular function. Nat Rev Mol Cell Biol *7*, 359-371.

Ono, K., Hattori, H., Takeshita, S., Kurita, A., and Ishihara, M. (1999). Structural features in heparin that interact with VEGF165 and modulate its biological activity. Glycobiology *9*, 705-711.

Orecchia, P., Conte, R., Balza, E., Pietra, G., Mingari, M.C., and Carnemolla, B. (2015). Targeting Syndecan-1, a molecule implicated in the process of vasculogenic mimicry, enhances the therapeutic efficacy of the L19-IL2 immunocytokine in human melanoma xenografts. Oncotarget.

Ostman, A., Yang, Q., and Tonks, N.K. (1994). Expression of DEP-1, a receptor-like protein-tyrosine-phosphatase, is enhanced with increasing cell density. Proc Natl Acad Sci U S A *91*, 9680-9684.

Ozaki, H., Okamoto, N., Ortega, S., Chang, M., Ozaki, K., Sadda, S., Vinores, M.A., Derevjanik, N., Zack, D.J., Basilico, C., *et al.* (1998). Basic fibroblast growth factor is neither necessary nor sufficient for the development of retinal neovascularization. Am J Pathol *153*, 757-765.

Pal-Ghosh, S., Tadvalkar, G., Jurjus, R.A., Zieske, J.D., and Stepp, M.A. (2008). BALB/c and C57BL6 mouse strains vary in their ability to heal corneal epithelial debridement wounds. Exp Eye Res *87*, 478-486.

Pan, Q., Chathery, Y., Wu, Y., Rathore, N., Tong, R.K., Peale, F., Bagri, A., Tessier-Lavigne, M., Koch, A.W., and Watts, R.J. (2007). Neuropilin-1 binds to VEGF121 and regulates endothelial cell migration and sprouting. J Biol Chem *282*, 24049-24056.

Pardali, E., Goumans, M.J., and ten Dijke, P. (2010). Signaling by members of the TGF-beta family in vascular morphogenesis and disease. Trends Cell Biol *20*, 556-567.

Park, H., Kim, Y., Lim, Y., Han, I., and Oh, E.S. (2002). Syndecan-2 mediates adhesion and proliferation of colon carcinoma cells. J Biol Chem *277*, 29730-29736.

Park, J.E., Keller, G.A., and Ferrara, N. (1993). The vascular endothelial growth factor (VEGF) isoforms: differential deposition into the subepithelial extracellular matrix and bioactivity of extracellular matrix-bound VEGF. Mol Biol Cell *4*, 1317-1326.

Patan, S., Alvarez, M.J., Schittny, J.C., and Burri, P.H. (1992). Intussusceptive microvascular growth: a common alternative to capillary sprouting. Archives of histology and cytology *55 Suppl*, 65-75.

Patterson, A.M., Gardner, L., Shaw, J., David, G., Loreau, E., Aguilar, L., Ashton, B.A., and Middleton, J. (2005). Induction of a CXCL8 binding site on endothelial syndecan-3 in rheumatoid synovium. Arthritis Rheum *52*, 2331-2342.

Paye, J.M., Phng, L.K., Lanahan, A.A., Gerhard, H., and Simons, M. (2009). Synectin-dependent regulation of arterial maturation. Dev Dyn *238*, 604-610.

Pepper, M.S., Ferrara, N., Orci, L., and Montesano, R. (1992). Potent synergism between vascular endothelial growth factor and basic fibroblast growth factor in the induction of angiogenesis in vitro. Biochemical and Biophysical Research Communications *189*, 824-831.

Phillips, G.D., Stone, A.M., Jones, B.D., Schultz, J.C., Whitehead, R.A., and Knighton, D.R. (1994). Vascular endothelial growth factor (rhVEGF165) stimulates direct angiogenesis in the rabbit cornea. In Vivo *8*, 961-965.

Phng, L.K., and Gerhardt, H. (2009). Angiogenesis: a team effort coordinated by notch. Dev Cell *16*, 196-208.

Phng, L.K., Potente, M., Leslie, J.D., Babbage, J., Nyqvist, D., Lobov, I., Ondr, J.K., Rao, S., Lang, R.A., Thurston, G., *et al.* (2009). Nrarp coordinates endothelial Notch and Wnt signaling to control vessel density in angiogenesis. Dev Cell *16*, 70-82.

Pinon, J.D., Klasse, P.J., Jassal, S.R., Welson, S., Weber, J., Brighty, D.W., and Sattentau, Q.J. (2003). Human T-cell leukemia virus type 1 envelope glycoprotein gp46 interacts with cell surface heparan sulfate proteoglycans. J Virol *77*, 9922-9930.

Pitulescu, M.E., and Adams, R.H. (2010). Eph/ephrin molecules--a hub for signaling and endocytosis. Genes Dev *24*, 2480-2492.

Plouet, J., Schilling, J., and Gospodarowicz, D. (1989). Isolation and characterization of a newly identified endothelial cell mitogen produced by AtT-20 cells. The EMBO journal *8*, 3801-3806.

Polte, T., Petzold, S., Bertrand, J., Schutze, N., Hinz, D., Simon, J.C., Lehmann, I., Echtermeyer, F., Pap, T., and Averbeck, M. (2015). Critical role for syndecan-4 in dendritic cell migration during development of allergic airway inflammation. Nature communications *6*, 7554.

Presta, M., Tiberio, L., Rusnati, M., Dell'Era, P., and Ragnotti, G. (1991). Basic fibroblast growth factor requires a long-lasting activation of protein kinase C to induce cell proliferation in transformed fetal bovine aortic endothelial cells. Cell Regul *2*, 719-726.

Pruessmeyer, J., Martin, C., Hess, F.M., Schwarz, N., Schmidt, S., Kogel, T., Hoettecke, N., Schmidt, B., Sechi, A., Uhlig, S., *et al.* (2010). A disintegrin and metalloproteinase 17 (ADAM17) mediates inflammation-induced shedding of syndecan-1 and -4 by lung epithelial cells. J Biol Chem *285*, 555-564.

Purushothaman, A., Chen, L., Yang, Y., and Sanderson, R.D. (2008). Heparanase stimulation of protease expression implicates it as a master regulator of the aggressive tumor phenotype in myeloma. J Biol Chem *283*, 32628-32636.

Purushothaman, A., Uyama, T., Kobayashi, F., Yamada, S., Sugahara, K., Rapraeger, A.C., and Sanderson, R.D. (2010). Heparanase-enhanced shedding of syndecan-1 by myeloma cells promotes endothelial invasion and angiogenesis. Blood *115*, 2449-2457.

Ramani, V.C., Purushothaman, A., Stewart, M.D., Thompson, C.A., Vlodavsky, I., Au, J.L., and Sanderson, R.D. (2013). The heparanase/syndecan-1 axis in cancer: mechanisms and therapies. FEBS J *280*, 2294-2306.

Rapraeger, A.C., Ell, B.J., Roy, M., Li, X., Morrison, O.R., Thomas, G.M., and Beauvais, D.M. (2013). Vascular endothelial-cadherin stimulates syndecan-1-coupled insulin-like growth factor-1 receptor and cross-talk between alphaVbeta3 integrin and vascular endothelial growth factor receptor 2 at the onset of endothelial cell dissemination during angiogenesis. The FEBS journal *280*, 2194-2206.

Rask-Madsen, C., and King, G.L. (2008). Differential regulation of VEGF signaling by PKC-alpha and PKC-epsilon in endothelial cells. Arterioscler Thromb Vasc Biol *28*, 919-924.

Reardon, D.A., Nabors, L.B., Stupp, R., and Mikkelsen, T. (2008). Cilengitide: an integrin-targeting arginine-glycine-aspartic acid peptide with promising activity for glioblastoma multiforme. Expert opinion on investigational drugs *17*, 1225-1235.

Reiland, J., and Rapraeger, A.C. (1993). Heparan sulfate proteoglycan and FGF receptor target basic FGF to different intracellular destinations. J Cell Sci *105 (Pt 4)*, 1085-1093.

Reynolds, A.R., Hart, I.R., Watson, A.R., Welti, J.C., Silva, R.G., Robinson, S.D., Da Violante, G., Gourlaouen, M., Salih, M., Jones, M.C., *et al.* (2009). Stimulation of tumor growth and angiogenesis by low concentrations of RGD-mimetic integrin inhibitors. Nature Medicine *15*, 392-400.

Reynolds, L.E., Wyder, L., Lively, J.C., Taverna, D., Robinson, S.D., Huang, X., Sheppard, D., Hynes, R.O., and Hodivala-Dilke, K.M. (2002). Enhanced pathological angiogenesis in mice lacking beta3 integrin or beta3 and beta5 integrins. Nat Med *8*, 27-34.

Risau, W. (1997). Mechanisms of angiogenesis. Nature *386*, 671-674.

Robinson, C.J., Mulloy, B., Gallagher, J.T., and Stringer, S.E. (2006a). VEGF165-binding sites within heparan sulfate encompass two highly sulfated domains and can be liberated by K5 lyase. J Biol Chem *281*, 1731-1740.

Robinson, C.J., Mulloy, B., Gallagher, J.T., and Stringer, S.E. (2006b). VEGF165-binding sites within heparan sulfate encompass two highly sulfated domains and can be liberated by K5 lyase. J Biol Chem *281*, 1731-1740.

Robinson, C.J., and Stringer, S.E. (2001). The splice variants of vascular endothelial growth factor (VEGF) and their receptors. J Cell Sci *114*, 853-865.

Roskoski, R., Jr. (2007). Vascular endothelial growth factor (VEGF) signaling in tumor progression. Crit Rev Oncol Hematol *62*, 179-213.

Ruhrberg, C., Gerhardt, H., Golding, M., Watson, R., Ioannidou, S., Fujisawa, H., Betsholtz, C., and Shima, D.T. (2002). Spatially restricted patterning cues provided by heparin-binding VEGF-A control blood vessel branching morphogenesis. Genes Dev *16*, 2684-2698.

Sainson, R.C., and Harris, A.L. (2008). Regulation of angiogenesis by homotypic and heterotypic notch signalling in endothelial cells and pericytes: from basic research to potential therapies. Angiogenesis *11*, 41-51.

Sanderson, R.D. (2001). Heparan sulfate proteoglycans in invasion and metastasis. Semin Cell Dev Biol *12*, 89-98.

Santambrogio, M., Valdembri, D., and Serini, G. (2011). Increasing traffic on vascular routes. Mol Aspects Med *32*, 112-122.

Saoncella, S., Echtermeyer, F., Denhez, F., Nowlen, J.K., Mosher, D.F., Robinson, S.D., Hynes, R.O., and Goetinck, P.F. (1999). Syndecan-4 signals cooperatively with integrins in a Rho-dependent manner in the assembly of focal adhesions and actin stress fibers. Proc Natl Acad Sci U S A *96*, 2805-2810.

Sarrazin, S., Lamanna, W.C., and Esko, J.D. (2011). Heparan sulfate proteoglycans. Cold Spring Harb Perspect Biol *3*.

Saunders, S., Jalkanen, M., O'Farrell, S., and Bernfield, M. (1989). Molecular cloning of syndecan, an integral membrane proteoglycan. J Cell Biol *108*, 1547-1556.

Sawamiphak, S., Seidel, S., Essmann, C.L., Wilkinson, G.A., Pitulescu, M.E., Acker, T., and Acker-Palmer, A. (2010). Ephrin-B2 regulates VEGFR2 function in developmental and tumour angiogenesis. Nature *465*, 487-491.

Sawano, A., Iwai, S., Sakurai, Y., Ito, M., Shitara, K., Nakahata, T., and Shibuya, M. (2001). Flt-1, vascular endothelial growth factor receptor 1, is a novel cell surface marker for the lineage of monocyte-macrophages in humans. Blood *97*, 785-791.

Scaringi, C., Minniti, G., Caporello, P., and Enrici, R.M. (2012). Integrin inhibitor cilengitide for the treatment of glioblastoma: a brief overview of current clinical results. Anticancer Res *32*, 4213-4223.

Schmidt, A., Echtermeyer, F., Alozie, A., Brands, K., and Buddecke, E. (2005). Plasmin- and thrombin-accelerated shedding of syndecan-4 ectodomain generates cleavage sites at Lys(114)-Arg(115) and Lys(129)-Val(130) bonds. J Biol Chem *280*, 34441-34446.

Scott, B.B., Zaratin, P.F., Colombo, A., Hansbury, M.J., Winkler, J.D., and Jackson, J.R. (2002). Constitutive expression of angiopoietin-1 and -2 and modulation of their expression by inflammatory cytokines in rheumatoid arthritis synovial fibroblasts. J Rheumatol *29*, 230-239.

Seegar, T.C., Eller, B., Tzvetkova-Robev, D., Kolev, M.V., Henderson, S.C., Nikolov, D.B., and Barton, W.A. (2010). Tie1-Tie2 interactions mediate functional differences between angiopoietin ligands. Mol Cell *37*, 643-655.

Seghezzi, G., Patel, S., Ren, C.J., Gualandris, A., Pintucci, G., Robbins, E.S., Shapiro, R.L., Galloway, A.C., Rifkin, D.B., and Mignatti, P. (1998). Fibroblast growth factor-2 (FGF-2) induces vascular endothelial growth factor (VEGF) expression in the endothelial cells of forming capillaries: an autocrine mechanism contributing to angiogenesis. J Cell Biol *141*, 1659-1673.

Seidel, C., Borset, M., Hjertner, O., Cao, D., Abildgaard, N., Hjorth-Hansen, H., Sanderson, R.D., Waage, A., and Sundan, A. (2000a). High levels of soluble syndecan-1 in myeloma-derived bone marrow: modulation of hepatocyte growth factor activity. Blood *96*, 3139-3146.

Seidel, C., Ringden, O., and Remberger, M. (2003). Increased levels of syndecan-1 in serum during acute graft-versus-host disease. Transplantation *76*, 423-426.

Seidel, C., Sundan, A., Hjorth, M., Turesson, I., Dahl, I.M., Abildgaard, N., Waage, A., and Borset, M. (2000b). Serum syndecan-1: a new independent prognostic marker in multiple myeloma. Blood *95*, 388-392.

Senger, D.R., Galli, S.J., Dvorak, A.M., Perruzzi, C.A., Harvey, V.S., and Dvorak, H.F. (1983). Tumor cells secrete a vascular permeability factor that promotes accumulation of ascites fluid. Science *219*, 983-985.

Serini, G., Maione, F., Giraudo, E., and Bussolino, F. (2009). Semaphorins and tumor angiogenesis. Angiogenesis *12*, 187-193.

Shafti-Keramat, S., Handisurya, A., Kriehuber, E., Meneguzzi, G., Slupetzky, K., and Kirnbauer, R. (2003). Different heparan sulfate proteoglycans serve as cellular receptors for human papillomaviruses. J Virol *77*, 13125-13135.

Shalaby, F., Rossant, J., Yamaguchi, T.P., Gertsenstein, M., Wu, X.F., Breitman, M.L., and Schuh, A.C. (1995). Failure of blood-island formation and vasculogenesis in Flk-1-deficient mice. Nature *376*, 62-66.

Shibuya, M. (2006). Vascular endothelial growth factor (VEGF)-Receptor2: its biological functions, major signaling pathway, and specific ligand VEGF-E. Endothelium *13*, 63-69.

Shono, T., Kanetake, H., and Kanda, S. (2001). The role of mitogen-activated protein kinase activation within focal adhesions in chemotaxis toward FGF-2 by murine brain capillary endothelial cells. Exp Cell Res *264*, 275-283.

Short, S.M., Derrien, A., Narsimhan, R.P., Lawler, J., Ingber, D.E., and Zetter, B.R. (2005). Inhibition of endothelial cell migration by thrombospondin-1 type-1 repeats is mediated by beta1 integrins. The Journal of cell biology *168*, 643-653.

Simons, M. (2012). An inside view: VEGF receptor trafficking and signaling. Physiology (Bethesda) *27*, 213-222.

Skidmore, M.A., Guimond, S.E., Rudd, T.R., Fernig, D.G., Turnbull, J.E., and Yates, E.A. (2008). The activities of heparan sulfate and its analogue heparin are dictated by biosynthesis, sequence, and conformation. Connective tissue research *49*, 140-144.

Slimani, H., Charnaux, N., Mbemba, E., Saffar, L., Vassy, R., Vita, C., and Gattegno, L. (2003a). Binding of the CC-chemokine RANTES to syndecan-1 and syndecan-4 expressed on HeLa cells. Glycobiology *13*, 623-634.

Slimani, H., Charnaux, N., Mbemba, E., Saffar, L., Vassy, R., Vita, C., and Gattegno, L. (2003b). Interaction of RANTES with syndecan-1 and syndecan-4 expressed by human primary macrophages. Biochim Biophys Acta *1617*, 80-88.

Soares, M.A., Teixeira, F.C., Fontes, M., Areas, A.L., Leal, M.G., Pavao, M.S., and Stelling, M.P. (2015). Heparan Sulfate Proteoglycans May Promote or Inhibit Cancer Progression by Interacting with Integrins and Affecting Cell Migration. BioMed research international *2015*, 453801.

Sondell, M., Lundborg, G., and Kanje, M. (1999). Vascular endothelial growth factor has neurotrophic activity and stimulates axonal outgrowth, enhancing cell survival and Schwann cell proliferation in the peripheral nervous system. The Journal of neuroscience : the official journal of the Society for Neuroscience *19*, 5731-5740.

Stalmans, I., Ng, Y.S., Rohan, R., Fruttiger, M., Bouche, A., Yuce, A., Fujisawa, H., Hermans, B., Shani, M., Jansen, S., *et al.* (2002). Arteriolar and venular patterning in retinas of mice selectively expressing VEGF isoforms. J Clin Invest *109*, 327-336.

Stauffer, M.E., Skelton, N.J., and Fairbrothe, W.J. (2002). Refinement of the solution structure of the heparin-binding domain of vascular endothelial growth factor using residual dipolar couplings. J Biomol NMR *23*, 57-61.

Steinfeld, R., Van Den Berghe, H., and David, G. (1996). Stimulation of fibroblast growth factor receptor-1 occupancy and signaling by cell surface-associated syndecans and glypican. J Cell Biol *133*, 405-416.

Stepp, M.A., Gibson, H.E., Gala, P.H., Iglesia, D.D., Pajoohesh-Ganji, A., Pal-Ghosh, S., Brown, M., Aquino, C., Schwartz, A.M., Goldberger, O., *et al.* (2002). Defects in keratinocyte activation during wound healing in the syndecan-1-deficient mouse. J Cell Sci *115*, 4517-4531.

Stickens, D., Zak, B.M., Rougier, N., Esko, J.D., and Werb, Z. (2005). Mice deficient in Ext2 lack heparan sulfate and develop exostoses. Development *132*, 5055-5068.

Stoeltzing, O., Liu, W., Reinmuth, N., Fan, F., Parry, G.C., Parikh, A.A., McCarty, M.F., Bucana, C.D., Mazar, A.P., and Ellis, L.M. (2003). Inhibition of integrin alpha5beta1 function with a small peptide (ATN-161) plus continuous 5-FU infusion reduces colorectal liver metastases and improves survival in mice. Int J Cancer *104*, 496-503.

Strand, M.E., Aronsen, J.M., Braathen, B., Sjaastad, I., Kvaloy, H., Tonnessen, T., Christensen, G., and Lunde, I.G. (2015). Shedding of syndecan-4 promotes immune cell recruitment and mitigates cardiac dysfunction after lipopolysaccharide challenge in mice. J Mol Cell Cardiol *88*, 133-144.

Strilic, B., Kucera, T., Eglinger, J., Hughes, M.R., McNagny, K.M., Tsukita, S., Dejana, E., Ferrara, N., and Lammert, E. (2009). The molecular basis of vascular lumen formation in the developing mouse aorta. Dev Cell *17*, 505-515.

Su, G., Blaine, S.A., Qiao, D., and Friedl, A. (2007). Shedding of syndecan-1 by stromal fibroblasts stimulates human breast cancer cell proliferation via FGF2 activation. J Biol Chem *282*, 14906-14915.

Subramanian, S.V., Fitzgerald, M.L., and Bernfield, M. (1997). Regulated shedding of syndecan-1 and -4 ectodomains by thrombin and growth factor receptor activation. J Biol Chem *272*, 14713-14720.

Suchting, S., Freitas, C., le Noble, F., Benedito, R., Breant, C., Duarte, A., and Eichmann, A. (2007). The Notch ligand Delta-like 4 negatively regulates endothelial tip cell formation and vessel branching. Proc Natl Acad Sci U S A *104*, 3225-3230.

Sutton, A., Friand, V., Brule-Donneger, S., Chaigneau, T., Ziol, M., Sainte-Catherine, O., Poire, A., Saffar, L., Kraemer, M., Vassy, J., *et al.* (2007). Stromal cell-derived factor-1/chemokine (C-X-C motif) ligand 12 stimulates human hepatoma cell growth, migration, and invasion. Mol Cancer Res *5*, 21-33.

Takahashi, K., Mernaugh, R.L., Friedman, D.B., Weller, R., Tsuboi, N., Yamashita, H., Quaranta, V., and Takahashi, T. (2012). Thrombospondin-1 acts as a ligand for CD148 tyrosine phosphatase. Proc Natl Acad Sci U S A *109*, 1985-1990.

Takahashi, T., Takahashi, K., Mernaugh, R., Drozdoff, V., Sipe, C., Schoecklmann, H., Robert, B., Abrahamson, D.R., and Daniel, T.O. (1999). Endothelial localization of receptor tyrosine phosphatase, ECRTP/DEP-1, in developing and mature renal vasculature. J Am Soc Nephrol *10*, 2135-2145.

Takahashi, T., Takahashi, K., Mernaugh, R.L., Tsuboi, N., Liu, H., and Daniel, T.O. (2006). A monoclonal antibody against CD148, a receptor-like tyrosine phosphatase, inhibits endothelial-cell growth and angiogenesis. Blood *108*, 1234-1242.

Takahashi, T., Takahashi, K., St John, P.L., Fleming, P.A., Tomemori, T., Watanabe, T., Abrahamson, D.R., Drake, C.J., Shirasawa, T., and Daniel, T.O. (2003a). A mutant receptor tyrosine phosphatase, CD148, causes defects in vascular development. Molecular and cellular biology *23*, 1817-1831.

Tammela, T., Zarkada, G., Wallgard, E., Murtomaki, A., Suchting, S., Wirzenius, M., Waltari, M., Hellstrom, M., Schomber, T., Peltonen, R., *et al.* (2008). Blocking VEGFR-3 suppresses angiogenic sprouting and vascular network formation. Nature *454*, 656-660.

Tan, X., Khalil, N., Tesarik, C., Vanapalli, K., Yaputra, V., Alkhouri, H., Oliver, B.G., Armour, C.L., and Hughes, J.M. (2012). Th1 cytokine-induced syndecan-4 shedding by airway smooth muscle cells is dependent on mitogen-activated protein kinases. Am J Physiol Lung Cell Mol Physiol *302*, L700-710.

Taraboletti, G., D'Ascenzo, S., Borsotti, P., Giavazzi, R., Pavan, A., and Dolo, V. (2002). Shedding of the matrix metalloproteinases MMP-2, MMP-9, and MT1-MMP as membrane vesicle-associated components by endothelial cells. Am J Pathol *160*, 673-680.

Thompson, C.A., Purushothaman, A., Ramani, V.C., Vlodavsky, I., and Sanderson, R.D. (2013). Heparanase regulates secretion, composition, and function of tumor cell-derived exosomes. J Biol Chem *288*, 10093-10099.

Thurston, G., Rudge, J.S., Ioffe, E., Zhou, H., Ross, L., Croll, S.D., Glazer, N., Holash, J., McDonald, D.M., and Yancopoulos, G.D. (2000). Angiopoietin-1 protects the adult vasculature against plasma leakage. Nat Med *6*, 460-463.

Tille, J.C., Wood, J., Mandriota, S.J., Schnell, C., Ferrari, S., Mestan, J., Zhu, Z., Witte, L., and Pepper, M.S. (2001). Vascular endothelial growth factor (VEGF) receptor-2 antagonists inhibit VEGF- and basic fibroblast growth factor-induced angiogenesis in vivo and in vitro. J Pharmacol Exp Ther *299*, 1073-1085.

Tkachenko, E., Elfenbein, A., Tirziu, D., and Simons, M. (2006). Syndecan-4 clustering induces cell migration in a PDZ-dependent manner. Circ Res *98*, 1398-1404.

Tkachenko, E., Lutgens, E., Stan, R.V., and Simons, M. (2004). Fibroblast growth factor 2 endocytosis in endothelial cells proceed via syndecan-4-dependent activation of Rac1 and a Cdc42-dependent macropinocytic pathway. J Cell Sci *117*, 3189-3199.

Tobe, T., Ortega, S., Luna, J.D., Ozaki, H., Okamoto, N., Derevjanik, N.L., Vinores, S.A., Basilico, C., and Campochiaro, P.A. (1998). Targeted disruption of the FGF2 gene does not prevent choroidal neovascularization in a murine model. Am J Pathol *153*, 1641-1646.

Tokunaga, Y., Yamazaki, Y., and Morita, T. (2005). Specific distribution of VEGF-F in Viperinae snake venoms: isolation and characterization of a VGEF-F from the venom of Daboia russelli siamensis. Arch Biochem Biophys *439*, 241-247.

Tolentino, M.J., Miller, J.W., Gragoudas, E.S., Chatzistefanou, K., Ferrara, N., and Adamis, A.P. (1996). Vascular endothelial growth factor is sufficient to produce iris neovascularization and neovascular glaucoma in a nonhuman primate. Archives of ophthalmology *114*, 964-970.

Tran, J., Master, Z., Yu, J.L., Rak, J., Dumont, D.J., and Kerbel, R.S. (2002). A role for survivin in chemoresistance of endothelial cells mediated by VEGF. Proc Natl Acad Sci U S A *99*, 4349-4354.

Tran, J., Rak, J., Sheehan, C., Saibil, S.D., LaCasse, E., Korneluk, R.G., and Kerbel, R.S. (1999). Marked induction of the IAP family antiapoptotic proteins survivin and XIAP by VEGF in vascular endothelial cells. Biochemical and Biophysical Research Communications *264*, 781-788.

Trikha, M., Zhou, Z., Nemeth, J.A., Chen, Q., Sharp, C., Emmell, E., Giles-Komar, J., and Nakada, M.T. (2004). CNTO 95, a fully human monoclonal antibody that inhibits alphav integrins, has antitumor and antiangiogenic activity in vivo. Int J Cancer *110*, 326-335.

Tzima, E., Irani-Tehrani, M., Kiosses, W.B., Dejana, E., Schultz, D.A., Engelhardt, B., Cao, G., DeLisser, H., and Schwartz, M.A. (2005). A mechanosensory complex that mediates the endothelial cell response to fluid shear stress. Nature *437*, 426-431.

Uchida, T., Nakashima, M., Hirota, Y., Miyazaki, Y., Tsukazaki, T., and Shindo, H. (2000). Immunohistochemical localisation of protein tyrosine kinase receptors Tie-1 and Tie-2 in synovial tissue of rheumatoid arthritis: correlation with angiogenesis and synovial proliferation. Ann Rheum Dis *59*, 607-614.

Underwood, P.A., Bean, P.A., and Gamble, J.R. (2002). Rate of endothelial expansion is controlled by cell:cell adhesion. Int J Biochem Cell Biol *34*, 55-69.

van der Flier, A., Badu-Nkansah, K., Whittaker, C.A., Crowley, D., Bronson, R.T., Lacy-Hulbert, A., and Hynes, R.O. (2010). Endothelial alpha5 and alphav integrins cooperate in remodeling of the vasculature during development. Development *137*, 2439-2449.

van Horssen, J., Wesseling, P., van den Heuvel, L.P., de Waal, R.M., and Verbeek, M.M. (2003). Heparan sulphate proteoglycans in Alzheimer's disease and amyloid-related disorders. Lancet Neurol *2*, 482-492.

van Lookeren Campagne, M., LeCouter, J., Yaspan, B.L., and Ye, W. (2014). Mechanisms of age-related macular degeneration and therapeutic opportunities. J Pathol *232*, 151-164.

Volk, R., Schwartz, J.J., Li, J., Rosenberg, R.D., and Simons, M. (1999). The role of syndecan cytoplasmic domain in basic fibroblast growth factor-dependent signal transduction. J Biol Chem *274*, 24417-24424.

Voskas, D., Jones, N., Van Slyke, P., Sturk, C., Chang, W., Haninec, A., Babichev, Y.O., Tran, J., Master, Z., Chen, S., *et al.* (2005). A cyclosporine-sensitive psoriasis-like disease produced in Tie2 transgenic mice. Am J Pathol *166*, 843-855.

Vuoriluoto, K., Jokinen, J., Kallio, K., Salmivirta, M., Heino, J., and Ivaska, J. (2008). Syndecan-1 supports integrin alpha2beta1-mediated adhesion to collagen. Exp Cell Res *314*, 3369-3381.

Wang, F., Li, H.M., Wang, H.P., Ma, J.L., Chen, X.F., Wei, F., Yi, M.Y., and Huang, Q. (2010). siRNA-mediated knockdown of VEGF-A, VEGF-C and VEGFR-3 suppresses the growth and metastasis of mouse bladder carcinoma in vivo. Exp Ther Med *1*, 899-904.

Weis, S.M., and Cheresh, D.A. (2011). Tumor angiogenesis: molecular pathways and therapeutic targets. Nat Med *17*, 1359-1370.

Whiteford, J.R., Behrends, V., Kirby, H., Kusche-Gullberg, M., Muramatsu, T., and Couchman, J.R. (2007). Syndecans promote integrin-mediated adhesion of mesenchymal cells in two distinct pathways. Exp Cell Res *313*, 3902-3913.

Whiteford, J.R., and Couchman, J.R. (2006). A conserved NXIP motif is required for cell adhesion properties of the syndecan-4 ectodomain. J Biol Chem *281*, 32156-32163.

Whiteford, J.R., Ko, S., Lee, W., and Couchman, J.R. (2008). Structural and cell adhesion properties of zebrafish syndecan-4 are shared with higher vertebrates. J Biol Chem *283*, 29322-29330.

Whiteford, J.R., Xian, X., Chaussade, C., Vanhaesebroeck, B., Nourshargh, S., and Couchman, J.R. (2011). Syndecan-2 is a novel ligand for the protein tyrosine phosphatase receptor CD148. Mol Biol Cell *22*, 3609-3624.

Wong, A.L., Haroon, Z.A., Werner, S., Dewhirst, M.W., Greenberg, C.S., and Peters, K.G. (1997). Tie2 expression and phosphorylation in angiogenic and quiescent adult tissues. Circ Res *81*, 567-574.

Woods, A., and Couchman, J.R. (1994). Syndecan 4 heparan sulfate proteoglycan is a selectively enriched and widespread focal adhesion component. Mol Biol Cell *5*, 183-192.

Woods, A., and Couchman, J.R. (2001). Syndecan-4 and focal adhesion function. Curr Opin Cell Biol *13*, 578-583.

Woods, A., Couchman, J.R., Johansson, S., and Hook, M. (1986). Adhesion and cytoskeletal organisation of fibroblasts in response to fibronectin fragments. EMBO J *5*, 665-670.

Xian, X., Gopal, S., and Couchman, J.R. (2010). Syndecans as receptors and organizers of the extracellular matrix. Cell Tissue Res *339*, 31-46.

Xu, J., Park, P.W., Kheradmand, F., and Corry, D.B. (2005). Endogenous attenuation of allergic lung inflammation by syndecan-1. J Immunol *174*, 5758-5765.

Xu, K., Sacharidou, A., Fu, S., Chong, D.C., Skaug, B., Chen, Z.J., Davis, G.E., and Cleaver, O. (2011). Blood vessel tubulogenesis requires Rasip1 regulation of GTPase signaling. Dev Cell *20*, 526-539.

Yang, Y., Macleod, V., Miao, H.Q., Theus, A., Zhan, F., Shaughnessy, J.D., Jr., Sawyer, J., Li, J.P., Zcharia, E., Vlodavsky, I., *et al.* (2007). Heparanase enhances syndecan-1

shedding: a novel mechanism for stimulation of tumor growth and metastasis. J Biol Chem *282*, 13326-13333.

Yoneda, A., Lendorf, M.E., Couchman, J.R., and Multhaupt, H.A. (2012). Breast and ovarian cancers: a survey and possible roles for the cell surface heparan sulfate proteoglycans. J Histochem Cytochem *60*, 9-21.

Yuan, F., Chen, Y., Dellian, M., Safabakhsh, N., Ferrara, N., and Jain, R.K. (1996). Time-dependent vascular regression and permeability changes in established human tumor xenografts induced by an anti-vascular endothelial growth factor/vascular permeability factor antibody. Proc Natl Acad Sci U S A *93*, 14765-14770.

Yuan, H.T., Suri, C., Yancopoulos, G.D., and Woolf, A.S. (1999). Expression of angiopoietin-1, angiopoietin-2, and the Tie-2 receptor tyrosine kinase during mouse kidney maturation. J Am Soc Nephrol *10*, 1722-1736.

Yuan, L., Moyon, D., Pardanaud, L., Breant, C., Karkkainen, M.J., Alitalo, K., and Eichmann, A. (2002). Abnormal lymphatic vessel development in neuropilin 2 mutant mice. Development *129*, 4797-4806.

Zeeb, M., Strilic, B., and Lammert, E. (2010). Resolving cell-cell junctions: lumen formation in blood vessels. Curr Opin Cell Biol *22*, 626-632.

Zeng, Y., Adamson, R.H., Curry, F.R., and Tarbell, J.M. (2014). Sphingosine-1-phosphate protects endothelial glycocalyx by inhibiting syndecan-1 shedding. American journal of physiology Heart and circulatory physiology *306*, H363-372.

Zhang, D., Pier, T., McNeel, D.G., Wilding, G., and Friedl, A. (2007). Effects of a monoclonal anti-alphavbeta3 integrin antibody on blood vessels - a pharmacodynamic study. Invest New Drugs *25*, 49-55.

Zhang, L., Martelli, M.L., Battaglia, C., Trapasso, F., Tramontano, D., Viglietto, G., Porcellini, A., Santoro, M., and Fusco, A. (1997). Thyroid cell transformation inhibits the expression of a novel rat protein tyrosine phosphatase. Experimental Cell Research *235*, 62-70.

Zhang, Y., Pasparakis, M., Kollias, G., and Simons, M. (1999). Myocyte-dependent regulation of endothelial cell syndecan-4 expression. Role of TNF-alpha. J Biol Chem *274*, 14786-14790.

Zhou, M., Sutliff, R.L., Paul, R.J., Lorenz, J.N., Hoying, J.B., Haudenschild, C.C., Yin, M., Coffin, J.D., Kong, L., Kranias, E.G., *et al.* (1998). Fibroblast growth factor 2 control of vascular tone. Nat Med *4*, 201-207.

Zhu, J.W., Doan, K., Park, J., Chau, A.H., Zhang, H., Lowell, C.A., and Weiss, A. (2011). Receptor-like tyrosine phosphatases CD45 and CD148 have distinct functions in chemoattractant-mediated neutrophil migration and response to S. aureus. Immunity *35*, 757-769.

Ziegler, W.H., Gingras, A.R., Critchley, D.R., and Emsley, J. (2008). Integrin connections to the cytoskeleton through talin and vinculin. Biochemical Society transactions *36*, 235-239.

Zimmermann, P., Zhang, Z., Degeest, G., Mortier, E., Leenaerts, I., Coomans, C., Schulz, J., N'Kuli, F., Courtoy, P., and David, G. (2005). Syndecan recycling [corrected] is controlled by syntenin-PIP2 interaction and Arf6. Dev Cell *9*, 377 - 388.

Zygmunt, T., Gay, C.M., Blondelle, J., Singh, M.K., Flaherty, K.M., Means, P.C., Herwig, L., Krudewig, A., Belting, H.G., Affolter, M., *et al.* (2011). Semaphorin-PlexinD1 signaling limits angiogenic potential via the VEGF decoy receptor sFlt1. Dev Cell *21*, 301-314.

Review Article

Novel Insight Into the Biological Functions of Syndecan Ectodomain Core Proteins

Giulia De Rossi
James R. Whiteford*

Centre for Microvascular Research, William Harvey Research Institute, Barts and the London School of Medicine and Dentistry, Queen Mary University of London, Charterhouse Square, London EC1M 6B, UK

Abstract

Syndecans are a four member family of multifunctional transmembrane heparan sulphate bearing cell surface receptors. Each family member has common molecular architecture but a distinct expression profile. Numerous molecular interactions between syndecan heparan sulphate chains, growth factors, cytokines, and extracellular matrix molecules have been reported and syndecans are intimately associated with cell adhesion and migration. Here, we describe the important emerging concept that contained within syndecan extracellular core proteins are "adhesion regulatory domains." Cell adhesion is driven by the integrins and syndecan ectodomain adhesion regulatory domains can alter integrin driven cellular responses. Cell adhesion and migration is central to numerous pathologies and an understanding of how syndecan ectodomains influence integrins will lead to novel therapeutic strategies. © 2013 BioFactors, 00(00):000–000, 2013

Keywords: *syndecan; extracellular matrix; heparan sulphate; proteoglycan; cell adhesion*

1. Introduction

1.1. The Syndecan Family

Syndecans are type I transmembrane heparan-sulphate proteoglycan (HSPG) cell surface receptors. In invertebrates, the syndecan family is represented by one member, while mammals have four with different tissue- and cell-specific expression profiles: syndecan-1 is highly expressed on epithelial and endothelial cells, monocytes, and fibroblasts, syndecan-2 is the principal syndecan of mesenchymal cells, syndecan-3 is present mostly in the nervous system, and syndecan-4 appears ubiquitously expressed but at lower levels (Fig. 1a) [1–3].

Syndecans have roles in cell adhesion, migration, proliferation, and growth factor signaling and through these functions contribute to important processes such as morphogenesis, wound healing, angiogenesis, and tumor development. Many of these activities are mediated by syndecan heparan-sulphate (HS) chains, due to their interactions with a wide range of molecules, including extra-cellular matrix (ECM) components, growth factors, chemokines and cytokines, enzymes, and so forth. Syndecans lack an intrinsic enzymatic activity, however, their cytoplasmic domains have several binding partners, including phospho-lipids and kinases important for cell adhesion and migration as well as forming a link between the ECM and the actin cytoskeleton [4,5].

Syndecan family members contain a shared molecular architecture. All possess a short highly conserved cytoplasmic domain which can be further divided into three sub-domains, the highly conserved C1 (membrane proximal) and C2 (membrane distal) flank a V region. The V region sequence is distinct for each of the four syndecan family members and may confer distinct functional characteristics for each molecule. The C2 sub-domain has a canonical PDZ binding motif, and is known to interact with several PDZ proteins including syntenin and is of importance particularly with regard to syndecan trafficking [6]. Syndecans exist on the cell surface as dimers and the formation of these is driven mainly through residues contained within the single pass syndecan transmembrane domain. The extracellular core proteins of syndecans range in size from 122aa (murine syndecan-4) to the largest 398aa (murine syndecan-3). There is very little conserved sequence

Address for correspondence to: James R. Whiteford, Ph.D., Centre for Microvascular Research, William Harvey Research Institute, Barts and the London School of Medicine and Dentistry, Queen Mary University of London, Charterhouse Square, London EC1M 6B, United Kingdom. Tel.: 0044(0)2078828241. Fax: 0044(0)207 882 8257; E-mail: j.whiteford@qmul.ac.uk.

Received 9 January 2013; accepted 18 February 2013

DOI: 10.1002/biof.1104

Published online in Wiley Online Library (wileyonlinelibrary.com)

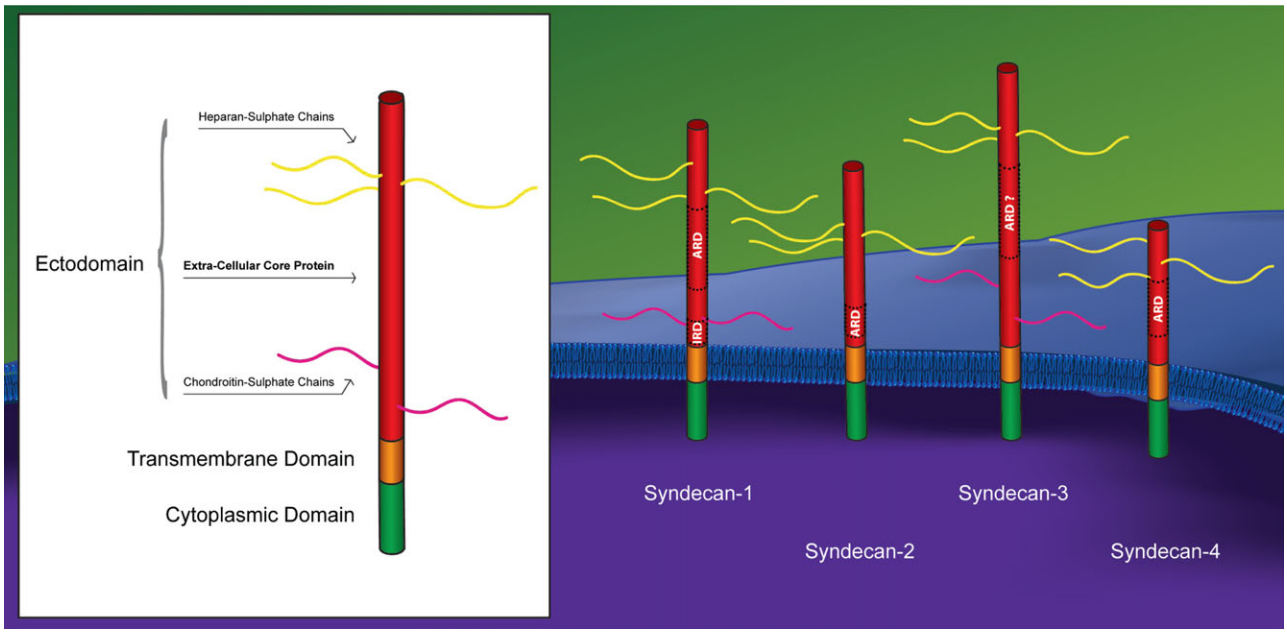

FIG 1

The syndecan family has adhesion regulatory domains within their extracellular core protein. (a) The syndecan family has four members each with a short cytoplasmic domain (green), a transmembrane domain (orange), and an ectodomain (red). (b) Adhesion regulatory domains (ARD) have been identified in the extracellular core proteins of syndecan-1, −2, and −4. In addition an invasion regulatory domain (IRD) has also been identified in syndecan-1.

between syndecan family member ectodomains, however, all four syndecans have Serine residues contained within Ser-Gly motifs situated toward the N-terminus to which HS (and in some cases chondroitin sulphate or dermatan sulphate) are covalently linked. HS is a complex polysaccharide consisting of repeating disaccharides (glucuronic acid and *N*-acetylglucosamine) which can form chains of up to 150 repetitions. HS chains can be sulfated by the action of several transferases during its biosynthesis which results in HS having a heterogeneous structure consisting of alternating high and low sulfated regions. The extent to which HS is sulfated can vary depending on tissue and cell type which also has ramifications for the functionality of HSPGs in any given tissue (for reviews see Refs. [7,8]).

The purpose of this review is to explore the biological roles that have been identified for syndecan ectodomain core proteins. There is a considerable body of work detailing syndecan HS interactions and the role of the full length molecule in pathology and development. These are briefly summarized in the subsequent sections, however, the main focus will be to examine the novel concept that regulatory protein sequences exist in syndecan ectodomains which can influence cell responses, particularly cell adhesion.

1.2. Syndecan Roles in Mammalian Development and Disease

Transgenic animals in which syndecans have either been deleted or their expression modified are viable, fertile, develop normally, and have no gross abnormalities. However, distinct phenotypes are observed in these animals after challenge or insult. For example, syndecan-1 null mice are more resistant to wnt-1 induced mammary tumorigenesis and show increased resistance to intranasally administered *P. aeruginosa* [9,10]. In models of inflammation syndecan-1 null mice also show enhanced leukocyte adhesion in both the retinal and mesenteric microvasculature and this enhanced leukocyte accumulation is associated with enhanced angiogenesis [11]. Syndecan-1 has also been shown to attenuate allergic inflammation in the lung. Airway epithelium detects allergenic adjuvants and secretes chemokines that specifically recruit Th2 immune cells to the site of inflammation; deletion of syndecan-1 promotes Th2 recruitment and ag-specific IgE responses. Moreover, allergens trigger ectodomain shedding leading to binding of CC chemokines inhibiting CCL-11 and −17-mediated T-cell migration [12]. Syndecan-1 is abundant on stratified epithelia and given its role in cell migration, several studies have been conducted to assess its role in wound healing. Corneal debridement wounds in syndecan-1 null mice re-epithelized slower than wild type controls, although more inflammatory cells were found beneath the wounds. In wildtype mice there is an increase in epithelial cell proliferation after wounding which decreases after 48 H, in contrast syndecan-1 null epithelial cells exhibit enhanced proliferation rates but this does not change in response to wounding [13]. Mice in which syndecan-1 is over-expressed in all tissues also exhibit delayed wound healing and this provides evidence that syndecan function may be dependent on gene dosage effects [14]. Evidence is

also accumulating that there is a correlation between decreased syndecan-1 expression and bad prognosis in poorly differentiated malignant tumors [15].

To date no mouse null for syndecan-2 has been reported, however, in zebrafish reduced expression of syndecan-2 leads to defects in sprouting angiogenesis and in *xenopus* there is a role for syndecan-2 in left/right axis formation [16,17].

Syndecan-3 is mainly expressed in the nervous system; interestingly, its loss doesn't affect mouse development, in particular basal synaptic transmission in hippocampus is comparable to that of wild types. However, syndecan-3 KO mice show an increased long-term potentiation (LTP) in the CA1 pyramidal neurons area of the hippocampus and impaired hippocampus-dependent memory, suggesting a role for syndecan-3 in suppressing LTP (probably through a mechanism involving heparin-binding growth-associated molecules (HB-GAM)) and in modulating hippocampus memory [18]. Syndecan-3 also has roles in regulating feeding behavior and body weight and can potentiate the activity of Agouti related protein or AgRP (an antagonist of melacortin) and therefore regulate the circuit of α-MSH (α-melanocyte stimulating hormone) and AgRP in the hypothalamus [14]. A balance between the activities of orexigenic AgRP and the anorexigenic α-MSH neurons regulate food intake, therefore, it is not surprising that the feeding behavior of syndecan-3 null mice differ from their wildtype counterparts [19]. Syndecan-3 null mice are hypersensitive to α-MSH and exhibit increased activation of melanocortin neurons, probably because in the hypothalamic paraventricular nuclei (PVN) AgRP expression is reduced, suggesting that syndecan-3 may have a role in the localization of AgRP in this hypothalamic area [20].

In common with syndecan-1 null mice, syndecan-4 null animals exhibit impaired wound healing. Syndecan-4 is expressed at low levels in all adherent cells but is up-regulated in the granulation tissue on endothelial cells and fibroblasts during wound healing [21]. Excisional wounds on syndecan-4 null mice healed significantly slower than in wild type controls and the granulation tissue is less vascularized. Syndecan-4 is intimately associated with cell adhesion and migration and syndecan-4 fibroblasts migrate slower and have both focal adhesion and cytoskeletal defects [22,23]. Syndecan-4 null mice are more susceptible to septic shock (induced by LPS) and this is thought to be related to interactions between syndecan-4 and TGFβ [24]. Syndecan-4 is known to modulate the activity of certain MMPs and this is reflected in the null mice which are more resistant to destruction of articular cartilage in models of osteoarthritis [25].

1.3. Syndecans as ECM Receptors

HS is known to interact with numerous ECM components such as fibronectin, collagens, tenascins, fibrillins, and laminins and key roles for syndecans have been identified during cellular interactions with these matrix components. The best characterized of these is the interaction between Fibronectin and the HS chains of syndecan-4 during fibroblast adhesion. Engagement of syndecan-4 HS chains leads to receptor clustering which results in the up-regulation of a PKCα dependant signaling pathway leading to cytoskeletal rearrangements and changes in the activation state of small GTPases such as RhoA and Rac1. This process occurs in conjunction with $\alpha 5\beta 1$ integrin signaling. Syndecans and integrins are intimately linked during ECM interactions and it seems likely that syndecan signaling can modulate integrin responses under these circumstances (Fig. 2), [for reviews see Refs. 5,7].

1.4. Syndecans as Growth Factor Co-Receptors

Growth factors such as VEGF, FGF, TGFβ, and PDGF are all known to interact with HS and there is strong evidence that syndecan-1, −2,and −4 contribute to the presentation of FGF to its receptor [26,27]. Furthermore, syndecan-2 has been shown to promote the interaction of VEGF165 with VEGFR2 [28]. Many chemokines and cytokines also possess putative HS binding motifs within their primary sequence and it is likely that syndecans also have a role in facilitating their ligand interactions. This is true of syndecan-1 HS chains which have been shown to engage CCL7, CCL11, and CCL17 which affects T-cell responses in allergic disease [12]. Studies on invertebrate syndecan have also shown that syndecan HS chains are also important for establishing gradients for morphogens which are essential for normal development and patterning (Fig. 2) [29].

1.5. Syndecan Shedding

Of importance is the fact that syndecan ectodomains can be shed from the cell surface by the action of MMPs. This process is thought to occur for a number of reasons, first shedding of cell surface syndecan results in the removal of growth factors and cytokines associated with the syndecan HS. Additionally, syndecan shedding will also result in the release of cells at points of adhesion between the cell and the ECM, leading to a more migratory cellular phenotype. It has also been suggested that the shed syndecan moiety could compete for ligands with its membrane anchored counterpart. It is also emerging that the core proteins of syndecan ectodomains have cell adhesion regulatory domains and these could exert their effects on cells as mobile effectors of cellular responses in the ECM (Fig. 2, for review see Refs. [30]).

2. Syndecan Ectodomains

It has been generally accepted that the extracellular core proteins of syndecans provide only an inert support for GAG chains and that all syndecan extracellular interactions are mediated by HS rather than the core protein. However, recent discoveries indicate that syndecan ectodomain core proteins have biological functions and can modulate cell behavior independent of HS. These adhesion regulatory sequences have been proposed to act with both autocrine and paracrine mechanisms (Fig. 3) and could well represent novel targets for

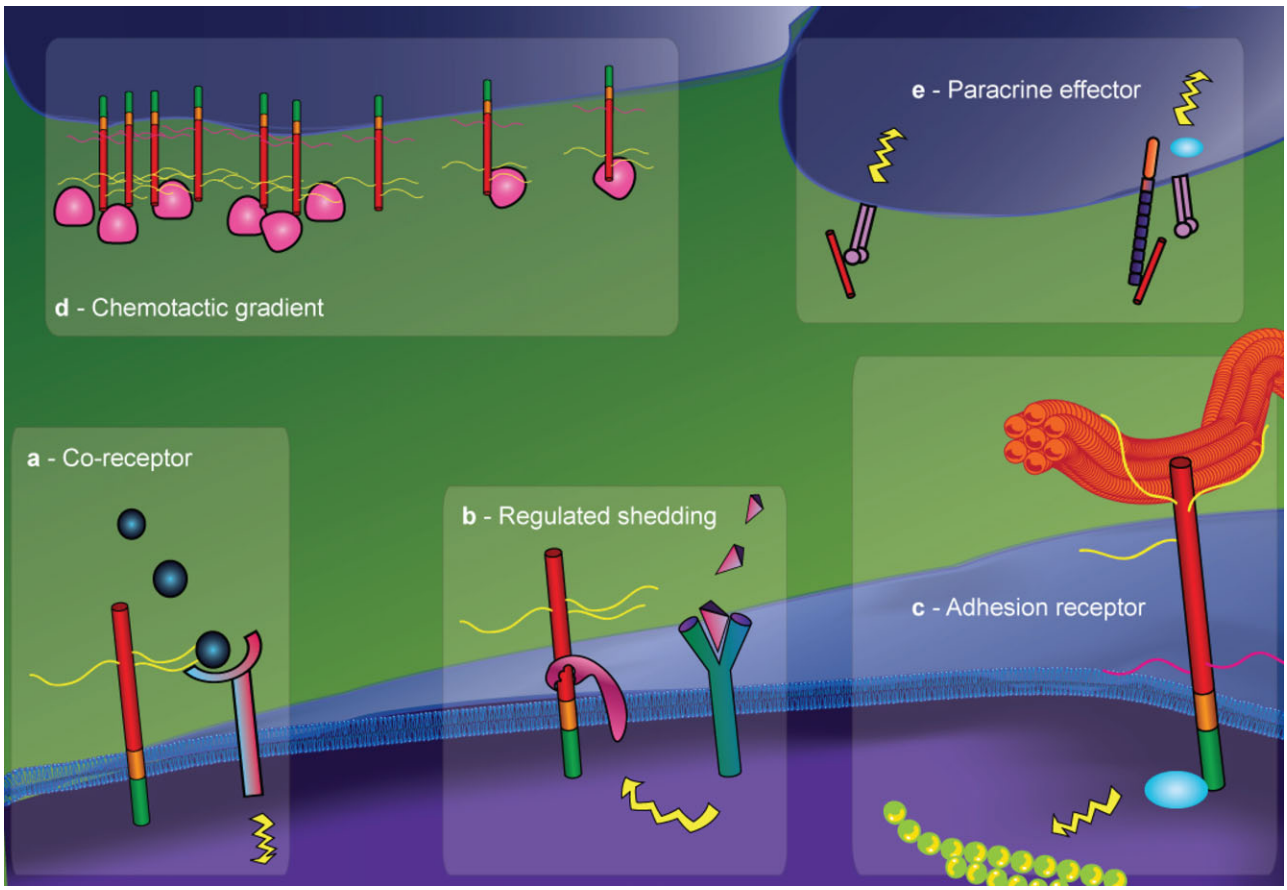

FIG 2 *Modes of action for syndecans. Syndecans can act as growth factor co-receptors (a), can be shed from the cell surface by the regulated action of proteases (b), can be act as adhesion receptors linking the ECM with the cytoskeleton (c), and finally can act as a paracrine effector of cell responses.*

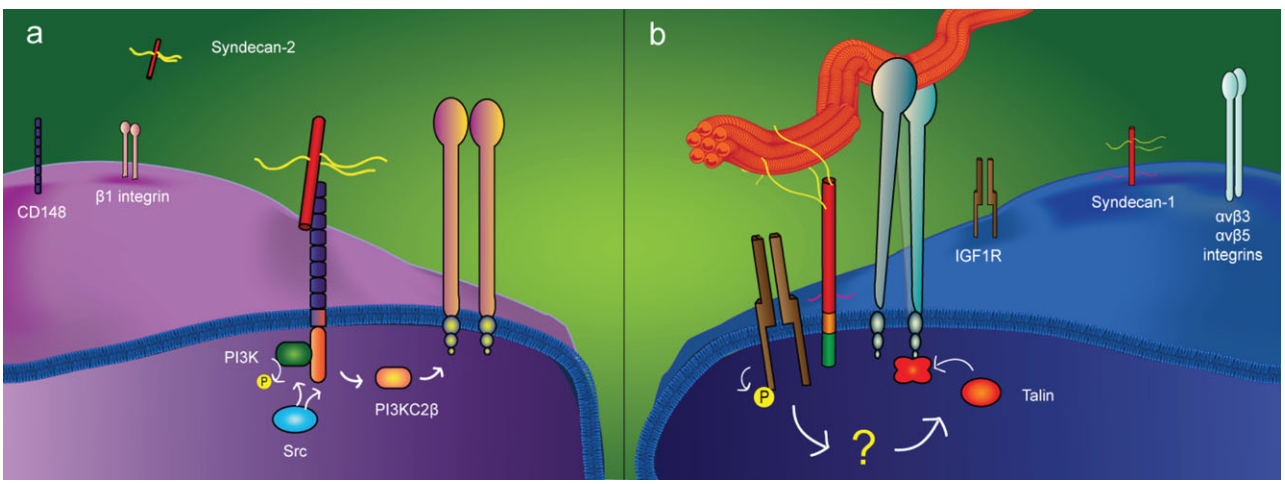

FIG 3 *Syndecan adhesion regulatory domains signal to integrins in a paracrine and autocrine fashion. (a) Shed syndecan-2 ectodomain acts as a mobile ligand for the protein tyrosine phosphatase receptor CD148. CD148 signals via isoforms of PI3 kinase to β1 integrin leading to changes in cell adhesion and migration. (b) Syndecan-1 forms a complex with IGF1R and αVβ3 or αVβ5 integrin leading to changes in integrin activation state.*

therapeutic interventions, particularly in diseases such as cancer. The purpose of the remainder of this review is to summarize the evidence demonstrating the importance of cell adhesion and migration regulatory domains present in syndecan extracellular core proteins and how these might be used as novel factors to treat disease.

2.1. Syndecan-1 Ectodomain

The first evidence that the syndecan-1 ectodomain core protein has biological function came from studies with mouse mammary tumor cells. A truncated mutant form of syndecan-1 lacking both the transmembrane and cytoplasmic domains was expressed in S115 (Shionogi 115) cells which resulted in soluble glycanated syndecan ectodomain being secreted into the culture medium. S115 cells lose their epithelioid morphology and become more proliferative when treated with testosterone, and this is thought to correlate with tumor growth. Interestingly, testosterone treatment results in a reduction in syndecan-1 expression in S115 cells. The epithelioid morphology of these cells could be restored by the addition of conditioned media containing the soluble syndecan-1 ectodomain to testosterone treated cells. This effect was found to be HS dependent but a role for the core protein was suggested since the addition of HS or heparin alone failed to restore the phenotype. Soluble syndecan-1 ectodomains also appeared to suppress tumor growth in soft agar colony formation assays [31].

Syndecan-1 expression correlates with a reduction in the invasiveness of cells into Collagen I matrices. The Human B lymphoid cell line ARH77 expresses very low levels of syndecan-1 and indeed other HSPGs, and is highly invasive. Expression of syndecan-1 in these cells inhibits migration through collagen I gels and this effect is HS dependent [32]. However, it also emerges that there is also an "invasion regulatory domain" mapped to an AVAAV sequence (aa 222–226) on the extracellular core protein of murine syndecan-1 [33]. ARH77 cells transfected with a mutant cDNA in which this motif had been deleted migrated faster through Collagen I gels than cells transfected with full length syndecan-1. Glypicans are another group of cell surface heparan sulphate bearing proteoglycans. Unlike syndecans they are linked to the cell surface by a glycosylphosphatidylinositol (GPI) anchor and do not possess a cytoplasmic domain. Chimeric proteins consisting of the glypican-1 extracellular core protein and the syndecan-1 cytoplasmic domain or the syndecan ectodomain fused to the glypican-1 GPI anchor were expressed in ARH77 cells and the effects on invasion determined. Cells expressing the glypican-1 ectodomain and the syndecan-1 cytoplasmic domain were as invasive as wild type cells, however, cells expressing the GPI-anchored form of syndecan-1 exhibited the same inhibited invasiveness that is characteristic of cells expressing full length syndecan-1 [34]. This data suggests that the syndecan-1 cytoplasmic domain is not required for the antimigratory properties of syndecan-1 and that the key determinants are a combination of the HS chains and regulatory motifs contained within the extracellular core protein.

The human lymphoblastic Raji suspension cell line does not express syndecan-1 but attaches and spreads on HS binding matrix substrates such as thrombospondin and fibronectin when transfected with full length syndecan-1. Attachment and spreading to these substrates is not dependent on the syndecan-1 cytoplasmic domain since cells expressing cytoplasmic domain deletion mutants attached and spread normally. Interestingly, attachment and spreading in Raji cells expressing syndecan-1 could also be observed in cells seeded on immobilized antibodies which recognize the syndecan-1 ectodomain and these effects could be observed even after treatment with heparanases. This suggests that the syndecan-1 core protein interacts with other cell surface receptors, leading to the formation of adhesion regulatory complexes [35].

Integrins are the key drivers of cell adhesion and migration and can exist in different activation states on the cell surface. Activated integrins are more able to engage their ECM ligands and the extent to which an integrin can be activated can be modulated by other cell surface receptors. For this reason, integrins were hypothesized to form part of the adhesion regulatory complexes stimulated by syndecan-1 extracellular domain clustering with antibodies. Some studies suggested that syndecans can trigger signaling leading to cell spreading either by exposing binding sites on fibronectin for ß1 integrin engagement [36] or by modulating the activation state of the β1 integrin [37]. However, evidence linking the syndecan-1 extracellular core protein with $\alpha V\beta 3$ integrin emerged from studies in which human mammary carcinoma cells (MDA-MB-231) were seeded on immobilized syndecan-1 antibodies. MDA-MB-231 cell adhesion to this antibody substratum resulted in the activation of αVß3 integrin and this could be inhibited by syndecan-1 extracellular fusion protein fused to GST [38]. This work implies that syndecan-1 interacts with integrins directly or indirectly on the cell surface via its extracellular core protein. The association between the syndecan-1 ectodomain and $\alpha V\beta 3$ driven cell adhesion is supported further by the fact that the syndecan-1 ectodomain is required for MDA-MB-231 cell spreading in response to vitronectin. Using deletion mutant forms of cDNA it was possible to establish that the amino acids lying between aa88 and aa252 (of murine syndecan-1) were required for the cell spreading response. This leads to the hypothesis that engagement of syndecan-1 by the ECM is a precursor step necessary for $\alpha V\beta 3$ activation and subsequent cell spreading in epithelial cells [39].

In later work, the question of what the effect of providing a native matrix ligand such as vitronectin or fibronectin on the adhesion responses of MDA-MB-231 cells was addressed. It was shown that syndecan-1 is directly responsible for cell spreading on vitronectin (but not on fibronectin) via activation of αVß3. Moreover, since the addition of soluble syndecan-1 ectodomain or transfection with a mutant form of syndecan-1 lacking a portion of the ectodomain (mS1Δ88–252) inhibits cell spreading on vitronectin, implying that the syndecan-1 extracellular core protein interacts with a partner on the cell surface to activate αVß3 integrin. This work resulted in a model

defined by the following features: in epithelial cells, syndecan-1 must engage a matrix ligand before triggering the activation of αVß3 leading to cell spreading, this mechanism is dependent on an unknown interaction mediated by motifs contained within the syndecan-1 ectodomain and is specific for αVß3 integrin [38].

Interactions between the syndecan-1 ectodomain and another integrin dimer αVβ5 have also been reported. Fibroblasts (B82L) were shown to spread in response to anti syndecan-1 ectodomain antibodies and this effect could be enhanced by the addition of serum. Further investigation revealed that B82L cell spreading on native matrix ligand ± anti-syndecan-1 ectodomain antibodies is dependent on αVß5 integrin and that the syndecan-1 ectodomain, independent of its HS chains or transmembrane and cytoplasmic domains, forms a complex with ß5 and that is sufficient and necessary to promote spreading [40,41].

This model is similar to that proposed for the regulation of αVß3 in epithelial cells [39] although they differ for some features: in B82L syndecan-1 is probably constitutively associated with ß5 through its extracellular core protein, only if integrin is in complex with the syndecan-1 ectodomain can it signal upon binding to vitronectin or fibronectin; in epithelial cells the engagement of syndecan-1 with a substratum (through its HS chains) is necessary to bring S1ED and αVß3 together in a complex and signal; in this case αVß3, unlike αVß5 in fibroblasts, does not require a ligand [42].

Given the importance of αVß3 and αVß5 integrins in angiogenesis, the possibility that syndecan-1 regulates these integrins in vascular endothelial cells has been investigated. Previously, it was shown that a GST-sydecan-1 fusion protein could block activation of αVß3 in MDA-MB-231 cells and, by doing so, spreading on vitronectin (spreading on fibronectin wasn't affected because the cells also express αVß1 [39]. The minimum sequence necessary to mediate this effect corresponds to aa82 to aa130 of the syndecan extra-cellular core protein and this region was required in order to co-immunoprecipitate αVβ3. Peptides corresponding to this region (termed synstatin) inhibit adhesion and spreading of B82L fibroblasts on vitronectin, which is mediated only by αVß5.

Syndecan-1, αVβ3, and αVβ5 are all expressed on endothelial cells and are also present on angiogenic sprouts derived from aortic rings seeded *ex vivo* in ECM. Treatment of rings with synstatin lead to a reduction in the angiogenic response and this was also the case in corneal angiogenesis models. The inhibition of angiogenesis has long been thought of as an attractive target for therapeutic intervention in cancer. In an orthotopic model of tumor formation in which MDA-MB-231 cells are subcutaneously injected into mice, synstatin treatment resulted in tumors considerably smaller than the untreated controls (Fig. 3) [41].

So does syndecan-1 activate integrin αVß3 and αVß5 by stabilizing its extracellular structure or does it mediate an inside-out signal? Treatment of MDA-MB-231 cells with metabolic inhibitors showed that syndecan-1-mediated integrin activation is energy-dependent and, by the use of different kinase inhibitors, it became clear that insulin-like growth factor-1 receptor (IGF1R) is involved in this process. In the model proposed by Beauvais and Rapraeger, syndecan-1 is clustered via engagement with vitronectin, interacts with αVß3 and ß5 integrin through its ectodomain and this complex is then able to engage with IGF1R. The formation of the syndecan-1/integrin/IGF1R is an essential step for later events and is required for IGF1R autophosphorylation on Y1131, subsequent activation of talin leading to inside out integrin activation (Fig. 3) [43].

There is also evidence that interactions with the syndecan-1 ectodomain can also lead to β1 integrin mediated effects. To mimic syndecan-1 over-expression often seen in breast carcinomas *in vivo,* three different human breast carcinoma cell lines were transfected with syndecan-1. The effect of syndecan-1 over-expression was unexpected in that cells which usually grow as adherent cohesive epithelial islands, spread poorly and assumed a rounded morphology in 2D culture and were more invasive in 3D culture. This was observed even when mutants were expressed lacking the GAG chains, transmembrane or cytoplasmic domains. Only cells expressing syndecan-1 lacking the ectodomain residues aa88–aa252 exhibited a wild type morphology. Moreover, the syndecan-1-dependent morphology change could be blocked by genistatin (a protein tyrosine kinase inhibitor), which is strongly indicative of the involvement of a signal transduction pathway. To determine whether the syndecan-1 extracellular core protein can interfere with adhesion-mediated signals, cells expressing a GPI-anchored form of the syndecan-1 ectodomain were tested for their ability to attach and spread on either E-cadherin or laminin-5. Cell attachment to laminin was disrupted in these cells confirming that the interactions with the syndecan-1 ectodomain could block β1 mediated adhesion pathways [40]. More recent evidence suggests there is an interaction between integrin $\alpha 2\beta 1$ and syndecan-1 via its extracellular core protein in bronchial epithelial cells. In this instance, syndecan-1 ectodomain promotes cell adhesion through activating β1 integrin [44].

2.2. Syndecan-2 Ectodomain

While in normal epithelium syndecan-2 is usually expressed at low levels, during epithelial cancer progression its expression increases; this is in contrast to syndecan-1 and syndecan-4 which for the most part exhibit reduced expression in malignancies. In colon carcinoma, for instance, syndecan-2 is highly expressed on tumor cells (both highly and weakly metastatic) when compared with normal colon cell lines. Speculation as to whether this HSPG was responsible for the poor prognosis of this tumor, led to the finding that the syndecan-2 ectodomain has specific roles in adhesion and tumorogenicity of epithelial cancer cells. Not only does recombinant syndecan-2 ectodomain (HS free) inhibit tumor cell attachment to the ECM, but it can also promote cell cycle arrest through an up-regulation of p53, p21, and p27 and down-regulation of cyclin E and D2.

Moreover, the addition of soluble syndecan-2 ectodomain to the medium of colon cancer cells inhibits EGF-mediated mitogen-activated protein kinase activation which is critical for the growth of many tumors [45].

Roles for syndecan-2 have also been identified in fibrosis. TGF-ß is a growth factor with multiple roles, among which is the ability to promote fibrosis by up-regulating matrix proteins and metalloproteinase inhibitors and down-regulating metalloproteinases. As a ligand, it binds and signals upon forming a complex with TGF-ß R I, II, and III. The latter (also known as ß-glycan) binds TGF-ß and transfers it to TGF-ß R II and, intriguingly, is a cell surface proteoglycan with very similar characteristics to syndecan-2. Since syndecan-2 controls left-right axis asymmetry in *Xenopus* through TGF-ß, a role for syndecan-2 in TGF-ß-induced fibrosis was suggested. Syndecan-2 was indeed found to regulate TGF-ß mediated matrix deposition via its cytoplasmic domain which is fundamental for its interaction with TGF-ß R III. Additionally, syndecan-2 in renal periphery fibroblasts was shown to interact with TGF-ß via its ectodomain (and partially through its HS chains) independently of the presence of the cytoplasmic domain [46].

Experiments with a GST/syndecan-2 ectodomain protein on brain microvascular endothelial cells (MvEC) in the context of glioma revealed that addition of as little as 0.1 μM of the protein to medium containing brain MvEC induced an increase in cell migration and tube formation on both fibronectin and growth factor-reduced matrigel [47].

Further studies with GST/syndecan-2 ectodomain fusion proteins revealed that this protein could act as a substrate for cell adhesion when immobilized on to culture dishes. Assays with numerous cell lines suggested that adhesion to the syndecan-2 ectodomain was a feature of mesenchymal cells [48]. Epithelial cell lines fail to attach and spread in response to this substrate although it was later found that this could be overcome if the cells were treated with neuraminidase, indicating that N-linked sugars are important in mediating this interaction [49]. Fibroblast attachment and spreading in response to GST/syndecan-2 ectodomain substrates is characterized by the formation of focal adhesions. Molecules associated with focal adhesion formation such as focal adhesion kinase and paxillin undergo phopshorylation and there is a requirement for RhoA and Rho kinase. Most striking is that cell adhesion to the syndecan-2 ectodomain has an absolute requirement for β1 integrin. A direct interaction between the syndecan-2 ectodomain and β1 integrin could not be demonstrated indicating that an intermediary receptor was required for this interaction [48].

Further characterization of the processes driving fibroblast attachment to the syndecan-2 ectodomain revealed that the adhesion regulatory motif on the syndecan-2 ectodomain lies in the membrane proximal region aa 124–141. The protein tyrosine phosphatase receptor CD148 was found to be the intermediary molecule which mediates the interaction with the syndecan-2 ectodomain and β1 integrin. In this study it was shown that engagement of CD148 with the syndecan-2 ectodomain lead to de-phopshorylation of the p85 subunit of PI3 kinase. This signal initiates a pathway involving Src kinase, and PI3KC2β (a novel isoform of PI3K) leading to inside out β1 integrin mediated cell adhesion (Fig. 3 [49]).

2.3. Syndecan-3 Ectodomain

Whether the syndecan-3 ectodomain has biological properties remains unclear. Adhesion assays with human dermal fibroblasts, Swiss 3T3 and NIH 3T3 on immobilized GST fused to the syndecan-3 ectodomain suggested that this protein could not support the cell attachment and spreading responses seen with the syndecan-1, −2, and −4 ectodomians [50]. However, the syndecan-3 ectodomain is unique as it possesses a mucin rich domain which may be extensively substituted with *O*-linked sugars and confer novel functionality [51]. Experiments to date have utilized fusion proteins expressed in bacteria which would not be post-translationally modified in the same way as if they were expressed in eukaryotic cells.

2.4. Syndecan-4 Ectodomain

As is the case with the syndecan-2, the syndecan-4 ectodomain when expressed as a GST fusion protein is a substrate for cell adhesion. Using fibroblast cell lines it was demonstrated that in the presence of divalent cations the syndecan-4 extracellular core protein is able to bind a cell surface receptor through a domain mapped to aa 56–109 [50,52]. Subsequent work isolated the key amino acids (NXIP) necessary for the syndecan-4 extracellular core protein to support cell adhesion and found that this motif is functionally conserved amongst vertebrates [53,54]. Syndecans form SDS insoluble dimers and one possible hypothesis is that immobilized ectodomain interacts with endogenous syndecan-4 on cells resulting in cell adhesive signals driven by full length syndecan-4 clustering. However, fibroblasts null for syndecan-4 attach and spread in the same manner as wild type cells when seeded on immobilized GST syndecan-4 fusion protein, indicating that cell surface receptors other than syndecan-4 are required for this adhesion response [48]. Like syndecan-2 adhesion to syndecan-4 is a characteristic of mesenchymal cells and some leukocytic cell lines after stimulation with phorbol ester and there is an absolute requirement for β1 integrin. In addition GST-syndecan-4 ectodomain can promote focal adhesion formation in fibroblasts in a Rho and Rho kinase dependant process. Jurkat T-cell adhesion to the syndecan-4 ectodomain requires $\alpha 4\beta 1$ integrin however solid phase binding assays between recombinant $\alpha 4\beta 1$ and GST-syndecan-4 ectodomain revealed that there was no direct interaction between these two molecules which led to speculation that an alternative receptor may be involved [48]. Screening with siRNA revealed that the protein tyrosine receptor CD148 may have a role in this process [49].

3. Discussion

Syndecans are involved in many aspects of cell behavior such as adhesion, cell spreading, migration, proliferation, and

morphology changes. Despite that, animals lacking one syndecan are viable and with no gross abnormalities, suggesting that syndecan loss is probably compensated during development. Nonetheless, when animals null for a syndecan are challenged with pathological stimuli, dramatic phenotypes are observed. Considerable attention has been focused on interactions between syndecan HS chains and numerous bioactive molecules such as chemokines, growth factors, and ECM components. There is considerable evidence that these interactions can contribute to syndecan signaling leading to changes in cell behavior. In this review, we have described a more novel aspect of syndecan biology relating to the biological properties of domains within the syndecan extracellular core protein. For the most part these molecular interactions occur independent of the HS chains. An adhesion regulatory domain within the syndecan-1 ectodomain has been shown to interact with both $\alpha V\beta 3$ and $\alpha V\beta 5$ integrins forming a complex with Insulin like growth factor receptor 1 (IGFR1). An autocrine interaction as described for syndecan-1 is thought to be a key priming step for cellular interactions with extracellular matrix ligands and blockade of this process can affect important processes such as angiogenesis. Similar effects on cell adhesion are observed in studies on adhesion regulatory domains contained within the syndecan-2 and −4 extracellular core proteins. In this instance a paracrine interaction is proposed in which syndecan-2 and −4 ectodomains are shed into the ECM and become mobilized ligands for the protein tyrosine phosphatase receptor CD148. CD148 signaling leads to $\beta 1$ integrin activation and alterations in cell adhesive properties.

Cell adhesion and migration and have vital roles in development and numerous pathologies and integrins are the key drivers of these processes. The fact that sequences contained within syndecan extracellular core proteins can modify or alter integrin mediated processes present them as possible agents for therapeutic use, indeed the synstatin peptide (derived from syndecan-1) has already been shown to have beneficial effects in tumor models. The amino acid sequences essential for the biological activities of syndecan-1, −2, and −4 have been mapped and they bear no homology to each other indicating that they may have different roles. To date the bulk of studies have focused on the effect of these syndecan adhesion regulatory domains in *in vitro* cell culture models. Attention should now focus on how these biologically active syndecan moieties affect biological processes *in vivo*. Syndecan adhesion regulatory domains affect cell behavior in a broad spectrum of cell types. Leukocytes have been shown to interact with the extracellular core proteins of syndecan-2 and −4 and it would be intriguing to see how these molecules affect processes associated with inflammation, such as leukocyte adhesion and extravasation. Furthermore the use of these proteins in tumor models should be further investigated. The body of work described here demonstrates that syndecan ectodomains are not simply structural moieties whose only role is to support syndecan HS chains but important molecules with great potential for therapeutic use in numerous pathologies.

Acknowledgements

JW is supported by Arthritis Research-UK (grant no. 19207) and the William Harvey Research Foundation. GDR is supported by Queen Mary University of London, Bart and the London School of Medicine and Dentistry.

References

[1] Couchman, J. R. (2003) Syndecans: proteoglycan regulators of cell-surface microdomains? Nat. Rev. Mol. Cell Biol. 4, 926–937.

[2] Kim, C. W., Goldberger, O. A., Gallo, R. L., and Bernfield, M. (1994) Members of the syndecan family of heparan sulfate proteoglycans are expressed in distinct cell-, tissue-, and development-specific patterns. Mol. Biol. Cell 5, 797–805.

[3] Couchman, J. R. (2010) Transmembrane signaling proteoglycans. Annu. Rev. Cell. Dev. Biol. 26, 89–114.

[4] Alexopoulou, A. N., Multhaupt, H. A., and Couchman, J. R. (2007) Syndecans in wound healing, inflammation and vascular biology. Int. J. Biochem. Cell Biol. 39, 505–528.

[5] Morgan, M. R., Humphries, M. J., and Bass, M. D. (2007) Synergistic control of cell adhesion by integrins and syndecans. Nat. Rev. Mol. Cell Biol. 8, 957–969

[6] Grootjans, J. J., Zimmermann, P., Reekmans, G., Smets, A., Degeest, G., Durr, J., and David, G. (1997) Syntenin, a PDZ protein that binds syndecan cytoplasmic domains. Proc. Natl. Acad. Sci. USA 94, 13683–13688

[7] Okina, E., Manon-Jensen, T., Whiteford, J. R., and Couchman, J. R. (2009) Syndecan proteoglycan contributions to cytoskeletal organization and contractility. Scand. J. Med. Sci. Sports 19, 479–489.

[8] Multhaupt, H. A., Yoneda, A., Whiteford, J. R., Oh, E. S., Lee, W., et al. (2009) Syndecan signaling: when, where and why? J. Physiol. Pharmacol. 60 (Suppl 4), 31–38.

[9] Alexander, C. M., Reichsman, F., Hinkes, M. T., Lincecum, J., Becker, K. A., et al. (2000) Syndecan-1 is required for Wnt-1-induced mammary tumorigenesis in mice. Nat. Genet. 25, 329–332.

[10] Park, P. W., Pier, G. B., Hinkes, M. T., and Bernfield, M. (2001) Exploitation of syndecan-1 shedding by *Pseudomonas aeruginosa* enhances virulence. Nature 411, 98–102.

[11] Gotte, M., Joussen, A. M., Klein, C., Andre, P., Wagner, D. D., et al. (2002) Role of syndecan-1 in leukocyte-endothelial interactions in the ocular vasculature. Invest. Ophthalmol. Visual. Sci. 43, 1135–1141.

[12] Xu, J., Park, P. W., Kheradmand, F., and Corry, D. B. (2005) Endogenous attenuation of allergic lung inflammation by syndecan-1. J. Immunol. 174, 5758–5765.

[13] Stepp, M. A., Gibson, H. E., Gala, P. H., Iglesia, D. D., Pajoohesh-Ganji, A., et al. (2002) Defects in keratinocyte activation during wound healing in the syndecan-1-deficient mouse. J. Cell Sci. 115, 4517–4531.

[14] Reizes, O., Lincecum, J., Wang, Z., Goldberger, O., Huang, L., et al. (2001) Transgenic expression of syndecan-1 uncovers a physiological control of feeding behavior by syndecan-3. Cell 106, 105–116.

[15] Teng, Y. H., Aquino, R. S., and Park, P. W. (2012) Molecular functions of syndecan-1 in disease. Matrix Biol. 31, 3–16.

[16] Chen, E., Hermanson, S., and Ekker, S. C. (2004) Syndecan-2 is essential for angiogenic sprouting during zebrafish development. Blood 103, 1710–1719.

[17] Kramer, K. L. and Yost, H. J. (2002) Ectodermal syndecan-2 mediates left-right axis formation in migrating mesoderm as a cell-nonautonomous Vg1 cofactor. Dev. Cell 2, 115–124.

[18] Kaksonen, M., Pavlov, I., Voikar, V., Lauri, S. E., Hienola, A., et al. (2002) Syndecan-3-deficient mice exhibit enhanced LTP and impaired hippocampus-dependent memory. Mol. Cell. Neurosci. 21, 158–172.

[19] Strader, A. D., Reizes, O., Woods, S. C., Benoit, S. C., and Seeley, R. J. (2004) Mice lacking the syndecan-3 gene are resistant to diet-induced obesity. J. Clin. Invest. 114, 1354–1360.

[20] Zheng, Q., Zhu, J., Shanabrough, M., Borok, E., Benoit, S. C., et al. (2010) Enhanced anorexigenic signaling in lean obesity resistant syndecan-3 null mice. Neuroscience 171, 1032–1040.

[21] Echtermeyer, F., Streit, M., Wilcox-Adelman, S., Saoncella, S., Denhez, F., et al. (2001) Delayed wound repair and impaired angiogenesis in mice lacking syndecan-4. J. Clin. Invest. 107, R9–R14.
[22] Ishiguro, K., Kojima, T., and Muramatsu, T. (2002) Syndecan-4 as a molecule involved in defense mechanisms. Glycoconj. J. 19, 315–318.
[23] Ishiguro, K., Kadomatsu, K., Kojima, T., Muramatsu, H., Tsuzuki, S., et al. (2000) Syndecan-4 deficiency impairs focal adhesion formation only under restricted conditions. J. Biol. Chem. 275, 5249–5252.
[24] Ishiguro, K., Kadomatsu, K., Kojima, T., Muramatsu, H., Iwase, M., et al. (2001) Syndecan-4 deficiency leads to high mortality of lipopolysaccharide-injected mice. J. Biol. Chem. 276, 47483–47488.
[25] Echtermeyer, F., Bertrand, J., Dreier, R., Meinecke, I., Neugebauer, K., et al. (2009) Syndecan-4 regulates ADAMTS-5 activation and cartilage breakdown in osteoarthritis. Nat. Med. 15, 1072–1076.
[26] Steinfeld, R., Van Den Berghe, H., and David, G. (1996) Stimulation of fibroblast growth factor receptor-1 occupancy and signaling by cell surface-associated syndecans and glypican. J. Cell Biol. 133, 405–416.
[27] Reiland, J. and Rapraeger, A. C. (1993) Heparan sulfate proteoglycan and FGF receptor target basic FGF to different intracellular destinations. J. Cell Sci. 105 (Part 4), 1085–1093.
[28] Kaji, T., Yamamoto, C., Oh-i, M., Fujiwara, Y., Yamazaki, Y., et al. (2006) The vascular endothelial growth factor VEGF165 induces perlecan synthesis via VEGF receptor-2 in cultured human brain microvascular endothelial cells. Biochim. Biophys. Acta 1760, 1465–1474.
[29] Rhiner, C., Gysi, S., Frohli, E., Hengartner, M. O., and Hajnal, A. (2005) Syndecan regulates cell migration and axon guidance in *C. elegans.* Development 132, 4621–4633.
[30] Manon-Jensen, T., Itoh, Y., and Couchman, J. R. (2010) Proteoglycans in health and disease: the multiple roles of syndecan shedding. FEBS J. 277, 3876–3889.
[31] Mali, M., Andtfolk, H., Miettinen, H. M., and Jalkanen, M. (1994) Suppression of tumor cell growth by syndecan-1 ectodomain. J. Biol. Chem. 269, 27795–27798.
[32] Liebersbach, B. F. and Sanderson, R. D. (1994) Expression of syndecan-1 inhibits cell invasion into type I collagen. J. Biol. Chem. 269, 20013–20019.
[33] Langford, J. K., Yang, Y., Kieber-Emmons, T., and Sanderson, R. D. (2005) Identification of an invasion regulatory domain within the core protein of syndecan-1. J. Biol. Chem. 280, 3467–3473.
[34] Liu, W., Litwack, E. D., Stanley, M. J., Langford, J. K., Lander, A. D., et al. (1998) Heparan sulfate proteoglycans as adhesive and anti-invasive molecules. Syndecans and glypican have distinct functions. J. Biol. Chem. 273, 22825–22832.
[35] Bernfield, M., Kokenyesi, R., Kato, M., Hinkes, M. T., Spring, J., et al. (1992) Biology of the syndecans: a family of transmembrane heparan sulfate proteoglycans. Annu. Rev. Cell Biol. 8, 365–393.
[36] Khan, M. Y., Jaikaria, N. S., Frenz, D. A., Villanueva, G., and Newman, S. A. (1988) Structural changes in the NH2-terminal domain of fibronectin upon interaction with heparin. Relationship to matrix-driven translocation. J. Biol. Chem. 263, 11314–11318.
[37] Iba, K., Albrechtsen, R., Gilpin, B., Frohlich, C., Loechel, F., et al. (2000) The cysteine-rich domain of human ADAM 12 supports cell adhesion through syndecans and triggers signaling events that lead to beta1 integrin-dependent cell spreading. J. Cell Biol. 149, 1143–1156.
[38] Beauvais, D. M. and Rapraeger, A. C. (2003) Syndecan-1-mediated cell spreading requires signaling by alphavbeta3 integrins in human breast carcinoma cells. Exp. Cell Res. 286, 219–232.
[39] Beauvais, D. M., Burbach, B. J., and Rapraeger, A. C. (2004) The syndecan-1 ectodomain regulates alphavbeta3 integrin activity in human mammary carcinoma cells. J. Cell Biol. 167, 171–181.
[40] Burbach, B. J., Ji, Y., and Rapraeger, A. C. (2004) Syndecan-1 ectodomain regulates matrix-dependent signaling in human breast carcinoma cells. Exp. Cell Res. 300, 234–247.
[41] Beauvais, D. M., Ell, B. J., McWhorter, A. R., and Rapraeger, A. C. (2009) Syndecan-1 regulates alphavbeta3 and alphavbeta5 integrin activation during angiogenesis and is blocked by synstatin, a novel peptide inhibitor. J. Exp. Med. 206, 691–705.
[42] McQuade, K. J., Beauvais, D. M., Burbach, B. J., and Rapraeger, A. C. (2006) Syndecan-1 regulates alphavbeta5 integrin activity in B82L fibroblasts. J. Cell Sci. 119, 2445–2456.
[43] Beauvais, D. M. and Rapraeger, A. C. (2010) Syndecan-1 couples the insulin-like growth factor-1 receptor to inside-out integrin activation. J. Cell Sci. 123, 3796–3807.
[44] Altemeier, W. A., Schlesinger, S. Y., Buell, C. A., Brauer, R., Rapraeger, A. C., et al. (2012) Transmembrane and extracellular domains of syndecan-1 have distinct functions in regulating lung epithelial migration and adhesion. J. Biol. Chem. 287, 34927–34935.
[45] Park, H., Kim, Y., Lim, Y., Han, I., and Oh, E. S. (2002) Syndecan-2 mediates adhesion and proliferation of colon carcinoma cells. J. Biol. Chem. 277, 29730–29736.
[46] Chen, L., Klass, C., and Woods, A. (2004) Syndecan-2 regulates transforming growth factor-beta signaling. J. Biol. Chem. 279, 15715–15718.
[47] Fears, C. Y., Gladson, C. L., and Woods, A. (2006) Syndecan-2 is expressed in the microvasculature of gliomas and regulates angiogenic processes in microvascular endothelial cells. J. Biol. Chem. 281, 14533–14536.
[48] Whiteford, J. R., Behrends, V., Kirby, H., Kusche-Gullberg, M., Muramatsu, T., et al. (2007) Syndecans promote integrin-mediated adhesion of mesenchymal cells in two distinct pathways. Exp. Cell Res. 313, 3902–3913.
[49] Whiteford, J. R., Xian, X., Chaussade, C., Vanhaesebroeck, B., Nourshargh, S., et al. (2011) Syndecan-2 is a novel ligand for the protein tyrosine phosphatase receptor CD148. Mol. Biol. Cell 22, 3609–3624.
[50] McFall, A. J. and Rapraeger, A. C. (1997) Identification of an adhesion site within the syndecan-4 extracellular protein domain. J. Biol. Chem. 272, 12901–12904.
[51] Carey, D. J., Evans, D. M., Stahl, R. C., Asundi, V. K., Conner, K. J., et al. (1992) Molecular cloning and characterization of N-syndecan, a novel transmembrane heparan sulfate proteoglycan. J. Cell Biol. 117, 191–201.
[52] McFall, A. J. and Rapraeger, A. C. (1998) Characterization of the high affinity cell-binding domain in the cell surface proteoglycan syndecan-4. J. Biol. Chem. 273, 28270–28276.
[53] Whiteford, J. R. and Couchman, J. R. (2006) A conserved NXIP motif is required for cell adhesion properties of the syndecan-4 ectodomain. J. Biol. Chem. 281, 32156–32163.
[54] Whiteford, J. R., Ko, S., Lee, W., and Couchman, J. R. (2008) Structural and cell adhesion properties of zebrafish syndecan-4 are shared with higher vertebrates. J. Biol. Chem. 283, 29322–29330.

Genetic Syndromes & Gene Therapy

De Rossi et al., J Genet Syndr Gene Ther 2013, 4:5
http://dx.doi.org/10.4172/2157-7412.1000147

Research Article Open Access

Critical Factors in Measuring Angiogenesis Using the Aortic Ring Model

De Rossi G, Scotland RS and Whiteford JR*

Centre for Microvascular Research, William Harvey Research Institute, Barts and the London School of Medicine and Dentistry, Queen Mary University of London, Charterhouse Square, London EC1M 6BQ, United Kingdom

Abstract

Angiogenesis is a feature of numerous pathologies including cancer and inflammatory conditions and as such is key therapeutic target for the treatment of disorders where excessive or insufficient formation of new blood vessels occurs. The study of angiogenesis *in vivo* provides many challenges, however the growth of new blood vessels *in vitro* from aortic explants has provided a highly useful model for the study of this process. In this manuscript we examine the critical factors which can affect this assay and demonstrate that aortas from both female rats and mice exhibit a reduced angiogenic response to males. These findings have implications not only for the experimental design of angiogenesis experiments but also in the use of therapies targeting angiogenesis in the treatment of pathologies, such as cancer.

Keywords: Angiogenesis; Tumour angiogenesis; Aortic ring; Gender; Endothelial cell

Abbreviations: FGF: Fibroblast Growth Factor; VEGF: Vascular Endothelial Growth Factor; ECM: Extracellular Matrix; EC: Endothelial Cell; FBS: Foetal Bovine Serum

Introduction

Angiogenesis, the formation of new blood vessels from pre-existing ones, occurs primarily during embryonic development and growth in order to remodel the primary network of vascular endothelial cells formed during *vasculogenesis* into a vast network of arteries, veins and capillaries that will form the blood circulatory system of the adult. Angiogenesis occurs during wound healing where angiogenic capillary sprouts invade the fibrin/fibronectin-rich wound clot and within a few days organize into a microvascular network throughout the granulation tissue. Additionally, in the female, angiogenesis happens during the reproductive cycle and pregnancy. In healthy unchallenged individuals angiogenesis is controlled by a fine balance of pro- and anti- angiogenic modulators. In particular conditions, such as tissue injury, the balance is tipped in favour of pro-angiogenic factors such as VEGF, FGF and angiopoietins. The quiescent vessels sense and respond to these molecules initiating the angiogenic process. A sequence of coordinated events culminate in the formation of a new capillary network: first, a so-called tip cell migrates from the vessel into the ECM guided by growth factor gradients; following the tip cell, stalk cells proliferate and eventually form the vessel lumen; mural cells such as pericytes and/or smooth muscle cells are recruited around the newly formed vessel and are necessary for its stabilisation. Angiogenesis involves the remodelling of the extracellular space through the action of proteases secreted by ECs and mural cells and is characterized by many interactions between adhesion receptors on the EC surface and ECM molecules [1-3].

Abnormal angiogenesis (either excessive or insufficient) is a common feature of many diseases such as cancer, cardiovascular and skin disorders, ischemia, retinopathies and arthritis and the importance of angiogenesis in these pathologies has led to considerable efforts to understand the mechanisms associated with new blood vessel formation in the hope that novel therapeutic targets for treatment can be established [1,4]. So far angiogenic and anti-angiogenic therapies have been developed but their efficiencies have rarely met expectations; a deeper understanding of the mechanisms underlying the angiogenic process is therefore crucial for designing better therapeutic strategies.

The aortic rings model of angiogenesis has been used to study new blood vessel formation [5-7]. Thoracic aortas from either rats or mice are dissected, sectioned and embedded in either a Collagen I or Matrigel matrix and angiogenesis is stimulated by the addition of pro-angiogenic factors such as VEGF or FGF. Angiogenic sprouts (new vessels) are visualised after 4-8 days in culture. In this study we describe the key factors that can affect this assay and show that the angiogenic response is different between males and females. This data has implications not only for experimental design of angiogenesis studies but also on the potential dosing of therapeutic interventions between male and female patients.

Materials and Methods

Aortic ring assay

Thoracic aortas dissected from cervically dislocated 180-200 g Wistar rats (Harlan laboratories) or C57BL/6 mice (Charles River) were sliced into 0.5 mm sections and incubated overnight in serum free OptiMEM (Invitrogen) at 37°C, 10% CO_2. Male and female rats and mice were aged matched unless stated otherwise and animals were fed a standard chow diet and housed under a 12hour light and dark cycle. Aortic rings were embedded in type I collagen (1mg/ml) in E4 media (Invitrogen). Wells were supplemented with OptiMEM with FBS (PAA) VEGF (R and D systems) at the concentrations indicated and incubated at 37°C, 10% CO_2. Emergent angiogenic sprouts from rat and mouse aortas were counted after 4 days and 8 days in culture respectively. All animal experiments were conducted in accordance with the British Home Office regulations (Scientific Procedures) Act 1986, United Kingdom.

***Corresponding author:** James R Whiteford, Centre for Microvascular Research, William Harvey Research Institute, Barts and the London School of Medicine and Dentistry, Queen Mary University of London, Charterhouse Square, London EC1M 6BQ, United Kingdom, Tel: 0044(0)2078828241; E-mail: j.whiteford@qmul.ac.uk

Received May 17, 2013; **Accepted** June 13, 2013; **Published** June 17, 2013

Citation: De Rossi G, Scotland RS, Whiteford JR (2013) Critical Factors in Measuring Angiogenesis Using the Aortic Ring Model. J Genet Syndr Gene Ther 4: 147. doi:10.4172/2157-7412.1000147

Imaging

Images were captured using an Olympus IX81 inverted microscope with a Hamamatsu Orca-ER digital camera. Image acquisition was performed using the CellM software (Olympus) and micrographs were prepared for publication using Adobe Photoshop.

Statistical analysis

Statistical analysis was performed using the Graphpad Prism software Version 6.0.

Results

The aortic ring model of angiogenesis is an *ex vivo* model and has been used extensively to study factors which affect angiogenesis particularly with regard to tumour angiogenesis [5-7]. The model entails growing blood vessels from sections of aorta. The resultant structures form branching tube like structures composed of both endothelial cells and pericytes (Figures 1A-1D). Rat aortas (Figure 1A) produce longer more branched sprouts than those obtained from murine aortas (Figures 1B-1D). Staining using a fluorescently labelled endothelial cell specific lectin from the bacteria *Bandeiraea simplicifolia* reveals, that the sprouts produced consist of vessel-like structures composed of endothelial cells surrounded by perivascular cells. These perivascular cells express the pericyte marker α-smooth muscle actin (αSMA) and envelop the newly formed vessel, as shown in Figure 1C and 1D in which sprouts have been induced from aortas from transgenic mice in which eGFP is under the control of the αSMA promoter.

Aortas from both rats and mice are used in these studies; rat aortas are longer and wider, enabling the collection of a greater number of rings and are more angiogenic in that they produce more sprouts and the chances of a given aortic section producing angiogenic sprouts is far higher than that observed in mice. Mice aortas are smaller, more susceptible to damage during dissection, particularly fat removal and there is a far higher chance of a given section failing to produce an angiogenic response (Figure 1E). The use of murine tissues is of course favourable owing to the number of genetically modified mice that are now available. Many factors can affect the aortic rings assay, and these can have major implications for the interpretation of the experimental data. The source of critical reagents can have an effect on the magnitude of the angiogenic response in these assays and it is inevitable that there will be differences between laboratories. We tried to standardize an aortic ring assay by examining the effect of VEGF, FBS and gender on the angiogenic response in tissues from both rats and mice (Figure 2).

Optimization of the rat aortic ring assay

As mentioned above rat aortas generally give a stronger angiogenic response than mice, indeed angiogenic sprouting can be observed in rings from male animals seeded in collagen only in the absence of FBS or VEGF. This response can be increased in the presence of 10ng/ml of VEGF. A similarly high response is observed in the presence of 30 ng/ml of VEGF although there is a reduction in angiogenic sprouts when 60ng/ml of VEGF is added. Interestingly in all conditions the angiogenic response from aortic rings from female rats is greatly reduced. There is still a response to increased concentrations of VEGF but this is significantly reduced when compared to samples from male rats.

In a second set of experiments we tested the effect of foetal bovine serum on sprout formation from rat aortic rings. The combination of 1% serum and 10 ng/ml VEGF elicited the highest angiogenic response in both male and female aortic rings, although as previously

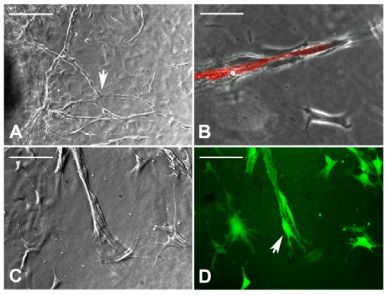

E

	Murine	Rat
No. of sections obtained/aorta	15	35
% sprouting sections	60%	80%
Time to sprout formation	6-8 days	3-4 days

Figure 1: Angiogenic sprouts from both rat and mouse aortas from microvessels consisting of endothelial cells surrounded by pericytes. (A) Vessel out growth from a rat aortic ring seeded in Collagen I, in the presence of 1% FBS and 10ng/ml VEGF (Scale bar 200μ). Sprouts from rat aortic rings are longer in length and tend to be more branched (arrow). (B) Murine angiogenic sprout stained with *Bandeiraea simplicifolia* (BS) lectin (red) showing endothelial cells comprising the microvessel surrounded by pericytes (Scale bar 100μ). (C and D) Angiogenic sprouts from aortas from transgenic mice expressing eGFP under the control of the αSMA promoter. GFP expressing pericytes (green) are observed surrounding ECs (D). (E) Table comparing the use of mouse and rat aortas for the study of angiogenesis.

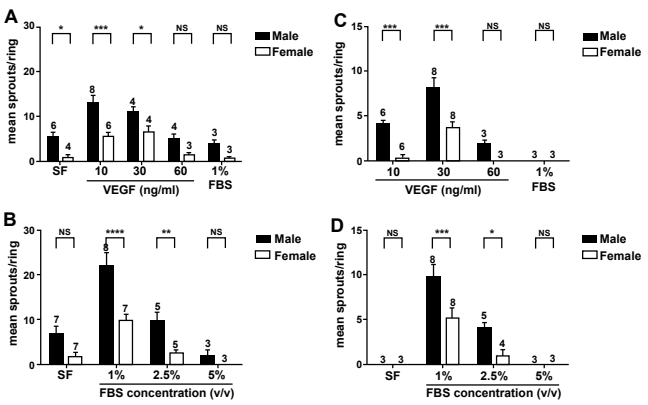

Figure 2: In all conditions tested aortas from females gave a reduced angiogenic response compared to males. (A) VEGF promotes angiogenesis in rat aortas embedded in collagen I in serum free conditions. Age matched Male and female rat aortic rings were seeded as described and supplemented with the concentrations of VEGF indicated. (B) High level of FBS can be inhibitory to the angiogenic response from both male and female rat aortas. Rings were embedded in collagen I and supplemented with 10ng/ml VEGF and the concentrations (v/v) of FBS indicated. (C) The formation of angiogenic sprouts from murine aortas requires VEGF. (D) High levels of serum also inhibit angiogenic sprout formation from murine vessels. Murine aortic explants were supplemented with 30ng/ml VEGF and the concentrations of FBS indicated. In (A-D) angiogenic sprouts were counted 4 days (rat) and 8 days (mouse) post embedding. At least 10 rings/animal, were counted and the mean calculated, data presented for each condition represents the mean of mean sprout formation obtained from at least 3 different animals (n-numbers for each condition are shown above data bars). Error bars represent the standard error of the mean and significance between male and female samples at each condition was calculated using a 2-way ANNOVA comparison.

the response was significantly lower in females versus males. Increased serum concentration (2.5% and 5% v/v) resulted in an inhibition of this

response. One of the issues with the aortic rings assay is that in addition to angiogenic sprouts emerging from the ring section there is also a significant amount of fibroblasts and smooth muscle cells. Higher serum concentrations tend to favour the emergence of fibroblasts and when this is excessive it appears to be inhibitory to sprout formation.

Optimization of the mouse aortic ring assay

The use of mouse aortas for the study of angiogenesis is more technically challenging. Unlike rat aortic rings murine sections do not sprout in serum free conditions and require both serum and VEGF to elicit a response. We have found that the best response is obtained from rings treated with 1% serum and 30ng/ml of VEGF. Higher concentrations of VEGF (>30 ng/ml) and serum (>1%v/v) are largely inhibitory to the response. As in the rat system higher serum levels favour the emergence of fibroblasts and smooth muscle cells which is not conducive to new blood vessel formation. As is also the case aortas from female mice give a significantly lower angiogenic response than males, regardless of the treatment. The use of murine aortic ring is also dependant on the age of the mice used (Figure 3). Aortas from younger mice give a more robust angiogenic response than that observed from older mice (Older than 8 weeks).

Discussion

In the work presented here we have examined in detail the factors which can affect a rodent model of angiogenesis. Although the effects of serum and VEGF are well established in this model, we also highlight the fact that the angiogenic response in this assay is greatly different between males and female donors. Results clearly showed a decreased angiogenic response in both female mice and rats when compared to their male counterparts. This difference was persistent throughout all the experiments regardless of the different conditions (VEGF or serum concentration).

Gender differences in cellular responses particularly inflammation have been identified [8]; however, differences in angiogenesis are less well characterised, particularly in an *ex vivo* model such as the aortic ring model where the tissues are isolated from the normal hormonal factors present *in vivo*. The reason why female samples are less angiogenic is not clear; however, it is intriguing to speculate that angiogenesis, like other physiological processes or disorders might have an epigenetic component [9-11]. Sexual dimorphism in angiogenic response could be caused by a different hormone-induced DNA methylation or histone modification in male and female resulting in different gene regulation. Microarray-based epigenetic profiles might shed some light on this hypothesis. Angiogenesis has been shown to be affected by gene dosage affects and it may be that sex linked genes contribute to this effect. This observation is highly relevant to gender specific pathologies such as testicular and ovarian cancer. Moreover, these findings are of considerable importance both in terms of experimental design relating to the study of angiogenesis but also for the development of angiogenic and anti-angiogenic therapies and represent the start point for further investigation.

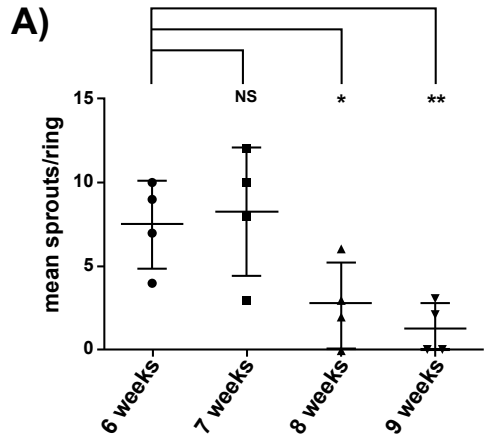

Figure 3: In the murine model of angiogenesis aortas from older mice show a reduced angiogenic response. (A) Male mice (aged as indicated) were embedded in Collagen I and supplemented with 1% FBS and 30 ng/ml VEGF. Mean sprout formation was calculated from at least 10 rings each point represents the mean value from one animal. Error bars represent the standard error of the mean and significance was calculated using individual student T tests compared to the 6 week value.

Acknowledgements

The bulk of this work was supported by a grant from the William Harvey Research Foundation. JRW is supported by Arthritis Research UK grant No. 19702 and GDR by Barts and the London School of Medicine and Dentistry.

References

1. Ramjaun AR, Hodivala-Dilke K (2009) The role of cell adhesion pathways in angiogenesis. Int J Biochem Cell Biol 41: 521-530.
2. Potente M, Gerhardt H, Carmeliet P (2011) Basic and therapeutic aspects of angiogenesis. Cell 146: 873-887.
3. Weis SM, Cheresh DA (2011) Tumor angiogenesis: molecular pathways and therapeutic targets. Nat Med 17: 1359-1370.
4. Silva R, D'Amico G, Hodivala-Dilke KM, Reynolds LE (2008) Integrins: the keys to unlocking angiogenesis. Arterioscler Thromb Vasc Biol 28: 1703-1713.
5. Baker M, Robinson SD, Lechertier T, Barber PR, Tavora B, et al. (2011) Use of the mouse aortic ring assay to study angiogenesis. Nat Protoc 7: 89-104.
6. Aplin AC, Fogel E, Zorzi P, Nicosia RF (2008) The aortic ring model of angiogenesis. Methods Enzymol 443: 119-136.
7. Goodwin AM (2007) In vitro assays of angiogenesis for assessment of angiogenic and anti-angiogenic agents. Microvasc Res 74: 172-183.
8. Scotland RS, Stables MJ, Madalli S, Watson P, Gilroy DW (2011) Sex differences in resident immune cell phenotype underlie more efficient acute inflammatory responses in female mice. Blood 118: 5918-5927
9. Gabory A, Roseboom TJ, Moore T, Moore LG, Junien C (2013) Placental contribution to the origins of sexual dimorphism in health and diseases: sex chromosomes and epigenetics. Biol Sex Differ 4: 5.
10. Guerrero-Bosagna C, Savenkova M, Haque MM, Nilsson E, Skinner MK (2013) Environmentally induced epigenetic transgenerational inheritance of altered Sertoli cell transcriptome and epigenome: molecular etiology of male infertility. PLoS One 8: e59922.
11. Takasugi M, Hayakawa K, Arai D, Shiota K (2013) Age- and sex-dependent DNA hypomethylation controlled by growth hormone in mouse liver. Mech Ageing Dev.

This article was originally published in a special issue, **Cancer Genetics** handled by Editor(s). Dr. Ahmed M Malki, Alexandria University, Egypt

Citation: De Rossi G, Scotland RS, Whiteford JR (2013) Critical Factors in Measuring Angiogenesis Using the Aortic Ring Model. J Genet Syndr Gene Ther 4: 147. doi:10.4172/2157-7412.1000147

SHORT RESEARCH ARTICLE

A novel role for syndecan-3 in angiogenesis [v1; ref status: indexed, http://f1000r.es/2g6]

Giulia De Rossi, James R. Whiteford

Centre for Microvascular Research, William Harvey Research Institute, Barts and the London School of Medicine and Dentistry, Queen Mary University of London, London, EC1 6BQ, UK

v1 **First Published:** 09 Dec 2013, **2**:270 (doi: 10.12688/f1000research.2-270.v1)
Latest Published: 09 Dec 2013, **2**:270 (doi: 10.12688/f1000research.2-270.v1)

Abstract

Syndecan-3 is one of the four members of the syndecan family of heparan sulphate proteoglycans and has been shown to interact with numerous growth factors via its heparan sulphate chains. The extracellular core proteins of syndecan-1,-2 and -4 all possess adhesion regulatory motifs and we hypothesized that syndecan-3 may also possess such characteristics. Here we show that a bacterially expressed GST fusion protein consisting of the entire mature syndecan-3 ectodomain has anti-angiogenic properties and acts via modulating endothelial cell migration. This work identifies syndecan-3 as a possible therapeutic target for anti-angiogenic therapy.

Article Status Summary

Referee Responses

Referees	1	2	3
v1 published 09 Dec 2013	✓ report	✓ report	✓ report

1 **Alberto Grossi**, Copenhagen University Denmark

2 **Mark Morgan**, University of Liverpool UK

3 **Jonas Jacobsen**, Chr. Hansen A/S Denmark

Latest Comments

No Comments Yet

Corresponding author: Giulia De Rossi (g.derossi@qmul.ac.uk)

How to cite this article: De Rossi G, Whiteford JR (2013) A novel role for syndecan-3 in angiogenesis [v1; ref status: indexed, http://f1000r.es/2g6] *F1000Research* 2013, **2**:270 (doi: 10.12688/f1000research.2-270.v1)

Grant information: This work was funded by Arthritis Research-UK (Grant No. 19207) and funds from the William Harvey Research Foundation both to JRW.
The funders had no role in study design, data collection and analysis, decision to publish, or preparation of the manuscript.

Competing Interests: No competing interests were disclosed.

First Published: 09 Dec 2013, **2**:270 (doi: 10.12688/f1000research.2-270.v1)
First Indexed: 20 Dec 2013, **2**:270 (doi: 10.12688/f1000research.2-270.v1)

Introduction

Angiogenesis is the process of new blood vessel formation from pre-existing vessels. This process is essential for embryonic development but it is also a feature of pathologies such as cancer and chronic inflammation (reviewed in[1]). For angiogenesis to occur, the release of pro-angiogenic factors, which promote the transition of endothelial cells (ECs) from a quiescent to a proliferative and migratory phenotype, is required[2–4]. The best characterized pro-angiogenic molecules are: vascular endothelial growth factor (VEGF), fibroblast growth factor (FGF) and platelet derived growth factor (PDGF) (reviewed in[5]). Angiogenesis represents an attractive target for the treatment of cancer, as during tumour development new blood vessels permeate the tumour mass and provide oxygen and nutrients to further enhance tumour growth. Therapies aimed at blocking angiogenesis have focused on targeting VEGF and its related receptors, however the prohibitive cost of such treatments and their side effects mean that there is still a need to discover new therapeutic anti-angiogenic targets[4].

Syndecans are a four member family of transmembrane adhesion receptors with diverse expression and functionality[6,7]. Syndecan-3 is the least well understood of the four family members. Like other syndecans, it possesses a short, highly conserved cytoplasmic domain, a single pass transmembrane domain and a large extracellular domain containing 6 glycosaminoglycan attachment sites which can be substituted by both heparan sulphate (HS) and chondroitin sulphate (CS). Syndecan-3 has the largest extracellular core protein of the syndecans and, in addition to the HS and CS modifications, the molecule possesses a number of potential sites for O-linked glycosylation resembling a mucin-rich domain which may affect both the structure and molecular interactions of syndecan-3[8,9].

Syndecan-3 Knock-Out mice, in common with other syndecan-KO animals, develop normally and only under conditions of challenge or insult are different phenotypes observed[6]. Syndecan-3 is mainly found in the nervous system and has been shown to be a co-receptor for a number of important growth factors, including Agouti related protein (AgRP), heparin binding growth associated molecule (HB-GAM), glial cell line derived growth factor (GDNF), neurturin (NRTN), artemin (PSPN) and NOTCH, via interactions with its HS chains[10–14]. Interactions with AgRP, an antagonist of melanocortin, lead to altered feeding behaviours in the syndecan-3 null mouse[14,15]. In addition, syndecan-3 deficiency leads to the mice exhibiting more addictive behaviours to opiates such as cocaine, and this occurs as a result of its interaction with GDNF[16]. Syndecan-3 is also expressed on satellite cells, adult skeletal muscle progenitors and has roles in the development of normal adult muscle[13,17–19].

An important emerging feature of syndecans is that sequences contained within their extracellular core domains have biological activity which can influence cell adhesion and migratory responses[20]. Such domains have been identified in syndecan-1, 2 and -4[21]. The syndecans can be divided into two subfamilies based on sequence homology: syndecan-1 and -3 and syndecans -2 and -4[22]. Since regions of the syndecan-1 core protein are anti-angiogenic, we hypothesized that the core protein of syndecan-3 may exhibit similar properties[23–25]. In this study we demonstrate that the syndecan-3 extracellular core protein is able to inhibit angiogenesis by reducing the migratory potential of endothelial cells and as such may be a candidate for use in anti-angiogenic therapy.

Materials and methods

Cell culture: Brain endothelial cells (bEND3.1) and skin endothelial cells (sEND) were obtained from Health Protection Agency UK and were grown in DMEM (PAA, GE Healthcare) supplemented with 10% FBS, 2 mM L-glutamine, 1% non-essential amino acids, 1 mM sodium pyruvate and 5 μM β-mercaptoethanol (all Invitrogen), at 37°C, 10% CO_2.

Syndecan-3 GST fusion protein: The full length syndecan-3 cDNA was obtained from Source BioScience. The entire length of the mature syndecan-3 ectodomain (A^{45}-L^{380}) was amplified by PCR using the primers S3forEcoRI (ttaattgaattcgctcaacgctggcgcaatg) and S3revHindIII (ttaattaagcttctacagtatgctcttctgaggga) (Integrated DNA Technologies) and the resultant product was digested with EcoRI and HIndIII and ligated into the equivalent sites of pET41 (Novagen) according to Manufacturer's instructions. Plasmids were verified by sequencing and transformed into the BL21 strain of *Escherichia coli* (Novagen). S3ED protein was purified from bacterial cultures which had reached an OD_{600} of 0.4 prior to the addition of 0.1 M Isopropyl β-D-1-thiogalactopyranoside (IPTG) and subsequent outgrowth for 4 hours. Affinity purification of both GST and S3ED was performed using glutathione-sepharose 4B (GE Healthcare) as described by the manufacturers.

Aortic ring assay: Angiogenic sprouts were induced from rat thoracic aortas according to the method of Nicosia and Ottinetti[26]. Briefly, aortas were dissected from cervically dislocated 180–200g 12 male Wistar rats (Harlan Laboratories) and sliced into 0.5 mm sections and incubated overnight in serum free OptiMEM (Invitrogen) at 37°C. Aortic rings were embedded in type I collagen (1 mg/ml) in E4 media (Invitrogen) containing either GST or S3ED in 48 well plates (Corning). Wells were supplemented with OptiMEM with 1% FBS and 10 ng/ml VEGF (R and D systems) and incubated at 37°C, 10% CO_2. Angiogenic sprouts from rat aortas were counted after 4 days and 8 days respectively. Animals were housed and treated in Accordance with UK Home Office Regulations.

EC tubule formation assay: Endothelial cell microtubule formation was measured as follows: ECs (5×10^4) were seeded into 24 well plates coated with 150 μl of Matrigel (BD sciences) in the presence of either GST or S3ED. Using the Cell-IQ controlled environmental chamber (CM technologies), the plates were incubated at 37°C, 10% CO_2 and images were captured every 15 minutes for 16 hours.

Scratch wound migration assay: Confluent monolayers of bEND cells were scratched with a pipette tip, cells were then washed twice with PBS prior to the addition of growth medium supplemented with 0.5 μM of either GST or S3ED. Wounds were monitored by time lapse microscopy using an Olympus IX81 Microscope Hamamatsu Orca ER digital camera. Images were acquired every 30 minutes and subsequently analysed using Adobe Photoshop. Cell speed was quantified by manually measuring the track of individual cells migrated for 9 hours (20 cells per conditions) using Adobe Photoshop, track lengths were then divided by the time to obtain cell speed.

Cell proliferation assay: EC proliferation was measured using the CellTiter 96 AQueous Cell proliferation assay kit as described by the manufacturer (Promega). bEND (5×10^3/spot) cells were seeded in a 96-well plate (Corning) and incubated in the presence of 0.5 μM either GST or S3ED.

Invasion assay: EC invasion assays through collagen matrices were performed in 24-well plates with trans-well inserts (Millipore; 8 μm pore size, polyester (PET) membrane). Membranes were coated with 10 μl of Collagen Type I mixture (Millipore; 1 mg/ml in E4 medium) containing 0.5 μM GST or S3ED. sEND cells were seeded on the gel in a homogenous single cell suspension of 5×10^3 cells/ insert in 200 μl of DMEM + 10% FBS; 1 ml of the same medium was added to the bottom well. Invasion was measured after 6 hours after which time gels were removed with a cotton swab, the filter washed in PBS and stained with calcein (Invitrogen) and the number of cells attached to the filter was counted.

Results

In keeping with previous studies from our group and others in the field[25,27–29], we set out to determine whether the extracellular core protein of syndecan-3 (S3ED) had any effect on cellular responses such as cell adhesion or migration and in particular on angiogenesis. To do this we generated a fusion protein consisting of the entire length of the syndecan-3 extracellular core protein (A^{45}-L^{380}) fused at the N-terminus to GST (S3ED). S3ED was expressed and purified from bacteria and therefore was not substituted with GAGs, or *O*-linked sugars, since bacteria lack the necessary transferases to perform these post-translational modifications (Figure 1).

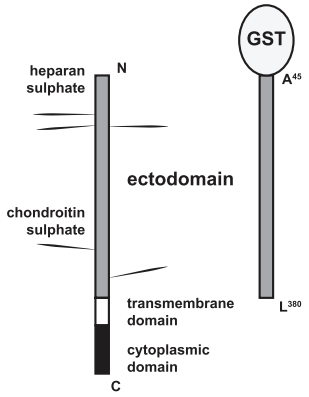

Figure 1. Syndecan-3 and S3ED-GST structures. Diagrammatic representation of the syndecan-3 fusion protein (S3ED) used in this study. The entire length of the syndecan-3 extracellular core protein (A^{45}-L^{380}) was fused at the N-terminus to GST.

In the aortic ring assay, angiogenic sprouts are formed from sections of rat aortas when embedded into a collagen I matrix (Figure 2a and b). Sprouting occurs in the absence of VEGF although a more robust response is observed when this growth factor is included in the medium (Figure 2c). We incorporated 0.5 μM of either GST or S3ED into the collagen I matrices to see if they affected sprout formation. Significantly fewer sprouts were observed in the presence of S3ED compared to either the untreated control or GST treated rings. This was true for both rings grown in the presence or in absence of VEGF (Figure 2c). We then demonstrated that this inhibition of angiogenesis is dose dependent; as little as 0.5 μM of S3ED had an inhibitory effect (Figure 3). Although 0.1 μM of S3ED also showed a statistically significant anti-angiogenic effect in this assay, we decided to use the higher dose (0.5 μM) for further experiments.

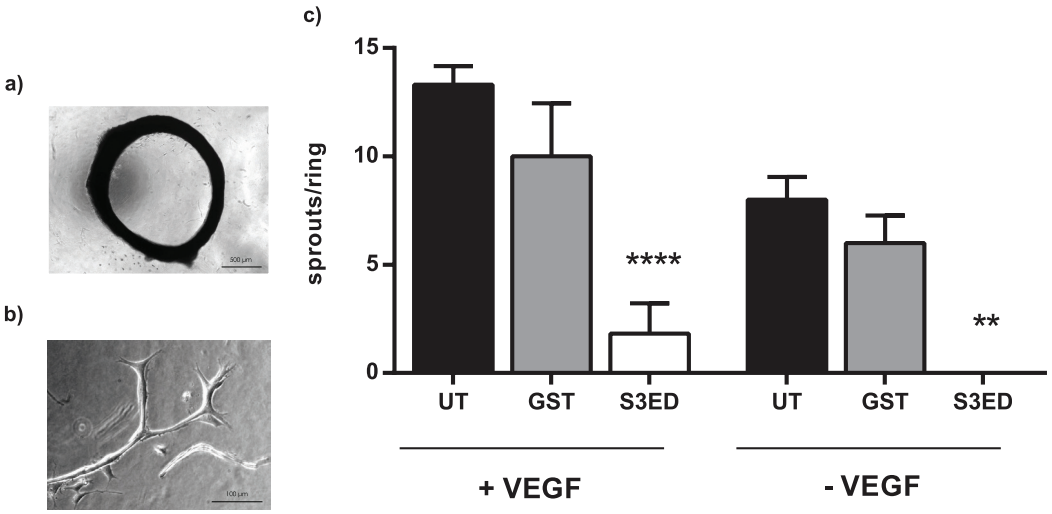

Figure 2. S3ED inhibits sprout formation in the rat aortic ring assay. (**a**) Low magnification (bar=500 μm) of a rat aortic ring and (**b**) high magnification (bar=100 μm) image of an angiogenic sprout grown under control conditions. (**c**) S3ED inhibits angiogenic sprout formation from rat aortic rings. Rat aortic rings were seeded in Collagen I gels with 0.5 μM of either S3ED or GST in the presence or absence of VEGF. Data is the mean taken from rings from 3 different animals and error bars represent the SEM. One-way ANOVA with Bonferroni multiple comparisons was used to compare S3ED to relative UT control.

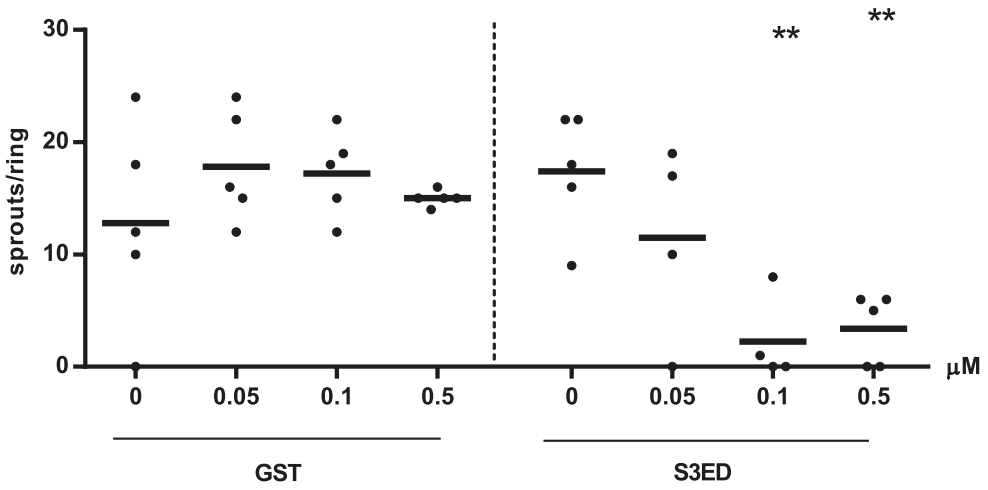

Figure 3. The anti-angiogenic effect of S3ED is dose dependant. Rat aortic rings were embedded in Collagen I with the indicated concentrations of either GST or S3ED in the presence of VEGF. Angiogenic sprouts were counted 4 days after seeding. Data is from 5 rings per condition. One-way ANOVA with Bonferroni multiple comparisons was used to compare S3ED 0.5 µM to S3ED 0 µM considered as a control.

Tubular network formation in response to matrigel is another measure of angiogenesis[30]. Brain endothelial cells form highly branched networks when seeded on matrigel and this was unaffected when GST was added to the culture medium (Figure 4a). In the presence of S3ED (0.5 µM) far fewer branch points were evident and the length of the microtubules was greatly reduced (Figure 4b and c; and Movie 1 and Movie 2). Together these data suggest that S3ED has anti-angiogenic properties.

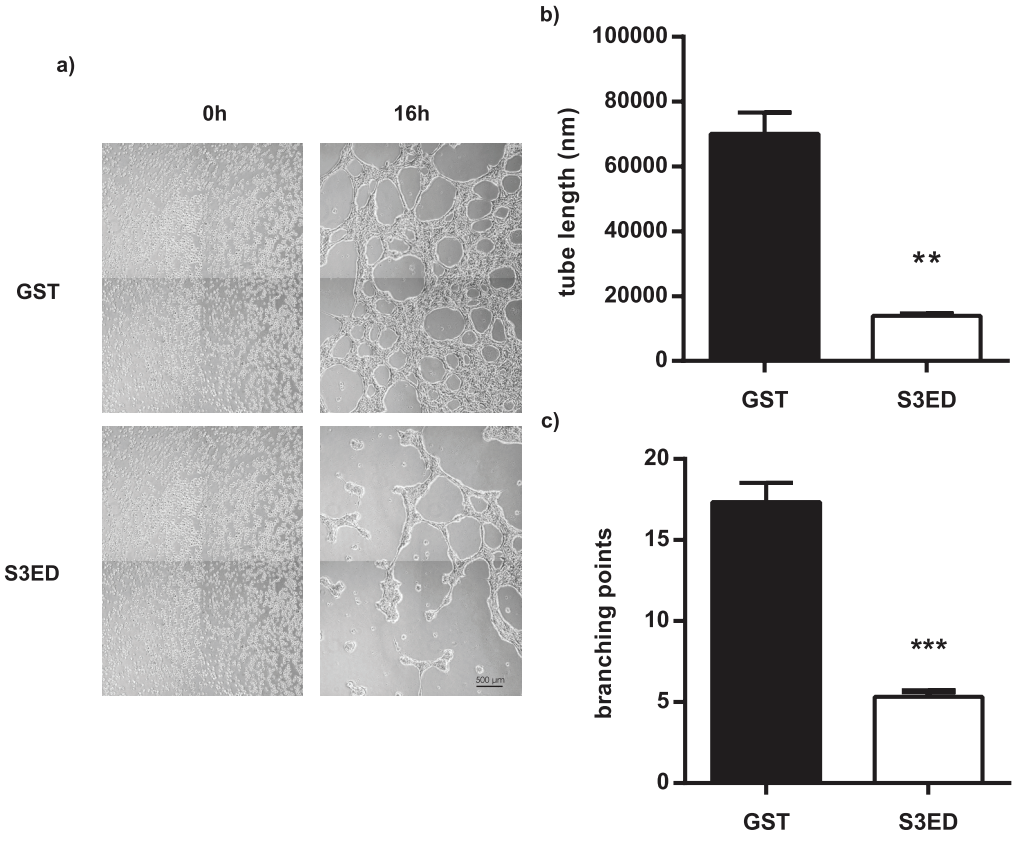

Figure 4. S3ED inhibits EC network formation in response to Matrigel. bEND3.1 cells were seeded on Matrigel in media containing GST or S3ED (0.5 µM) and micrographs were obtained after 16 hours (**a**). Tube length (**b**) and branch points (**c**) were calculated and both were reduced in the presence of S3ED. Error bar represents SEM. T-test was used to compare S3ED to GST control.

Movies 1 and 2

2 Data Files

http://dx.doi.org/10.6084/m9.figshare.870448

The ectodomains of syndecan-1,-2 and -4 have all been shown to affect cell behaviour through interactions with integrins (for review see[21]). For example, the anti-angiogenic properties of syndecan-1 have been demonstrated to occur through interactions with the αV sub-family[25]. Integrins are the major drivers of cell migration[31,32] so we set out to determine whether the inhibitory properties of S3ED were due to effects on EC migration. Scratch wound cell migration assays revealed that S3ED significantly inhibited brain endothelial cell migration as compared to GST and untreated controls (Figure 5a). This was reflected in both percentage of wound closure and single cell speed measurements (Figure 5b and c). We further confirmed that S3ED inhibits EC migratory potential by using a 3D culture system where we observed that S3ED, when incorporated into a collagen I matrix, inhibited endothelial cell invasion through the collagen (Figure 6a and b). Although we demonstrate that S3ED inhibits EC migration, it could be argued that these effects may also be associated with anti-proliferative effects of this protein. To test this we performed proliferation assays on brain ECs in the presence of S3ED or GST and observed no differences in the proliferation of these cells compared with controls (Figure 7).

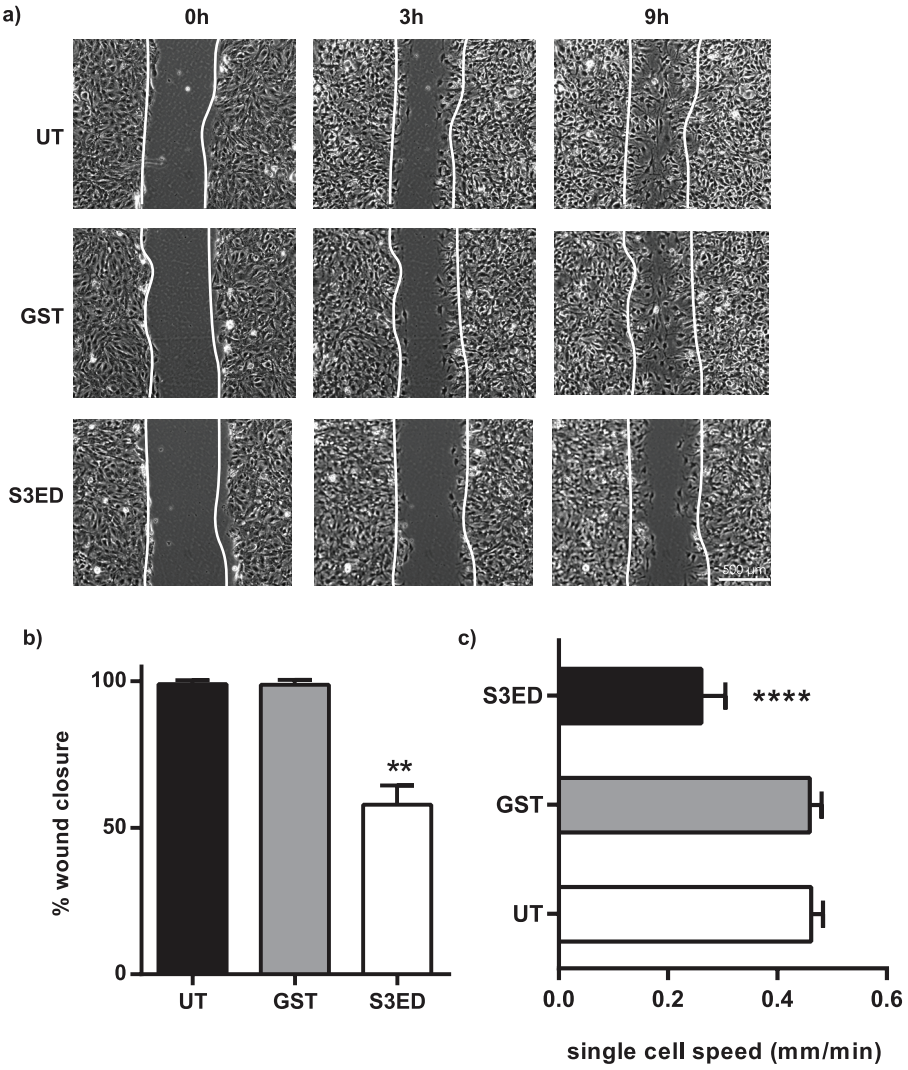

Figure 5. S3ED inhibits brain EC migration. Scratch wounds were made to confluent monolayers of bEND3.1 cells and micrographs were captured after 9 hours clearly showing that wound closure is reduced in the presence of S3ED 0.5 µM (**a**). Scratch wound closure (**b**) and single cell speeds (**c**) were calculated. Single cell speed was calculated from 15–25 cells per condition. Error bars represent SD for (**a**) and SED for (**b**). One-way ANOVA with Bonferroni multiple comparisons was used to compare S3ED to relative UT control.

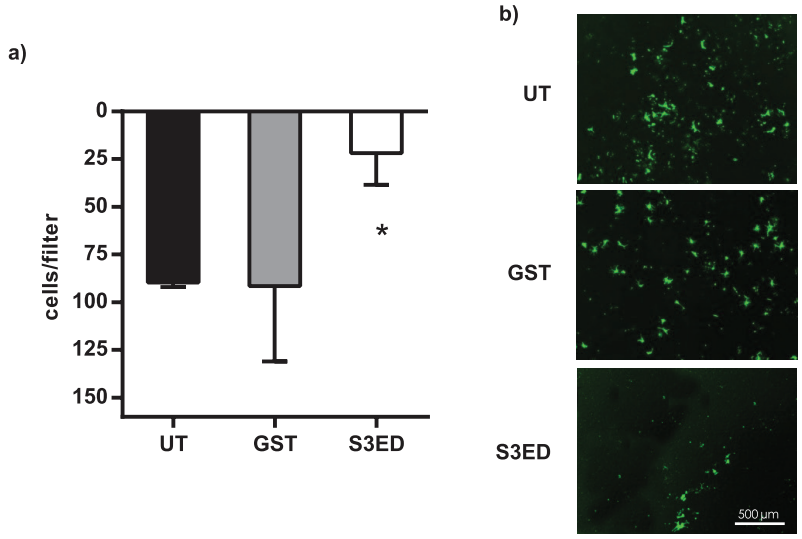

Figure 6. S3ED inhibits EC invasion into Collagen I. 5 × 10^3 sEND cells were seeded on 10 µl of Collagen I and were allowed to migrate for 6 hours. Numbers of transmigrated cells are shown in (**a**) and micrographs of transmigrated Calcein-labelled cells are in (**b**). Error bars represent SD. One-way ANOVA with Bonferroni multiple comparisons was used to compare S3ED to relative UT control.

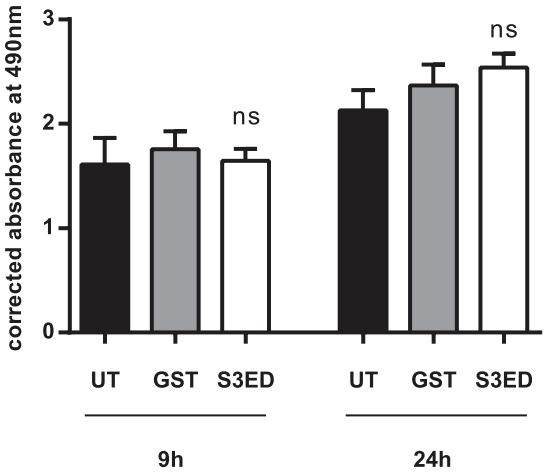

Figure 7. EC proliferation is unaffected by either GST or S3ED. 5 x 10^3 bEND 3.1 cells were incubated in the presence of 0.5 µM of either GST or S3ED. Error bars represent SD. One-way ANOVA with Bonferroni multiple comparisons was used to compare S3ED to relative UT control showing no statistically significant difference between the two at after 9 and 24 hours.

Syndecan-3 raw data

8 Data Files

http://dx.doi.org/10.6084/m9.figshare.870449

Discussion

Here we show for the first time that the ectodomain of syndecan-3, like the other syndecan family members, has cell adhesion regulatory properties and acts as an inhibitor of angiogenesis. This strongly suggests that adhesion regulatory domains in syndecan extracellular core domains exist in all four family members and also provides further insight as to how these molecules function. Interestingly, there is very little sequence homology between syndecan ectodomains[32], and the adhesion regulatory motifs identified in syndecan-1,-2 and -4 are not present in S3ED. In addition, syndecan-3 is unique amongst the family since its core protein possesses a mucin-rich domain and it is likely that these *O*-linked sugars will also have a role in its molecular interactions. Although syndecan-3 expression is mostly associated with cells of the nervous system, it has also been found to be associated with cells related to maternal and foetal circulation[33]. Vascular defects in the syndecan-3 null mouse have not been reported but the identification of S3ED as a regulator of angiogenesis suggests that this may be a fertile area for future research. This work identifies syndecan-3 as a potential therapeutic target in pathologies where angiogenesis is a feature.

Author contributions

GDR and JRW conceived of the study, designed the experiments and carried out the research.

Competing interests

No competing interests were disclosed.

Grant information

This work was funded by Arthritis Research-UK (Grant No. 19207) and funds from the William Harvey Research Foundation both to JRW.

The funders had no role in study design, data collection and analysis, decision to publish, or preparation of the manuscript.

References

1. Potente M, Gerhardt H, Carmeliet P: **Basic and therapeutic aspects of angiogenesis.** *Cell.* 2011; **146**(6): 873–887.
PubMed Abstract | Publisher Full Text
2. Holderfield MT, Hughes CC: **Crosstalk between vascular endothelial growth factor, notch, and transforming growth factor-beta in vascular morphogenesis.** *Circ Res.* 2008; **102**(6): 637–652.
PubMed Abstract | Publisher Full Text
3. Chung AS, Ferrara N: **Developmental and pathological angiogenesis.** *Annu Rev Cell Dev Biol.* 2011; **27**: 563–584.
PubMed Abstract | Publisher Full Text
4. Carmeliet P, Jain RK: **Molecular mechanisms and clinical applications of angiogenesis.** *Nature.* 2011; **473**(7347): 298–307.
PubMed Abstract | Publisher Full Text
5. Weis SM, Cheresh DA: **Tumor angiogenesis: Molecular pathways and therapeutic targets.** *Nature Medicine.* 2011; **17**(11): 1359–1370.
PubMed Abstract | Publisher Full Text
6. Alexopoulou AN, Multhaupt HA, Couchman JR: **Syndecans in wound healing, inflammation and vascular biology.** *Int J Biochem Cell Biol.* 2007; **39**(3): 505–528.
PubMed Abstract | Publisher Full Text
7. Couchman JR: **Transmembrane signaling proteoglycans.** *Annu Rev Cell Dev Biol.* 2010; **26**: 89–114.
PubMed Abstract | Publisher Full Text
8. Chernousov MA, Carey DJ: **N-syndecan (syndecan 3) from neonatal rat brain binds basic fibroblast growth factor.** *J Biol Chem.* 1993; **268**(22): 16810–16814.
PubMed Abstract
9. Asundi VK, Carey DJ: **Self-association of n-syndecan (syndecan-3) core protein is mediated by a novel structural motif in the transmembrane domain and ectodomain flanking region.** *J Biol Chem.* 1995; **270**(44): 26404–26410.
PubMed Abstract | Publisher Full Text
10. Bespalov MM, Sidorova YA, Tumova S, *et al.*: **Heparan sulfate proteoglycan syndecan-3 is a novel receptor for gdnf, neurturin, and artemin.** *J Cell Biol.* 2011; **192**(1): 153–169.
PubMed Abstract | Publisher Full Text | Free Full Text
11. Creemers JW, Pritchard LE, Gyte A, *et al.*: **Agouti-related protein is posttranslationally cleaved by proprotein convertase 1 to generate agouti-related protein (agrp)83–132: Interaction between agrp83–132 and melanocortin receptors cannot be influenced by syndecan-3.** *Endocrinology.* 2006; **147**(4): 1621–1631.
PubMed Abstract | Publisher Full Text
12. Nolo R, Kaksonen M, Raulo E, *et al.*: **Co-expression of heparin-binding growth-associated molecule (hb-gam) and n-syndecan (syndecan-3) in developing rat brain.** *Neurosci Lett.* 1995; **191**(1–2): 39–42.
PubMed Abstract | Publisher Full Text
13. Pisconti A, Cornelison DD, Olguin HC, *et al.*: **Syndecan-3 and notch cooperate in regulating adult myogenesis.** *J Cell Biol.* 2010; **190**(3): 427–441.
PubMed Abstract | Publisher Full Text | Free Full Text
14. Reizes O, Benoit SC, Strader AD, *et al.*: **Syndecan-3 modulates food intake by interacting with the melanocortin/agrp pathway.** *Ann N Y Acad Sci.* 2003; **994**: 66–73.
PubMed Abstract | Publisher Full Text
15. Zheng Q, Zhu J, Shanabrough M, *et al.*: **Enhanced anorexigenic signaling in lean obesity resistant syndecan-3 null mice.** *Neuroscience.* 2010; **171**(4): 1032–1040.
PubMed Abstract | Publisher Full Text | Free Full Text
16. Chen J, Repunte-Canonigo V, Kawamura T, *et al.*: **Hypothalamic proteoglycan syndecan-3 is a novel cocaine addiction resilience factor.** *Nat Commun.* 2013; **4**: 1955.
PubMed Abstract | Publisher Full Text | Free Full Text
17. Cornelison DD, Filla MS, Stanley HM, *et al.*: **Syndecan-3 and syndecan-4 specifically mark skeletal muscle satellite cells and are implicated in satellite cell maintenance and muscle regeneration.** *Dev Biol.* 2001; **239**(1): 79–94.
PubMed Abstract | Publisher Full Text
18. Kosher RA: **Syndecan-3 in limb skeletal development.** *Microsc Res Tech.* 1998; **43**(2): 123–130.
PubMed Abstract | Publisher Full Text
19. Dealy CN, Seghatoleslami MR, Ferrari D, *et al.*: **Fgf-stimulated outgrowth and proliferation of limb mesoderm is dependent on syndecan-3.** *Dev Biol.* 1997; **184**(2): 343–350.
PubMed Abstract | Publisher Full Text
20. De Rossi G, Whiteford JR: **Novel insight into the biological functions of syndecan ectodomain core proteins.** *BioFactors.* 2013; **39**(4): 374–382.
PubMed Abstract | Publisher Full Text
21. De Rossi G, Whiteford JR: **Novel insight into the biological functions of syndecan ectodomain core proteins.** *BioFactors.* 2013; **39**(4): 374–382.
PubMed Abstract | Publisher Full Text
22. Couchman JR, Woods A: **Syndecans, signaling, and cell adhesion.** *J Cell Biochem.* 1996; **61**(4): 578–584.
PubMed Abstract | Publisher Full Text
23. Rapraeger AC, Ell BJ, Roy M, *et al.*: **Vascular endothelial-cadherin stimulates syndecan-1-coupled insulin-like growth factor-1 receptor and cross-talk between alphavbeta3 integrin and vascular endothelial growth factor receptor 2 at the onset of endothelial cell dissemination during angiogenesis.** *FEBS J.* 2013; **280**(10): 2194–2206.
PubMed Abstract | Publisher Full Text | Free Full Text
24. Rapraeger AC: **Synstatin: A selective inhibitor of the syndecan-1–coupled igf1r-alphavbeta3 integrin complex in tumorigenesis and angiogenesis.** *FEBS J.* 2013; **280**(10): 2207–2215.
PubMed Abstract | Publisher Full Text | Free Full Text
25. Beauvais DM, Ell BJ, McWhorter AR, *et al.*: **Syndecan-1 regulates alphavbeta3 and alphavbeta5 integrin activation during angiogenesis and is blocked by synstatin, a novel peptide inhibitor.** *J Exp Med.* 2009; **206**(3): 691–705.
PubMed Abstract | Publisher Full Text | Free Full Text
26. Nicosia RF, Ottinetti A: **Growth of microvessels in serum-free matrix culture of rat aorta - a quantitative assay of angiogenesis *in vitro*.** *Lab Invest.* 1990; **63**(1): 115–122.
PubMed Abstract
27. Whiteford JR, Couchman JR: **A conserved nxip motif is required for cell adhesion properties of the syndecan-4 ectodomain.** *J Biol Chem.* 2006; **281**(43): 32156–32163.
PubMed Abstract | Publisher Full Text
28. Whiteford JR, Behrends V, Kirby H, *et al.*: **Syndecans promote integrin-mediated adhesion of mesenchymal cells in two distinct pathways.** *Exp Cell Res.* 2007; **313**(18): 3902–3913.
PubMed Abstract | Publisher Full Text
29. Whiteford JR, Xian X, Chaussade C, *et al.*: **Syndecan-2 is a novel ligand for the protein tyrosine phosphatase receptor cd148.** *Mol Biol Cell.* 2011; **22**(19): 3609–3624.
PubMed Abstract | Publisher Full Text | Free Full Text
30. Passaniti A, Taylor RM, Pili R, *et al.*: Methods in laboratory investigation **A simple, quantitative method for assessing angiogenesis and antiangiogenic agents using reconstituted basement-membrane, heparin, and fibroblast growth-factor.** *Lab Invest.* 1992; **67**(4): 519–528.
PubMed Abstract
31. Streuli CH, Akhtar N: **Signal co-operation between integrins and other receptor systems.** *Biochem J.* 2009; **418**(3): 491–506.
PubMed Abstract | Publisher Full Text
32. Couchman JR, Chen L, Woods A: **Syndecans and cell adhesion.** *Int Rev Cytol.* 2001; **207**: 113–150.
PubMed Abstract
33. Chui A, Zainuddin N, Rajaraman G, *et al.*: **Placental syndecan expression is altered in human idiopathic fetal growth restriction.** *Am J Pathol.* 2012; **180**(2): 693–702.
PubMed Abstract | Publisher Full Text

Current Referee Status:

Referee Responses for Version 1

Jonas Jacobsen
Enzymes, Chr. Hansen A/S , Hørsholm, Denmark

Approved: 07 January 2014

Referee Report: 07 January 2014
The work described by researchers Whiteford and De Rossi is placed in the scientific field angiogenesis. The research group has identified the mature syndecan-3 ectodomain in fusion with a GST protein as a possible therapeutic target for anti-angiogenic therapy. A therapy that could prove relevant in the treatment of cancer.
The biological activities of extracellular core domain of Syndecan-3 is both novel and interesting and deserve publication.

The only minor point of criticism to the authors is the following:

In the discussion it is mentioned that O-linked glycosylation in the mucin-rich region of Syndecan-3 may also engage in molecular interactions. While this may be true it is also a fact that the expressed syndecan-3 fusion protein is not glycosylated because in was produced in the BL21 strain of *Escherichia coli*.

I have read this submission. I believe that I have an appropriate level of expertise to confirm that it is of an acceptable scientific standard.

Competing Interests: No competing interests were disclosed.

Mark Morgan
Institute of Translational Medicine, University of Liverpool, Liverpool, UK

Approved: 20 December 2013

Referee Report: 20 December 2013
This is an interesting study highlighting the potential role of syndecan-3 in the regulation of angiogenesis. The study was well executed and the manuscript well written.

The authors show that recombinant syndecan-3 ectodomain (S3ED) inhibits angiogenic sprouting in a dose-dependent manner, using *ex vivo* aortic ring assays. They further show that S3ED inhibits endothelial cell migration and suggest that this is responsible for its anti-angiogenic effect.

This work warrants publication as it raises many new questions (beyond the realms of this project), about the non-neuronal roles of a relatively understudied syndecan. For example:

- What are the effects of S3ED *in vivo* and can syndecan-3 be targeted therapeutically?

- Does endogenous syndecan-3 (either shed or membrane-bound) serve a role for fine-tuning angiogenic processes *in vivo*?
- What is the specific mechanism by which S3ED inhibits endothelial cell migration and angiogenesis? Does it involve modulation of integrin and/or growth factor receptor function?

No doubt these questions will form the basis of many future studies.

Minor Points:

1. In Fig 2 it would be useful to include a representative image of an S3ED-treated aortic ring. Are angiogenic sprouts completely absent or are they just stumps?

2. The Transwell "invasion" assays described use a very thin coating (10ul) of non-crosslinked collagen type 1 and a relatively short time period (6Hrs). Consequently, they are not a good read-out of "invasion" *per se*, but rather of a mode of migration. Therefore the process should be described as "migration through collagen", or perhaps "invasive migration".

I have read this submission. I believe that I have an appropriate level of expertise to confirm that it is of an acceptable scientific standard.

Competing Interests: No competing interests were disclosed.

Alberto Grossi
Department of Food Science and Food Microbiology, Copenhagen University, Copenhagen, Denmark

Approved: 10 December 2013

Referee Report: 10 December 2013
This is a well conducted study which highlights an unforeseen role for the heparan sulphate proteoglycan syndecan-3. Additionally, beyond the realms of this study, these data suggest more detailed knowledge of the syndecan-3 expression profile is required.

I have read this submission. I believe that I have an appropriate level of expertise to confirm that it is of an acceptable scientific standard.

Competing Interests: No competing interests were disclosed.

© 2014. Published by The Company of Biologists Ltd | Journal of Cell Science (2014) 127, 4788–4799 doi:10.1242/jcs.153015

RESEARCH ARTICLE

Shed syndecan-2 inhibits angiogenesis

Giulia De Rossi[1], Alun R. Evans[1], Emma Kay[1], Abigail Woodfin[1], Tristan R. McKay[2], Sussan Nourshargh[1] and James R. Whiteford[1,*]

ABSTRACT

Angiogenesis is essential for the development of a normal vasculature, tissue repair and reproduction, and also has roles in the progression of diseases such as cancer and rheumatoid arthritis. The heparan sulphate proteoglycan syndecan-2 is expressed on mesenchymal cells in the vasculature and, like the other members of its family, can be shed from the cell surface resulting in the release of its extracellular core protein. The purpose of this study was to establish whether shed syndecan-2 affects angiogenesis. We demonstrate that shed syndecan-2 regulates angiogenesis by inhibiting endothelial cell migration in human and rodent models and, as a result, reduces tumour growth. Furthermore, our findings show that these effects are mediated by the protein tyrosine phosphatase receptor CD148 (also known as PTPRJ) and this interaction corresponds with a decrease in active β1 integrin. Collectively, these data demonstrate an unexplored pathway for the regulation of new blood vessel formation and identify syndecan-2 as a therapeutic target in pathologies characterised by angiogenesis.

KEY WORDS: Angiogenesis, Inflammation, Syndecan, Integrin, Endothelial cell migration

INTRODUCTION

Angiogenesis is a feature of development, wound healing, tumorigenesis and chronic inflammatory conditions, such as rheumatoid arthritis and atherosclerosis (Carmeliet, 2003; Mapp and Walsh, 2012). The process requires the transition of endothelial cells from a quiescent state to a migratory and proliferative phenotype, and is stimulated and controlled by growth factors, most notably vascular endothelial growth factor (VEGF) (Sakurai and Kudo, 2011). Endothelial cell migration is a crucial component of angiogenesis and integrins are the major drivers of this response (Ramjaun and Hodivala-Dilke, 2009). Integrins exist in various activation states on the cell surface and this modulates the migratory and adhesive characteristics of cells through interactions with the extracellular matrix (ECM). Other cell surface receptors also interact with ECM ligands leading to signalling cascades that can alter the activation state of integrins (Streuli and Akhtar, 2009). The four-member syndecan family of heparan sulphate proteoglycans (HSPGs) are an example of such molecules.

The syndecans are a family of transmembrane receptors with roles in cell adhesion, migration and growth factor signalling. In common with the other family members, syndecan-2 has a short cytoplasmic domain, a single-pass transmembrane domain and a larger extracellular domain, which is modified toward the N-terminus with heparan sulphate (HS) side chains and can be shed from the cell surface. Many cell types shed syndecan ectodomains through the action of matrix metalloproteinases (MMPs) in response to a variety of stimuli including inflammatory mediators, but the biological implications of this response are not fully understood (Manon-Jensen et al., 2010). In the present study, the possibility that shed syndecan-2 might be a regulator of angiogenesis was investigated.

There is a considerable body of work to suggest that syndecan extracellular core proteins have domains that influence cell behaviour. For example, cell adhesion regulatory domains have been identified in all four syndecan family members (De Rossi and Whiteford, 2013a; De Rossi and Whiteford, 2013b; McFall and Rapraeger, 1997; McFall and Rapraeger, 1998; Whiteford et al., 2007; Whiteford and Couchman, 2006). How and when these regulatory sequences function and their relevance to biological processes has yet to be determined. Previously, we have shown that the syndecan-2 extracellular core protein (S2ED) can support fibroblast attachment and spreading (Whiteford et al., 2007). Here, we show that S2ED shed from cells acts to inhibit angiogenesis in both rodent and human models through a paracrine interaction with the protein tyrosine phosphatase receptor CD148. This interaction leads to a de-activation of β1 integrins resulting in a reduction in endothelial cell migration.

RESULTS

Constitutively released syndecan-2 ectodomain inhibits angiogenesis in a xenograft tumour model

To investigate the potential effects of shed syndecan-2 on angiogenesis we established a mammalian expression system in which a constitutively released form of the molecule (lacking both transmembrane and cytoplasmic domains, M^{1}–F^{141}, eS2ED) was expressed in HEK293t cells (Fig. 1A). The HA epitope was also incorporated into eS2ED between D^{27} and K^{28} enabling us to readily detect eS2ED in conditioned media as compared to controls transfected with empty vector (Fig. 1B; supplementary material Fig. S1). Using these cell lines, we investigated the anti-angiogenic properties of shed syndecan-2 in a xenograft tumour model. Specifically, SCID-SHO mice were injected with empty vector cells or cells that constitutively released syndecan-2 (eS2ED) and tumour sizes were quantified at 21 days. Mice injected with control (empty vector) cells developed vascularised tumours that were significantly larger both in terms of diameter

[1]William Harvey Research Institute, Barts and The London School of Medicine and Dentistry, Queen Mary University of London, Charterhouse Square, London EC1M 6BQ, UK. [2]Division of Biomedical Sciences, St. George's University of London, Cranmer Terrace, London SW17 0NE, UK.

*Author for correspondence (j.whiteford@qmul.ac.uk)

Received 14 April 2014; Accepted 6 August 2014

Journal of Cell Science

Journal of Cell Science (2014) 127, 4788–4799 doi:10.1242/jcs.153015

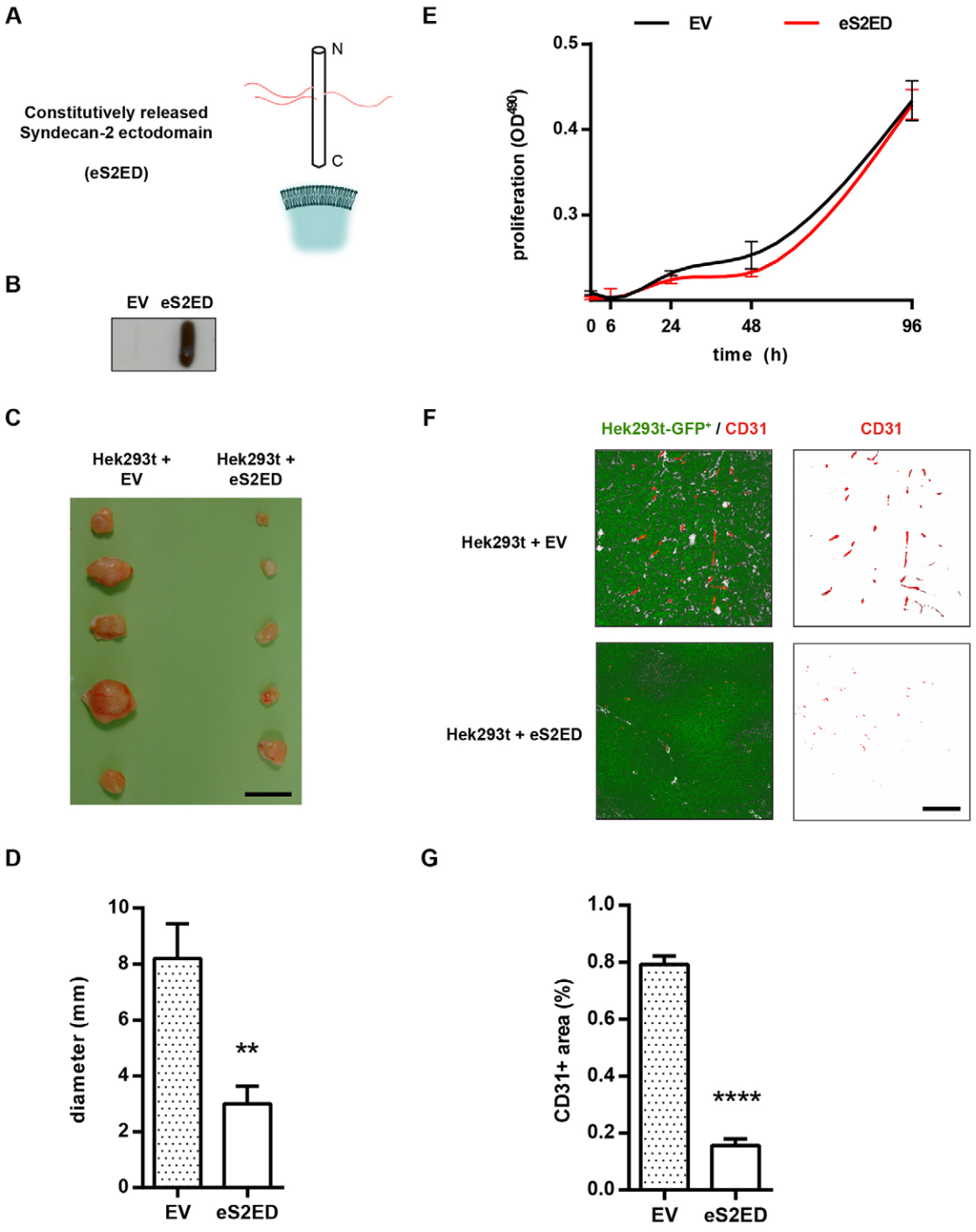

Fig. 1. Constitutively released syndecan-2 extracellular core protein from HEK293t cells inhibits angiogenesis in a xenograft tumour model. (A) Schematic diagram of syndecan-2 lacking both cytoplasmic and transmembrane domains (eS2ED), which is constitutively released from HEK293t cells. (B) Dot blot of conditioned media from cells transfected with either empty vector (EV) or eS2ED constructs. Dot blots were probed with the anti-HA antibody, and a strong signal is obtained from cells transfected with eS2ED. (C) Constitutively released syndecan-2 inhibits tumour growth. Micrograph of tumours from SCID-SHO mice injected with either empty vector cells or eS2ED cells. Scale bar: 1 cm. (D) Tumours derived from eS2ED cells have smaller diameter. Error bars represent the s.e.m. $^{**}P<0.01$ ($n=5$ tumours per condition, Student's *t*-test. (E) Empty vector cells and S2ED cells have the same growth kinetics over 96 h in culture. (F) Immunofluorescence staining of tumour sections derived from empty vector cells and eS2ED-transfected cells for the endothelial cell marker CD31 (red; tumour cells are GFP positive). Considerably more CD31-positive structures are evident in tumours derived from cells transfected with empty vector as compared the tumours in which syndecan-2 is constitutively released. Scale bar: 200 μm. (G) Quantification of the area of micrographs positive for CD31 was performed and expressed as a percentage of the GFP-positive tumour cells. Data are the mean from three separate images from sections of three tumours per group. Error bars represent the s.e.m. $^{****}P<0.0001$ (unpaired Student's *t*-test).

Journal of Cell Science (2014) 127, 4788–4799 doi:10.1242/jcs.153015

and weight as compared to tumours generated in mice injected with the eS2ED cells (Fig. 1C,D; supplementary material Fig. S2). We compared the growth kinetics in culture between empty vector cells and eS2ED-transfected cell lines and found no differences, indicating that cell proliferation defects were not the reason tumours derived from eS2ED cells failed to develop (Fig. 1E). Immunofluorescence staining of tumour sections for the endothelial cell marker CD31 (also known as PECAM1) revealed that tumours derived from empty vector control cells contained CD31-positive structures consistent with blood vessels. CD31-positive cells were greatly reduced in tumour sections derived from cells constitutively releasing syndecan-2 (Fig. 1F,G). These findings suggest that constitutive release of the syndecan-2 ectodomain in this model is inhibitory to angiogenesis.

The shed syndecan-2 ectodomain inhibits angiogenesis

We next explored the possibility that the syndecan-2 ectodomain cleaved from the cell surface in response to a known inducer of syndecan shedding, the pro-inflammatory mediator TNFα, could regulate angiogenesis (Pruessmeyer et al., 2010). HEK293t cells transfected with full-length HA-tagged syndecan-2 cDNA (eFLS2, Fig. 2A) expressed an abundance of cell surface syndecan-2 as demonstrated by flow cytometry, and the presence of HS chains was confirmed by western blotting (supplementary material Fig, S3B,C). These cells were stimulated with TNFα for 4 h and the medium was analysed for the HA-tagged shed syndecan-2 ectodomain. TNFα was found to induce shedding of syndecan-2 in a concentration-dependent manner (Fig. 2B). To investigate the potential impact of the shed molecule on angiogenesis, we performed anion exchange on conditioned media to isolate the HSPGs from empty vector and eFLS2-transfected cells stimulated with TNFα, and also on conditioned media from cells constitutively releasing eS2ED. The resulting HSPG-enriched samples were incorporated into collagen matrices into which rat aortic rings were embedded. Rings grown in the presence of empty vector eluates exhibited normal sprout formation. However, eluates containing shed syndecan-2, either TNFα-induced (eFLS2) or constitutively released (eS2ED), strongly inhibited angiogenic sprout formation (Fig. 2C). These data suggest that the anti-angiogenic properties of the syndecan-2 ectodomain are retained when syndecan-2 is shed from the cell surface.

The anti-angiogenic properties of shed syndecan-2 reside in the extracellular core protein of the molecule

In the following series of experiments, we further explored the impact of the extracellular core protein moiety of shed syndecan-2 on angiogenesis. For this purpose, we used a bacterial expression system to produce a fusion protein consisting of the extracellular core protein [of murine syndecan-2 (E^{19}–F^{141}) fused at the N-terminus to GST (S2ED, Fig. 3A) (Whiteford et al., 2007; Whiteford et al., 2011)]. The resulting protein is easily purified using glutathione and is not modified with HS chains because prokaryotes lack the requisite transferases (Whiteford et al., 2007). We incorporated S2ED into Matrigel plugs injected sub-dermally in the abdomen of C57BL/6 mice. After 5 days, plugs containing GST alone contained both CD31+ endothelial cells and blood, a possible indication of new blood vessel formation (Fig. 3B,C). In contrast plugs containing S2ED showed a notable reduction in angiogenesis as indicated by a reduced number of CD31+ endothelial cells (Fig. 3B,C). In addition, analysis of Matrigel plugs for haemoglobin content indicated less blood, indicative of reduced vascular formation in plugs incorporating S2ED as compared to those with GST alone (Fig. 3B; supplementary material Fig. S4A).

Having demonstrated the regulatory effects of S2ED on angiogenesis *in vivo*, we expanded these studies to both *ex vivo* and *in vitro* models of angiogenesis. Rat aortic explants were embedded into collagen I gels in which either GST (control) or S2ED was incorporated in the presence of VEGF. Whereas S2ED inhibited sprout formation in a concentration-dependent manner, rings grown in the presence of GST were unaffected by this treatment and sprouted to the same degree as untreated controls (Fig. 3D). S2ED also inhibited VEGF-induced angiogenesis in a model employing aortic rings from C57BL/6 mice (supplementary material Fig. S4B). The effect of S2ED *in vitro* was tested on

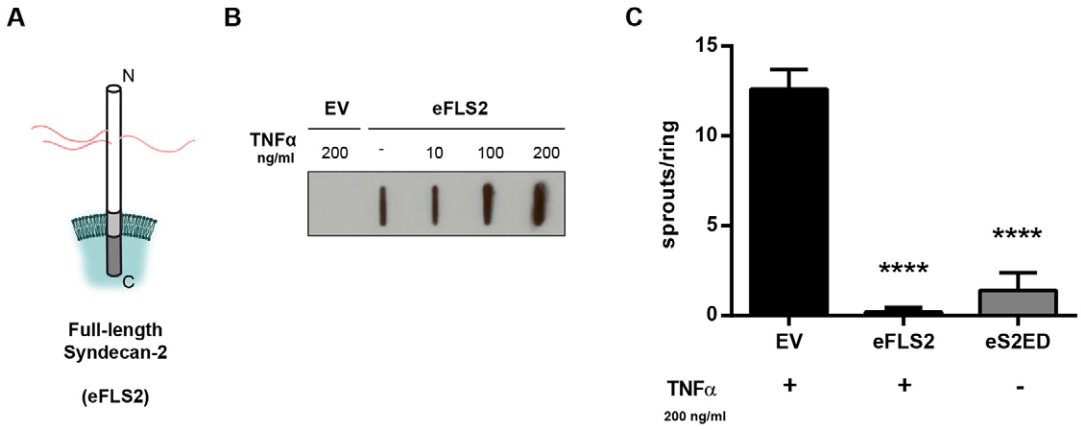

Fig. 2. Shed syndecan-2 from HEK293t cells has anti-angiogenic properties. (A) Schematic diagram of full-length HA-tagged syndecan-2 (eFLS2), which was expressed in HEK293t cells. (B) Syndecan-2 is shed from HEK293t cells after stimulation with TNFα in a dose-dependant manner. eFLS2 cells were incubated for 4 h in serum-free media with the indicated concentration of TNFα, and conditioned media were assayed by dot blot using the anti-HA antibody. EV, empty vector. (C) Shed syndecan-2 is anti-angiogenic. Empty vector cells and eFLS2 cells were treated with TNFα (200 ng/ml) for 4 h and the shed proteoglycans were purified by anion exchange. Proteoglycans were also isolated from conditioned media from eS2ED transfected cells using the same methodology. 10 μg of each protein preparation was incorporated into collagen I gels and then seeded with rat aortic rings as described in the Materials and Methods. Sprouts from eight rings were counted and results are mean±s.e.m. ****$P<0.0001$ (one-way ANOVA comparing to empty vector controls using the Tukey's camparisons test).

Journal of Cell Science (2014) 127, 4788–4799 doi:10.1242/jcs.153015

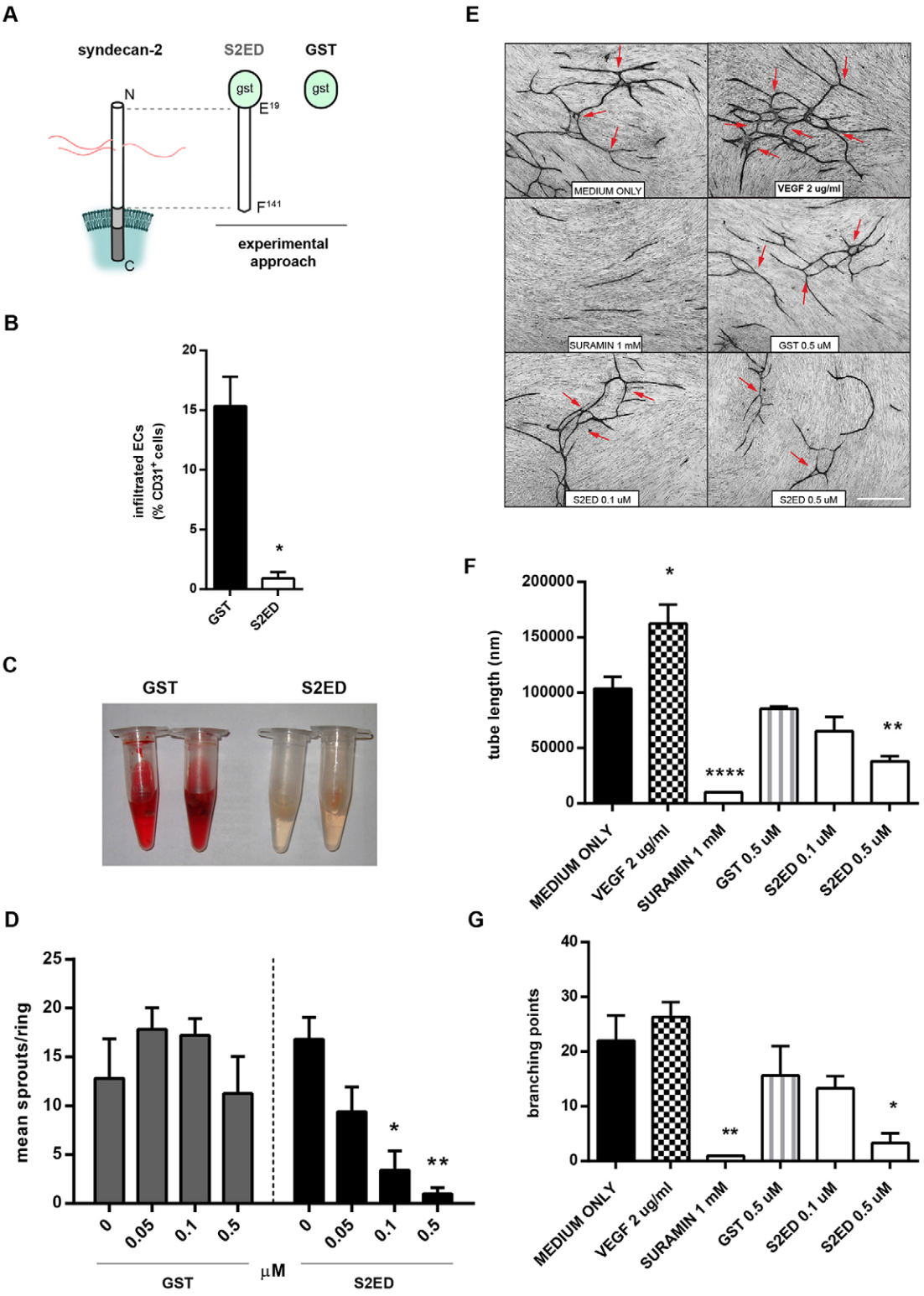

Fig. 3. See next page for legend.

human umbilical vein endothelial cell (HUVEC) tube formation when in 3D co-culture with human dermal fibroblasts using the commercially available V2A vasculogenesis to angiogenesis kit. After 2 weeks in culture under control conditions, tubule structures were formed with branch points (Fig. 3E). This effect could be augmented with the addition of VEGF and inhibited by the addition of Suramin. The addition of GST to the culture medium had little effect on either the length of tubules formed or the number of branch points as compared to the control medium. In contrast, in the presence of S2ED a significant reduction in tubule length and branch points was noted (Fig. 3F,G). Taken together, these results demonstrate that the syndecan-2 extracellular core protein has

Fig. 3. The syndecan-2 extracellular core protein inhibits angiogenesis. (A) Schematic diagram of S2ED consisting of GST fused to the syndecan-2 ectodomain core protein. (B) Angiogenesis is inhibited by S2ED when incorporated into Matrigel. C57BL/6 mice were given sub-dermal injections of Matrigel supplemented with VEGF and FGF containing either 0.5 μM of S2ED or GST. Excised sections of Matrigel plugs were immunostained for CD31 (endothelial cells) and DRAQ5 (all cell nuclei) and analysed by confocal microscopy, and the percentage of cells positive for CD31 calculated. Less endothelial cells migrate into Matrigel plugs containing S2ED. Error bars represent the s.e.m. of four separate images. $*P<0.05$ (Mann–Whitney *t*-test). (C) Photographs of plugs after excision. (D) The anti-angiogenic effects of S2ED are dose dependant. Rat aortic rings were seeded in collagen I containing the indicated concentrations of GST or S2ED and the angiogenic sprouts counted after 4 days. Data were obtained from at least 10 rings from four separate rats per condition. $*P<0.05$, $**P<0.01$ (one-way ANOVA comparing to untreated controls using the Tukey's comparisons test). (E) S2ED inhibits tubule formation in a HUVEC co-culture system. Using the V2a kit, HUVECs and fibroblasts were co-cultured in the presence of VEGF, Suramin, S2ED and GST. Micrographs, showing fewer tubules, were obtained in the presence of S2ED and these were shorter (F) and less branched (G; branch points denoted by arrows). Scale bar: 500 μm. Error bars represent the s.e.m. of four separate images. $*P<0.05$, $**P<0.01$, $****P<0.0001$ (Mann–Whitney *t*-test).

anti-angiogenic properties in both rat, murine and human model systems.

The anti-angiogenic properties of S2ED reside in the syndecan-2 adhesion regulatory domain

Given that we have previously shown that fibroblast adhesion to S2ED is regulated by the C-terminal 18-amino-acid domain between P^{124} and F^{141} of murine syndecan-2 (Whiteford et al., 2011), we hypothesised that this adhesion regulatory region of syndecan-2 might also be responsible for the inhibition of angiogenesis. This was initially investigated by performing rat aortic ring assays with deletion mutants of S2ED (Fig. 4A). Full length S2ED, S2EDΔP^{124}–F^{141} (lacking the adhesion regulatory domain) or S2EDΔL^{73}–G^{123} (a truncated form containing only the adhesion regulatory residues) were incorporated into collagen matrices in which aortic ring sections were embedded (Fig. 4A,B). Although angiogenic sprouts were observed in both untreated and GST controls, sprout formation was severely compromised when rings were embedded in matrices with S2ED or S2EDΔL^{73}–G^{123} both of which contain the regulatory 18-amino-acid motif (Fig. 4B). These data indicate that the anti-angiogenic properties of S2ED are dependent on the adhesion regulatory domain lying between P^{124} and F^{141} of murine syndecan-2.

S2ED inhibits endothelial cell migration

As endothelial cell migration is a crucial component of angiogenesis, the following series of experiments aimed to investigate the effect of S2ED on this response. To establish whether the anti-angiogenic effect of S2ED is due to the inhibition of endothelial cell migration by residues contained within the 18-amino-acid regulatory domain, we performed migration assays on brain endothelial cells in the presence of either S2ED or the truncated forms of this protein (S2EDΔP^{124}–F^{141} and S2EDΔL^{73}–G^{123}). As found with the full-length protein, the truncated fusion protein containing only the adhesion regulatory domain (S2EDΔL^{73}–G^{123}), inhibited endothelial cell migration (Fig. 4C,D). In contrast, the mutant protein lacking the syndecan-2 adhesion regulatory domain did not affect cell migration, with the wound closure being equivalent to that noted with cells treated with GST alone. The inhibitory effect of S2ED on endothelial cell migration was evident regardless of the vascular bed from which the endothelial cells originated because both skin and lung endothelial cells responded to S2ED and the mutant proteins in a similar manner (supplementary material Fig. S4C). Taken together, these data show that the effect of S2ED on endothelial cell migration is regulated by the C-terminal 18-amino-acid regulatory domain.

We also tested the effects of S2ED on endothelial cell invasion into collagen I gels and observed that cell invasion was greatly inhibited when S2ED was incorporated as compared to controls (Fig. 4E). Of importance, neither protein impacted upon cell proliferation (Fig. 3F). These data are in disagreement with the findings of a previous report (Fears et al., 2006) in which it was suggested that S2ED could promote endothelial cell invasion and stimulate longer microtubules in networks formed when endothelial cells are seeded on Matrigel. In trying to recapitulate this work we observed that S2ED inhibited endothelial cell invasion through Matrigel and had no measurable effect on network formation when sEND cells were seeded on Matrigel (supplementary material Fig. S4D,E). These results also show an inhibitory effect on endothelial cell invasion by S2ED and this is likely to be through inhibition of cell migration.

The inhibition of angiogenesis by S2ED is driven by CD148, leading to changes in β1 integrin activation

In fibroblasts the protein tyrosine phosphatase receptor CD148 (also known as PTPRJ) interacts directly with the adhesion regulatory domain of S2ED leading to β1-integrin-mediated cell attachment and spreading (Whiteford et al., 2011). To determine whether CD148 is a mediator for endothelial cell responses to S2ED, we first confirmed that endothelial cells from brain, lung and skin expressed CD148. Western blot analysis using an antibody directed to the cytoplasmic domain of CD148 revealed that all three cell lines expressed this receptor (Fig. 5A). We then demonstrated that there was an interaction between CD148 and the syndecan-2 ectodomain by performing a pulldown assay using GST–S2ED beads as bait. No CD148 was evident in precipitates in which GST- or GST–S2EDΔP^{124}–F^{141}-coated beads were used (Fig. 5B). S2ED and S2EDΔL^{73}–G^{123}, which both contain the C-terminal 18-amino-acid adhesion regulatory domain successfully pulled down CD148 from endothelial cell lysates indicating that the interaction point between CD148 and S2ED resides in this region of the molecule.

We next performed rat aortic ring experiments using a purified recombinant form of the CD148 extracellular domain comprising the first five type III fibronectin repeats of the human form of this molecule. This also proved inhibitory to angiogenesis to the same degree as S2ED, and when used in conjunction with S2ED the anti-angiogenic effect appeared enhanced (Fig. 5C).

The impact of S2ED on endothelial cell β1 integrin activation was examined next. Endothelial cells treated with S2ED showed reduced binding of the β1 integrin activation marker, the monoclonal antibody (mAb) 9EG7, as demonstrated by fluorescence activated cell sorting (FACS) (Fig. 6A). Using this antibody for immunofluorescent staining of endothelial cells, a substantial reduction in active β1 integrins was observed in cells treated with S2ED (Fig. 6B,C). Interestingly this effect was most pronounced at the leading edge of scratch wounds, where the highest expression of active β1 integrins was noted in control and GST-treated cells. We further tested the effect of S2ED on β1

Journal of Cell Science (2014) 127, 4788–4799 doi:10.1242/jcs.153015

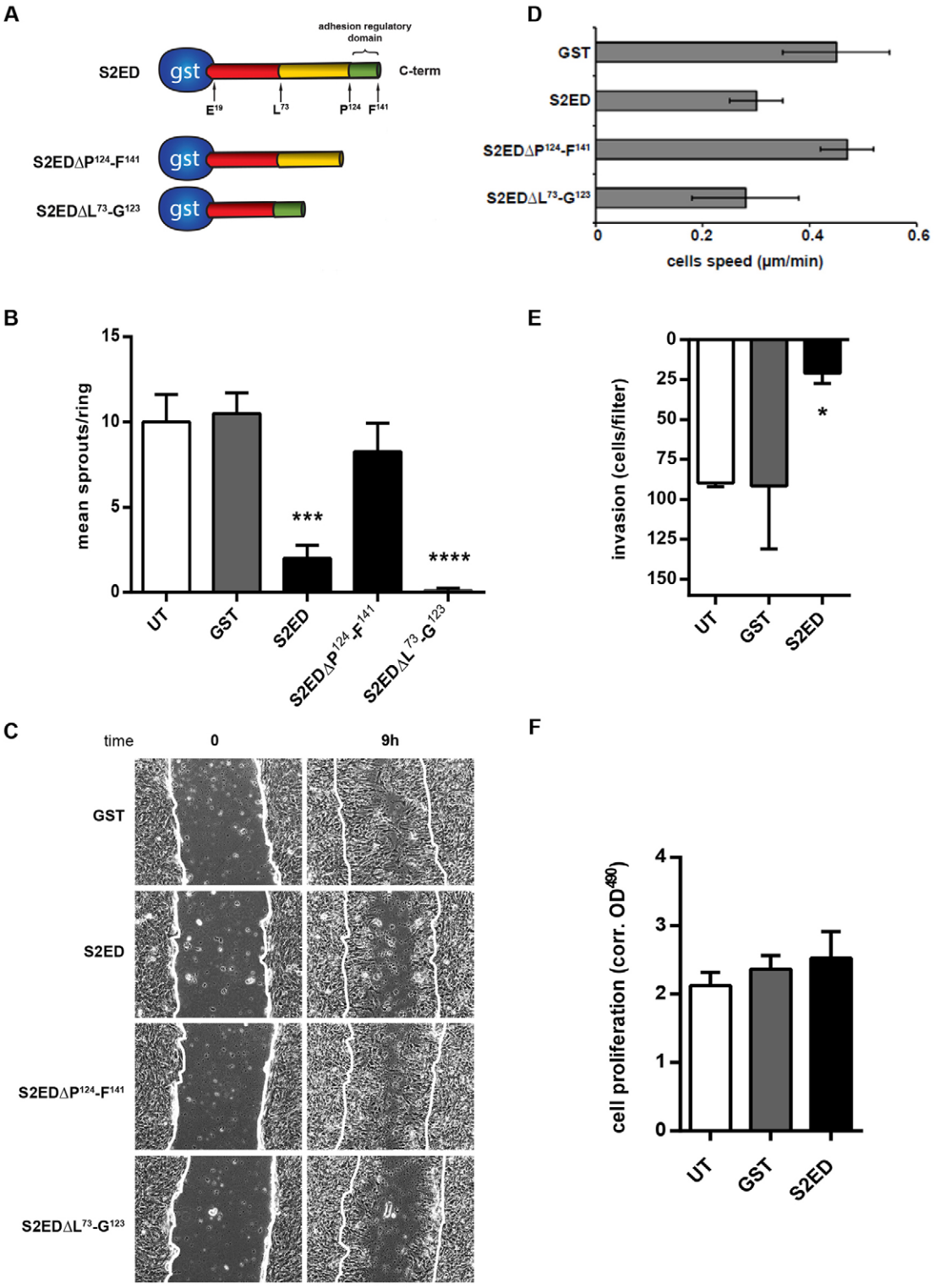

Fig. 4. See next page for legend.

integrin activation in HUVECs. Stimulation of HUVECs with Mn^{2+} lead to an increase in structures that bound the mAb HUTS4 and this was unaffected by the addition of GST. Positive staining was greatly reduced when cells were treated with S2ED (Fig. 6D). Taken together, these results suggest that the anti-migratory effects of S2ED on endothelial cells might be mediated by CD148 signalling, an interaction that could lead to a reduction in active β1 integrins on the surface of endothelial cells (Fig. 6).

DISCUSSION

The use of inhibitors for the suppression of pathological angiogenesis is well established, although clinical evidence

Journal of Cell Science (2014) 127, 4788–4799 doi:10.1242/jcs.153015

Fig. 4. The anti-angiogenic properties of S2ED are due to inhibition of endothelial cell migration and are mediated by amino acids P^{124}–F^{141}. (A) Diagram of the mutant proteins used in this study. Full-length syndecan-2 extracellular core protein S2ED comprising E^{19}–F^{141}, a truncated form of S2ED lacking the adhesion regulatory domain, S2EDΔP^{124}–F^{141} (green), and a mutant containing only the GAG attachment domain and the C-terminal adhesion regulatory domain, S2EDΔL^{73}–G^{123}. (B) The adhesion regulatory domain of syndecan-2 inhibits angiogenic sprout formation. Rat aortas were seeded in collagen I matrices containing 0.5 μM of GST, S2ED or the mutant forms of S2ED. Sprouts from eight rings per condition were counted and the mean calculated. Error bars represent the s.e.m. ***$P<0.005$, ****$P<0.0001$ (one-way ANOVA with Bonferroni multiple comparison). (C,D) Scratch wound migration assays were performed in the presence of 0.5 μM of the indicated fusion proteins on brain endothelial cells. (D) Endothelial cell migration speed is reduced in the presence of S2ED proteins containing the 18-amino-acid regulatory domain. Cell speed data represents mean±s.e.m. measurements from at least 25 individual cells at the leading edge per treatment. (E) S2ED inhibits endothelial cell invasion into collagen I matrices. GST or S2ED (0.5 μM) were incorporated into collagen I matrices in transwells. After 6 h, cells that had migrated were counted and the data represents the mean±s.e.m. of triplicate assays. *$P<0.05$ (by Student's *t*-test). (F) Cell proliferation is unaffected by S2ED. Confluent monolayers of sEND cells were grown in the presence of 0.5 μM of the proteins indicated and mean proliferation measurements were calculated from four wells per condition.

suggests that there are a number of complications and side effects (Duda et al., 2007). There is therefore a need for greater understanding of the regulatory mechanisms that both promote and inhibit new blood vessel formation in order to develop new more effective therapeutic targets. We propose a previously unreported role for syndecan-2, in that, in its shed form, syndecan-2 can act to inhibit angiogenesis by slowing endothelial cell migration, through an interaction with CD148 leading to changes in β1 integrin activation (Fig. 7). The identification of the syndecan-2 adhesion regulatory domain as a strong negative regulator of angiogenesis mean that both it and its binding partner CD148 are potential novel therapeutic targets in pathologies where angiogenesis is a feature, such as atherosclerosis, arthritis and cancer.

Angiogenesis requires the action of numerous pro- and anti-angiogenic factors that collectively provide the signals necessary for the generation of new blood vessels. Here, we demonstrate that one such factor is the extracellular core protein of syndecan-2 that, when shed from cells, can negatively regulate angiogenesis. Syndecan shedding is a feature of many cell types and occurs in response to stimuli such as inflammatory mediators and growth factors (Manon-Jensen et al., 2010; Pruessmeyer et al., 2010). Both MMP-7 and MMP-9 have been identified as having a role in the shedding of syndecan-2 (Fears et al., 2006; Kwon et al., 2014). As yet the cleavage sites for syndecan-2 shedding have not been identified; however, the eukaryotic expression system described here will provide an useful tool to address this important question. Shedding studies on syndecan-4, the most closely related member of this family to syndecan-2, suggest that the entire ectodomain can be cleaved from the cell surface (Manon-Jensen et al., 2013). The fact that shed syndecan-2 influences angiogenesis and that the regulatory region resides between P^{124} and F^{141} of the ectodomain, close to the syndecan-2 transmembrane domain, suggests that, like syndecan-4, the entire ectodomain is shed in response to inflammatory stimuli.

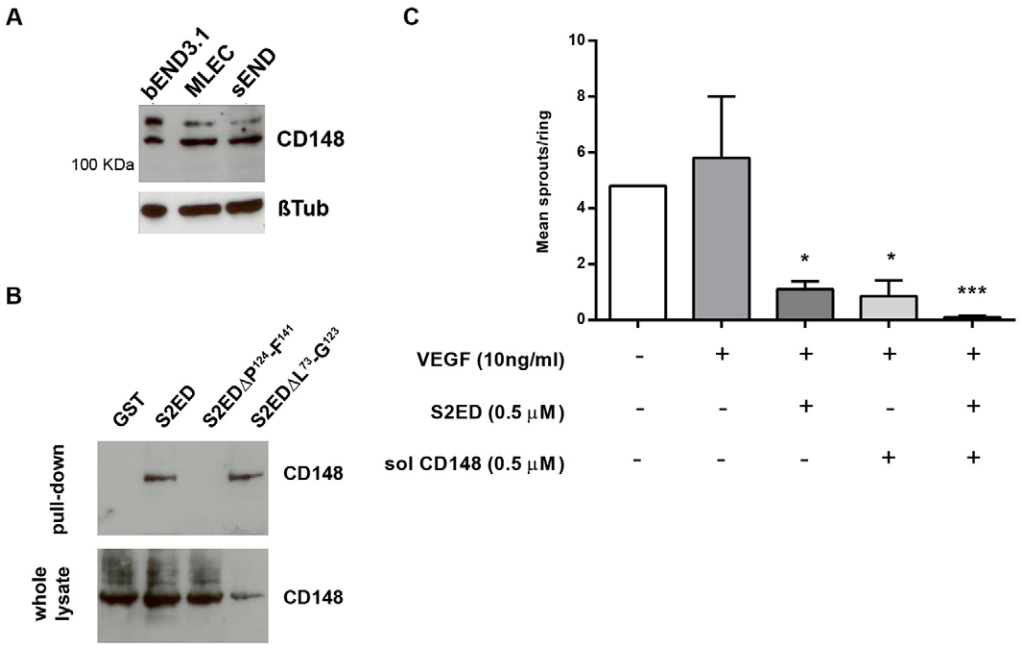

Fig. 5. S2ED interacts with CD148, resulting in the inhibition of angiogenesis. (A) bEND3.1, MLEC and sEND cells express CD148. Western blot of lysates from the endothelial cell lines indicated were probed with antibodies against CD148 or β-tubulin. (B) CD148 interacts with S2ED. Cell lysates from sEND cells were incubated with beads coated with GST, S2ED, S2EDΔP^{124}–F^{141} or S2EDΔL^{73}–G^{123}. Precipitates were analysed by western blotting for the presence of CD148. CD148 was only pulled down by forms of S2ED which contain the C-terminal 18-amino-acid adhesion regulatory domain. The blot is representative of four experiments. (C) Soluble CD148 inhibits angiogenesis. Rat aortic rings were embedded in collagen I with either 0.5 μM S2ED or 0.5 μM of soluble (sol) CD148, or both proteins in combination, in the presence of VEGF. Both S2ED and soluble CD148 inhibited sprout formation to the same degree, and also inhibited angiogenesis when used in combination. Data are the mean from aortas from five animals and errors bars reflect the s.e.m. *$P<0.05$, ***$P<0.001$ (Student's *t*-test comparing values to the untreated VEGF control).

Journal of Cell Science (2014) 127, 4788–4799 doi:10.1242/jcs.153015

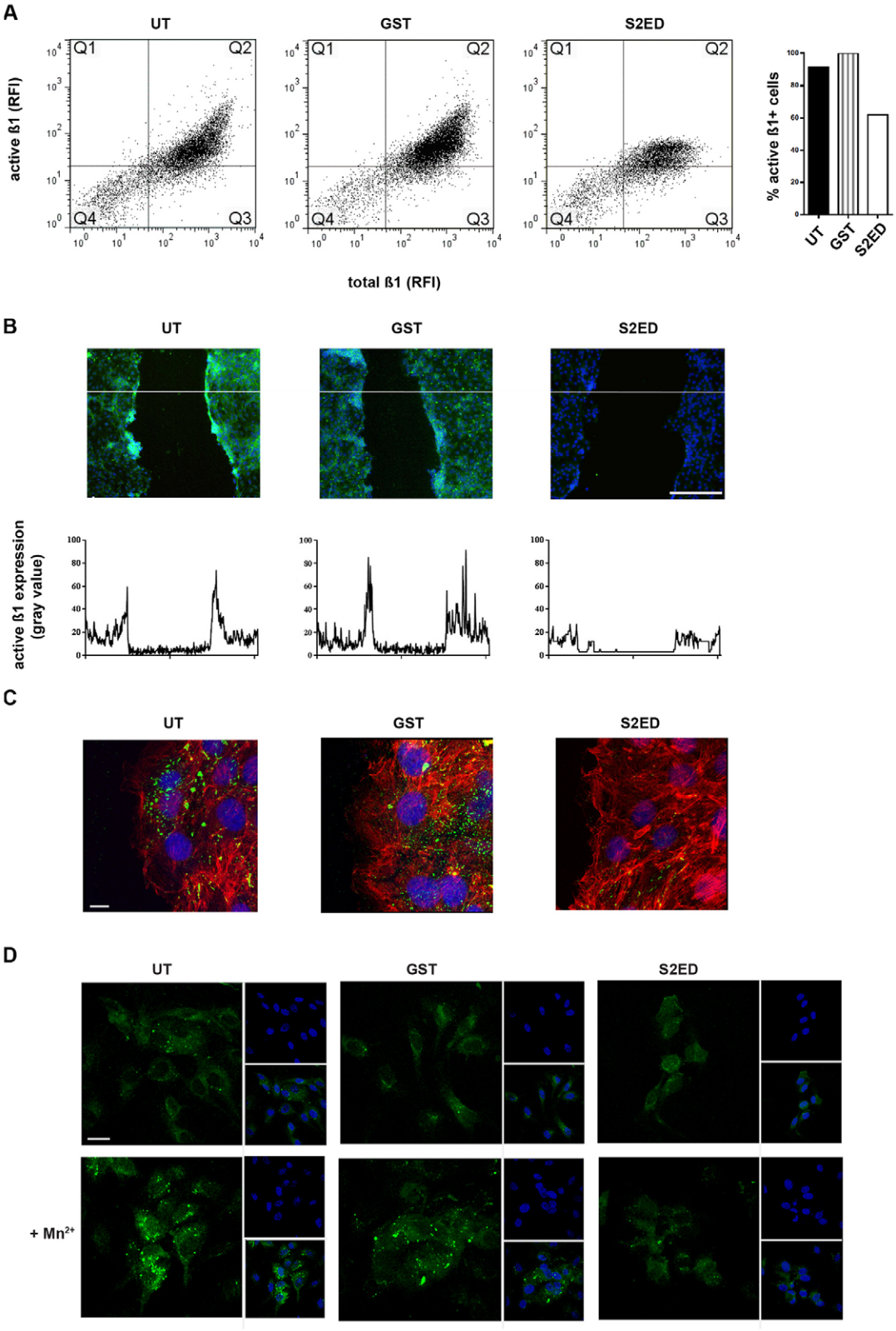

Fig. 6. See next page for legend.

Regulatory sequences in the syndecan-1 and, more recently, the syndecan-3 ectodomain have been identified and these have also been shown to be anti-angiogenic (Beauvais et al., 2004; Beauvais et al., 2009; De Rossi and Whiteford, 2013b). However, the evidence presented here suggests that shed syndecan-2 acts on endothelial cells through a mechanism distinct to that associated with syndecan-1 and -3. Syndecan-1 is thought to interact directly with αV integrins, leading to changes in cell adhesion

Journal of Cell Science (2014) 127, 4788–4799 doi:10.1242/jcs.153015

Fig. 6. Active β1 integrin is reduced on endothelial cells in the presence of S2ED. (A) Active β1 integrin on sEND cells positive for total β1 integrin is reduced in S2ED-treated cells as measured by FACS. The number of endothelial cells with active β1 integrin (as recognised by the monoclonal antibody 9eG7) was expressed as a percentage of total β1-integrin-expressing cells and plotted on the bar chart (right) left and dot blots corresponding to each treatment (left). (B) Micrographs of scratch wounds showing that active β1 integrin is reduced in endothelial cells treated with S2ED. Active β1 integrin is shown in green and DAPI in blue. Scratch wounds were performed on confluent monolayers and were incubated in the presence of the indicated proteins (0.5 μM) for 30 min prior to staining. Graphs represent the fluorescent intensity profile of active β1 integrin across the scratch wounds. The data was obtained from the section represented by the lines indicated on the micrographs. Scale bar: 200 μm. (C) Higher magnification micrographs (63×) of endothelial cells treated as indicated. Scale bar: 10 μm. Cells were stained for F-actin (red), DRAQ5 (blue) and active β1 integrin (green). (D) S2ED causes a reduction in active β1 integrin on HUVECs. HUVECs were treated with 1 mM $MnCl_2$ in the presence of 0.5 μM GST or S2ED. Untreated cells or cells treated with GST showed an increase in structures recognised by the monoclonal antibody HUTS4 (green). This was not the case with cells treated with S2ED. Inlays show DAPI staining (blue) and merged images. Scale bar: 20 μm.

characteristics through an autocrine interaction with IGFR-1 (Beauvais and Rapraeger, 2010; Rapraeger et al., 2013). We propose that shed syndecan-2 acts in a paracrine fashion given that the adhesion regulatory domain of syndecan-2 is situated very close to the transmembrane domain of the full-length molecule. The presence of glycosaminoglycan (GAG) chains and the respective sizes of the receptors involved make it hard to envisage how an autocrine interaction between these CD148 and syndecan-2 could occur. Whether regulation of angiogenesis is a common feature of all four syndecan ectodomains is an attractive possibility that requires further investigation.

We showed that the anti-angiogenic effect of the syndecan-2 ectodomain is observed in both rodent and human models of angiogenesis, and involves the interaction with the protein tyrosine phosphatase receptor CD148 on the surface of endothelial cells, which corresponds with the inactivation of β1 integrins. β1 integrins are intimately associated with angiogenesis and endothelial cell migration (Mettouchi and Meneguzzi, 2006). Our previous work using fibroblasts has shown that engagement of CD148 with S2ED leads to the de-phosphorylation of the p85 subunit of phosphoinositide 3-kinase (PI3K) and that there is a requirement for Src kinase in this process. Furthermore, clustering of CD148 with cognate antibodies leads to β1-integrin-mediated fibroblast adhesion responses (Whiteford et al., 2011). It is likely that this same signalling pathway is functional in endothelial cells, and that these signalling molecules are involved in the reduction in active β1 integrins on the surface of endothelial cells in response to S2ED. CD148 is known to be involved in the inhibition of cell migration in leukocytes, notably neutrophils and macrophages (de la Fuente-García et al., 1998; Zhu et al., 2008; Zhu et al., 2011), and, here for the first time we show it also has a role in regulating endothelial cell migration. Another ECM component, thrombospondin, has also been identified as a ligand for CD148, and this molecule is also known to bind HS, and is an inhibitor of angiogenesis (Takahashi et al., 2012). It is tempting to speculate that these three molecules are involved in some form of cell migration regulatory complex within the ECM, particularly as endothelial cell responses to thrombospondin-1 have been shown to involve β1 integrin.

Syndecan-2 and CD148 are molecules intimately associated with the vasculature. Syndecan-2 is expressed on fibroblasts, leukocytes and endothelial cells, and studies in zebrafish have revealed that syndecan-2 is essential for branching angiogenesis (Chen et al., 2004). Here, we show that CD148 is present on endothelial cells from three distinct vascular beds (brain, skin and lung). CD148-null mice are viable and show no gross defects; however, a knock-in mouse expressing a catalytically dead form of CD148 in which the cytoplasmic domain is replaced by eGFP dies early in development due to a failure in vascularisation (Takahashi et al., 2003; Trapasso et al., 2006). Quite why the cytoplasmically mutated form of CD148 elicits such a strong

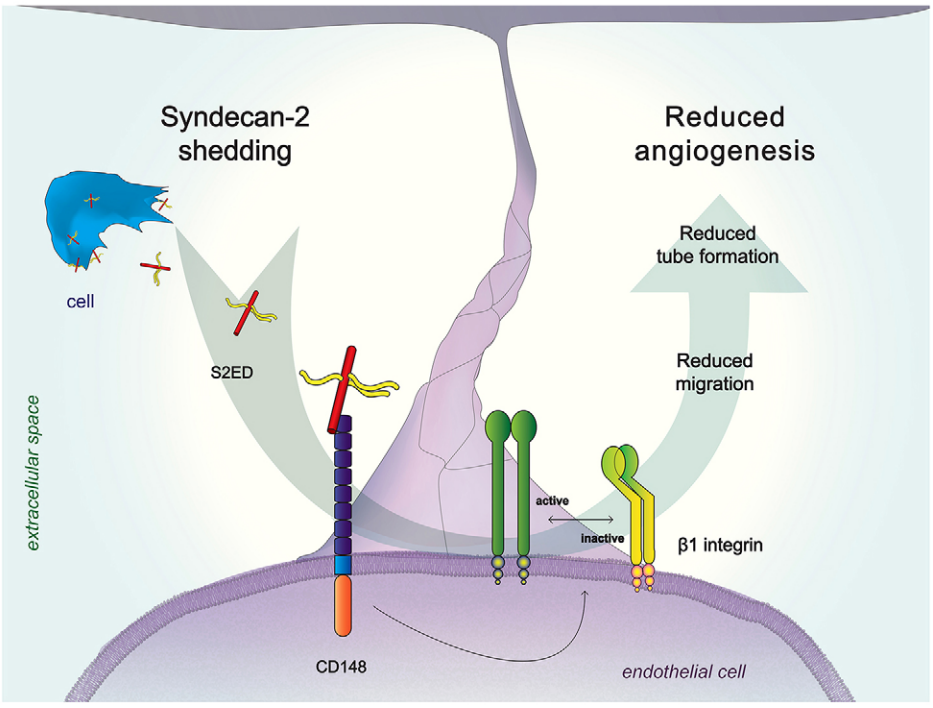

Fig. 7. Engagement of CD148 by shed syndecan-2 corresponds with a reduction in active β1 integrin in endothelial cells leading to inhibition of cell migration and less angiogenesis.

Journal of Cell Science

phenotype is not clear. Our study suggests that engagement of CD148 by its ligands results in an ablation of the angiogenic process and this is supported by the fact that antibodies targeting CD148 have anti-angiogenic affects (Takahashi et al., 2006). We hypothesize that this CD148-driven response to S2ED represents a signal whereby new blood vessel formation is halted, for example at the site of tissue injury. In as much as promoting new blood vessel formation is an important feature of wound healing, the cessation of this process also represents an important step. Syndecan-null animals also breed normally, are fertile and have no gross abnormalities and it is only under challenge or insult that these animals exhibit phenotypes (Ishiguro et al., 2002). It is conceivable that the CD148-null mouse would exhibit similar responses. An intriguing question would be how this mouse would respond to wounding or models where excessive angiogenesis occurs, such as in retinal angiogenesis or tumour models. This work presents an unreported pathway for the inhibition of angiogenesis and presents an alternative therapeutic target for anti-angiogenic therapy to those currently on the market.

MATERIALS AND METHODS

Fusion proteins and antibodies

GST, S2ED, S2EDΔP^{124}–F^{141}, S2EDΔL^{73}–G^{123} and soluble CD148 were purified as described previously (Whiteford et al., 2011). Antibodies used were anti-CD148 (R and D Systems), anti-CD29 clone 9EG7 (BD Pharmingen), anti-mouse CD29 clone HMβ1-1 (Biolegend), anti-CD29 clone HUTS4 (Millipore), Anti-HA (clone HA.11, Covance), anti-syndecan-2 (AF6585, R and D systems) and anti β-tubulin (clone TUB2.1, Sigma) antibodies, and Alexa-Fluor-488-conjugated anti-mouse CD31 antibody (Clone MEC 13.3, Biolegend). Alexa-Fluor-568-conjugated phalloidin was from Life Technologies.

Cell culture

All cells used in this study were grown at 37℃ under 10% CO_2 in Dulbecco's modified Eagle's medium (DMEM; PAA), supplemented with 10% FBS, 2 mM L-glutamine, 1% non-essential amino acids, 1 mM sodium pyruvate and 5 µM β-mercaptoethanol (all Invitrogen). Primary murine lung endothelial cells were isolated and maintained as described previously (Reynolds et al., 2002). HUVECs (HPA laboratories) were grown and maintained in Endothelial Growth Medium (HPA laboratories) and maintained as above.

Generation of syndecan-2-expressing cell lines

Gene synthesis of the complete murine syndecan-2 cDNA and the cDNA encoding only the syndecan-2 ectodomain coding sequence was performed by GeneArt (Invitrogen). Both full-length and truncated syndecan-2 cDNAs were mutated such that the HA epitope was inserted between D^{27} and K^{28} (supplementary material Fig. S1). *Bam*HI sites were also incorporated at the 5′ and 3′ end of the two synthetic genes. The cDNAs were cloned into the *Bam*HI site of the lentiviral vector pLNT-SFFV-MCS-EGFP (available from T.R.M.). Lentiviruses were produced in HEK293t cells and packaged into a VSVG coat using conventional procedures. HEK293t cells were transfected using the supernatant transfer method. Cells expressing high levels of eGFP were sorted by flow cytometry and these were cultured in DMEM as described.

Tumour xenograft model

Six-week-old SCID SHO mice (Charles River) were subcutaneously injected in the left flank with 3×10^6 HEK293t cells stably transfected with either empty vector or eS2ED in 100 µl PBS. Mice were left for 21 days prior to being killed by cervical dislocation. All experiments were performed under the UK legislation for the protection of animals in accordance with UK Home Office regulations. Tumours were dissected and photographed and tumour mass and diameter was measured. Tumours were then snap-frozen in liquid nitrogen prior to embedding in OCT and sectioning (20 µm sections). Sections were fixed using ice-cold methanol and immunostained with anti-CD31 antibodies conjugated to Alexa Fluor 564 and imaged using a PASCAL laser-scanning confocal microscope (Carl Zeiss) with a 10× objective.

Matrigel plug assay

Male 6-week-old C57BL/6 mice were given subdermal abdominal injections consisting of 600 µl of Matrigel (BD Biosciences) mixed with 100 µl of PBS containing 100 ng/ml VEGF, 100 ng/ml FGF and 20 U/ml of heparin and 0.5 µM of either GST or S2ED (following the method described in Passaniti et al., 1992). Mice were killed after three days and the plugs excised, photographed and incubated overnight in PBS. Haemoglobin was quantified using Drabkin's reagent (Sigma) as described by the manufacturer. All experiments were performed under the UK legislation for the protection of animals, and at the end of all *in vivo* procedures involving anaesthesia, animals were humanely killed by cervical dislocation in accordance with UK Home Office regulations. Excised plugs were frozen in liquid nitrogen and subsequently embedded in ice cold OCT, 15-µm sections were made using a cryostat at −20℃. Following fixation with 4% paraformaldehyde (PFA) for 5 min and blocking with 10% normal goat serum for 15 min, sections were stained for nuclei (DRAQ5) and the endothelial cell marker CD31 overnight. Images were captured using a PASCAL laser-scanning confocal microscope (Carl Zeiss, 10×objective). Quantification was performed using the IMARIS software and Photoshop (Adobe), endothelial cells were identified by co-localization of nuclei with CD31 staining.

Aortic ring assay

Thoracic aortas dissected from cervically dislocated 180–200 g male wistar rats (Harlan laboratories) or 6-week-old C57BL/6 mice (Charles River), and were sliced into 0.5-mm sections and incubated overnight in serum-free OptiMEM (Invitrogen) at 37℃. Aortic rings were embedded in type I collagen (1 mg/ml) in E4 medium (Invitrogen) containing GST, syndecan-2 mutant proteins or peritoneal exudates in 48-well plates. Wells were supplemented with OptiMEM with 1% FBS and 10 ng/ml VEGF (R and D systems, 30 ng/ml for murine rings) and incubated at 37℃ under 10% CO_2. Angiogenic sprouts from rat and mouse aortas were counted after 4 days and 8 days respectively (method based on that of Nicosia and Ottinetti, 1990 and modified in De Rossi et al., 2013).

In vitro tubule formation assays

HUVECs and human dermal fibroblasts were co-cultured using the Cell Works V2a kit (Caltag Media Systems as described by the manufacturer). Medium containing control compounds, GST or S2ED was changed every second day and at day 14 endothelial cells were stained for CD31 to assess the tube formation. Imaging was performed using an Olympus IX81 inverted microscope (10× objective); tube length and branch points were quantified using Photoshop (Adobe). A branch point was defined as the point at which two or more tubules met, and the tubule length as the length of tubules between branch points. In a second type of microtubule assay, sEND cells (5×10^4) were seeded into 24-well plates coated with 150 µl of Matrigel (BD sciences) in the presence of either GST or S2ED. Using the Cell-IQ controlled environmental chamber (CM technologies) plates were incubated at 37℃ under 10% CO2 and images were captured every 15 min for 16 h.

Scratch wound migration assays

Scratch wound migration assays were performed on confluent monolayers of endothelial cells. Wounds were made using a pipette tip, and fusion proteins were added to the medium and images were captured every 30 min for 12 h by time lapse microscopy using an Olympus IX81 microscope. Percentage wound closure was calculated and individual cells were tracked using Image J.

Invasion assay

Invasion assays through collagen and Matrigel matrices were performed in 24-well plates with transwell inserts [Millipore; 8-µm pore size, polyester (PET) membrane]. Membranes were coated with 10 µl of a collagen type I mixture (Millipore; 1 mg/ml in E4 medium) containing

0.5 µM GST or S2ED. sEND cells were seeded on the gel in a homogenous single cell suspension of 5,000 cells/insert in 200 µl of DMEM plus 10% FBS; 1 ml of the same medium was added to the bottom well. Invasion was measured after 6 h after which time gels were removed with a cotton swap, the filter washed in PBS and stained with calcein (Invitrogen) and the number of cells attached to the filter counted.

Proliferation

Cell proliferation was measured using the CellTiter 96 AQ_{ueous} Cell proliferation assay kit as described by the manufacturer (Promega).

CD148 pulldown and western blotting

Confluent bEND3.1 cells were lysed in 1% Triton X-100 in Tris-buffered saline (TBS) containing HALT protease and phosphatase inhibitors (Pierce). GST and S2ED were bound to glutathione–Sepharose beads (GE Healthcare) and were added to cell lysates and incubated for 1 h. Beads were isolated by centrifugation and washed twice in TBS, prior to incubation in Laemmli buffer and analysis by western blotting using standard procedures.

Dot blotting

Samples were diluted in blotting buffer (0.15 M NaCl buffered to pH 4.5 with 50 mM sodium acetate, with 0.1% Triton X-100) and applied under vacuum to cationic nylon membranes (GE Healthcare; Amersham Hybond^{TM}-N+). Membranes were washed three times with blotting buffer, blocked for 1 h in blocking buffer (3% milk, 0.5% BSA, 0.15 M NaCl in 10 mM Tris-HCl pH 7.4) and incubated overnight with primary antibody in blocking buffer plus 0.3% Tween-20. After washing, blots were incubated for 2 h with the appropriate horseradish peroxidase (HRP)-conjugated secondary antibody and signals were detected by chemi-luminescence using conventional procedures. Quantification of the signal intensity was performed using ImageJ software.

FACS and immunofluorescence staining for active integrin

Confluent bEND3.1 cells were trypsinised and the trypsin inactivated with BSA. Cells were re-suspended in Hank's buffer (without Ca^{2+} and Mg^{2+}) containing the treatments described (0.5 µM GST or S2ED) and incubated for 30 min at 37℃. Cells were then fixed in 2% PFA prior to FACS analysis for both total and active β1 integrin and the percentage of cells expressing active β1 calculated. For immunofluorescence staining of active β1 integrin, confluent monolayers of sEND cells were grown on microscope slides and scratch wounds were made and either 0.5 µM GST or S2ED was added. After 30 min, cells were fixed with 4% PFA (Sigma) and permeabilised in 0.1% Triton X-100 (Sigma) in PBS. Samples were incubated with active β1-integrin-specific antibody 9EG7 in 1% normal goat serum in PBS overnight at 4℃. Slides were washed in PBS and incubated in anti-rabbit-IgG antibody conjugated to Alexa Fluor 488 (Molecular Probes) and DAPI, and images were captured on an Olympus IX81 inverted microscope. Fluorescent intensity profiles from the resulting images were calculated using ImageJ. For higher resolution images, cells were imaged using a PASCAL laser-scanning confocal microscope (Carl Zeiss) with a 63× objective and the resulting stacks were processed using IMARIS software. HUVECs were seeded on coverslips coated with fibronectin (10 µg/ml) and collagen I (30 µg/m) in 0.1% gelatin. Once ~60% confluent, cells were washed with serum-free OptiMEM then treated either with or without 1 mM $MnCl_2$ in the presence of either 0.5 µM GST or S2ED for 30 min. Cells were then fixed in 2% PFA and stained using a monoclonal active β1-integrin-specific antibody (clone HUTS4, at 1:300). After washing, cells were stained with an anti-mouse-IgG antibody conjugated to Alexa Fluor 594 (Molecular Probes). Cells were analysed by confocal microscopy as described above.

Acknowledgements

We would like to acknowledge the technical help of Kairbaan Hodivala-Dilke and Bruce Williams (Barts Cancer Institute, Queen Mary University of London, UK).

Competing interests

The authors declare no competing interests.

Author contributions

J.R.W., G.D.R., A.R.E., E.K. and A.W. performed the research. J.R.W. and S.N. designed the study. T.M. provided the lentiviral reagents. The manuscript was written by J.R.W., S.N. and G.D.R.

Funding

J.W. is supported by grants from Arthritis Research UK [grant number 19207]; G.D.R. is supported by Barts and the London School of Medicine and Dentistry; A.W. is supported by the British Heart Foundation [grant number FS/11/19/28761]; and S.N. by the Wellcome Trust [Senior Investigator Award 098291/Z/12/Z]. Deposited in PMC for immediate release.

Supplementary material

Supplementary material available online at
http://jcs.biologists.org/lookup/suppl/doi:10.1242/jcs.153015/-/DC1

References

Beauvais, D. M. and Rapraeger, A. C. (2010). Syndecan-1 couples the insulin-like growth factor-1 receptor to inside-out integrin activation. *J. Cell Sci.* **123**, 3796-3807.

Beauvais, D. M., Burbach, B. J. and Rapraeger, A. C. (2004). The syndecan-1 ectodomain regulates alphavbeta3 integrin activity in human mammary carcinoma cells. *J. Cell Biol.* **167**, 171-181.

Beauvais, D. M., Ell, B. J., McWhorter, A. R. and Rapraeger, A. C. (2009). Syndecan-1 regulates alphavbeta3 and alphavbeta5 integrin activation during angiogenesis and is blocked by synstatin, a novel peptide inhibitor. *J. Exp. Med.* **206**, 691-705.

Carmeliet, P. (2003). Angiogenesis in health and disease. *Nat. Med.* **9**, 653-660.

Chen, E., Hermanson, S. and Ekker, S. C. (2003). Syndecan-2 is essential for angiogenic sprouting during zebrafish development. *Blood* **103**, 1710-1719.

de la Fuente-García, M. A., Nicolás, J. M., Freed, J. H., Palou, E., Thomas, A. P., Vilella, R., Vives, J. and Gayá, A. (1998). CD148 is a membrane protein tyrosine phosphatase present in all hematopoietic lineages and is involved in signal transduction on lymphocytes. *Blood* **91**, 2800-2809.

De Rossi, G. and Whiteford, J. R. (2013a). Novel insight into the biological functions of syndecan ectodomain core proteins. *Biofactors* **39**, 374-382.

De Rossi, G. and Whiteford, J. R. (2013b). A novel role for syndecan-3 in angiogenesis. *F1000Res.* **2**, 270.

De Rossi, G., Scotland, R. and Whiteford, J. (2013). Critical factors in measuring angiogenesis using the aortic ring model. *J. Genet. Syndr. Gene Ther.* **4**, 1000147.

Duda, D. G., Batchelor, T. T., Willett, C. G. and Jain, R. K. (2007). VEGF-targeted cancer therapy strategies: current progress, hurdles and future prospects. *Trends Mol. Med.* **13**, 223-230.

Fears, C. Y., Gladson, C. L. and Woods, A. (2006). Syndecan-2 is expressed in the microvasculature of gliomas and regulates angiogenic processes in microvascular endothelial cells. *J. Biol. Chem.* **281**, 14533-14536.

Ishiguro, K., Kojima, T. and Muramatsu, T. (2002). Syndecan-4 as a molecule involved in defense mechanisms. *Glycoconj. J.* **19**, 315-318.

Kwon, M. J., Hong, E., Choi, Y., Kang, D. H. and Oh, E. S. (2014). Interleukin-1α promotes extracellular shedding of syndecan-2 via induction of matrix metalloproteinase-7 expression. *Biochem. Biophys. Res. Commun.* **446**, 487-492.

Manon-Jensen, T., Itoh, Y. and Couchman, J. R. (2010). Proteoglycans in health and disease: the multiple roles of syndecan shedding. *FEBS J.* **277**, 3876-3889.

Manon-Jensen, T., Multhaupt, H. A. and Couchman, J. R. (2013). Mapping of MMP cleavage sites on syndecan-1 and syndecan-4 ectodomains. *FEBS J.* **280**, 2320-2331.

Mapp, P. I. and Walsh, D. A. (2012). Mechanisms and targets of angiogenesis and nerve growth in osteoarthritis. *Nat. Rev. Rheumatol.* **8**, 390-398.

McFall, A. J. and Rapraeger, A. C. (1997). Identification of an adhesion site within the syndecan-4 extracellular protein domain. *J. Biol. Chem.* **272**, 12901-12904.

McFall, A. J. and Rapraeger, A. C. (1998). Characterization of the high affinity cell-binding domain in the cell surface proteoglycan syndecan-4. *J. Biol. Chem.* **273**, 28270-28276.

Mettouchi, A. and Meneguzzi, G. (2006). Distinct roles of beta1 integrins during angiogenesis. *Eur. J. Cell Biol.* **85**, 243-247.

Nicosia, R. F. and Ottinetti, A. (1990). Growth of microvessels in serum-free matrix culture of rat aorta. A quantitative assay of angiogenesis in vitro. *Lab. Invest.* **63**, 115-122.

Passaniti, A., Taylor, R. M., Pili, R., Guo, Y., Long, P. V., Haney, J. A., Pauly, R. R., Grant, D. S. and Martin, G. R. (1992). A simple, quantitative method for assessing angiogenesis and antiangiogenic agents using reconstituted basement-membrane, heparin, and fibroblast growth-factor. *Lab. Invest.* **67**, 519-528.

Pruessmeyer, J., Martin, C., Hess, F. M., Schwarz, N., Schmidt, S., Kogel, T., Hoettecke, N., Schmidt, B., Sechi, A., Uhlig, S. et al. (2010). A disintegrin and metalloproteinase 17 (ADAM17) mediates inflammation-induced shedding of syndecan-1 and -4 by lung epithelial cells. *J. Biol. Chem.* **285**, 555-564.

Ramjaun, A. R. and Hodivala-Dilke, K. (2009). The role of cell adhesion pathways in angiogenesis. *Int. J. Biochem. Cell Biol.* **41**, 521-530.

Rapraeger, A. C., Ell, B. J., Roy, M., Li, X., Morrison, O. R., Thomas, G. M. and Beauvais, D. M. (2013). Vascular endothelial-cadherin stimulates syndecan-1-coupled insulin-like growth factor-1 receptor and cross-talk between αVβ3 integrin and vascular endothelial growth factor receptor 2 at the onset of endothelial cell dissemination during angiogenesis. *FEBS J.* **280**, 2194-2206.

Reynolds, L. E., Wyder, L., Lively, J. C., Taverna, D., Robinson, S. D., Huang, X., Sheppard, D., Hynes, R. O. and Hodivala-Dilke, K. M. (2002). Enhanced pathological angiogenesis in mice lacking beta3 integrin or beta3 and beta5 integrins. *Nat. Med.* **8**, 27-34.

Sakurai, T. and Kudo, M. (2011). Signaling pathways governing tumor angiogenesis. *Oncology* **81 Suppl. 1**, 24-29.

Streuli, C. H. and Akhtar, N. (2009). Signal co-operation between integrins and other receptor systems. *Biochem. J.* **418**, 491-506.

Takahashi, T., Takahashi, K., St John, P. L., Fleming, P. A., Tomemori, T., Watanabe, T., Abrahamson, D. R., Drake, C. J., Shirasawa, T. and Daniel, T. O. (2003). A mutant receptor tyrosine phosphatase, CD148, causes defects in vascular development. *Mol. Cell. Biol.* **23**, 1817-1831.

Takahashi, T., Takahashi, K., Mernaugh, R. L., Tsuboi, N., Liu, H. and Daniel, T. O. (2006). A monoclonal antibody against CD148, a receptor-like tyrosine phosphatase, inhibits endothelial-cell growth and angiogenesis. *Blood* **108**, 1234-1242.

Takahashi, K., Mernaugh, R. L., Friedman, D. B., Weller, R., Tsuboi, N., Yamashita, H., Quaranta, V. and Takahashi, T. (2012). Thrombospondin-1 acts as a ligand for CD148 tyrosine phosphatase. *Proc. Natl. Acad. Sci. USA* **109**, 1985-1990.

Trapasso, F., Drusco, A., Costinean, S., Alder, H., Aqeilan, R. I., Iuliano, R., Gaudio, E., Raso, C., Zanesi, N., Croce, C. M. et al. (2006). Genetic ablation of Ptprj, a mouse cancer susceptibility gene, results in normal growth and development and does not predispose to spontaneous tumorigenesis. *DNA Cell Biol.* **25**, 376-382.

Whiteford, J. R. and Couchman, J. R. (2006). A conserved NXIP motif is required for cell adhesion properties of the syndecan-4 ectodomain. *J. Biol. Chem.* **281**, 32156-32163.

Whiteford, J. R., Behrends, V., Kirby, H., Kusche-Gullberg, M., Muramatsu, T. and Couchman, J. R. (2007). Syndecans promote integrin-mediated adhesion of mesenchymal cells in two distinct pathways. *Exp. Cell Res.* **313**, 3902-3913.

Whiteford, J. R., Xian, X., Chaussade, C., Vanhaesebroeck, B., Nourshargh, S. and Couchman, J. R. (2011). Syndecan-2 is a novel ligand for the protein tyrosine phosphatase receptor CD148. *Mol. Biol. Cell* **22**, 3609-3624.

Zhu, J. W., Brdicka, T., Katsumoto, T. R., Lin, J. and Weiss, A. (2008). Structurally distinct phosphatases CD45 and CD148 both regulate B cell and macrophage immunoreceptor signaling. *Immunity* **28**, 183-196.

Zhu, J. W., Doan, K., Park, J., Chau, A. H., Zhang, H., Lowell, C. A. and Weiss, A. (2011). Receptor-like tyrosine phosphatases CD45 and CD148 have distinct functions in chemoattractant-mediated neutrophil migration and response to S. aureus. *Immunity* **35**, 757-769.

SUPLEMENTARY MATERIAL

Supplemental Figure 1

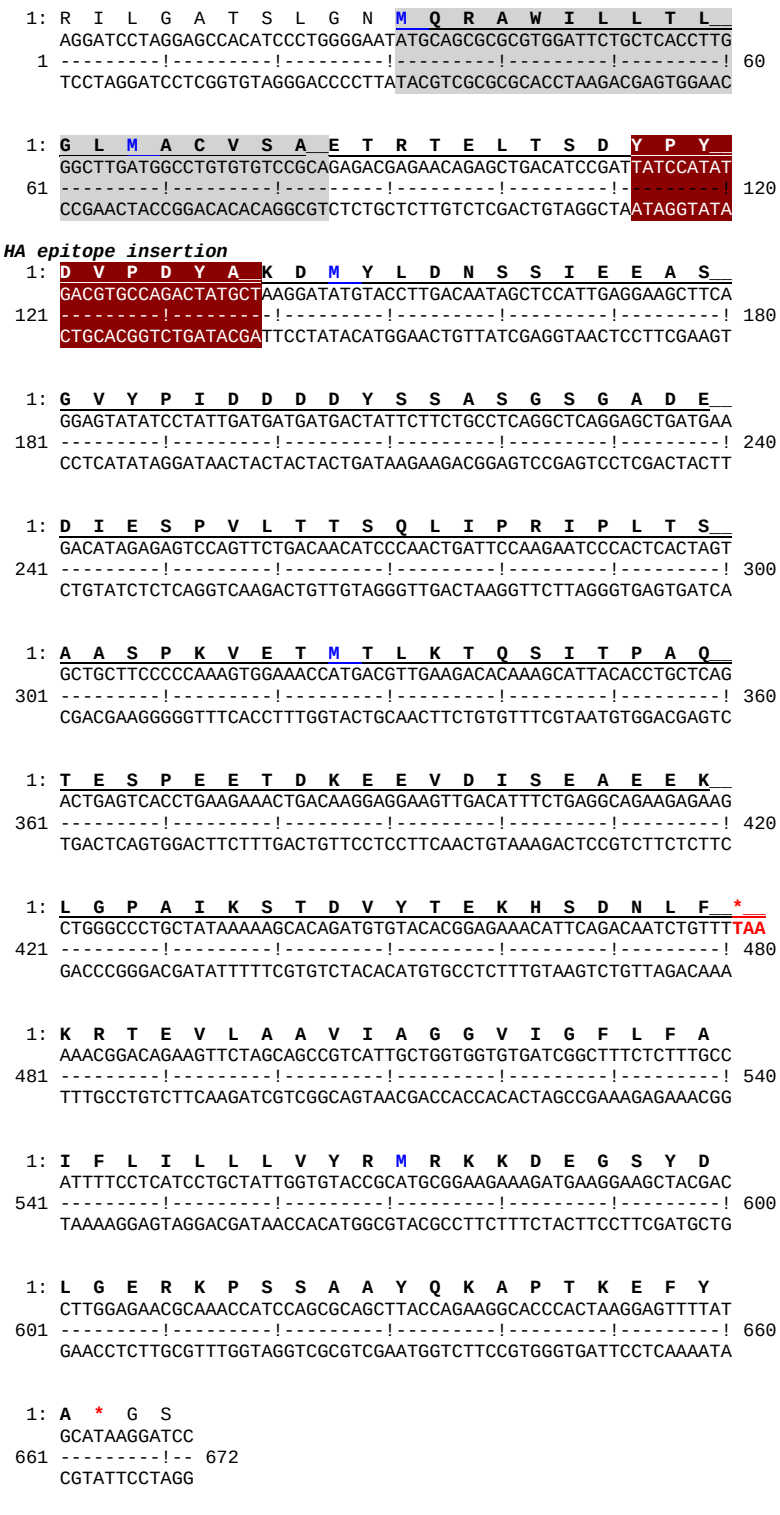

Murine syndecan-2 cDNA with HA tag insertional mutation (white text, red background). Syndecan coding sequence for eFLS2 is in bold and sequence encoding eS2ED is underlined with the addition of a stop codon (red).

Supplemental Figure 2

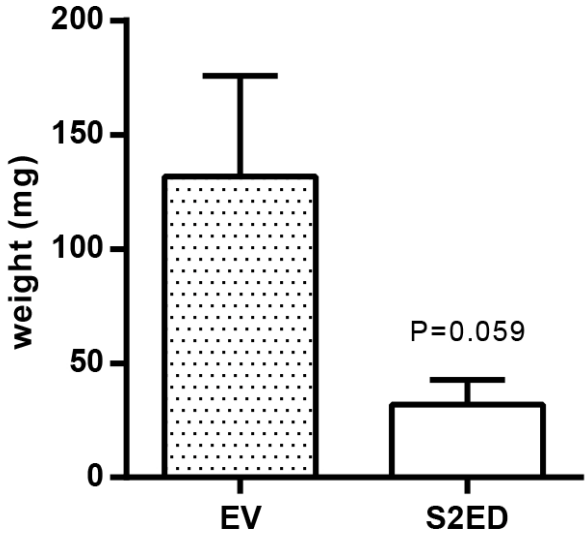

Tumours derived from eS2ED cells have smaller diameter and mass. Error bars represent the SEM and significance was calculated using a Students t test.

Supplemental Figure 3

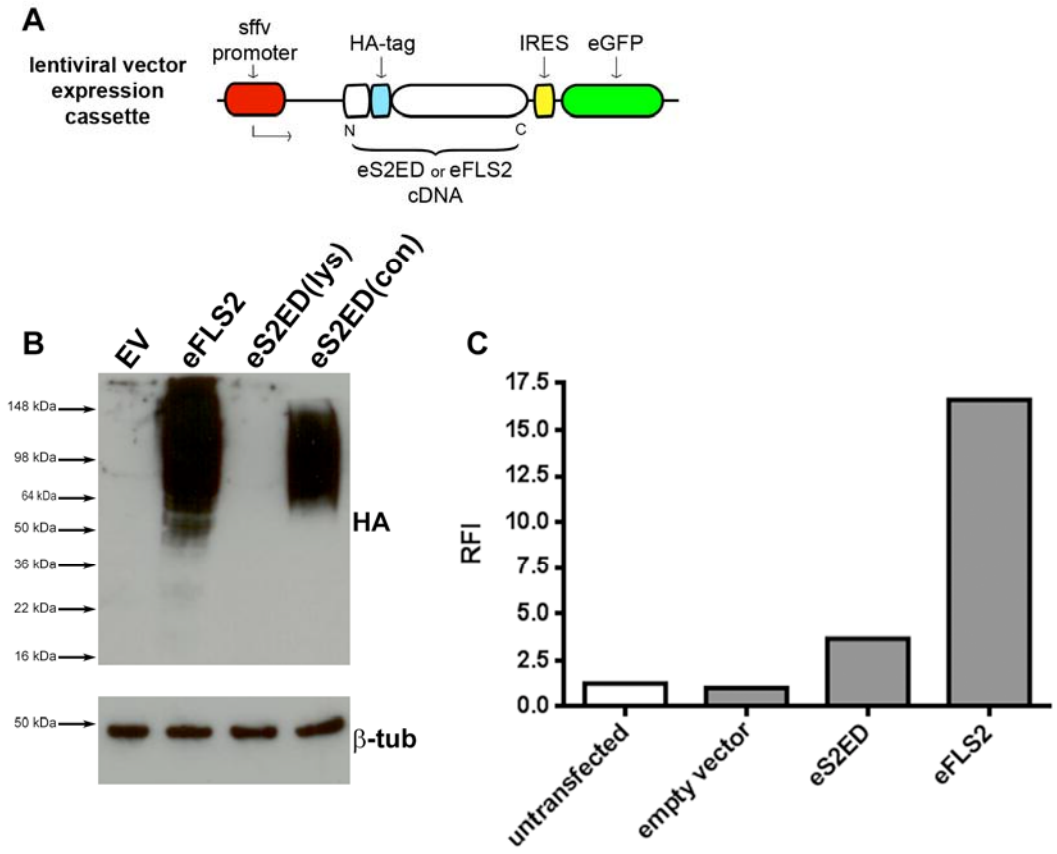

Characterisation of the syndecan-2 expressing HEK293t cell lines. (A) Schematic diagram of the lentiviral expression cassette used for transfection. (B) Expression of full length syndecan-2 was demonstrated by western blot using anti-HA antibodies. A high molecular weight smear is observed in cells expressing eFLS2 indicating that the protein is substituted with HS. No smear or band is evident in lysates from cells transfected with eS2ED (eS2EDlys) however HSPGs isolated from the conditioned media by anion exchange (eS2EDcon) contain a high molecular weight smear indicating that the constitutively secreted syndecan-2 core protein is glycanated. (C) The full length form of syndecan-2 is expressed on the cell surface. Flow cytometry using the anti-HA antibody was performed on the cell lines indicated.

Supplemental Figure 4

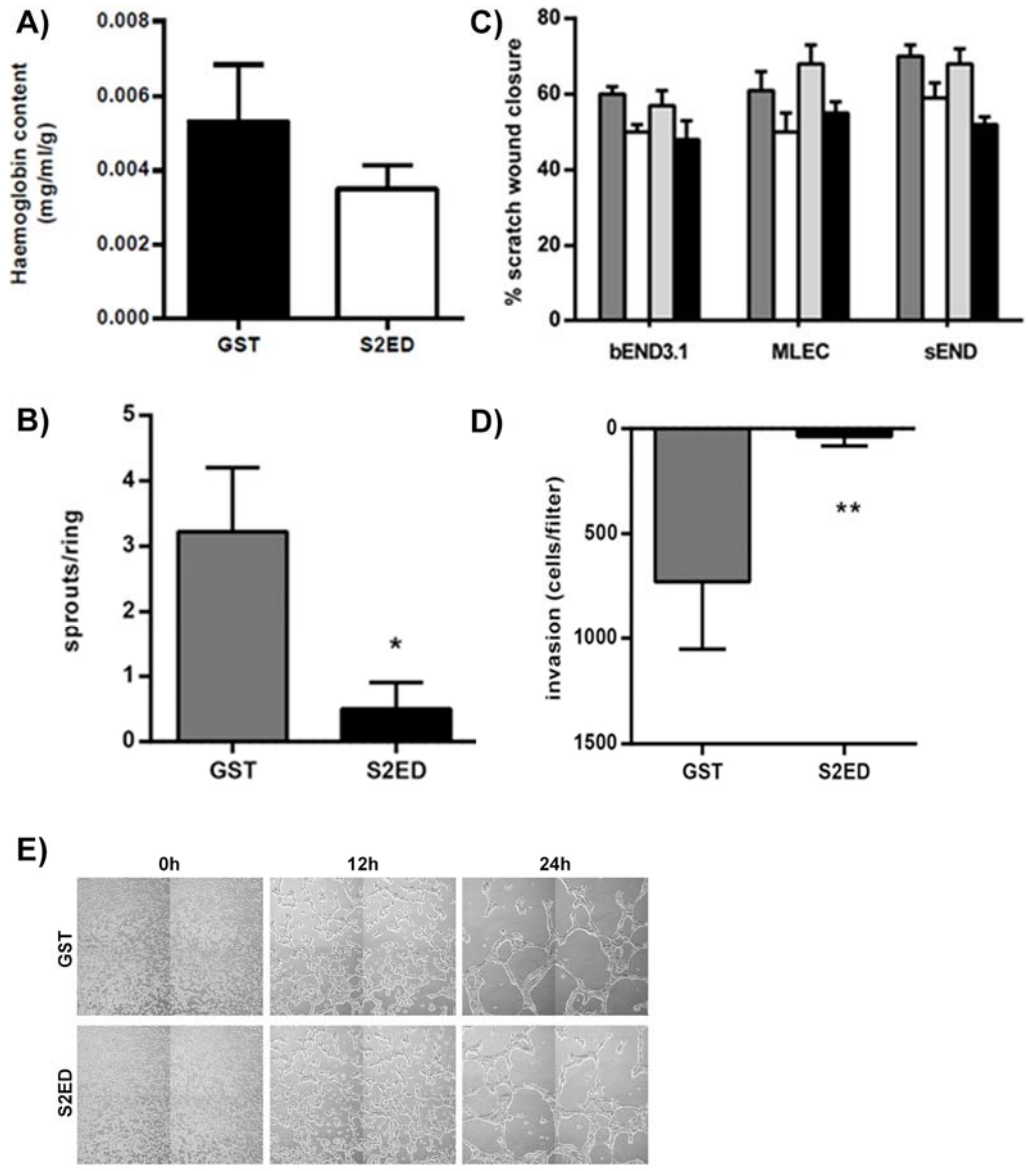

A) Quantification of haemoglobin content of Matrigel plugs. Plugs containing S2ED (white bar) contained less blood than GST control (black bar). Error bars represent the highest and lowest mean measurements obtained from 2 mice injected with 2 plugs.

B) S2ED is inhibitory to angiogenic sprout formation from murine aortas. Murine aortic rings were seeded in collagen I gels containing 0.5μM of GST or S2ED and supplemented with 1% FBS and VEGF. (Statistical analysis was performed using a Student's t-test, n=5; $p<0.05$).

C) S2ED inhibits migration of ECs from different vascular beds. Scratch wound migration assays were performed in the presence of 0.5μM of the fusion proteins indicated on the EC cell lines from brain, lung and skin. Percentage scratch wound closure was measured after 9 hours of incubation. Proteins containing the adhesion regulatory domain S2ED (white bars) and S2EDΔL^{73}-G^{123} (black bars) inhibit EC migration whereas migration is unaffected by treatment with GST (grey bars) and S2EDΔP^{124}-G^{123} (light grey bars).

D) S2ED slows EC migration through Matrigel. S2ED inhibits EC invasion through Matrigel. GST or S2ED (0.5μM) was incorporated into Matrigel layers in transwells. After 6 hours migrated cells were counted and the data represents the mean of triplicate assays.

E) EC microtubule formation is not affected by S2ED. sEND cells were seeded on layers of Matrigel and micrographs were obtained at the times indicated.

Biochemical Society TRANSACTIONS
www.biochemsoctrans.org
Biochemical Society Transactions

Syndecans in angiogenesis and endothelial cell biology

Giulia De Rossi*[1] and James R. Whiteford*

*Centre for Microvascular Research, William Harvey Research Institute, Barts and the London School of Medicine and Dentistry, Queen Mary University of London, Charterhouse Square, London EC1M 6B, U.K.

Abstract

Syndecans are multifunctional heparan sulfate proteoglycans (HSPGs) with roles in cell adhesion, migration, receptor trafficking and growth-factor interactions and signalling. Studies using syndecan null animals have revealed limited roles for syndecans during development; however, under conditions of challenge or insult, several phenotypes have emerged. Angiogenesis is an important process both in development and in wound healing, but also in pathologies such as cancer and chronic inflammatory conditions. In the present paper, we summarize the main studies elucidating the role of syndecans in angiogenesis and their potential as novel therapeutic targets.

Introduction

Syndecans are type I transmembrane glycoproteins that belong to the heparan sulfate proteoglycan (HSPG) superfamily. Four members have been characterized in vertebrates with different functions and expression profiles. Most cell types, with the exception of erythrocytes, possess at least one syndecan; although syndecan-1 appears principally in epithelia and in some leucocyte subsets, syndecan-2 is mainly expressed in mesenchymal tissues, syndecan-3 is primarily neuronal whereas syndecan-4 is ubiquitously expressed but at lower levels compared with the other three [1–3]. However, this traditional description of syndecan expression profiles is being challenged by new studies (some of which are reviewed in the present paper) showing that syndecan expression is more plastic and not only dependent on cell type, but also on the developmental stage, the environment and stimuli present.

Syndecans possess a linear single-pass transmembrane protein core which includes a highly conserved short cytoplasmic domain, a transmembrane domain and a more divergent (except for the sugar-attachment sites) syndecan-specific extracellular domain which varies in length among the four members (with syndecan-4 being the shortest and syndecan-3 being the longest) and this is covalently substituted with heparan sulfate (HS) chains (and chondroitin or dermatan-sulfate chains, in some cases). The HS chains consist of 50–150 repetitions of disaccharide units (mainly glucoronic acid and *N*-acetylglucosamine) with alternating high- and low-sulfated domains attached to conserved Ser-Gly dipeptides in the extracellular core protein [4].

Syndecans have the ability to interact with a great repertoire of ligands including extracellular matrix (ECM) molecules, growth factors, enzymes, cytokines, chemokines and pathogens. These interactions occur mainly through syndecan HS chains and there are a considerable number of angiogenesis-related growth factors, cytokines and chemokines that have heparin-binding properties, including fibroblast growth factors (FGFs), platelet-derived growth factor (PDGF), vascular endothelial growth factors (VEGFs), pleiotrophin, placental growth factor (PlGF), platelet factor-4 (PF-4), heparin-binding endothelial growth factor (EGF)-like growth factor, interleukin-8 (IL-8), hepatocyte growth factor (HGF), macrophage inflammatory protein-1 (MIP-1), transforming growth factor-β (TGF-β) and interferon-γ (IFN-γ). Surprisingly, no direct interaction between many of these molecules and syndecans has been reported yet, possibly because of the technical challenges and limited knowledge of the specific sugar composition and level of modification of the four different syndecans HS chains.

The cytoplasmic domain of syndecans is composed of two conserved regions (C1 and C2) flanking a variable region (V), unique for each syndecan. These domains can interact with a number of cytoplasmic proteins and lipids and as such promote specific cell functions. The V region generally confers syndecan-specific properties whereas the C-terminus (C2) domain contains a PDZ-binding domain shared among the four members [5].

It is becoming increasingly evident that many functions of syndecans depend on their extracellular domains [6]. Once engaged in an interaction, syndecans can act as cell-surface receptors transmitting signals to inside the cell (although they do not possess intrinsic enzymatic activity), as co-receptors presenting the ligand to another receptor and, upon ectodomain shedding, as soluble effectors. It is then unsurprising that syndecans can regulate a number of complex signalling events contributing to cell proliferation, differentiation, adhesion and migration [1,5,7].

The formation of new blood vessels from pre-existing ones, also known as angiogenesis, is a complex process

Key words: angiogenesis, endothelial cell, heparan sulfate, integrin, syndecan.

Abbreviations: EGF, endothelial growth factor; FGF, fibroblast growth factor; HMEC, human microvascular endothelial cell; HS, heparan sulfate; HSPG, heparan sulfate proteoglycan; MvEC, murine vein endothelial cell; PGE_2, prostaglandin E_2; PKCα, protein kinase Cα; SSTN, synstatin; TSP-1, thrombospondin-1; VEGF, vascular endothelial growth factor; VN, vitronectin.

[1]To whom correspondence should be addressed (email g.derossi@qmul.ac.uk).

which involves all the cell processes mentioned above and more. The basic steps of angiogenesis include enzymatic degradation of capillary basement membrane, endothelial cell proliferation and migration, tubulogenesis, vessel fusion and stabilization [8–10]. A large number of factors and cell types participate in the regulation of this important physiological (and pathological) process; the purpose of the present article is to summarize the recent findings on how syndecan functions can affect endothelial cell behaviour in the context of angiogenesis.

Syndecan-1

Syndecan-1 is probably the best characterized of the syndecans; it appears to be implicated in a variety of physiological processes associated with the endothelium, both during development and during adulthood. This is unsurprising since syndecan-1 is a major constituent of the endothelial glycocalyx [11]. In an interesting study, increased new blood vessel formation in syndecan-1-deficient mice was observed where corneal neovascularization was induced by inflammation rather than pro-angiogenic growth factors. However, a direct correlation between increased endothelial cell–leucocyte interactions in these animals and increased angiogenesis was observed which suggested that the increase in the latter is due to an increased local accumulation of leucocytes [12]. Other studies have shown that syndecan-1 can associate directly via its extracellular domain with the $\alpha V\beta 3$ and $\alpha V\beta 5$ integrins leading to their activation. This has been shown to happen in a variety of cell types [13–15] including endothelial cells from both mice and humans. In fact, immunoprecipitation experiments with human microvascular endothelial cells (HMECs) revealed that it was possible to co-precipitate $\beta 3$ and $\beta 5$ integrins in complex with syndecan-1 and that by silencing syndecan-1 expression, the HMEC-1 line was not able to spread on the $\alpha V\beta 3$ ligand vitronectin (VN) [16]. The same group previously showed that cells seeded on syndecan-1 antibody would spread and activate $\alpha V\beta 3$ and $\alpha V\beta 5$ even in the absence of integrin ligands [15]. They could replicate this result with endothelial cells and show that integrin activation could be prevented by adding synstatin ($SSTN_{82–130}$, a peptide corresponding to amino acids 82–130 of the syndecan-1 extracellular core protein). Interestingly, the SSTN peptide showed promising results in being able to inhibit tumour angiogenesis in a mouse model of mammary carcinoma [16].

Later, the same group discovered the mechanism through which syndecan-1 is able to activate $\alpha V\beta 3$ and $\alpha 5\beta 3$ integrins. They were able to co-precipitate syndecan-1 with $\alpha V\beta 3$ and insulin-like growth factor receptor 1 (IGF1R) from endothelial cells in a way which suggested integrin and syndecan-1 were acting as a docking site for IGFR1. Also, they showed the presence of this ternary complex on focal contacts when cells were plated on VN [17]. In further investigations, they found that SSTN, the peptide able to disrupt syndecan-1–$\alpha V\beta 3$ interaction, can block VEGF-induced angiogenesis, but only in the early phase (in the aortic ring assay) when endothelial cell dissemination is preceded by breakdown of adherens junctions. VEGF-stimulated migration of endothelial cells depends on $\alpha V\beta 3$ and can be blocked by SSTN, suggesting that syndecan-1 has a role VEGF-dependent migration in endothelial cells. Indeed, stimulation of cells with VEGF activates not only VEGFR2, but also IGFR1 and $\alpha V\beta 3$; activation of the latter can be abolished by adding SSTN. They propose a model whereby during the early phase of angiogenesis, syndecan-1, in its ternary complex with $\alpha V\beta 3$ and IGFR1, is necessary for VEGF-induced integrin activation. This is key to endothelial cell dissemination and can be prevented by SSTN and also by disruption of the vascular endothelial (VE)–cadherin homophilic interaction, thus supporting the finding that SSTN is not able to stop angiogenesis in its late phase when adherens junctions are disrupted [18].

Syndecan-2

The most important study linking syndecan-2 to angiogenesis dates back to 10 years ago when Chen et al. [19] showed that lack of syndecan-2 in zebrafish (achieved by morpholino gene-targeting approach) dramatically impairs developmental angiogenesis. In the least severe case, corresponding to a less efficient syndecan-2 knockdown, intersegmental vessels either sprouted abnormally or failed to form and the vascular plexus of the tail region was less complex compared with that of wild-type embryos. Primary formation of the axial vessels was normal. However, although axial expression of fli-1, flk-1 and tie-1 was retained in the trunk, this was lost in the intersegmental vessels. In an elegant twist to the work, they not only showed that the phenotype could be reverted by injection of exogenous zebrafish syndecan-2 cDNA but also that a similar effect could be obtained by injecting human syndecan-2 cDNA, giving clear clues of an important functional conservation among species. The exact mechanism through which syndecan-2 asserts its pro-angiogenic function remains unclear. However, they showed that injection of a cytoplasmically-truncated form of syndecan-2 phenocopied the lack of its full-length form, suggesting the importance of its cytoplasmic domain in syndecan-2 vascular function [19].

Syndecan-2 may also play a role in pathological angiogenesis. It was found to be up-regulated both on vessels in gliomas and from normal brain whereas not present in the surrounding parenchyma [20]. The same study showed that knockdown of syndecan-2 in murine vein endothelial cells (MvEC) resulted in decreased migration on fibronectin and tube formation on Matrigel. However, those same pro-angiogenic factors such as EGF, basic FGF (bFGF) and VEGF, known to be up-regulated in gliomas, showed an ability to promote syndecan-2 shedding from MvECs. Further studies showed that the shed molecule can have a pro-angiogenic effect on MvECs, suggesting that the vascular function of syndecan-2 might result from a quite complicated balance of its functions on the cell surface, the regulation of its shedding and a possible autocrine or paracrine role as a shed effector [20].

Furthermore, the HMEC-1 line predominantly expresses syndecan-2 (~80% of all HSPG on the cell surface) and its expression is increased in response to angiogenic stimuli (especially FGF) and is dependent on the type of matrix cells are seeded on. Interestingly, down-regulation of syndecan-2 resulted in decreased cell attachment and spreading and accelerated cell migration but also impaired the HMEC-1 line's ability to form capillary-like structures on Matrigel [21].

In the light of these few but important studies, it appears that syndecan-2 plays a pivotal role in angiogenesis. Unfortunately, unlike the other three members of the syndecan family, a knockout mouse model for syndecan-2 has not yet been developed; therefore the question as to whether a syndecan-2-knockout mouse would develop normally or die prematurely due to angiogenic defects is still left unanswered.

Syndecan-3

Syndecan-3-knockout mice are viable and develop normally. Syndecan-3 is considered the main syndecan of the nervous system and as such it is been mainly investigated in behavioural studies.

However, recent work highlighting a role for syndecan-3 in the inflammatory response of different tissues also served to demonstrate that its expression is not limited to the nervous system but it can also be found on the endothelium of different vascular beds (joints, dermis and cremaster muscle) [22].

We recently showed a potential therapeutic effect of the syndecan-3 extracellular core protein in pathologies where angiogenesis is increased. Recombinant bacterially-derived (hence lacking the glycosaminoglycan chains) syndecan-3 extracellular domain was shown to be able to significantly inhibit angiogenesis in the *ex vivo* model of the aortic ring assay and also inhibit skin and brain endothelial cell-tube formation and cell migration through collagen in 2D and 3D [23]. These data support the idea that syndecan core proteins, when released from the cell surface, can act as important effectors of cell behaviour.

Syndecan-4

Although syndecan-4 was found up-regulated throughout the granulation tissue during skin injury on endothelial cells [24], the first clear evidence that it could play a functional role in angiogenesis came from the work of Echtermeyer et al. [25]. They generated a syndecan-4-knockout mouse which showed significantly delayed wound healing in a model of skin injury. Although the number of newly generated vessels populating the regenerating tissue was not affected by the lack of syndecan-4, the vessels were smaller compared with the wild-type littermates.

Syndecan-4 has since been found to be essential in mediating the pro-angiogenic effects of thrombospondin-1 (TSP-1). The study proposed a model whereby two heparin-binding sequences contained within TSP-1 are able to compete with fibronectin for the interaction with syndecan-4, thus interfering with syndecan-4-mediated endothelial cell adhesion [26].

In vitro experiments on endothelial cells have shown that syndecan-4 is also key player in FGF signalling [27,28]. Interestingly, this is achieved not just by facilitating the interaction between FGF2 and its receptor FGF receptor 1 (FGFR1), but the syndecan-4 cytoplasmic domain seems to have a key role, as chimaeras and deletion mutants of this portion lacking the V or the C2 regions fail to promote an effective intracellular response to FGF2. In particular, lack of the C2 region (which contains the PDZ binding domain) prevents the binding of GAIP (Gα-interacting protein)-interacting protein C-terminus (GIPC)/synectin, which results in a failure to activate Rac1 and thus inhibits endothelial cell migration [29,30].

Quite recently, syndecan-4 has been shown to participate in the signalling initiated by another pro-angiogenic molecule, prostaglandin E_2 (PGE_2). The study revealed that in murine endothelial cells lacking syndecan-4, PGE_2-mediated pro-angiogenic effects (i.e. endothelial cell migration and tube formation) were decreased. It also showed that syndecan-4 activation of protein kinase Cα (PKCα) is necessary for the phosphorylation of extracellular-signal-regulated kinase (ERK) following PGE_2 stimulation. This molecular mechanism was confirmed *in vivo* by showing a diminished angiogenic response to PGE_2, both in the syndecan-4- and in the PKCα-knockout mice compared with the wild-type [31].

Concluding remarks

The studies demonstrate the importance of syndecans in endothelial cell biology during the process of angiogenesis. Remarkably, despite sharing a common structure, the four members of the syndecan family appear to have specific functions, and studies using knockout animals clearly show that lack of one syndecan can be compensated by another structurally-similar member (at least during adulthood and in pathophysiological conditions).

In the light of the few but promising results summarized in the present review, a more thorough investigation of syndecan biology is needed as not only will it increase our understanding of the complex process of new blood vessel formation but also it could potentially present syndecans as molecular targets in anti-angiogenic therapies.

Funding

G.D.R. is supported by Queen Mary University of London, Bart's and the London School of Medicine and Dentistry. J.R.W. is supported by Arthritis Research-UK [grant number 19207].

References

1 Couchman, J.R. (2003) Syndecans: proteoglycan regulators of cell-surface microdomains? Nat. Rev. Mol. Cell Biol. **4**, 926–937 CrossRef PubMed

2 Xian, X., Gopal, S. and Couchman, J.R. (2010) Syndecans as receptors and organizers of the extracellular matrix. Cell Tissue Res. **339**, 31–46 CrossRef PubMed

3 Couchman, J.R. (2010) Transmembrane signaling proteoglycans. Annu. Rev. Cell Dev. Biol. **26**, 89–114 CrossRef PubMed
4 Leonova, E.I. and Galzitskaya, O.V. (2013) Structure and functions of syndecans in vertebrates. Biochemistry **78**, 1071–1085 PubMed
5 Lambaerts, K., Wilcox-Adelman, S.A. and Zimmermann, P. (2009) The signaling mechanisms of syndecan heparan sulfate proteoglycans. Curr. Opin. Cell Biol. **21**, 662–669 CrossRef PubMed
6 De Rossi, G. and Whiteford, J.R. (2013) Novel insight into the biological functions of syndecan ectodomain core proteins. Biofactors **39**, 374–382 CrossRef PubMed
7 Alexopoulou, A.N., Multhaupt, H.A. and Couchman, J.R. (2007) Syndecans in wound healing, inflammation and vascular biology. Int. J. Biochem. Cell Biol. **39**, 505–528 CrossRef PubMed
8 Folkman, J. (1995) Angiogenesis in cancer, vascular, rheumatoid and other disease. Nat. Med. **1**, 27–31 CrossRef PubMed
9 Carmeliet, P. and Jain, R.K. (2011) Molecular mechanisms and clinical applications of angiogenesis. Nature **473**, 298–307 CrossRef PubMed
10 Carmeliet, P. (2005) Angiogenesis in life, disease and medicine. Nature **438**, 932–936 CrossRef PubMed
11 Zeng, Y., Adamson, R.H., Curry, F.R. and Tarbell, J.M. (2014) Sphingosine-1-phosphate protects endothelial glycocalyx by inhibiting syndecan-1 shedding. Am. J. Physiol. Heart Circ. Physiol. **306**, H363–H372 CrossRef PubMed
12 Gotte, M., Joussen, A.M., Klein, C., Andre, P., Wagner, D.D., Hinkes, M.T., Kirchhof, B., Adamis, A.P. and Bernfield, M. (2002) Role of syndecan-1 in leukocyte–endothelial interactions in the ocular vasculature. Invest. Ophthalmol. Vis. Sci. **43**, 1135–1141 PubMed
13 Beauvais, D.M. and Rapraeger, A.C. (2003) Syndecan-1-mediated cell spreading requires signaling by αvβ3 integrins in human breast carcinoma cells. Exp. Cell Res. **286**, 219–232 CrossRef PubMed
14 Beauvais, D.M., Burbach, B.J. and Rapraeger, A.C. (2004) The syndecan-1 ectodomain regulates αvβ3 integrin activity in human mammary carcinoma cells. J. Cell Biol. **167**, 171–181 CrossRef PubMed
15 McQuade, K.J., Beauvais, D.M., Burbach, B.J. and Rapraeger, A.C. (2006) Syndecan-1 regulates αvβ5 integrin activity in B82L fibroblasts. J. Cell Sci. **119**, 2445–2456 CrossRef PubMed
16 Beauvais, D.M., Ell, B.J., McWhorter, A.R. and Rapraeger, A.C. (2009) Syndecan-1 regulates αvβ3 and αvβ5 integrin activation during angiogenesis and is blocked by synstatin, a novel peptide inhibitor. J. Exp. Med. **206**, 691–705 CrossRef PubMed
17 Beauvais, D.M. and Rapraeger, A.C. (2010) Syndecan-1 couples the insulin-like growth factor-1 receptor to inside-out integrin activation. J. Cell Sci. **123**, 3796–3807 CrossRef PubMed
18 Rapraeger, A.C., Ell, B.J., Roy, M., Li, X., Morrison, O.R., Thomas, G.M. and Beauvais, D.M. (2013) Vascular endothelial-cadherin stimulates syndecan-1-coupled insulin-like growth factor-1 receptor and cross-talk between αVβ3 integrin and vascular endothelial growth factor receptor 2 at the onset of endothelial cell dissemination during angiogenesis. FEBS J. **280**, 2194–2206 CrossRef PubMed
19 Chen, E., Hermanson, S. and Ekker, S.C. (2004) Syndecan-2 is essential for angiogenic sprouting during zebrafish development. Blood **103**, 1710–1719 CrossRef PubMed
20 Fears, C.Y., Gladson, C.L. and Woods, A. (2006) Syndecan-2 is expressed in the microvasculature of gliomas and regulates angiogenic processes in microvascular endothelial cells. J. Biol. Chem. **281**, 14533–14536 CrossRef PubMed
21 Noguer, O., Villena, J., Lorita, J., Vilaro, S. and Reina, M. (2009) Syndecan-2 downregulation impairs angiogenesis in human microvascular endothelial cells. Exp. Cell Res. **315**, 795–808 CrossRef PubMed
22 Kehoe, O., Kalia, N., King, S., Eustace, A., Boyes, C., Reizes, O., Williams, A., Patterson, A. and Middleton, J. (2014) Syndecan-3 is selectively pro-inflammatory in the joint and contributes to antigen-induced arthritis in mice. Arthritis Res. Ther. **16**, R148 CrossRef PubMed
23 De Rossi, G. and Whiteford, J.R. (2013) A novel role for syndecan-3 in angiogenesis. F1000Res. **2**, 270 PubMed
24 Gallo, R., Kim, C., Kokenyesi, R., Adzick, N.S. and Bernfield, M. (1996) Syndecans-1 and -4 are induced during wound repair of neonatal but not fetal skin. J. Invest. Dermatol. **107**, 676–683 CrossRef PubMed
25 Echtermeyer, F., Streit, M., Wilcox-Adelman, S., Saoncella, S., Denhez, F., Detmar, M. and Goetinck, P. (2001) Delayed wound repair and impaired angiogenesis in mice lacking syndecan-4. J. Clin. Invest. **107**, R9–R14 CrossRef PubMed
26 Nunes, S.S., Outeiro-Bernstein, M.A., Juliano, L., Vardiero, F., Nader, H.B., Woods, A., Legrand, C. and Morandi, V. (2008) Syndecan-4 contributes to endothelial tubulogenesis through interactions with two motifs inside the pro-angiogenic N-terminal domain of thrombospondin-1. J. Cell. Physiol. **214**, 828–837 CrossRef PubMed
27 Murakami, M., Horowitz, A., Tang, S., Ware, J.A. and Simons, M. (2002) Protein kinase C (PKC) δ regulates PKCalpha activity in a syndecan-4-dependent manner. J. Biol. Chem. **277**, 20367–20371 CrossRef PubMed
28 Volk, R., Schwartz, J.J., Li, J., Rosenberg, R.D. and Simons, M. (1999) The role of syndecan cytoplasmic domain in basic fibroblast growth factor-dependent signal transduction. J. Biol. Chem. **274**, 24417–24424 CrossRef PubMed
29 Tkachenko, E., Lutgens, E., Stan, R.V. and Simons, M. (2004) Fibroblast growth factor 2 endocytosis in endothelial cells proceed via syndecan-4-dependent activation of Rac1 and a Cdc42-dependent macropinocytic pathway. J. Cell Sci. **117**, 3189–3199 CrossRef PubMed
30 Tkachenko, E., Elfenbein, A., Tirziu, D. and Simons, M. (2006) Syndecan-4 clustering induces cell migration in a PDZ-dependent manner. Circ. Res. **98**, 1398–1404 CrossRef PubMed
31 Corti, F., Finetti, F., Ziche, M. and Simons, M. (2013) The syndecan-4/protein kinase Cα pathway mediates prostaglandin E_2-induced extracellular regulated kinase (ERK) activation in endothelial cells and angiogenesis *in vivo*. J. Biol. Chem. **288**, 12712–12721 CrossRef PubMed

Received 26 August 2014
doi:10.1042/BST20140232